Université Fédérale
Toulouse Midi-Pyrénées

THÈSE

En vue de l'obtention du
DOCTORAT DE L'UNIVERSITÉ DE TOULOUSE
Délivré par l'Université Toulouse 3 - Paul Sabatier

Présentée et soutenue par

Léo CLEMENT

Le 17 juillet 2023

Navigation visuelle chez les fourmis : approche comportementale et de modélisation

Ecole doctorale : **SEVAB - Sciences Ecologiques, Vétérinaires, Agronomiques et Bioingenieries**

Spécialité : **Ecologie, biodiversité et évolution**

Unité de recherche :
CRCA - Centre de Recherches sur la Cognition Animale

Thèse dirigée par
Jacques GAUTRAIS et Antoine WYSTRACH

Jury

M. Andrew PHILIPPIDES, Rapporteur
M. Simon BENHAMOU, Rapporteur
Mme Emily BAIRD, Examinatrice
M. Franck RUFFIER, Examinateur
M. Antoine WYSTRACH, Co-directeur de thèse
Mme AUDREY DUSSUTOUR, Présidente

Navigation visuelle chez les fourmis : approche comportementale et de modélisation

Visual navigation in ants: behavioural and modelling approach

Léo Clement

2023

Contents

Abstract

Navigation in natural environments is an essential ability for animals, but it can be highly challenging to achieve due to the complex, ever-changing, nature of the environment they navigate through. Solitary foraging hymenopterans, such as ants, have evolved remarkable abilities to navigate in these complex environments despite a nervous system much simpler than those of vertebrates. What's more, ants' displacements can be easily tracked, thus providing a powerful system to investigate the mechanisms underlying navigation in the wild.

Thanks to the development and application of neurobiological tools in insects, we now have an increasingly detailed description of the circuits in these "mini-brains". These networks, composed of a large number of interacting units (neurons), are the site of very dynamic internal activity that allows for an effective coupling of the organism with its environment. The field of insect navigation has integrated this neurobiological knowledge with a long-standing tradition of behavioural experiments, as well as in-silico modelling approaches, to gain a deeper understanding of the mechanisms and emergent properties in these systems. This multi-level approach has provided valuable insights into how complex behaviour emerges.

This thesis presents an integrative approach combining behavioural experiments and computational modelling with the aim to gain further understanding of the mechanisms of ant navigation.

First, I investigate the dynamics of visual learning when ants navigate in natural conditions. There are already good insights into how the insect brain can memorize and recognize views, and how these views might be used for navigation. However, practically nothing is known about how learning is orchestrated in the first place. Learning a route cannot be governed only by rewards and punishments but may happen 'continuously'; a vague concept so-called 'latent learning' in the vertebrate literature. By combining field experiments and modelling, I show that ants learn the route they travel in a continuous fashion. I also explain how such a continuous mechanism of learning and recalling can be implemented in the light of the known insect brain circuitry. Our work shows that such a continuous spatial learning is supported by egocentric route memories rather than a map-like reconstruction of space.

Secondly, I shed light on how higher-level visual recognition and lower-level motor control interact. Most -if not all-studies in animal navigation have focused on higher level strategies

such as the use of path integration, the recognition of learnt visual cues and the reconstruction of so-called cognitive maps. However, how these higher-level strategies are supported by lower level (often more ancestral) motor behaviours remains largely unexplored. We used a multidirectional treadmill set up -a trackball- to record with high precision the motor behaviour of ants directly in their natural environment. Results explain how higher-level navigation strategies are supported by lower-level motor control and demonstrate the existence – and importance – of an intrinsic oscillator at the core of navigational behaviours.

Finally, I investigate the specific cues encoded by ants in visual scenes. Insects' visual system performs various feature extractions. I used virtual reality (VR) to explore which visual cues are encoded by ants to consider the presence of a natural panorama and trigger exploratory behaviours. Through this approach, I shed light on the perceptual encoding of naturalistic environments and provide a promising avenue for further investigation using virtual reality setups.

Taken together, this thesis allowed me to understand that behaviour, rather than being a set of discrete actions, is a continuous process where intelligence can be seen as an emergent property. I employed various approaches, some successful, some failing, but all improved my vision of how I should ask and answer a scientific question.

Résumé

La navigation est une capacité essentielle pour les animaux, mais est une tâche complexe en raison de la nature de l'environnement qui est en constante évolution. Les hyménoptères, tels que les fourmis, ont développé des capacités remarquables pour naviguer dans ces environnements complexes malgré un système nerveux beaucoup plus simple que celui des vertébrés. Ainsi, les fourmis sont un modèle puissant pour étudier les mécanismes sous-jacents à la navigation.

Grâce au développement d'outils neurobiologiques chez les insectes, nous avons maintenant une description de plus en plus détaillée des circuits de ces "mini-cerveaux". Ces réseaux, composés d'un grand nombre d'unités en interactions (neurones), sont le site d'une activité interne très dynamique qui permet un couplage efficace de l'organisme avec son environnement. Le domaine de la navigation des insectes a intégré cette connaissance neurobiologique avec une tradition de longue date d'expériences comportementales, couplé, plus récemment, à de la modélisation. Cette approche intégrative a fourni des informations précieuses sur la manière dont les comportements complexes émergent.

Cette thèse présente une approche intégrative combinant des expériences comportementales et de modélisation dans le but de mieux comprendre les mécanismes de la navigation chez les fourmis.

Premièrement, je m'intéresse à la dynamique de l'apprentissage visuel lorsque les fourmis naviguent dans des conditions naturelles. Il y a déjà de bonnes connaissances sur la manière dont le cerveau des insectes peut mémoriser et reconnaître des vues, et comment ces vues peuvent être utilisées pour la navigation. Cependant, on ne sait pratiquement rien sur la façon dont l'apprentissage est orchestré en premier lieu. Apprendre une route ne peut pas être régie uniquement par des récompenses et des punitions, mais peut se produire de manière continue ; un concept vague appelé "apprentissage latent" dans la littérature des vertébrés. En combinant modélisation et expériences de terrain, je montre que les fourmis apprennent les routes de manière continue, soutenue par des mémoires égocentriques plutôt qu'une reconstruction de l'espace sous forme de ‘carte cognitive’.

Deuxièmement, je mets en lumière comment la reconnaissance visuelle de niveau « supérieur » et le contrôle moteur basal interagissent. La plupart, voire toutes, les études sur la navigation

animale se concentrent sur l'utilisation des stratégies de haut niveau telles que l'intégration du trajet, la reconnaissance de repères visuels appris et l'utilisation de cartes cognitives. Cependant, comment ces stratégies de haut niveau sont soutenues par les comportements moteurs de bas niveau (souvent plus ancestraux) reste largement inexploré. J'ai enregistré avec une grande précision le comportement moteur des fourmis directement dans leur environnement naturel et montré que les stratégies de navigation de haut niveau sont soutenues par un contrôle moteur de bas niveau. Nous révélons ici l'existence - et l'importance - d'un oscillateur intrinsèque au cœur des comportements de navigation.

Finalement, j'ai étudié les indices spécifiques encodés par les fourmis dans les scènes visuelles. J'ai utilisé la réalité virtuelle (RV) pour explorer quels indices visuels sont encodés par les fourmis pour déclencher leurs comportements de navigation. Grâce à cette approche, j'ai pu déterminer sur quelles caractéristiques les fourmis se basent pour déterminer si l'environnement perçu déclenche ou non un comportement d'exploration.

Dans l'ensemble, cette thèse m'a permis de comprendre que le comportement, plutôt que d'être un ensemble d'actions discrètes, est un processus continu où l'intelligence peut être considérée comme une propriété émergente. J'ai utilisé diverses approches, certaines réussies, d'autres infructueuses, mais toutes ont amélioré ma vision de la façon dont je dois poser et répondre à une question scientifique.

Acknowledgements

Back to my first field season in July 2017, I had the chance to join Antoine Wystrach and Sebastian Schwarz (Seppie) for a one-month internship. Everything about the field pleased me, from the experiments to the temporary life we created in Sevilla. We were more than co-workers during that period; we were roommates. I want to thank you for allowing me to be a part of that and for bringing out with you a little "punk". Most importantly, Seppie, our field mama, taught me everything about the delicate art of ant painting. I will always remember that first season with you guys and the chaos that came with Evripides (another intern from the Sussex lab) while trying to identify ants. I still laugh when I think about the moments of uncertainty, like when he questioned, "Are you sure it was pink?". You, mama Seppie, were trying to supervise two young researchers. To Evripides, thank you, we started together our journeys. I am proud of you, my dear friend, always available for small chats and scientific discussions.

Surprisingly, both Antoine and Seppie took me back to the field for subsequent internships and for my thesis. I want to thank you both for passing on your knowledge and, more importantly, for being more than co-workers but true friends. You always trusted me and gave me the opportunity to be not just an intern but a member of the team and a friend from the very beginning. I wonder how many GnTs we enjoyed together; I didn't bother keeping count because it would be impossible to achieve. So, Antoine, thank you for being so supportive, humorous, and witty, and for allowing me to find my own path while trusting me. Seppie, thank you for your honesty, kindness, outspokenness, and for simply being yourself. I don't know if you remember, but you helped me name my dogs, which means everything to 'me' - to us - and shows how highly I regard you. Both of you were like my unconventional science parents: I love you.

Last but not least, one of the first members of the *AntNavigationTeam* was Florent Le Moël, aka Floflo. Floflo, I don't know how to express how much you were and still are important to me. I read your acknowledgement in your thesis, and you said, "I know I can always count on you." Once again, you demonstrated this recently to me. You are an amazing

friend, from our casual chats to the serious conversations, including all the science in between. I hope we can go back to the field together and have some more 'defile' moments while doing science (or the other way around). Thank you, Floflo, for being you, for always being there to support me, and most importantly, for being so reassuring. As you said, we share many similarities despite our outward differences. This thesis would not have been the same without you. Just one last thing... Stop using Json; it gives headaches to students.

I am aware that I can always count on you guys.

From my first experience in Sevilla to now, I want to thank you, Mike, aka el Capitan. I feel a strong connection with you, and I'm not sure why, considering you're one of the meanest persons I've ever met... No, seriously, you are so kind and caring, with a good amount of irony and a particular humor that I enjoy so much (maybe it's your British side; oops, I did it again). See you soon (I hope).

Since the beginning of this team, many students have joined us, not only as temporary internship slaves but as true members of the team, from work to the bar. So, guys, friends, I want to thank you. Cricri, “I mean” Cricri, we spent so much time enjoying Sevilla together. I like you a lot more than I would admit. Blandine, we spent such a significant amount of time together in the VR room, going crazy without windows and endlessly joking. Thank you for those moments. And Erwan, you are a very good person. You taught me a lot about ant evolution and identification. Many thanks for the many cigarette break and beers we shared together. Lastly, the team had the opportunity to have Océane as a new PhD student. Océane, I've already told you that you are truly amazing and smart. You will go far in science and life. Thanks for your honesty, kindness, and humor. We didn't spend as much time together as I would have wanted, but the couple of times we did were truly amazing. Thank you.

Considering lab life, I would like to thank all my comrades of the CRCA. A special thanks to Mathieu K. My god, man, you are so crazy, but in a good way. I miss you. And of course, this acknowledgement wouldn't be complete without mentioning Emily M., Charlotte D., and Mathilde L., with whom we enjoyed some crazy road trips together. Thanks for all the moments we spent combining friendship, science, and beer pong. Thank you, guys: Louis D.,

Nour S., Jordan D., Gregory L., Manon T. I guess we spent more Friday afternoons drinking and playing than conducting experiments, which we would readily admit. Finally, thanks to everyone who crossed my path and for the moments we enjoyed together, from the bar to the lab life: Ana, Flora, Fares, Matthias, Stéphane, Inès, Laure-Anne, Renaud, Benjamin, Marco, and Louise.

Finally, I would like to express my gratitude for all these years to L'AEUPS and all its members, particularly my close friends and roommates: Yanis, Theo, Dodo, Mika, Marc&Barbs, Dragon, Callu, Alex, Romy, Océane, AnneGa, and all those whom I may have forgotten, who endured all my discussions about ants, navigation, science, epistemology, and more. I especially want to thank my roommates, who served as my control sample for all my presentations and posters. Thank you for that and for all the moments we shared together. Lastly, I want to extend my heartfelt appreciation to Josephine. We have shared our lives together for more than 8 years, and you have been incredibly supportive during my thesis crisis, helping me overcome obstacles. I believe you have almost become an expert in ant navigation now. Initially, you were a bit scared of ants, but I have seen you collecting ants and gathering data in the field. I would even say that you have come to like them now. I love you. And to my beloved dogs, Kha, you are the most beautiful dogs on earth. Although you can't read, you have participated a lot during our walks, helping me clear my mind and refocus as I think out loud.

To my friend and family.

Introduction

0.1. The insect world: - and me-

"If one could conclude as to the nature of the Creator from a study of creation it would appear that God has an inordinate fondness for stars and beetles."

— J.B.S. Haldane

Insects are one of the most diverse groups on the planet, with estimates suggesting there are more than 5 to 10 (up to 30) million species (1 million currently named) [1–4], representing the major part of the total animal biomass [1,5]. Insects fulfil essential ecological tasks in their ecosystem, from pedogenesis to pollination; they are crucial for Earth -and human-survival. Arthropods are omnipresent on our planet, and have colonized all biomes, from the rainforest canopy to desert salt pans [1,2,4]. I had the opportunity to observe these omnipresent creatures -insects- in my childhood. Mainly, what's piqued my curiosity, is their robotic appearance and external armour, offering an inexhaustible source for my imagination. From observation of the dragonfly's "mechanical" precision with which they caught the small dead flies I threw at them, to the epic wars of little tanks -ants-. I used to perceive them as little machines [6] straight out of a science-fiction movie. Now I realise that such a diversity is the product of more than 400 million years of evolution -without any designer behind them-. Darwin's theory suggests that all living beings on Earth, including humans and insects, have evolved through a continuous process of adaptation and natural selection over millions of years. Therefore, it may be wise not to segregate human and insect intelligence as separate entities, but rather view them as part of the same evolutionary process [7]. As we – including insects – live in a complex environment, we are likely to face analogous problems as navigation. Insects, much like other animals, have developed similar strategies that have evolved at the phylogenetic level, and develop at the ontogenetic one. These adaptations enable them to thrive in ecological niches, via moment-to-moment adjustments based on internal and external conditions.

I have had the opportunity to observe these creatures since my childhood until now. Although the way I used to perceive them has evolved over time, my fascination, and the inspiration they provide me remains unchanged.

0.2. Why studying insect navigation: a lesson of simplicity

Foraging is one of the most ubiquitous tasks in the animal kingdom, as it is necessary for an individual's survival. In the case of central place foragers, such as social hymenopterans, the stakes are even higher because the survival of the entire colony depends on their ability. Also, central place foragers, by definition, must not only collect food but also be able to bring it back to their nest.

"Take a lesson from the ants, you lazybones. Learn from their ways and become wise! Though they have no prince or governor or ruler to make them work, they labor hard all summer, gathering food for the winter."

—Bible Proverbs 6:6-8

Fabre's [8] and Darwin's [9] who noticed the incredible and almost magical hymenopterans skills to fix a route and navigate over long distances, sparked an ever-growing interest for the study of insect navigation. These early observations were facilitated by the ubiquitous presence of insects, the ease to manipulate them, and the ability to control their experiences during their brief lifetimes, in ecologically relevant -or abstract- environments. As such, insect navigation research has been conducted across more than a century in multiple species, from dung beetles to drosophila maggots. Most importantly, these studies have focused on different questions, such as: which cues are used [10–14,14–20]; which sensory structures are involved [21–25]; how routes are developed and followed [14,26–31]; or how sensory-motor control operates in closed-loop with the environment [32–41].

In addition, insects' incredible navigation skills result from a nervous system much simpler than that of vertebrates [1]. It is precisely this -apparent- simplicity that made insect navigation a ground of interest. Their neural networks, still composed of a reasonably large number of interacting neurons, are the site of very dynamic internal activity that allows for effective coupling of the organism with its environment. Thanks to the development of neurobiological tools and modelling techniques in insects, we now have an increasingly detailed description of their neural circuits and functions [42–47,47–50], and the ability to silence, activate or record individual neurons to understand their role in sensory-motor control [48,51–56]. Regarding navigation, this ever-growing knowledge has allowed us to understand how neural

circuits enable an insect to maintain a bearing [55,57–63], what are the brain structures implicated in learning and memory [64–68], and how memories are encoded through synaptic plasticity in specific brain regions [62,63,69–75].

> *"There may be extraordinary mental activity with an extremely small absolute mass of nervous matter: thus the wonderfully diversified instincts, mental powers, and affections of ants are notorious, yet their cerebral ganglia are not so large as the quarter of a small pin's head. Under this point of view, the brain of an ant is one of the most marvellous atoms of matter in the world, perhaps more so than the brain of a man."*
>
> —Charles Darwin (1871)

Viewing insects through the belief of simplicity led scientists to seek for parsimonious explanations of their behaviour, detached from higher-level cognitive processes. The parsimonious insights stemming from this approach have proven excellent to understand the insect of navigation from early naturalistic observations to a multi-level integrative approach, providing a holistic understanding of the mechanisms[76] at both the ontogenetic and phylogenetic levels. The 'simple' mechanisms stemming from this field have also proven to be useful in understanding more complex organisms such as vertebrates [1,77–79]. Finally, this mechanistic explanations, have inspired simple algorithm of navigation that led to application in robotics [1,80–88].

0.3. Insect navigation: The navigational toolkits in the light of an integrative approach

In the mid-18th century, giants such as Darwin [9] and Fabre [8] already displaced -humble-bees and marvelled at their incredible ability to find their nest. However, they were unable to uncover the precise cues or mechanisms that underlie this prowess. On the shoulders of these giants, other experimentalists[89] soon revealed that hymenopterans derive celestial information to find back their way to their nest [90–92], as well as learn useful terrestrial visual information for their decision-making[93] and orientation [89,94–96].

The field of insect navigation has progressed from early naturalistic observations to an experimental approach, proving that insect relies on two main strategies to navigate: Path Integration (PI) involving celestial cues, and view-based navigation that relies on learnt terrestrial visual information. These two strategies, coupled with the ability to produce a systematic search when lost, have been later characterized as the insects' "navigational toolkit" [97].

0.3.1. Path integration

The first strategy, called "path integration", allows insects to return to their nest in an almost straight line after a meandering outbound trip [98]. While travelling, insects build a so-called "home-vector" by continuously estimating and integrating the direction and distance that separates them from their nest [98–100]. When motivated to home, they can then use this 'home vector' to return to the origin of their trip. Direction estimation relies on the use of allocentric information, such as celestial cues like the sun position or the pattern of polarized skylight [100,101]- which are perceived through specialized part of eyes-[22,98,102]. It is important to note that other sensory modalities also contributed to this vector navigation, such as wind [17,103,104], magnetic fields [14,105,106], the moon [107], or the Milky Way [13] as well as terrestrial cues and self-motion cues [55]. In contrast, distance estimation involves an egocentric [108] estimation, which can be achieved through optic flow -mainly in flying insects- [109,110] but also to a certain degree in ants [111,112]. In ants, what contributes the most to their distance estimation is the use of "pedometers" [25,113]. Our actual understanding of compass navigation in insects comes from a cross transfer of knowledge between many different arthropods [108,114–118] from shrimps [119] to bees, passing by dung beetles [120].

Thanks to neurobiological approaches that have been developed in parallel in several arthropod species, these multiple sources of sensory information have been shown to be integrated in a brain area called the Central Complex (CX) – a preserved structured in arthropods-[60,121,122], to build a representation of the current heading relative to the environment, [42,43,47,55,60,61,123–131]. Neurobiological works coupled with modelling efforts provided insight into how directional information is integrated into the CX, and modulates the current heading to the desired one through connections to the premotor centres [57,60,132–134]. We also understand how the central complex combines such compass information with odometric information [134] to produce a path integration home vector. Further works have shown how the central complex

circuits could enable a home vector to be memorised, and reversed, to enable ants and bees to reach a known food source from their nest [133] as observed in these insects [103,135–138].

0.3.2. Learnt visual navigation

The second navigation strategy, known as view-based navigation, involves the process of learning and recognizing visual terrestrial information [12,15,20,71,72,72,75,137,139,140,140,141,141–144,144]. During their foraging life, insects acquire knowledge about their visual surrounding: first around their nest trough stereotyped movements so-called learning walks or flights [31,40,41,145–148], to the establishment of full idiosyncratic routes [20,26–28,149–152]. This route establishment occurs even after only one or a few trials [153,154]. But what kind of visual information is encoded and memorised by insects to display learnt visual navigation is still debated. On the one hand, early works suggested that insects extract and encode so-called "landmarks" (i.e., as we humans can distinguish individual "objects"). Notably in poor visual surroundings, such as in desert salt pans or controlled lab rooms, the manipulation of landmark configurations can disrupt navigational performance [142,154–159]. On the other hand, richer environments showed that changes in local landmark configurations do not necessarily impair homing [20,160,161]. These studies showed that insects rather rely on the wide input spanning their full panoramic views [15,20,141,143,162,163], and do not need to extract individual "landmarks" as identified objects from the rest of the scenery. This theory does not only account for insect behaviour in visually rich environments but also does for the studies achieved in visually poor environments, where subtle changes, such as displacing the only objects that constitute the scene, drastically modify the panoramic scenery indeed [20,75].

In parallel, there is ever-growing work to determine the brain structures underlying visual navigation, from memory formation to retrieval [67,68,164]. Lesion experiments in a specific brain structure, the Mushroom Bodies (MB), showed that learnt view-based navigation is disrupted when this structure is silenced by pharmacological injections or physical lesion [64,165,166]. The hundreds of thousands of neurons called Kenyon Cells [65,167] that compose this structure present a random pattern of connectivity with sensory input. This connectivity actually provides a suitable substrate for the encoding of complex sensory information, including full panoramic views [62,69,71,72,75]. Also, MBs' structure undergoes drastic structural changes in synaptic circuits at the early stages of the foraging life, during and right after the first learning walks [168–171], further supporting its implication into sensory encoding. Additionally, the wide field of view

of insects and their low resolution eyes (1 to 5 degrees resolution [69,172,173]) seems to facilitate navigational performance: low resolution vision reduces the mushroom bodies "memory space" needed to encode multiple views; and filters out the high-resolution visual details that are useless for navigation while retaining information that is useful to recognise the overall scenes [62,69,143,174,175].

From the integration of knowledge about the brain and behaviour into neurobiologically plausible models, we now have a better understanding of how natural scenes are stored in the mushroom body and how this memory can be recalled to modulate motor control for route following [69,176] and homing[62,63,177], thereby enabling the capture of behavioural signatures observed in insects.

0.4. Evolutionary and ontogenetic consideration

Ultimately, by analysing the differences of related species occupying different habitats, as well as unrelated species that colonize the same ecological niche, valuable insights can be gleaned regarding the evolutionary development of sensory structures, behaviours, and brains in different environments.

"*Nothing in Biology Makes Sense Except in the Light of Evolution*"

—Theodosius Dobzhansky

Brain structures involved in navigation are largely preserved among arthropods [60,67,68,121,178]. However, it has been observed that the precision of navigation strategies based on the path integration and based on learnt views also depend on the foraging ecology, visual structure of the environment and phylogeny of the species. Thus, differences in how individuals rely on both strategies reflect the experience, environmental and ecological aspects of the studied species, allowing us to dive into evolutionary considerations. For instance, ant species, or even colonies, that live in richer visual environments are typically good visual learners, rely more on learned terrestrial cues and do not trust their PI as much as others [179–182]. Inversely, species living in visually very poor environments display more precise path integration and trust this information more: they followed their home vector for a longer distance when compared to ants living in visually rich environments [150,179,182–185].

Finally, along the foraging experience of individuals the weight between these two strategies change. With growing experience, foragers trust less their PI and rely more on learnt terrestrial information [186], showing that the weight of both strategies can be modulated along a foraging carrier. Also, even during a foraging trip weights of both strategies seem to vary according to the distance of the nest [187]. First, PI weight depends on the current vector length [188], whereas view weight depends on the current familiarity [189], suggesting an online modulation of these weights during a foraging trips. Additionally, view weight can drop with under unnatural conditions, where ants are forced to repeat a same portion of their path, thus impairing their ability of route following strategies [190,191]. Hence, weights of navigational strategies vary throughout the ant's foraging journey and along their foraging carrier.

Thus, by this comparative approach, we now get a better understanding of how the weight of these strategies is shaped by phylogenetic, ontogenetic factors, and the structure of the environments.

0.5. How simple computational modules of navigation are integrated to produce robust navigation.

Rather than acting independently, PI and view-based navigation work in synergy, each strategy compensating for the gaps of the other. While PI is prone to error accumulation with increasing distance travelled [98,192–195], view-based navigation is not. However, the latter involves learning and is thus inoperant in novel, unfamiliar situations or during the first inbound trip. As a result, newly trained foragers can reach back their nest using PI, while simultaneously visually learning the route [28]. With enough experience, the visual familiarity gains weight over the PI system, allowing for detours and enabling the ant to compensate for passive displacement within the familiar area [104]. Therefore, PI is more useful for naïve ants or unfamiliar areas [186], while view-based navigation overpowers PI in experienced foragers on well-known ground [26,140,196,197]. Interestingly, evidence suggests that ants use both strategies simultaneously and in a weighted manner, with the weight varying instead of the strategies being turned on or off. This optimal balanced use of the two strategies provides ants with remarkable behavioural flexibility. Thus, both strategies seem to be weighted optimally [140,188,189,197].

The weighting between the two strategies suggests that there is an interaction between different brain areas, but the nature of this interaction remains unclear. Specifically, it is unclear whether this interaction occurs upstream of the motor controls, indicating a segregation of brain function, or if the integration occurs within the same brain structures that are involved in both strategies. Complicating matters, it is not possible to define brain regions based solely on their involvement in specific behavioural functions, as different behaviours can involve the same brain structures, and a single behaviour can involve multiple brain regions[198,199]. Regarding navigation, recent studies have emphasized that CX is not solely involved in the generation of PI but is also involved in various other behaviours, including navigation using terrestrial cues by working together with the MB. For instance, lesions of the CX impair learnt visual navigation [200,201]. Additionally, during visual-only navigation -without involvement of the PI- mirroring the apparent position of the sun by 180 degrees results in a temporary reorientation of the ant's path [63]. This suggests that information from learnt views rather than directly used to control motor command rather acts in two-step, recognition of the visual scene in the MB produces a signal that is sent to the central complex, which in turn controls guidance (based on terrestrial info) using compass cues. Further emphasized by combination of anatomical, experimental, and modelling approaches has shown that this integration occurs in the CX, where mushroom body (MB) signals update the desired heading [60,63,68,200,202–205].

Controlling guidance by integrating information into the CX provides a great advantage. Indeed, visual recognition was thought to be rather egocentric and therefore can't allowed for guidance and recognition if the body orientation is not precisely oriented as during learning. Recent models' have emphasized that guidance based on the PI can be decoupled from the body orientation [122,134]. Therefore, updating a heading based on visual memory in the central complex also enables to follow routes independently of the actual body orientation, as noticed during backward navigation [206]. However, the CX acting as a bottleneck for navigational strategies is not the exclusive way to modulate motor control, as premotor areas are also connected with various brain regions such as the MB or the visual lobes in a way that bypasses the CX [50]. These diversities of pathways emphasize that various brain regions are working in parallel and synergy to control behaviour [140,188,189,207,208].

0.6. Insect navigation: is there something else to learn?

0.6.1. Ants: a fertile ground for studying navigation

Among Hymenopterans, one order is particularly interesting and easy to study: ants. They display sophisticated and robust navigation, they walk rather than fly and can thus be easily followed even in the field, and finally, they can be found in a wide range of ecological niches, from desert salt-pans to pristine rainforest, allowing inter- and intra-specifics comparisons [181]. But what mainly amazed me at first when working in this field is the ease with which one can manipulate them, from individually marking (painting) to designing colony-sized experimental apparatuses. With some simple wood planks and plastic, it is possible to quickly purpose-build setups in the wild within which the ants will navigate. While tracking their movements using pen and paper to technology-based precise recordings of their motor behaviour using a multidirectional treadmill (trackball) while controlling their visual sensory information, sometimes throughout their whole lifetime, [141,150,209–212] thus providing a powerful system to investigate the mechanisms underlying navigation in the wild.

0.6.2. Science: a continuous process

Overall, the brain structure of insects benefits from transfer of knowledge of ever-growing works among arthropods, providing a dwelling ground to tackle neural correlates that underpin -ants'- navigation through an integrative approach. Insect -ant- navigation is a mix between innate and learnt behaviour enabling a robust outcome. Our understanding of the mechanisms, from sensory structures to the brain, has been shaped by centuries of experimentation, and more recent successful integrations of multilevel approaches, such as notably neurobiology and modelling. This draws a good picture of how ants might use full panoramic views to navigate in complex and ecologically relevant situations. But thankfully,

science often leads to more mysteries as we answer questions. Therefore, there is always something else to learn.

First, when new behaviours are unearthed, they are sometimes not accounted by current models and even challenge them, thus require a novel effort to explain these new results in the light of the brain circuitry. For instance, there is yet no satisfying mechanistic explanation for the fact that ants displaced off route are attracted to their route. Models that align with our understanding of the brain circuitry propose a different outcome, and efforts to elucidate this phenomenon result in models that deviate from the biological relevance of the brain. Also, it was previously believed that memory in ants is independent of the temporality of views along their route. However, recent studies suggest that memory retrieval may also have a temporal component, as disturbing the sequence of views during homing can trigger a scanning behaviour that ants typically display when they are lost [213]. Here again, current models do not consider these new results. This suggests that the field of insect navigation still has some beautiful days ahead to understand how views are encoded according to temporality, the lateralization in the brain, and how the brain integrates them with other sources of information. How exactly do the MB encode views and how their input is integrated into the CX is still unclear. [60,68,202].

0.7. Questions I asked during my thesis: outline

As just explained, there is ever-growing work to do on how memories are encoded in both their temporal and spatial aspects. During my first day on the field in 2017 and my first years as a PhD student, I worked on visual memory retrieval and how ants could follow a route, leading me to tackle ant navigation at different levels from motor control to how ants route learning is orchestrated in this thesis. Notably, I tackled three main questions that form the 3 chapters of my thesis:

1 – How is learning orchestrated in the first place?

The primary and most extensively researched mechanism of learning and recalling memories is based on the delivery of rewards and punishments, and it has been studied mainly

in laboratory settings, particularly for the sense of smell [214–217]. Here, classical paradigms of associative learning coupled with neurobiological approaches have given a good understanding of how insects learn, and which mechanism are involved [214–217]. Although this comprehension did help to improve models for visual navigation [68], our understanding of how the learning process occurs in the navigational task is still limited. Considering the reward/punishment paradigm, it is possible that running down the PI or reaching the nest act as rewards for learning. However, our current knowledge has reached a standstill regarding how learning is facilitated by PI [28,29]. The principles that govern spatial learning are unclear, and it seems unlikely that the learning of a route is solely guided by reward and punishment as in associative learning.

Here, I ask whether ants require distinct rewards to learn, or, alternatively, if they can learn continuously. In addition, I asked whether spatial learning in these ants relies on a map-like representation as in vertebrates. This will allow us to shed light on a much-debated issue of whether insects indeed create a complex representation of space [218–223].

Specifically, I investigated how ants orchestrate learning by recording the paths of desert ants *Catagliphys velox* in their natural habitat. Through the combination of experimental data, detailed path analysis, and modelling, I revealed that ants learn continuously. However, the learning mechanisms we highlighted seem rigid: ants could not solve straightforward navigation tasks even when the goal was visible. Overall, our results suggest that ants rely on egocentric visual memories instead of building a representation of the space around them, as would vertebrates do. This chapter is intended to be submitted in the coming month.

2 – How does basal-level motor control carry higher-level strategies?

The majority of studies on animal navigation have focused on higher level strategies such as the use of Path Integration, the recognition of learnt visual cues and the reconstruction of so-called cognitive maps, with little exploration of the role that lower-level motor behaviours may play in supporting these strategies. One good and widespread example of basal motor control is lateral oscillations between left and right along the trajectory. Oscillations are displayed by various taxa from vertebrates [224,225] to invertebrates [51,226–229] and may have an important role in fine-tuning navigational decisions. Oscillations are closely linked with perceptual cues [228] such as olfaction, auditory and visual modality tasks such as route-following. This coupling appears to involve a brain structure that is highly conserved in

arthropods, the Lateral Accessory Lobes (LAL) [50]. This brain region upstream to thoracic motor ganglia presents an internal connectivity well-suited to triggering oscillations [50,53,209,227,228]. In addition, the LAL is connected with other brain regions, providing a substrate to integrate sensory information and adjust oscillations-based behaviours.

However, it is currently unclear whether lateral oscillations are generated internally and what is their precise role for visual navigation.

Using state-of-the-art multidirectional treadmills, we examined the motor output of two ant species, *Myrmecia crosslandi* and *Iridomyrmex purpureus*, in their natural environment. The results revealed a finely tuned oscillatory movement dynamic that optimizes information sampling and distance covered. This dynamic is produced internally but modulated by learnt and innate visual information. It is conserved across distant ant species and navigational contexts, suggesting an ancestral movement strategy based on the lateral accessory lobes. We showed that a simple neural model of this brain circuit indeed reproduced the observed movement dynamics, linking our findings about oscillations and vision to oscillations displayed in other context in other insect species, and shedding light on the evolutionary pathway of visual navigation in hymenopterans. This chapter has been published in Current Biology.

3 – How can we access the Umwelts -self world- of insects?

It is known that ants can memorize visual information, but it is unclear which features are crucial for their perception of a navigable panorama. Insects' visual system extracts various types of information from their environment. For example, lab experiments have demonstrated that insects, such as ants, can derive information about the centre of mass of visual cues [162,230–233], extract information about boundaries/edges [16,56,234,235], or relative brightness and colour [230,231]. Also, ants rely on global cues like the skyline (which refers to the boundary line where terrestrial structures meet the sky). The mere presence of this visual feature is enough to facilitate navigation for insects [12,15,208,236,237]. Additionally, some insects can also use dynamic cues, such as translational and rotational optic flow, for guidance. It is however currently unclear how this particular feature contributes to the visual perception of a natural scene.

This study delved into the visual perception of a panorama for an ant - their Umwelt world. Virtual reality setups were used to precisely record the movements of *Cataglyphis velox*

while being able to fully manipulate the visual scene perceived by the animal. The study aimed to understand what visual cues would be sufficient to trigger navigational behaviour in ants. The findings revealed that, although not exclusively, ants rely on edge orientations to interpret a visual scenery as something worth exploring. The findings have implications for memory formation and representations of insect's world, which can improve our understanding of how they navigate and interact with their environments. This chapter is intended to be submitted in the coming month.

4-General discussion.

After these three chapters, I discuss how this approach allowed me to bring together different aspects of navigation, from ancestral motor components to representations of space. I will also focus on how apparently simple mechanisms can lead to a wide range of behaviours, where complexity emerges from simplicity. Notably, emphasizing how complex behaviour emerges from the interaction between simple computational modules. Finally, I will discuss how the various approaches I employed - some successful, some failing - both improved my vision of how I should ask and answer a scientific question.

Appendix I: the formatted publication of chapter II.

- **Clement L, Schwarz S, Wystrach A.** (2023). An intrinsic oscillator underlies visual navigation in ants. *Current Biology* **33**:411-422.e5. doi:10.1016/j.cub.2022.11.059

Appendix II: Other formatted publication which I contributed.

- **Haalck L, Mangan M, Wystrach A, Clement L, Webb B, Risse B.** (2023). CATER: Combined Animal Tracking & Environment Reconstruction. *SCIENCE ADVANCES*.
- **Schwarz S, Clement L, Gkanias E, Wystrach A.** (2020). How do backward-walking ants (Cataglyphis velox) cope with navigational uncertainty? *Animal Behaviour* **164**:133–142. doi:10.1016/j.anbehav.2020.04.006

- **Schwarz S, Clement L, Haalck L, Risse B, Wystrach A.** (2023). Compensation to visual impairments and behavioral plasticity in navigating ants (preprint). Animal Behavior and Cognition. doi:10.1101/2023.02.20.529227

- **Wystrach A, Le Moël F, Clement L, Schwarz S. (2020).** A lateralised design for the interaction of visual memories and heading representations in navigating ants (preprint). Animal Behavior and Cognition. doi:10.1101/2020.08.13.249193

Chapter I

Latent learning without map-like representation of space in navigating ants

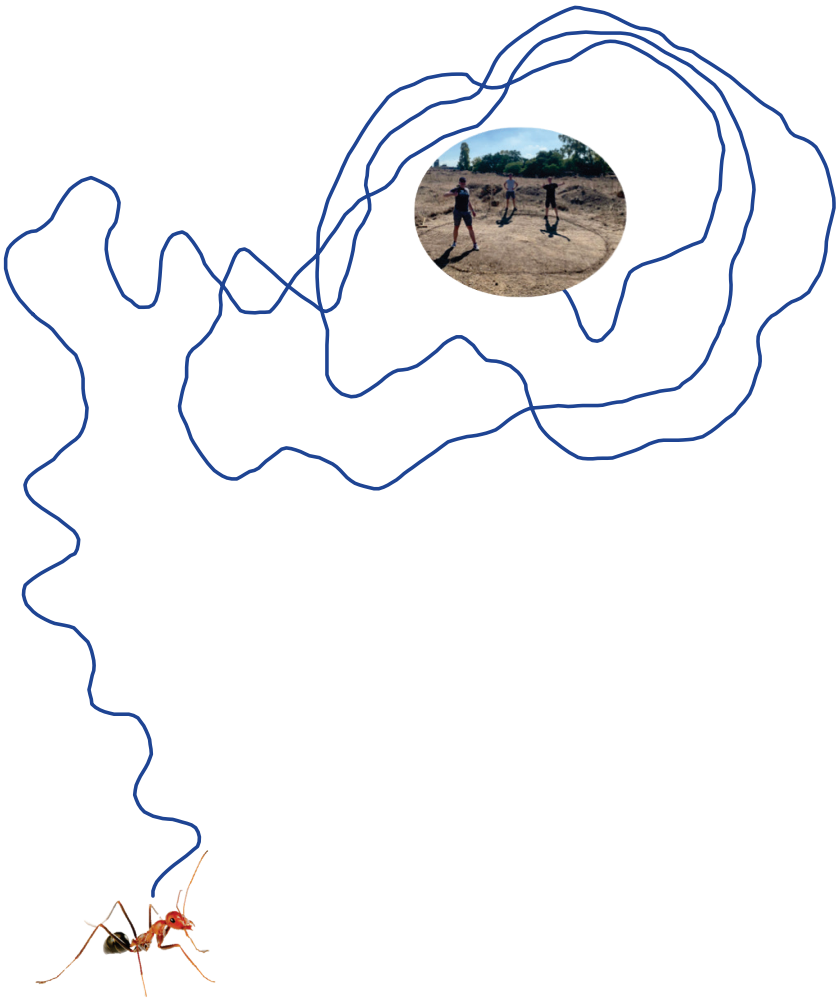

Latent learning without map-like representation of space in navigating ants

Leo Clement*, Sebastian Schwarz and Antoine Wystrach

Centre de Recherches sur la Cognition Animale, CNRS, Université Paul Sabatier, Toulouse 31062 cedex 09, France

Abstract

Desert ants are excellent navigators. Each individual learns long foraging routes meandering between scattered trees and bushes in their natural habitat. It is well-known how the insect memorizes and recognizes views, and how this recognition enables them to find their way. However, next to nothing is known about how spatial learning is orchestrated in the first place. Here we recorded the paths of desert ants navigating in their natural habitat under various displacement conditions. We demonstrate that ants do learn *continuously* the routes they travel, even if these routes are meandering and do not lead to a place of interest: a concept so-called 'latent learning'. Our results also unveil the online mechanism by which ants ignore or recall 'latent memories' as they are being built. A simple model shows that this mechanism can be implemented in the insect's Mushroom bodies brain area through the continuous formation and dynamic interaction between two parallel route-memories. This mechanism captures present and past evidence, as well as the failure of ants to solve simple artificial navigation tasks – even with a rewarded goal being clearly visible. These failures reveal that navigating ants relied on egocentric route memories rather than a map-like representation of the surrounding space.

Introduction

Navigation is a complex task solved by many animals. During spatial learnings, individuals need to acquire spatial knowledge to be able to return to – or avoid – some specific locations. In some instances, spatial learning fits with the more general learning theory, where learning is dependent on a reward or punishment (the unconditioned stimulus US) that happens concomitantly with the stimulus to learn (the conditioned stimulus CS). That way, insects and vertebrates associate a specific location (CS) with a feeding site (US reward,[221,238,239]) or a negative event to be avoided (US punishment [74,240,241]).

However, such discrete rewarding or punishing events only occur sporadically along the path of a navigator. Most of the time, navigation is a reward-less continuous task and animals can learn long routes and the space around them despite the lack of an apparent reward [242], a feat so-called latent learning [243–245]. Latent learning has been mostly demonstrated in vertebrates and is typically assumed to involve – or be associated with – the continuous reconstruction of a map-like representation of space [246], which requires the interaction between path integration and the learning of visual scenes [247–250]. As for vertebrates, insect navigators such as ants and bees are known to rely on both path integration (PI), and the learning of visual scenes [98,99,137,139–141,251–253]. But whether they require distinct rewards or learn continuously is unclear, and whether they form map-like representations is much debated [218–223]. Here, we investigated those questions through a series of manipulations with Iberian desert ants (*Cataglyphis velox*) navigating in their natural habitat. Our results demonstrate that they do learn continuously the route they travel without the need of any reward. Ants use a sophisticated online mechanism (i.e., running continuously) to recall their 'latent memories', but do not use a map-like representation of the space around them.

Results

One trial is sufficient to learn a route

We first investigated whether ants would memorize a route encountered only once in a distant unfamiliar test field. To do so, ants trained to a 7.0 m familiar route were captured at the feeder just before starting their homing journey and released on a distant unfamiliar test field (Fig. 4). These foragers are called full vector (FV) ants as they possess a path integrator (PI) homing vector, pointing to the feeder-to-nest compass direction. Unsurprisingly, when released at the centre of the test field, these FV ants followed their PI vector direction (Rayleigh test with PI as theoretical direction p: FV< 0.001; Fig.1 A, third row). Upon reaching the rim of the test field (3.0 m) the ants were captured again and released directly inside their nest (N) (Figure 1 A first column). On their subsequent exit of the nest, the same individuals were free to run to the feeder and back along their familiar route. This time, those foragers were caught just before entering their nest and released for the second time on the distant test field. These ants are so-called zero-vector (ZV) ants because they have already run out their PI homing vector, therefore they can only rely on visual memory to guide their path [27,254]. Surprisingly, ZV ants released on the test field followed the same direction as during their first trial as FV ants (Rayleigh test with PI as theoretical direction p: FV< 0.01; Figure 1A, first column), showing that they relied on memories, built during the first trial. To investigate if ants have learned a route rather than a general direction of travel, we compared the shape of the paths displayed on the test field using dynamic time warping analysis (DTW). Between the first training trial (FV) and subsequent test trial (ZV), paths shapes were more similar within individuals than between individuals (Figure 1A, last row, $W = 11$, $p < 0.05$), showing that one trial was sufficient for ants to learn an idiosyncratic route.

Learning a route needs no reward

In the previous experiment, ants were released inside their nest right after their first trial on the test field. We hypothesized that entering the nest may constitute a reward for the ants to consolidate memories of the route they just had experienced before entering the nest.

To test for this hypothesis, we replicated the experiment but, this time, ants were prevented to enter their nest. After their first trial as FV ants on the test field, foragers were released either on their familiar route (Figure 1A, second column, F) or in another distant unfamiliar location (Figure 1A, third column, U). In both cases, the ants were free to run off their PI vector before they were captured again (as ZV ants) and released on the test field for the second trial. Here again, the paths of these ZV ants resembled mostly their previous FV paths (Figure 1A, last row, $p< 0.01$), demonstrating that they had learned an idiosyncratic route. Thus, ants memorize a route in a single trial and subsequently recall it regardless of whether they have experienced the nest, a familiar or unfamiliar terrain in between.

Learning a route needs no path integration vector

We next wondered whether route-learning occurred because ants were running down their PI home vector (feeder-to-nest compass direction) during the first trial. Indeed, running down the home vector indicates to the ant that she is moving toward the nest direction and thus might act as a reward signal for learning the current route [29].

To test for this hypothesis, we captured ZV ants (near their nest and thus deprived of PI homing vector) and released them on the test field for their first trial. As expected, these ZV ants (Figure 1B) displayed a typical search path [30,255–257]. on the test field, meandering in all directions, and walking in average 21.5 m (sd = 9.5 m) before reaching the rim of the test field (3.0 m radius from the release point) Once the foragers had reached the rim, they were captured and subjected to one of the two following experimental groups: either they were released inside their nest (Fig. 1B, first column, N) or released for ~30s in another unfamiliar terrain (Fig. 1B second column, U). Once released for the second time on the test field, ants of both groups showed a strong idiosyncrasy by reproducing characteristic signatures of their own previous meandering path (ps < 0.05, Fig. 1B, last row). Consequently, even without running down their PI vector, ants had memorized their previous meandering search and used this memory to guide their subsequent trip. What more, they did so even if their previous trial lead to nowhere but another unfamiliar location.

Overall, we are left with the conclusion that ants navigating in unfamiliar areas continuously learn the route they are travelling and subsequently recognize and recall these memories to guide their path, even in the absence of any sort of external or functional reward.

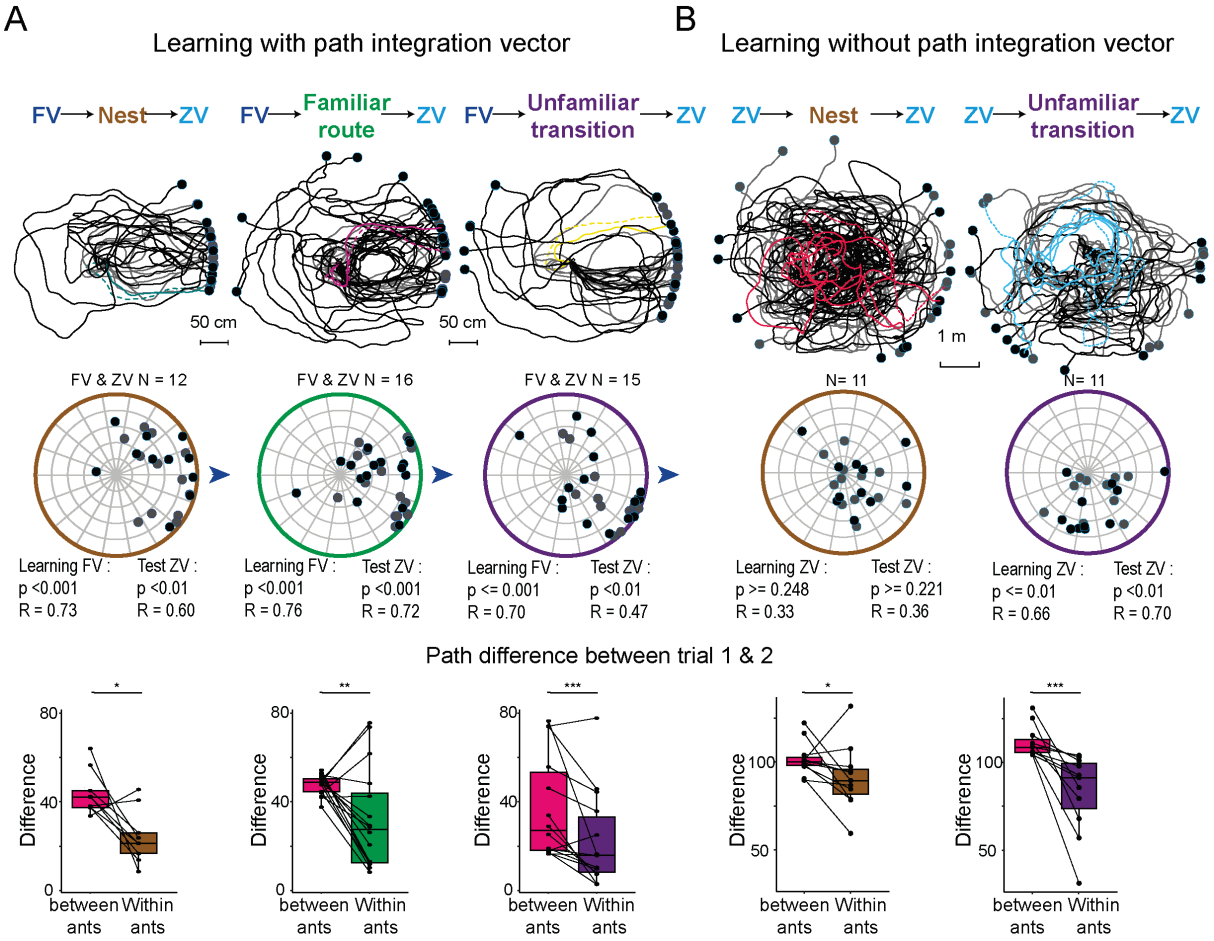

Figure 1. Ants learn and recall their route even if it leads to nowhere. Trajectories of *C. velox* ants recorded on the test field. For their first trials ants were released as full-vector (A) or zero-vector (B) at the centre of the test field. Ants were then released either in their nest (brown), on their familiar route (green) or on another unfamiliar terrain (purple) and captured again as ZV ants. For their second trial, these ZV ants were released again at the centre of the test field. The first row shows the training path (grey) and test path (black). Within each condition, an example-coloured path has been emphasized for the training (dashed) and test (solid) path. The colour of the path corresponds to the ant identity. The second row is a circular plot showing the average circular vector calculated over a portion of the path during the first trial (grey) and the test (black). Each dot is the mean direction taken and the mean resultant vector (i.e., a point closer to the periphery indicates straighter paths). The third row shows the results of the similarity analysis (DTW). This analysis was made between the first and second trial (see methods). Each ant's path has been cut into segments of 2.4 m and each segment has been compared with the closest neighbour segment of the subsequent trial to estimate their similarity. We did this analysis by comparing two trials of same ants (within ants, right boxplot) or between ants (left boxplot).

Ants recall memories of the previous, but not the current, trial

We reasoned that if learning is continuous, the memories currently formed should not be recalled instantaneously. Otherwise, the ant would not be able to distinguish what is familiar and what is not.

To test for this, we focused on the search patterns displayed by ZV ants on the test field. The first and second trial on the test field had very different characteristics. During their first trials, ants displayed a typical systematic search: exploring novel areas as they go (Figure 2A, B, first column, third row; grey path). Contrastingly, on their second trials, ants tended to explore less areas (Fig. 2A, B first column; exploration index between path 1 and 2: p-value: Nest < 0.01, Unfamiliar > 0.05) and walked along portions of the route they had already travelled, sometimes getting stuck while running along the same portion multiple times (Fig. 2A, B black paths, Fig. S1A, B). The paths during the second trials showed more overlapping portions than the first trial did (Fig. 2 A, B second column; DWT ($N = 11$, $T = 3$, ps < 0.05). As mentioned earlier, individual paths during the second trials resembled more their own previous trials (Figure 1B). Together, this confirms that the route memories acquired during the first trial were not recalled during the first trials but during the second trials. In other words, during the first trials, ants were performing a systematic search (as they typically do in unfamiliar areas); and during the second trials, ants were following the route they had learnt in the first trial, even though this route sometimes led them to turn into circles (Fig. 2A, B black paths, Figure S1A, B).

Recall is triggered when ants experience a discrete change of viewpoint

We next wondered what mechanisms trigger the recall of route memories. In our experimental manipulation, something happened between trial 1 and 2 that led to the recall of the memories acquired during trial 1. It could be the fact that the ants were released in another location (either their nest or another unfamiliar terrain) and thus experienced a discrete change of view in between both trials (hypothesis 1) or the fact that ants spent time (~60s) in the catching vial between both trials (hypothesis 2). To test for these two non-mutually exclusive hypotheses, we performed the following experiment. We captured a new cohort of ants as they exited their nest (ZV ants), gave them a cookie to trigger homing motivation and released them at the centre of the test field for the first time. As expected, these ants displayed a tight systematic search at

the centre of the test field (Fig. 2 C trial 1). If, during their exploration, ants would venture further away than 1.8 m and then return to the centre of the test field, they were captured again (at the centre) and kept for 60s in the vial. From there we created two experimental groups: some ants were released at a different location in the test field and thus experienced a discrete change and a novel viewpoint (group 1), while the others were released again in the centre of the test field, that is, where they had just been caught, and thus spent time in the vial but experienced no discrete change in view point (group 2). As in trial 1, ants of both groups were free to explore and were captured again if reaching the centre of the test field. After sixth trials of this regime, ants were recorded while exploring the test field without interference.

Remarkably, ants of group 1, who were released at a novel location and had experienced discrete changes of views between catch and release, concentrated their path densely at the centre of the test field (Figure 2E; mean distance from the centre: group1 vs group2 one-tail test = $p < 0.001$). This is what is expected if ants are recalling their memories of the previous trials, which were concentrated at the centre of the test field from the first trial onwards. Remarkably, this strong attraction to the centre is visible from trial 2 onwards (Figure 2C, trial 2-5) and confirms that ants are recalling memories rather than pursuing a systematic search (Figure 2D, F; exploration index: group1 vs group2 one-tail test = $p < 0.05$).

Inversely, ants from group 2, who were systematically caught and released at the centre of the test field, and thus did not experience a discreet change of view, searched mostly around the peripheries of the test field (Fig. 2D, E). This is what is expected if ants are not recalling their memories of the previous trials but instead simply pursuing their systematic search, which is indeed expected to expand toward the periphery with time[30,255]. Together, this demonstrates that spending time in a vial does not trigger the recall of the previously formed route memories; however, experiencing a discrete change of location, and thus novel views does. Perhaps counter-intuitively, this makes functional sense. By doing so, the ants are safeguarded against the risk of recognizing the currently experienced route as familiar when it is not. Instead, novel routes experiences will always be treated as unfamiliar while being explored as no discrete change of views occurs, enabling other mechanisms, that are adapted to unfamiliar environments (such as path integration or a systematic search) to control guidance. A discrete change of view ensures that the ant is no longer perceiving the previously learnt route (or route section), thus the inhibition of the recall of these memories can be safely lifted.

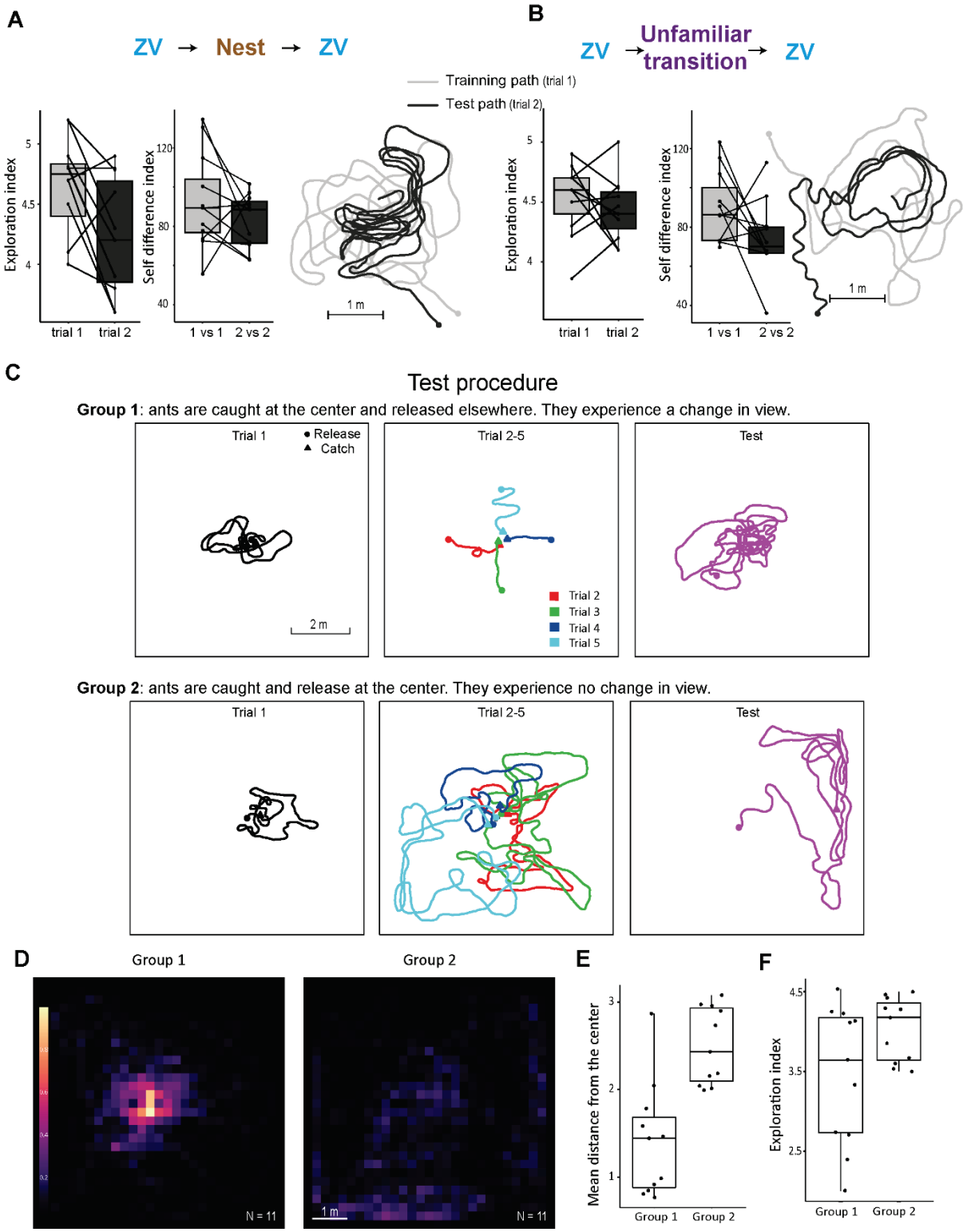

Figure 2. A discrete change in view triggers memory recall. (A, B) Path analysis for both visual transitions conditions. Exploration index: the first 10 m of the path are discretized into an X/Y matrix with a resolution of 25 cm. The exploration index is then calculated by dividing the number of explored cells divided by the length of the path. Self-difference index indicates how much ants tended to repeat signatures of their current path. Each ant's path has been cut into segments of 2.4 m and each segment has been compared with the closest neighbour segment to estimate their similarity (DTW, see method). For each ant, we used the median score of all its route segments. Example paths showing that ants tend to explore during trial 1

(grey) but repeat their route segment guided by visual memory during the subsequent trial (black). (C) Example paths illustrating the test procedure. For the first trial, ZV ants are released and captured at the centre of the test field. For the next four trials, ants were captured at the centre, and either systematically released at a different location (group 1) or at the centre again (group 2). During tests (the sixth trial) ants are recorded without interference. (D) Density heat map at the population scale of the ants' position during the test for group 1 and 2. The density maps have been done on the first 28 m walked of each ant. More examples of paths are presented in Figure S1C. (E) Distribution of the mean distance from the centre reached during the test. (F) Distribution of exploration index, the first 28 m of the path have been discretized into an X/Y matrix with a resolution of 25 cm. The exploration index is then calculated by dividing the number of explored cells divided by the length of the path.

Neural implementation of latent memories and recall.

We investigated how the observed dynamic of learning and recall could be implemented in the insects' neural circuit using a modelling approach. Route memories, which are mainly visual in solitary foraging ant species [26,142,143,150,151,153,222,258] are stored in a brain area called the mushroom bodies (MB) [64,68,165]. Each perceived view triggers the sparse activation of a unique set of MB Kenyon's cells (KC) and learning occurs through the modulation of the output synapses of these KC's to MB output neurons (MBON) [68,69]. As a result, MBON activity provides information about the familiarity of the current view. Insects possess multiple MBONs mediating parallel memory banks with different proprieties [259,260], such as: short vs. long-lasting memories [66,261–263]; 'views of the way out' vs. 'views for homing' [62,68], or in the context of olfaction, odours associated with sugar vs. odours associated with punishment [264–268]. The recall of memories is then usually controlled by a complex system of local (between MBONs) and external modulations of the MBONs, typically conveying information of the animal's current state and needs [68,264,269–271].

Based on this type of connectivity, we present here a simple circuit that explains the surprising dynamic of visual learning and recalling in ants, while strictly respecting known features of the interactions between different MBONs. Our model assumes that:

1- A long-lasting 'persistent memory' (PM) and a short-lasting 'transient memory' (TM) of the route experienced are continuously built in parallels in different MB lobes compartments and thus conveyed by different MBONs (as observed in [66,261–263]).

2- The MBON conveying the PM controls steering behaviour [62,63,69], and the MBON conveying the TM inhibits the expression of this control through direct lateral inhibition [264,272] onto the PM MBON (Fig. 3A).

3- The TM memory is reset if the ant enters its nest, or if a discrete change of location with a novel view is experienced. The reset can occur by having the input synapses of the TM MBON switched to default again (as in [259,269]). Information about such a 'novel discrete change of view' can be obtained by having the TM MBON activity itself (which would indicate strong unfamiliarity only given a discrete change towards a view that hasn't been experienced during the current trial) providing (direct or indirect) modulatory feedback on its own input synapses. More likely, this could be implemented as a third party MBON, acting as 'novelty detectors' that send a lateral connection to modulate the TM MBON input synapses (as in [73]).

As a proof of concept, we implemented this circuit in a navigating agent. The agent is guided by 3 forces (on which noise is added): 1-path integration, that tends to make it walk towards the ZV point; 2- Inertia, that tends to make it carry on straight; 3- current visual familiarity, as given by the output activity of the PM MBON (resulting from the circuit described above, Figure 3A) for the current location and heading. Indeed, visual recognition in ants is rotationally dependent [206]. This vector tends to make the agent turn in the most familiar direction at this location (as shown in [63]). The driving force of the current visual familiarity gains weight as a function of the PM MBON activity itself [189,197], so that a strong familiarity yields the agent to pursue almost perfectly along its route direction, while a weak familiarity lets path integration and noise take more control over the behaviour.

Despite continuous learning, this model explains the absence of memory recall in a novel environment. This is because during the first trial in a novel environment, both TM and PM are building memories in parallel (Figure 3A). Any views that have already been experienced (for instance when performing a loop) is simultaneously 'recognized' by both memories, that is, it triggers the equivalent activity in both PM and TM pathways. The signal of the TM MBON matches and thus suppresses the activity of the PM MBON which therefore does not influence behaviour. In other words, the route memories of the current trial are not recalled and do not impact the behaviour, letting instead path integration and noise having full control over the agent's movements: a search pattern would naturally emerge. During the second trial, however, the transition (in the nest or in unfamiliar terrain for real ants) resets the TM, which therefore, no longer inhibits the visual familiarity signals of the PM, enabling the recall of the previous

trial route memories. As a result, when the agent is on a portion of its route effected during trial 1, views are recognized, and the non-inhibited PM pathway leads the agent to carry on and recapitulate its previous trajectory (Fig 3A, S3A).

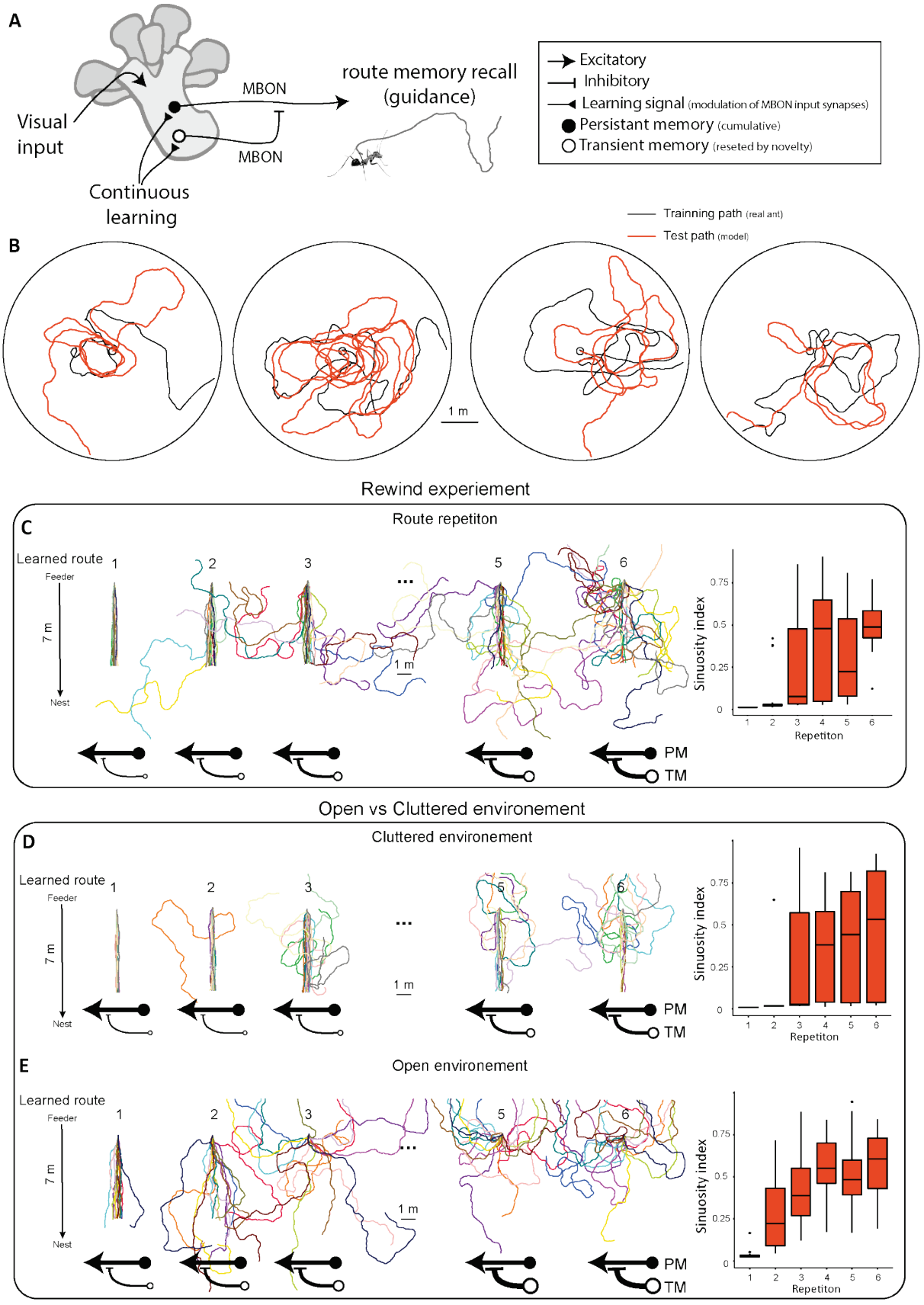

Figure 3. A simple circuit captures the dynamic of route memories in ants. (A) Scheme of the model. Model with a continuous build of two memory banks (persistent long-lasting memory (PM) and a transient short-lasting memory (TM) that inhibit each other. (B) Example paths of test (trail 2, orange). The model has been trained once on real data (black path) and then we simulated 10 replicas of the test trails (orange) guided by memory bank acquired during training, we selected parameters to prevent the model to being more efficient in route following than our real ants (Figure S3). (C-E) Reproduction of the experiment made by Wystrach et al., 2020[191]. First 20 ant agents are trained 50 times to establish a route between the feeder and the nest located 7.0 m away. During training, ants navigate with a home vector and progressively update their memory banks. Under each path, the thickness of the black arrow corresponds to the relative strength of the TM. While the thickness of flat head arrow is relative to the strength of the TM. (C) Test the effect of repetition of route on route following. After 6 repletion the path meander away significantly (sinuosity index trial 1 vs 6, N= 20: V = 210, $p<0.001$). (D, E) Test the effect of the structure of the panorama: cluttered (D) and open (E). (C-E) Boxplot shows the distribution of sinuosity according to the repletion.

Interestingly, this model captures further puzzling evidence from the current and previous works in ants, even-though it was not designed for it. First, it explains why ants during their trial 2 repeat portions of their first trials multiple times but never stay stuck turning in a loop and eventually ignore their route and reach the border of the test field (Figure 3B, S3A, C). This is because, as the agent navigates its second trial, the TM is building up again and eventually catches up with the PM if a route segment is being repeated. In other words, as the agent repeats a route portion, the inhibition of TM on PM yields it to increasingly ignore the repeated segments and therefore no longer recapitulate them. This property turns out to be vital to prevent the agent getting stuck in an infinite loop and captures the wide variation observed across individuals in our experiment (Figure 3B, S3A). Second, the model captures the evidence from previous work that ants forced to repeat a route segment several times consecutively eventually stop following the route and increasingly meander away (Figure 3C)[190,191] . Indeed, as the agent repeats its route segment, the TM memories build up and increasingly inhibit the PM (Figure 3C). Third, and perhaps most impressive, our model captures the fact that this disruption of route-following through repetition occurs more quickly in a visually open environment than in a cluttered environment (with added proximal objects on the side of the route)[74] (Figure 3D, E). This is because views change slower with displacement in an open environment, and therefore, this longer lasting exposition to the same views (repeated activation of the same KCs) leads the PM memory to build up and thus inhibit the TM memory more quickly (Figure 3D, E).

Discussion

We demonstrated that *Cataglyphis velox* ants navigating in their natural habitat memorize a route in a single trial without reward and independent of their path integration state. Foragers subsequently recall these route memories regardless of whether they have experienced the nest, a familiar or unfamiliar terrain in between. Such continuous learning, occurring in the absence of any external or functional reward, echoes the so-called 'latent learning' observed in vertebrates spatial learning [243–245] and demonstrates that the smaller brain size of insects is capable to continuously store visual information (see [273], for an example of how neurons can store such info).

In the vertebrate literature, latent learning is often associated with the reconstruction of map-like representation of space [246]. However, our results highlight a profound difference of the representation of space between ants and vertebrates. Whereas vertebrates spontaneously optimize their paths between a start and a goal location – a signature of map-like representation [274–277]–, ants did not (Figure S2). ZV ants released – up to ten consecutive times – at the centre of a 3.0 m radius open field with ample visual information did not learn to simply walk to the periphery, where they would systematically be transferred to their nest (Figure 2A, S1, S2). Instead, they follow their route memories even when it led them to walk into circles on the test field (Figure 2A, B, S1; see also [278,279]), with no improvement over trials (Figure S2) and despite the fact that the goal was in plain sight. This aberrant, non-functional behaviour seems impossible to conciliate with the idea that ants build a unified representation of the space around them. Instead, it reveals the heuristics that are at play: homing ants continuously learn to associate the egocentric visual scenery perceived to the motor command performed, even if the movements effected leads to nowhere. In natural conditions, this heuristic is perfectly functional as path integration ensures that the early motor command effected leads the naïve insect to its nest, thus acting as a scaffold to guide visual learning of route that do lead to the goal [28,153].

Previous studies have suggested that hymenopterans – such as ants or bees – could build a map-like representation by using their PI system to associate visual information to actual locations in space [248,250], although this is much debated [137,196,218–223]. If this was the case, ants should not remember two different visual scenes for a same PI coordinate, as this would create a conflict when attempting to build a map-like representation. Our result show that ants released

on the test field had no difficulties to learn and recall a new route (Figure 1A), as well as to recall their usual foraging route along their actual nest – even though these two distinct routes correspond to same path integration coordinates. Thus, further suggests that path integration and visual memories in ants are not integrated into a unified representation of space [196].

Finally, while it is unclear how a map-like representation could be implemented in the light of our knowledge of insect neural circuits [45,166,170,280], the latter explains well how a wide variety of the behaviours observed can emerge without building such a unified representation of space[60,63,68,69,69,76,133,281]. Here, we showed that the complex dynamic of visual latent learning and recall can simply result from an interaction between the expression of two memory banks in the Mushroom bodies (Figure 3). The different temporal dynamics of these memory banks ensure that route memories are not recalled inappropriately, and most importantly, safeguard the insect of being stuck walking along a loop infinitely, a risk that exists only if using egocentric route-following heuristics indeed. How such a memory dynamic is actually implemented, whether it has evolved for this navigational reason, or whether it is equally present in other context of insect learning involving interaction across the MB lobes [263,264,272], remains to be seen.

Methodology

Study Animal & Experimental site

All experiments took place within an open semi-arid landscape near Seville (Spain) from Sep. to Oct. 2021. We had the opportunity to work with the thermophilic ant *Cataglyphis velox.* Foragers, rather than using pheromone, are known to navigate solitarily relying mainly on learnt terrestrial visual cues and path integration (PI). For the main experiments, four nests have been located and used within an area of about 200 square meters. Each nest has been enclosed in a corridor (7.0 × 1.5 m), with a feeder placed 7.0 m away from the nest and foragers were free to familiarize themselves with the route for 24h before being tested.

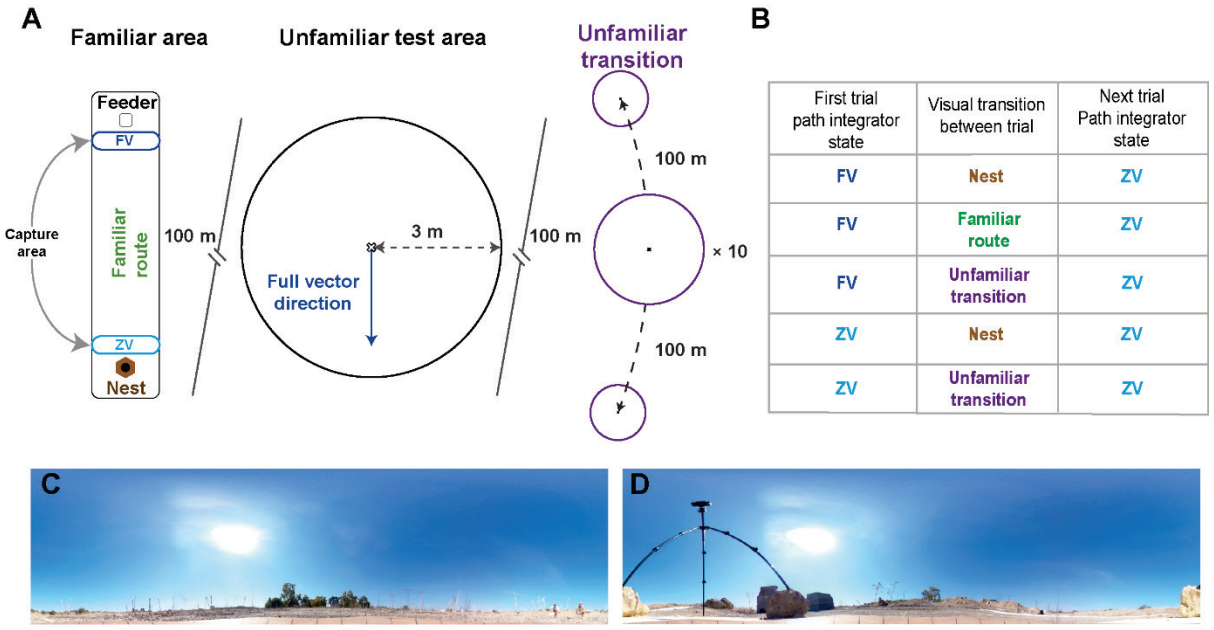

First trial path integrator state	Visual transition between trial	Next trial Path integrator state
FV	Nest	ZV
FV	Familiar route	ZV
FV	Unfamiliar transition	ZV
ZV	Nest	ZV
ZV	Unfamiliar transition	ZV

Figure 4. Experimental set up. (A)Scheme of the experimental set-up. A familiar route consisting of a straight route of 7.0 m enclosed in a corridor (7×1.5 m). A feeder is placed 7.0 m away from the nest at least 24h before the experiment. (Unfamiliar test field 100 m away from the familiar area. Unfamiliar transition areas placed at least 100 m away from the test field and 200 m from the closet nest. We used 10 distinct unfamiliar transition. (B) Table of experimental condition. (C, D) panoramic picture of the (C) familiar area and (D) Unfamiliar test area.

Experimental procedure and data collection

We investigated whether ants would learn a novel route in a distant unfamiliar test field (Figure 4A) during their homing path. For all experiments, the test area was covered with a gridded string pattern (1×1.0 m) to record the path of the ants.

First trial as Full vector ants.

Ants were captured at the beginning of their homing path along their familiar route corridor. Hence, those foragers are called full vector ants as they possess a homing vector (FV) pointing to the food-to-nest compass direction. Ants were trained in an unfamiliar test field (TF) at least 100 m away from their usual route. Paths were recorded until the foragers reached the outer rim of a 3.0 m radius circle. When they reached the rim, ants were captured and released in one of three distinct visual transitions: (1) directly inside their nest (N); (2) along the ant's familiar route (F) therefore in presence of familiar terrestrial cues; (3) or in an unfamiliar location (U) 100 m away from the test field (Figure 4A). Crucially, for the subsequent trips in the TF ants

were tested without homing vector (ZV ants). Hence, they could not rely on their PI vector but only on visual memory acquired during the previous trail. To do so, we let the ants run off their vector (approximately 3.0 m) either within the unfamiliar (U) transition or along their familiar route (F). For the group of ants released inside their nest (N), we observed the nest entrance, followed foragers until they picked up a food item at the feeder and finished their inbound trip and captured them just before the nest entrance. Hence, they were tested at ZV ants.

First trial as Zero vector ants.

To test whether ants would learn a route on the unfamiliar test field without PI homing vector, homing ants were caught on their familiar corridor just before entering their nest and thus no longer possess a PI homing vector (ZV). As before, ants were released at the centre of the test field for their first trial. Once the ants reach the rim (3.0 m radius around the release point) they were captured and attributed to one out of two visual conditions (U or N; Figure 4). They were released either for a few seconds in U or N before being released again on the TF. Here again for the test, ants were captured and released on the test field for their second trial as ZV ants. For the unfamiliar transition where the centre of the test field is the ZV point, we forced the ant to run in the opposite direction of their exit point in the TF. This permits to keep the release point in the test field as the ZV point.

Recall experiment.

During the final test of this experiment, ants released on the test field were no longer captured when reaching a 3.0 m distance from the release point. The search area was constrained with white barriers about 3 cm height, forming a square shape (6×6.0 m). For this experiment, we used ZV ants captured while exiting their nest and provided with a cookie to trigger homing motivation. ZV ants were released at the centre of the test field and free to explore. If during their exploration ants depart from the centre about 1.8 meters and return to the released point, they were captured again (at the centre of the test field). From there we created two groups. Group 1 ants were released at a novel location at least 1.8 m away from the centre. Group 2 ants were released again at the centre of the test field (the point of capture) (Figure 2C). After 4 repetitions of this procedure, ants were tested by letting them free to explore for at least 3 min.

Data extraction Analysis of the ants' direction of movement.

Data was extracted and analysed have been run using the free software R (v 3.6.2. R Core Development Team). The recorded paths were digitized as (X, Y) coordinates using ImageJ. After digitization, all paths were discretized with a constant step length of 0.02 m. Descriptive statistics of this path such as the mean direction of movement (mu) as well as the mean circular vector length (r, a measure of dispersion) were extracted on R with the package Circular. The mean directions (mu) were analysed using a Rayleigh test (from R package: Circular) that also includes a theoretical direction (analogous to the V-test). To test whether the angular data are distributed uniformly as a null hypothesis or if they are oriented toward the theoretical direction of the nest as indicated by the state of the PI.

For the recall experiment, we did a density heat map of the ants' position during the first trial and the test for group 1 and 2. The density maps have been done on the first 28 m of the test path. Path have been discretized into an X/Y matrix representing the space of the test field with a resolution of 25 cm.

We thus obtain with which frequency the ant has been in each square (0.25*0.25 cm^2). From this matrix, we calculated an exploratory index (Fig; 2F) that correspond to the number of squares explored divided by the distance walked (28 m). This index between groups has been compared by using a one-tails permutation test.

Then we computed a density map at the population scale (Fig.2 D) by summing individuals density map within each group. To facilitate meaningful comparisons between the two groups, we normalized the heat maps accordingly.

Data Time Warping (DTW) analysis:

To reveal the occurrence of identical pattern between paths, we run a Dynamic Time Warping (DTW) analysis (from R package: SimilarityMeasures). This analysis allows for a comparison of two X, Y trajectories. The DTW computes a similarity value that corresponds to the sum of the distance between each point of trajectories. High values indicate that the two trajectories are rather dissimilar, while low values indicate that both trajectories are similar.

Rather than comparing the entire path, we compared segments between two trajectories of the same ants. To extract a segment, we choose a focal path. Then we indexed a focal point p0 and extracted the corresponding X, Y coordinates. These coordinates served to identify the closet point p1 in the subsequent path. We extracted a segmentof 1.2 m around these focal points p0 and p1. We choose a focal point p0 every 10 steps. Between all segments, we did a DTW analysis. We used the median of all DTW within two paths for statistical tests.

To test whether the paths of ants were more similar within rather than between individuals, we compared the path of trial 1 of an individual to the path of trial 2 of all other ants. Then we obtain the median of these DTW analysis value across all ant comparisons. Medians of DTW values were then compared between the 'between individuals' and 'within individuals' paths comparisons using a permutation test for paired data.

Computational model:

We designed an agent-based model (Figure 3) using Python (Version 3.7.4).

The agent consists of a point with position x,y and an associated heading orientation θ (we inferred that ants do not walk sideways and therefore heading θ is defined as the direction between the previous and current point location). The model runs in discrete time steps, with each time-step representing an iteration of the algorithm. The test field was modelled as a 3 m radius X,Y space in which the agent could update its position with a step length of 0.02 cm at each time step.

Agent memories:

The agent's memories of its routes on the test field were modelled as a 3D matrix, representing the space of the test field. Two dimensions correspond to the X,Y space of the field (steps of 10 cm) while the third dimension corresponds to all possible headings θ for each location (0°→360°, steps of 5°). At first, the 3D memory matrix is filled with 0 values (i.e., unfamiliar) representing the absence of memory for any location*heading. As the agent explores the world, at each time step the memory matrix values increase towards 1 (i.e. familiar) for the X,Y,θ (position*heading) of the agent, based on a defined learning rate (see

table 1). To account for the fact that a view memorized at a given X,Y, θ can be recognized at neighbouring locations*headings[141,282,283] , the familiarity value was diffused around the X,Y, θ in the memory space following an exponential decay towards 0 (see 'diffusion' parameters in Table 1). Note that the value of the diffusion parameter in X,Y captures the visual openness of the environment: because more open environments visually change slower with displacement, a given learnt view can be recognized from further away.

Two such memory matrixes were built and updated in parallel: one representing the persistent memory PM and on the transient memory TM.

Training phase (Trial 1):

For trial 1, the naïve agent (both TM and PM memory matrix initially set at 0) was moved along one of the paths of our real ants recorded during their first trails as ZV (N =23) while updating both its PM and TM memory matrixes.

Test phase (Trial 2)

We realized 10 replicas of the test trails. For each replica, the trained agent's TM memory matrix was reset to 0, but the PM memory matrix values acquired during the training phase persisted. For One test (replicas), the agent was positioned at the middle of the test field in a random heading θ and let to guide its second path. At each time step, the agent performs a 0.02 cm step in a novel heading θ, which is determined by three directional forces integrated together as in vector-based navigation [71,284] :

1) Familiarity vector: Because learnt view recognition is dependent on both position and orientation[141] the agent extracts the 'familiarity' values of its current position and heading X,Y, θ in space by sampling the corresponding X,Y, θ values of both its PM and TM memories. Because TM inhibit PM, the 'recalled familiarity' is then obtained as 'PM (X,Y, θ) – TM (X,Y, θ)', and provides the weight (norm) of the familiarity vector for the current time step. To account from the fact that ants can learn view in multiple orientation at a same position and can associate these views to the most familiar route direction at this location[63] , the direction of the familiarity vector is obtained as the average of the θs familiarity of that location (X,Y) in the PM. To account for biological noise in retrieving the direction of a learnt route, a

directional noise is added to this vector's direction, drawn randomly from a Gaussian distribution of ± SD = 5°.

2) Path Integration vector: Path Integration (PI) continuously attracts homing ants towards their so-called Zero-Vector point location, usually at the nest position [99]. Here we modelled ZV ants (captured at their nest) displaced to the centre of the test field, therefore, their PI vector always points from the agent's current X,Y position to the centre of the test field. To account for biological noise in computing a PI home vector, a directional noise is added to this vector's direction, drawn randomly from a Gaussian distribution of ± SD = 5°. The weight (norm) of this vector was fixed at 0.015 (see explanation below).

3) Inertia vector: To account for the fact that running ants are not constantly stopping and reassessing their orientation, we added an inertial vector, which direction correspond to the current heading θ of the agent. To account for biological motor noise, a directional noise is added to this vector's direction, drawn randomly from a Gaussian distribution of ± SD = 10°. The weight (norm) of this vector was fixed at 0.8 (see explanation below).

At each time step, the new heading of the agent θ is obtained by summing the three vectors mentioned above (note that the norm of each vector function therefore as a weight, mimicking the weighted integration of directions achieved by ants[188,189,197,284]. The agent would then perform a step of 0.02 cm in this new θ to arrive at a new X,Y location in the test field, and both PM and TM memory matrixes would be updated to account from the ongoing learning of the current location.

Note that the familiarity weight of the current view varies from 0 (unfamiliar) to 1 (perfectly familiar). The weight of the PI and Inertial vectors have been manually selected to ensure that the agent did not follow routes more consistently than our real ant data (Figure S3B, C). Note that an agent guided only by the PI and inertia vectors (as in an exploration of a novel environment) would spontaneously display a systematic search centred on the PI Zero Vector point, as observed in ants [30,255–257].

Parameters	Description	Continuous learning Experiment (fig. 3 B,C)	Rewind Experiment (fig. 3 D,E)
Learning rate	Familiarity value for the current position*orientation in memory matrixes are updated such as: New value = Old value + (1 – Old value) *learning rate.	TM = 0.35 PM = 0.35	
Weight PI	Weight of direction indicated by the PI.	0.015	
Weight view	Weight of the direction indicated by the recalled familiarity.	Range between 0 and 1	
Weight inertia	Weight of the tendency to continue straight	0.8	
Diffusion accros location (X,Y)	Parameters of the exponential law for memory diffusion.	0.6 Meaning that the memory diffuses 40 cm on either side of the position.	Open: 0. 5; spill = 50 cm. Cluttered: 1; spill = 20 cm.
Diffusion across heading (θ)	Parameters of the exponential law for memory diffusion.	0.7 Meaning that the memory diffusion spill around 25 degrees around the orientation.	
Step length	The distance made by the agent at each step	0.02 meters	

Table 1. Default parameters used for both models. The first column corresponds to the parameter name. The second column to their description. The third and fourth column are the actual value used in different simulation.

Modelled agent path analysis

The path model was analysed using R (version 3.6.2). To access to the similarity between two successive trajectories, we conducted a DTW (see method: “DTW analysis"). The median of the DTW between the first (training) and second trial (test) was extracted, as for the real ant data.

We compared DTW obtained from our ant's path with the ones obtained from ants agents' path (Fig. S3) using linear mixed models with the ant identity as random variable. It is important to note that as we realized 10 replicas of the test path (see *Test phase)* for the agent, we average the DTW value through replicas.

To estimate if ant agent indeed stays stuck in a particular trajectory pattern, we used a focal segment of the training path (trials one) with multiple other segments in subsequent test paths (trials two) to determine if the agent has followed a similar pattern. The comparison is made if the centre-to-centre distance between two segments is less than 60 cm and has a similar direction (within 25 degrees). The number of resulting comparisons is then used as a proxy for the number of times the agent repeated the pattern of the trial's one.

Rewind experiment.

To determine if our model could replicate behavioural signatures observed in the literature, we virtually reproduced an experimental paradigm where ants are forced to repeat a route segment several times consecutively. Typically, repetition after repetition, ants typically stop following their route and start to meandering away [190,191].

We replicated this experimental paradigm. First, we conducted 50 training sessions where the ant agent was trained along a direct route from the feeder to their nest located 7.0 m away. During training, the agents navigate with a home vector and progressively update their memory banks.

For a first test, we aimed to investigate the specific effect of visual repetition by re-running one portion of the route. We forced the agent to repeatedly traverse the same portion of the route by systematically catching the agent when reaching 1 m from its virtual nest and releasing it at the beginning of the inbound trip again. Between each repetition, as the agent does not encounter novel views, the TM is not reset, and the agent therefore accumulates familiarity in its TM memory across repetition. We did 6 replicates of this procedure for 20 ants' agents. We then analysed paths, by using a sinuosity index (The inverse of the mean resultant vector calculated over the entire path). We then compared this value between the first and the last trials with a Wilcoxon test for paired data.

Lastly, we explored how the environmental structure influences the impact of route repetition on route disturbance. To achieve this, we modified the memory diffusion along the X and Y

axes (see Table 1). Because more open environments visually change slower with displacement, a given learnt view can be recognized from further away, which can be modelled by having the familiarity values diffusing further along the X,Y of the memory matrixes. We thus simulated cluttered areas by reducing memory diffusion, simulating scenarios where the ant agent moves through a cluttered scene that therefore changes rapidly with displacement (see Table 1). Note that because ants were tested as 'zero-vector ant' captured at their nest and released at the beginning of the route, their PI home vector points in a direction opposite to the route familiarity direction from the first trial onwards [196], to account for his effect the PI vector weight was fixed at 0.015.

Acknowledgments

We express our gratitude to Xim Cerda and the helpful team at Spanish National Research Council (CSIC Seville) and appreciate the help during field work preparation and data collection of Joséphine Gouleau, and Christelle Gassama.Finally, we thank the ants tested in these experiments for their participation.

Funding: European Research Council, Grant reference number: EMERG-ANT 759817, Author: Antoine Wystrach.

Supplemental information

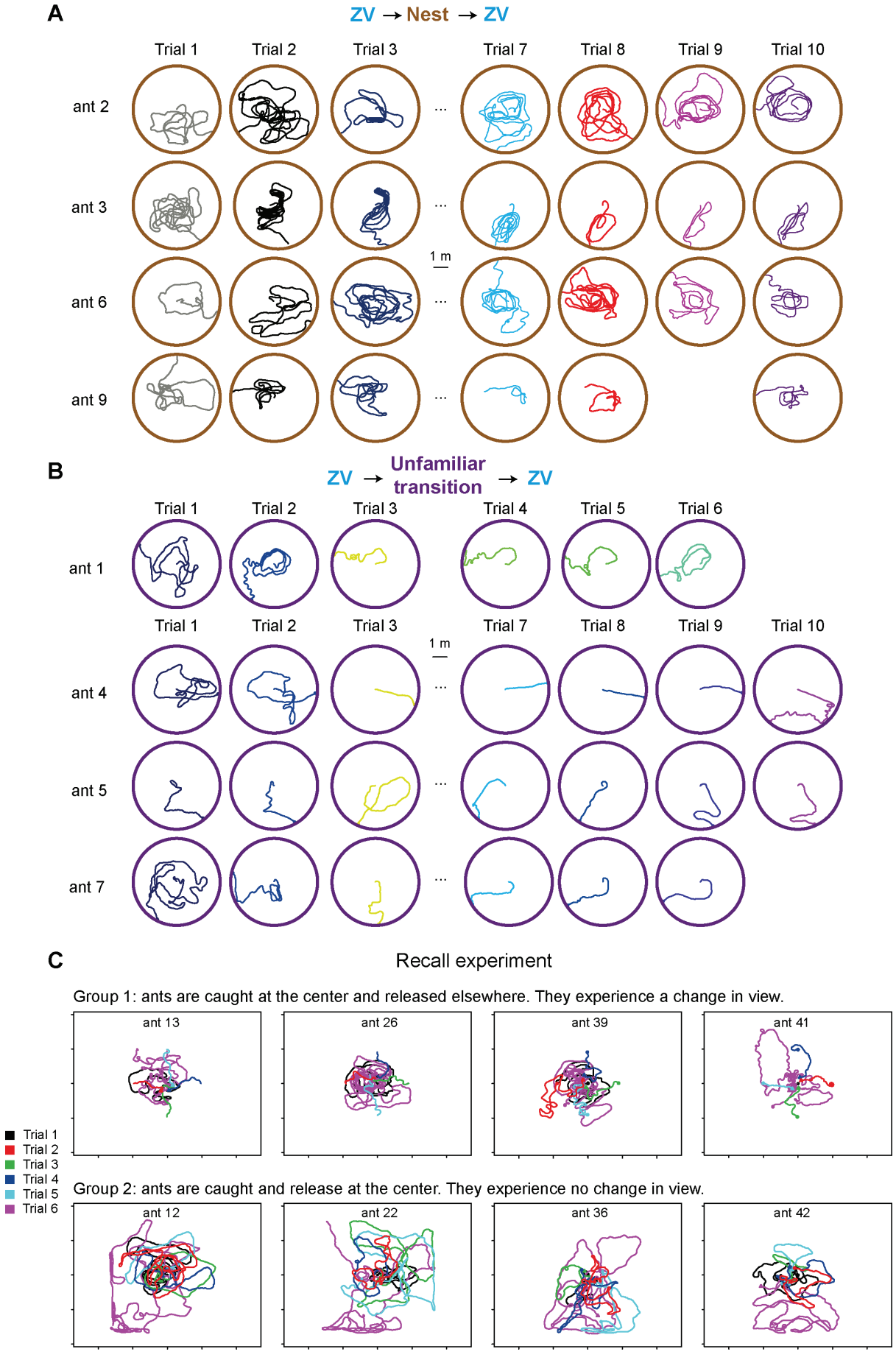
A
ZV → Nest → ZV
Trial 1
Trial 2
Trial 3
Trial 7
Trial 8
Trial 9
Trial 10
ant 2
ant 3
ant 6
ant 9
1 m
B
ZV → Unfamiliar transition → ZV
Trial 1
Trial 2
Trial 3
Trial 4
Trial 5
Trial 6
ant 1
Trial 1
Trial 2
Trial 3
Trial 7
Trial 8
Trial 9
Trial 10
ant 4
ant 5
ant 7
1 m
C
Recall experiment
Group 1: ants are caught at the center and released elsewhere. They experience a change in view.
ant 13
ant 26
ant 39
ant 41
Trial 1
Trial 2
Trial 3
Trial 4
Trial 5
Trial 6
Group 2: ants are caught and release at the center. They experience no change in view.
ant 12
ant 22
ant 36
ant 42

Figure S1: Experimental manipulations in ZV Ants: samples Paths (A,B) Path of ants trains as ZV in the test field. After the first trials, ants were either released at the nest between each recording session (A) or in another unfamiliar place (B). (C) Example path of the "recall experiment". For the first trial ZV ants are released and capture at the centre of the TF. Then for the next four trial ants are split into two groups that will experience either a changement of view (C, group 1) or not (C, group2). Finally, during the test (sixth trial, purple path) – for both group- ants are recorded without interfering with their path. On these examples' path we can clearly see an attraction for the centre for the group 1 since trials 2. While group 2 tend to continue and widen their search.

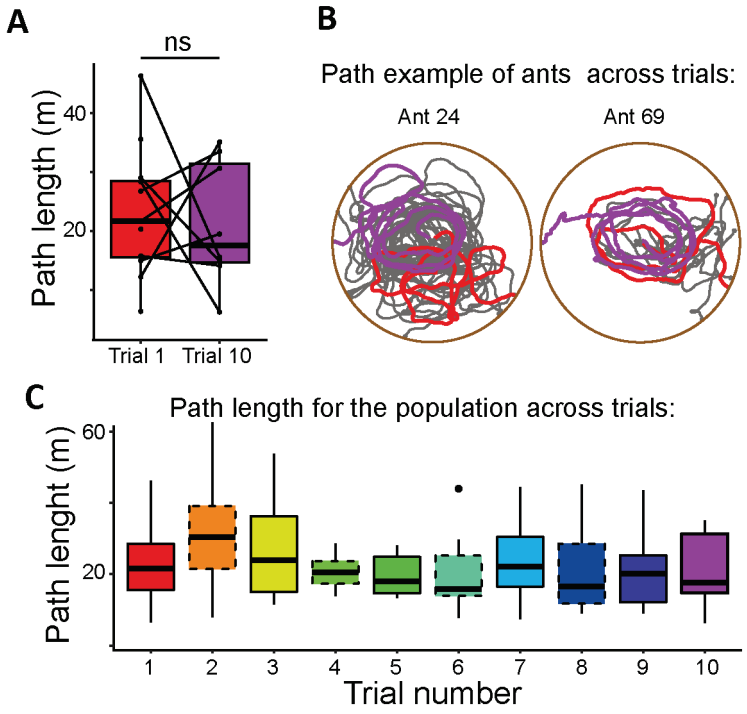

Figure S2: Ants do not optimize the distance covered trials after trials. Analysis of distance covered for the groups of ants trained as ZV and released directly inside their nest between two training sessions. (A) The distribution of distance covered during trials one and ten are identical ($p > 0.05$). Showing that's ants do not optimize the distance covered (B) Two examples path, highlighting that the distance covered between trials one (red) and ten (purple) are rather similar (C) Path length distribution of trials after trials.

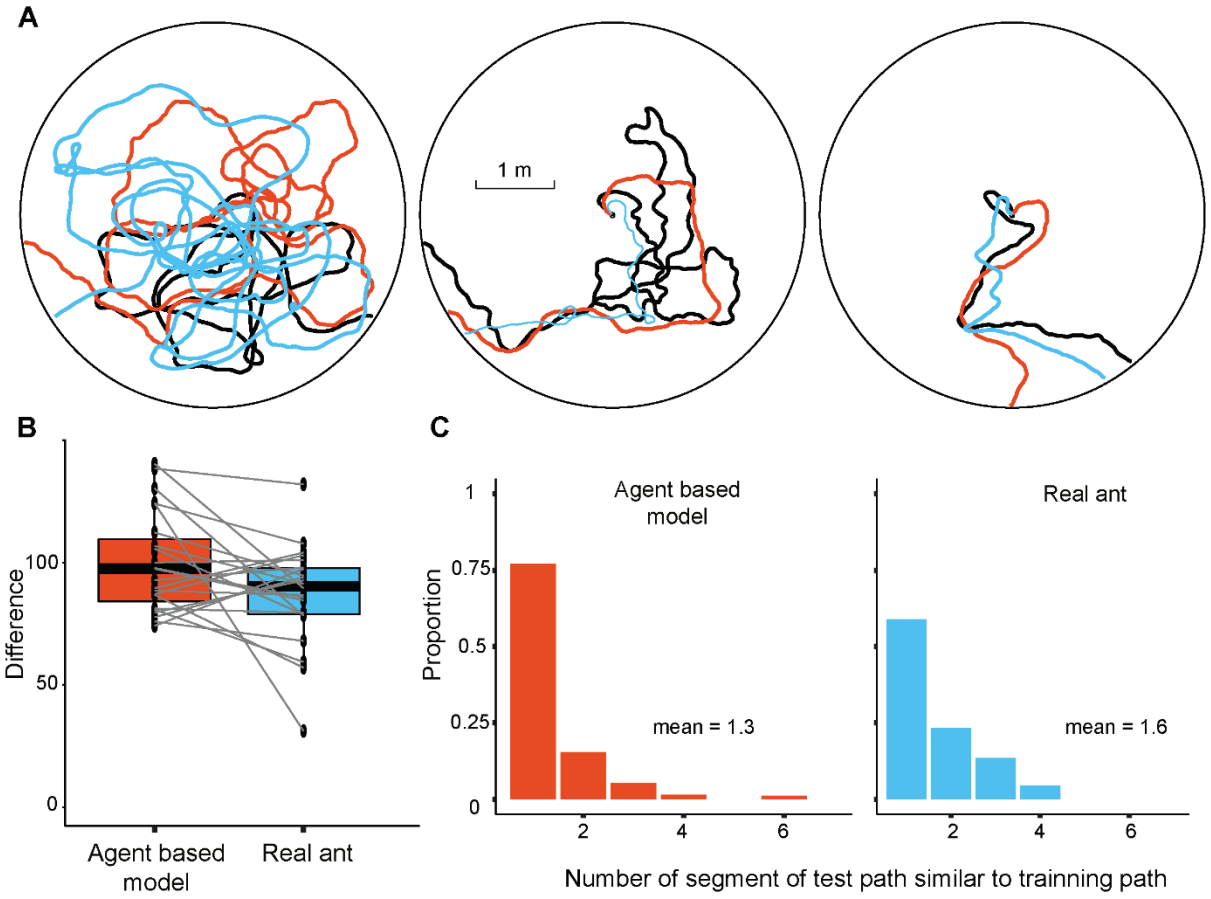

Figure S3. The feedforward inhibition model prevents to stay stuck too long in path signature. (A) Example path of the test path for model (orange) and real ant data train in ZV learning protocol (blue). The model has been trained once on the first path (see method) of real data (black path). (B) Comparison of the Similarity analysis (DTW) between models and real ants' data trained as ZV (see method). Each path has been cut into segments of 2.4 meters, and each segment has been compared with the closest neighbour segment in a subsequent trial to estimate their similarity. Data obtained from the models has been average through replica. (C) Show the distribution of overlapping segments between the test path (trial two, A, coloured path) and training path (trial one, A, black path) for both model and real ant data. We compared one training path segment (trials one) with multiple test path segments (trials two). Two comparable segments are defined if their centre-to-centre distance is less than 60 cm and have a similar direction (within 25 degrees). The number of comparisons was used to estimate how many times a portion of route from trials one was repeated during the test path. We selected this range of parameters as the model crucially not follow route better than our real data (B, Anova < 0.05, post hoc analysis ps <0.05, mean DWT and SD: model = 99, 20; real ant data = 87, 20).

Chapter II

An intrinsic oscillator underlies visual navigation in ants

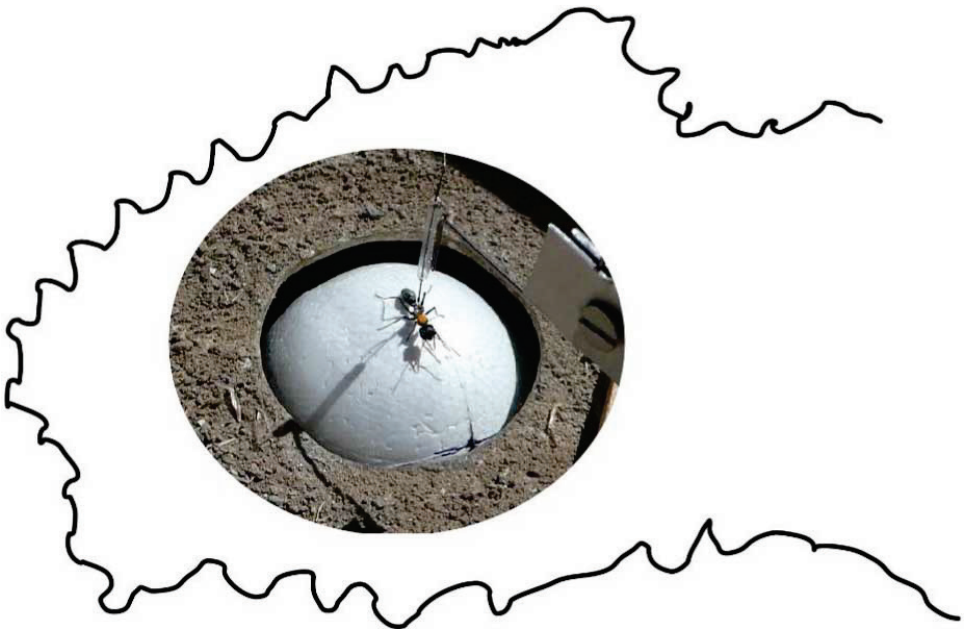

An intrinsic oscillator underlies visual navigation in ants

Leo Clement*, Sebastian Schwarz and Antoine Wystrach

Centre de Recherches sur la Cognition Animale, CNRS, Université Paul Sabatier, Toulouse 31062 cedex 09, France

Abstract

Many insects display lateral oscillations while moving, but how these oscillations are produced and participate in visual navigation remains unclear. Here, we show that visually navigating ants continuously display regular lateral oscillations coupled with variations of forward speed that strongly optimize the distance covered while simultaneously enabling them to scan left and right directions. This pattern of movement is produced endogenously and conserved across navigational contexts in two phylogenetically distant ant species.

Moreover, the oscillations' amplitude can be modulated by both innate or learnt visual cues to adjust the exploration/exploitation balance to the current need. This lower-level motor pattern thus drastically reduces the degree of freedom needed for higher-level strategies to control behavior. The observed dynamical signature readily emerges from a simple neural circuit model of the insect's conserved pre-motor area known as the lateral accessory lobe, offering a surprisingly simple but effective neural control and endorsing oscillation as a core, ancestral way of moving in insects.

Introduction

Navigating through space implies both to acquire information (exploration) and to use this information to move in the correct direction (exploitation). A way to acquire information is to sample the environment by actively moving. Such 'active-sampling' is common across the animal kingdom spanning from invertebrates [285–287] to vertebrates [224,288–291]. However, active sampling entails movements that are typically different than moving towards the goal and thus requires the animal to solve a trade-off. Achieving a balance between sampling actions (exploration) and goal-directed actions (exploitation) lies at the core of the behavioural control, but how it is achieved and evolved in animals remains unclear.

A way of sampling the world is through the production of regular alternations between left and right turns along the path: lateral oscillations. Lateral oscillations are observed in wide range of taxa (vertebrates [224,225]; invertebrates[51,226–229]) and have been mainly studied in the context of olfactory behaviours such as plume following in moths[51–53,292], trail following in ants[21] or odour gradient climbing in Drosophila larvae[229] and *Caenorhabditis elegans*[293]. The intrinsic production of oscillations enables an efficient sampling of odour across locations and models show that oscillations modulated by odour perception enables to reach the source in a remarkably effective way[229,293,294].

Modelling studies have shown that lateral oscillations can also be useful for visual navigation. For instance, having the amplitude of oscillation modulated by the familiarity of the perceived visual scenes, can produce robust visual navigational behaviours such as route-following[295] or homing[62], and captures particular behavioural signatures observed in ants[37]. Moreover, visually guided insects such as ants[31,34,35,37,144,148], wasps[41,296] or bumblebees[40] do display oscillations, whose expression appears to be coupled with visual perceptual cues. But whether these lateral oscillations are produced internally, how exactly they interact with visual cues and how they participate to the visual navigational task remains unclear.

We focused on the expression of oscillations in two ecologically and phylogenetically distant ant species: *Myrmecia croslandi* are solitary foragers relying heavily on vision[37,148–150,297] ; and *Iridomyrmex purpureus* that uses mass recruitment and pheromone trials but also other modalities for navigation[298]. The replication of the experiments in two distant species enables to tell apart whether the observed signatures are species-specific or shared across ants.

As most central place foragers, these ants species are known to rely on two main strategies to guide their foraging journeys [150,298]. The first strategy, commonly called Path Integration, allows individuals to continuously estimate the distance and compass direction that separates them from their nest (or other starting points) during their foraging trip[98,99,251]. The second, commonly called view-based navigation, involves the learning and subsequent recognition of the learnt visual panorama[98,141,299]. To see how these navigational strategies interact with oscillations, we mounted ants on a spherical treadmill device[300] (see Star methods), directly in their natural environment. This device enables to record the ants motor behaviour in detail, without interference of the uneven ground, while facilitating the control of the surrounding visual cue perceived. We characterised whether the obtained trajectories show a regular oscillatory pattern of movements and how these patterns are influenced by the presence or absence of: (1) visual input, (2) learnt visual terrestrial cues, (3) path integration homing vector and (4) rotational visual feedback. In both species, our results revealed the presence of a conserved pattern of oscillations generated intrinsically, which comprises both angular and forward velocity components. This pattern of movement provides a remarkable trade-off between exploration and exploitation and the amplitude of the oscillations can be flexibly adjusted by visual information in a way that is adapted to the navigational tasks at hand. Finally, we propose a simple neural circuit model of reciprocal inhibition between left and right pre-motor area to explore how these movement dynamics could be produced.

Results

Ants mounted on the trackball display their natural navigational behaviour

We first investigated whether ants mounted on the trackball display their natural navigational behaviours across different experimental conditions. When released on the ground in their natural environment, both species studied here (*Myrmecia croslandi* and *Iridomyrmex purpureus* see Figure S1) are known to rely on learnt terrestrial cues as well as, to a lesser extent, on Path Integration (PI)[37,150,297,298]. We first tethered ants and placed them on top of the trackball in a way that enabled them to physically rotate and control their actual body orientation[300] (Figure S2A). The trackball was placed in three distinct visual conditions: (1) along the individual ant's familiar route (F) therefore in presence of familiar terrestrial cues; (2) in an unfamiliar location (U) 50 meters away from their usual route; or (3) without any visual input: in complete darkness (D). For each of these visual conditions, ants were tested

either with (full-vector (FV) ants) or without (zero-vector (ZV) ants) PI information. While FV ants were captured at their feeding place and thus possess a PI homing vector pointing in the food-to-nest compass direction, ZV ants were caught just before entering their nest and thus no longer possess a PI homing vector.

Irrespectively of the PI state (FV or ZV), ants mounted on the trackball within their familiar visual route (i.e., in the presence of learnt terrestrial cues) displayed paths that were oriented toward the nest direction (Figure 1A; Rayleigh test with nest as theoretical direction ps: FV & ZV < 0.001), proving that they recognised and used the familiar terrestrial cues to orient even without PI information (ZV). When tested in unfamiliar surroundings, FV ants were oriented towards the theoretical direction of the nest as indicated by their PI (Figure 1B first row; Rayleigh test with PI as theoretical direction p: FV< 0.001); but ZV ants (Figure 1B second row) showed random orientations (Rayleigh test p: ZV=0.443). This confirms that the distant release points were indeed unfamiliar to the ants and that the ants relied on their PI when tested as FV ants. When tested in total darkness, ants displayed randomly orientated paths in all conditions (Figure 1C; Rayleigh test p: FV=0.354; ZV=0.360;), showing that the chosen dark condition was effective in preventing the ants to use neither terrestrial nor celestial cues for orientation. Overall, these results demonstrate that *M.croslandi* foragers rely on learnt terrestrial cues as well as their PI to navigate when mounted on the trackball system (Figure1).

We then looked at the individual's path straightness (R values in Figure 1 that indicate whether the ant's travel directions were rather constant across time (R=1) or not (R=0)). Independent of the PI state, the ants' paths were straighter in familiar terrain as compared to the other conditions (Figure 1; Familiar vs. Unfamiliar & Familiar vs. Dark: p*s* < 0.001), showing that the recognition of learnt terrestrial cues was most effective at helping the ant to maintain a constant direction of travel. With regards to the effect of PI state, there was no difference on the path straightness within each visual condition (FV vs ZV ps <0.1, Figure 1).

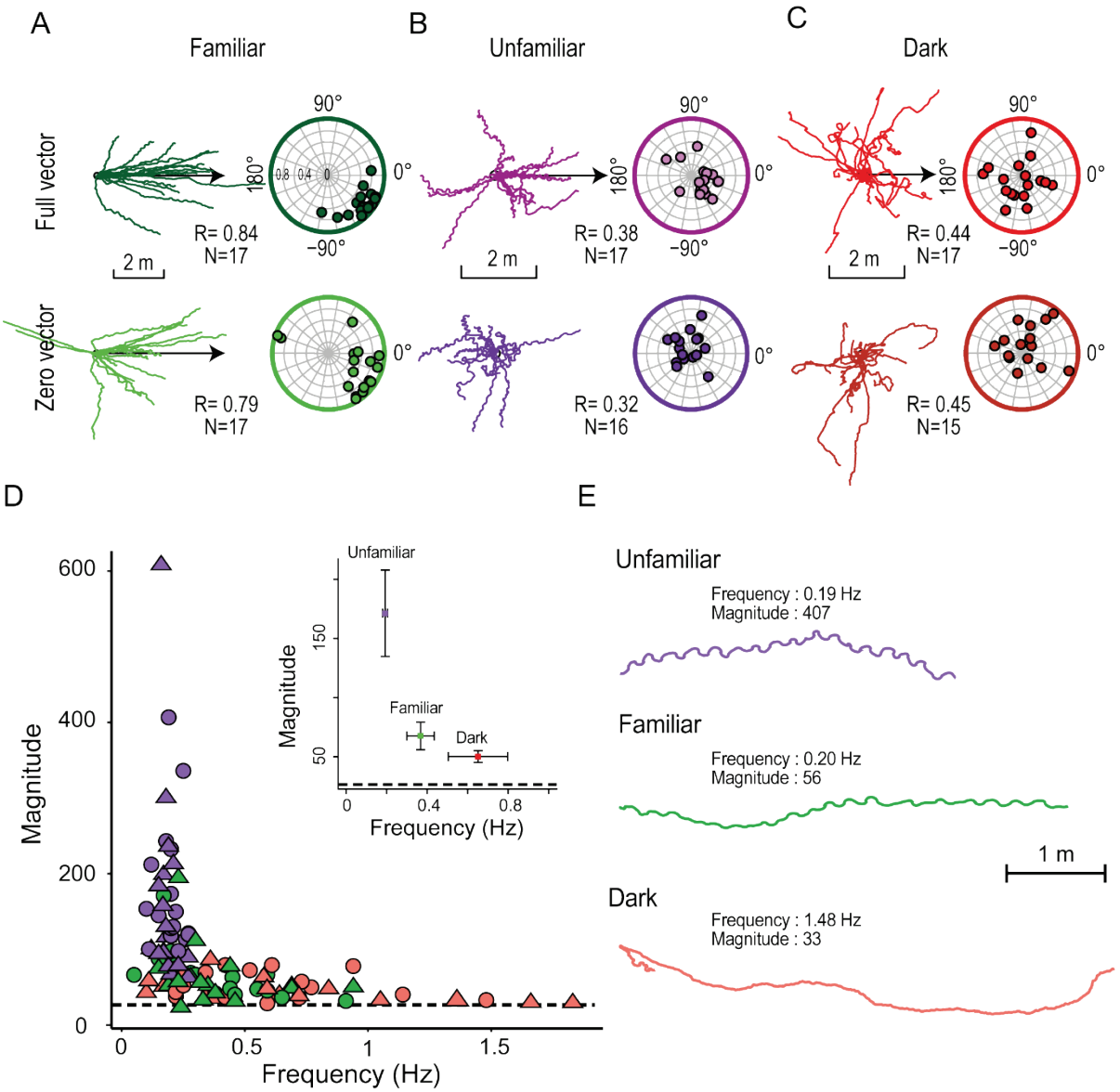

Figure 1. Oscillation characteristics vary across visual conditions. Trajectories of *M. croslandi* tested on the trackball in a familiar panorama along their known route ((A) green), an unfamiliar panorama ((B) purple) or in the dark ((C) red). For each condition, individuals were tested either with (full-vector, top row) or without (zero-vector, bottom row) path integration information. Reconstructed paths over 60 s are displayed relative to the real (in familiar) or theoretical (in full-vector) direction of the nest (arrow). In the circular plots, each dot indicates the average circular vector calculated over the entire path of an individual, showing the mean direction and the average vector length (i.e., a point closer to the periphery indicates straighter paths). The R values ('Straightness' between 0 and 1) indicate the length of the average resulting vector of the population. The direction (in familiar terrain) or theoretical direction (for FV in unfamiliar terrain) of the nest is 0°. (D) The graphs show the frequency and spectral density magnitude of the dominant oscillation (highest magnitude) for method see method see Figure S2). High frequencies indicate a fast-oscillatory rhythm and high magnitudes indicate a strong presence of this oscillation. Individuals were tested within a familiar panorama (green), an unfamiliar panorama (purple) or in the dark (red). Symbols indicate whether the state of the Path Integration vector was full (round) or zero (triangles) at

the beginning of the experiment. Inserts show the mean frequency against the mean magnitude of each visual condition with the associated 95% confidence interval around the mean. The dashed black line represents the mean of the spectral density peak magnitudes resulting from 200 Gaussian white noise signals. (E) example path for each condition for *M. croslandi* across 100s. For similar results on *M. croslandi* recorded directly on the ground and on our second species *I. purpureus* see also Figures S1, S3 and S4. See also Figure S2 for methods.

Overall, these results show that *M.croslandi* rely greatly on learnt visual cues and to a lesser extent on their PI. The latter still enables them to guide their general direction in unfamiliar terrain, but has only a limited impact on their path's straightness. Qualitatively similar results were obtained with our second species *I. purpureus* (see Figure S1). These results are consistent with what is observed in these species when navigating on their natural environnement [150,298].

Ants display regular lateral oscillations

To determine whether ants display regular lateral oscillations – that is, alternate between left and right turns at a steady rhythm – we first used our video recordings to track the ant's change in body orientation when mounted on the trackball. The body angular velocity signal is independent of the ant's actual forward movement and thus a direct reading of its motor control for turning. We conducted a Fourier analysis on autocorrelation coefficients of the angular velocity time series to obtain a 'power spectral density' (PSD) (see Figures S2 C-E) for detailed method). This PSD provides information about the regularity and frequency of oscillation, with higher magnitude values (y axis; Figure S2E) indicating more regular oscillation at the corresponding frequency (x axis; Figure S2E). For each ant, we selected the frequency corresponding to the highest magnitude (peak), that is, the most salient rhythm in the signal. In all experimental conditions, the obtained peak fell in the expected range of 0.2 to 1.5 Hz, as observed in other insect species[229,301]. It should be noted that this rhythm is 10 to 50 times slower than ants' typical stepping frequency[302] and thus are not the consequence of their rhythmic walking gait and hence must be the product of a different oscillatory mechanism. For both species, the obtained highest PSD magnitudes obtained with the ant's signal were higher than the ones obtained with a Gaussian white noise (Figure 1D dashed line; Wilcoxon one-tail test: $p \leq 0.001$, see Figures S3 A, C for *I. purpureus*), showing that ants displayed lateral oscillations with a higher regularity than random. We also replicated the same analysis using tracks of *M. croslandi* ants recorded directly on the ground while displaying learning walks

around their nest (Figure S4), which confirms that these regular oscillations are not a consequence of being mounted on the trackball set-up.

The navigational context modifies the regularity and frequency of oscillations

We tested whether the visual condition and the state of the path integrator influenced how regular the oscillations are, which can be measure with the magnitude of the individuals' power spectral density peak, (PSD, see S2 C-E for individual example and star methods) (Figures 1D, E). The statistical model revealed no interaction between both effects (AIC=-198.8, $F_{2,101}$=0.434, p=0.647) however the additive model (i.e., without interaction AIC=-215.8) explains the variation of the magnitude peaks relatively well (R^2 marginal=56% & conditional=67%). PI state did not affect the regularity of oscillations (PSD peak magnitudes (Figure 1D; Anova: vector effect: $F_{1,101}$=1.291, p>0.200)), however, the three visual conditions did (Figure 1D; Anova: visual condition effect: $F_{2,101}$=83.663, p < 0.001; Post-hoc: F vs. U: p<0.001; F vs. D: p=0.016; U vs. D: p<0.001): oscillations were most regular in unfamiliar terrain, intermediate in familiar environment and least regular in the dark (Figures, 1D, E; mean±se: $U_{(FV+ZV)}$ =171±19; $F_{(FV+ZV)}$ =68±6; $D_{(FV+ZV)}$ =50±3). The effect of individuality is significant (p=0.015), indicating that some individuals show more regular oscillations than others, across conditions.

We then investigated whether our different conditions influenced the oscillations' frequencies (Figure 1D, x axis), which indicates how quick the turn alternation happens. Here again, the PI state had no observable effect (Wilcoxon test for repeated measures; F: FV vs. ZV p=0.635; U: FV vs. ZV p=0.343, mean±se in F: FV=0.38±0.05 Hz, ZV=0.34±0.04 Hz; U: FV=0.19±0.01Hz, ZV=0.18±0.0009 Hz, Figure 1 D), however, independent of the PI state, the oscillatory frequencies were significantly higher in a familiar (F) than in an unfamiliar (U) visual panorama (p=0.023, mean±se: $F_{(FV+ZV)}$ =0.37±0.036 Hz; $U_{(FV+ZV)}$ =0.19±0.008 Hz; Figure 1D). Thus, the presence of familiar visual cues tends to increase the frequency of oscillations.

In the dark however, peak magnitudes are significantly weaker, closer to Gaussian noise and with a wider frequency range, suggesting that the PSD peak in some individuals may result from noise (Figures 1D, E). Oscillations seems to persist in the dark, however their expression is greatly inhibited suggesting that visual input is important for the expression of oscillation (Figure 1).

Overall, these results confirm the existence of regular oscillations and that their expression are influenced by the perceived familiarity of the visual surrounding, with slower and most regular oscillations being expressed in unfamiliar terrain (Figures 1D, E, S4A). The second ant species *I. purpureus* showed significantly regular oscillations, too, with the same tendency to produce slower oscillation in visually unfamiliar terrain and to inhibit their expression when in the dark (Figure S3).

The navigational context modulates the angular and forward velocity of oscillations

To investigate the dynamics of the ant oscillatory movements in more details, we combined for each ant its body angular velocity signal – obtained from video recording – with the forward movement signal – obtained from the trackball movements. We reconstructed 'average cycles' for each individual by pooling the angular and forward velocity recordings 3s before and 3s after the moments when ants switch from a left to a right turn (i.e., when the time series of the angular velocity crosses zero from negative to positive; see Figures S2F-I). That way, we can quantify each individual's average dynamic of angular and forward velocity and compare them across conditions.

The visual surrounding had a strong effect ($p<0.001$): ants displayed higher peak of angular velocities (Figure 3B, upper row; mean±se: $U_{(FV+ZV)}$=129±4.8 deg/s; $F_{(FV+ZV)}$=67.5±4.4 deg/s) and higher forward velocities amplitude (Figure 3B, second row, mean±se: $U_{(FV+ZV)}$=4.8±0.34 cm/s; $F_{(FV+ZV)}$=2.3± 0.2 cm/s) in an unfamiliar environment. There was however neither an effect of the PI state on turn or forward velocity ($p>0.05$) nor an interaction between the visual surrounding and the PI state (mean peak of angular velocity model: AIC=160.9, interaction $p>0.05$; amplitude of forward velocity model: AIC=109.9, interaction $p=0.22$). Therefore, the amplitude of lateral oscillations within the path are larger in an unfamiliar panorama than in a familiar one, independently of the PI sate (Figure 1E).

Lateral oscillations are combined with specific forward velocities variations.

To test for the existence of conserved oscillatory dynamics across individuals, each individual average cycle (Figures S2 F-I for method example) was normalised and averaged to obtain a cycle at the population level. To ensure that we pooled ants oscillating at similar frequency ranges, we separated data from familiar and unfamiliar terrain and selected only individuals showing a peak frequency within 0.1 to 0.27 Hz for *M. croslandi* (N=12). These frequency ranges correspond to high magnitude, ensuring that they are not a consequence of noise. The emerging population-averaged oscillation patterns show the existence of movement dynamics that are consistent across individuals, for both familiar and unfamiliar environments (Figure 2 A). Forward velocity co-varies with angular velocity in a particular way. Forward velocity is quite low when the ants reverse their turning direction (i.e., when angular velocity crosses zero). In contrast, we observe significant peaks of forward velocity, which happen briefly (up to 1s) while the ant is sweeping to the left or right (Figure 2A).

Remarkably, these peaks coincide well with the moment when the ants' body orientation is aligned with its overall direction of travel (Figure 2A, dashed lines) even though during these moments the ants' angular velocity is quite high. The same covariation is present in our second species *I. purpureus* (Figures S3C, D), showing that this signature is not a specificity of *M. croslandi*.

We replicated the same analysis using tracks of *M. croslandi* ants recorded directly on the ground while displaying learning walks around their nest and observed the same relationship between forward and angular speed (Figure S4), which confirms that these dynamics are not a consequence of being mounted on the trackball set-up.

Thus, ants (Figures 2, S4, S3) display large sweeps from one side to the other and thus spend a minimal amount of time facing their goal direction (i.e. the middle of the sweep), as angular speed is high at this moment. However, they produce a burst of forward velocity during this moment, that is, when aligned with their direction of travel (Figures 2A, C, D). On the contrary, they slow down, sometimes up to a pause, at the end of each left and right sweep, that is, when their body is facing away from their overall direction of travel (Figures 2A, C, D, G).

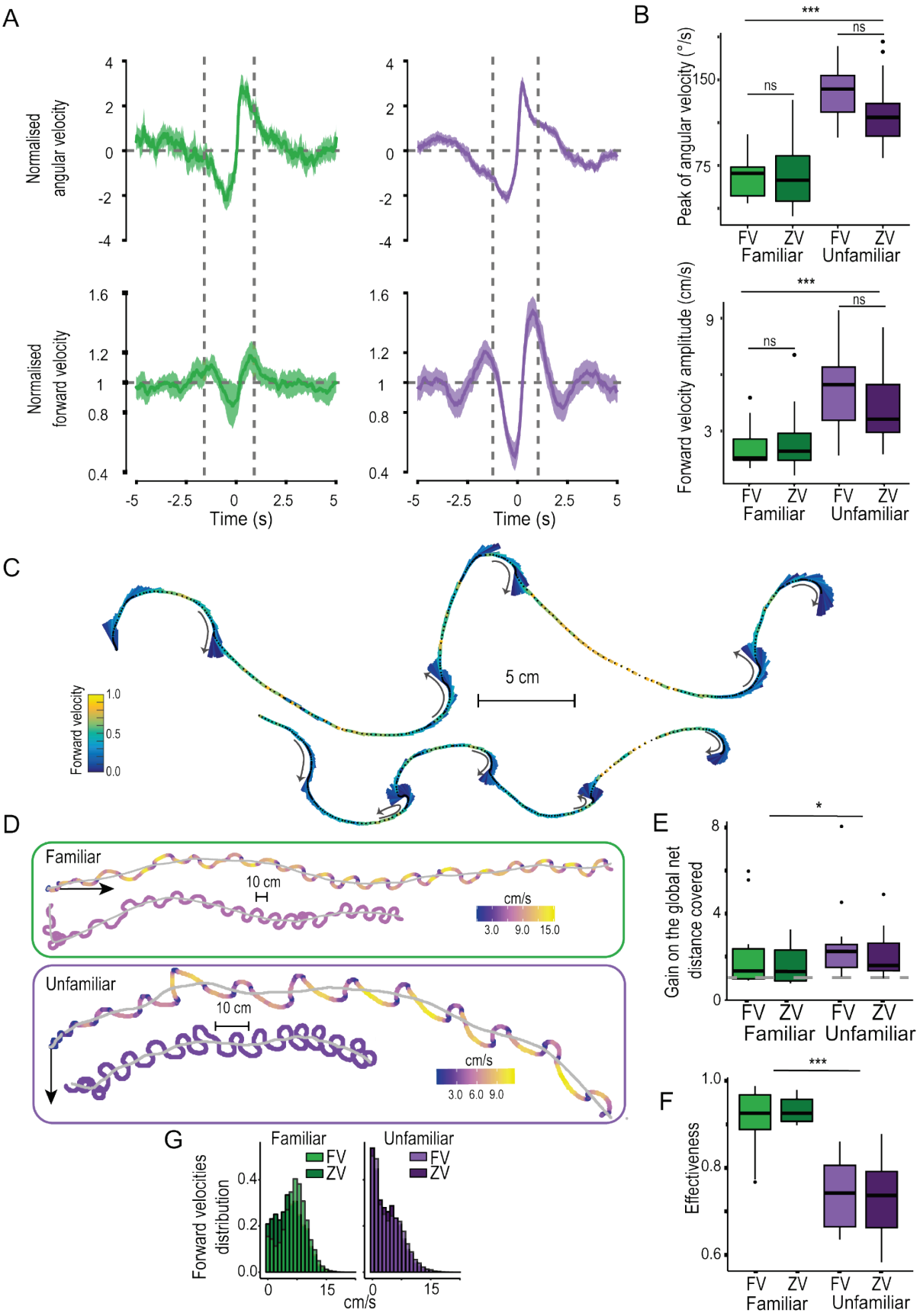

Figure 2: Co-variation of forward velocity and angular velocities optimize the distance covered and visual exploration. (A) Angular velocities (top-row) and forward velocity (bottom row) co-vary in a way that seem conserved across visual condition (on familiar route

(green, N = 12) or in unfamiliar terrain (purple, N=34)). Population cycles have been reconstructed by merging full- (FV) and zero-vector (ZV) data and normalising the data amplitude within the individual's average cycle (Figures S2 F-I). Colour areas around the mean curves represent the 95% confidence interval, based on the inter-individual variation. Dashed lines represent the moment when the ants are facing their overall direction of travels. (B) boxplots show the actual distribution of the non-normalised mean peak of angular speed (top row) and forward velocity amplitude (bottom row) for the individuals' average cycle (FV on the left, ZV on the right). (C) Details of paths (12s) displayed by two different individuals in unfamiliar terrain. Black dots indicate the successive positions of the animal and vectors indicate the current heading direction. Variation of forward velocities are indicated by both the colour and the length of the vectors (the longer the vector, the smaller the forward speed and thus the higher the time spent in this direction). Grey arrows emphasise the directions of turns. (D) Reconstructed path (100s) of two individuals recorded in a familiar (green panel) and in an unfamiliar (purple panel) panorama. Each path has been either reconstructed with the actual forward velocity signal of the ant (top path) or with a constant speed (mean of the individual's forward velocity signal, bottom path). Colour scales indicate the forward velocity. For each path, the global trajectory is shown in grey (i.e., path smoothed to remove the lateral oscillations). Straight black arrows indicate the direction of the nest. (E-G) Population statistics across conditions. (E) Ratio of the effective distance covered (length of grey path in (D)) between the reconstructed path with variation speed against path with constant speed for the different condition. A ratio >1 (dashed grey line) indicates that the effective distance covered is longer with forward speed variation than without. (F) Ratio between the effective distance covered (length of grey path in (D)) and the actual distance walked. (G) Distribution of the forward velocity in cm/s for each condition. (B,E-G) N = 17 for each conditions. For similar results on *M. croslandi* recorded directly on the ground and on our second species *I. purpureus* see also Figures S1, S3 and S4. See also Figure S2 for methods.

The dynamics of lateral oscillations optimise the distance covered.

To investigate the benefit of such regular variations of forward movements within the oscillations' cycle, we compared the ant's real paths with reconstructed versions of their path where we kept the original angular speed signal but averaged the forward speed, so it became constant (Figure 2D). By doing so the actual distance walked remains identical, but remarkably, the effective ground distance covered (length of the grey paths in Figure 2D) by the original paths (with forward speed variation) increased by up to a factor 8 (median =1.5; 25 / 75 percentiles = 1.08 / 2.5) compared to the paths with constant speed. This positive gain concerns 81% of our individuals and is significant in all our conditions (ratio above 1: ps<0.009, Figure 2E).

We then looked at the ratio between the effective ground distance covered (length of the grey path in Figure 2F) and the actual distance walked across conditions. The smaller the ratio the

more local oscillations are impeding the ants to cover effective ground (a ratio of 1 indicates a straight path, without local oscillations). Such an 'effectiveness ratio' is impacted by the presence of familiar visual surrounding but not by the PI state (panorama effect: $F_{1,101}$=142.090, $p < 0.001$; PI effect: $F_{1,101}$=0.683, $p = 0.407$). Paths displayed when on familiar terrain are more effective to cover ground than in an unfamiliar environment (Post-hoc, Figure 4D, F vs. U: $p<0.001$). This is in line with the fact that ants displayed smaller amplitude of oscillation in the presence of a familiar panorama (Figures 2A, B). In addition, we observed that ants in familiar environment displayed less pauses (Figure 2G) and higher forward velocities (N =34, $p < 0.001$, mean±se: F =6.087±0.336, U=3.961±0.182 cm/s).

Oscillations are modulated **by rotational feedback**

To test whether oscillations result from an intrinsic oscillator rather than a control mechanism based on an external directional reference (i.e., servo-mechanism), we investigated whether ants deprived of rotational feedback (either via optic-flow or compass cues) would still oscillate. To do so, ants were mounted on the trackball in a way that prevented them from physically rotating their body on the ball: when the ant tries to turn, it is the ball that counterturns. In other words, the fixed ant experiences neither a change of body orientation nor visual rotational feedback when trying to turn (see Figure S2B). For this experiment, we recorded *M. croslandi* ants in unfamiliar terrain as this condition produced the clearest oscillations in our previous experiments (Figure 1D). To control for potential effects of facing directions (depending on celestial or terrestrial visual cues), we tested each ant fixed in eight subsequent different orientations with a 45° rotational shift.

Despite the absence of visual rotational feedback, the obtained peak magnitudes of the angular velocity power spectral density (PSD: see Star Method) were much higher than expected from a Gaussian white noise ($p<0.001$) clearly showing the presence of a regular alternation between left and right turns (Figures 3A, B). The ants' body orientation relative to the world had no effect on the magnitudes (orientation: $F_{7,83}$=0.3729, $p=0.914$) nor did the other random parameters (individual $p=0.933$, sequence $p=0.473$).

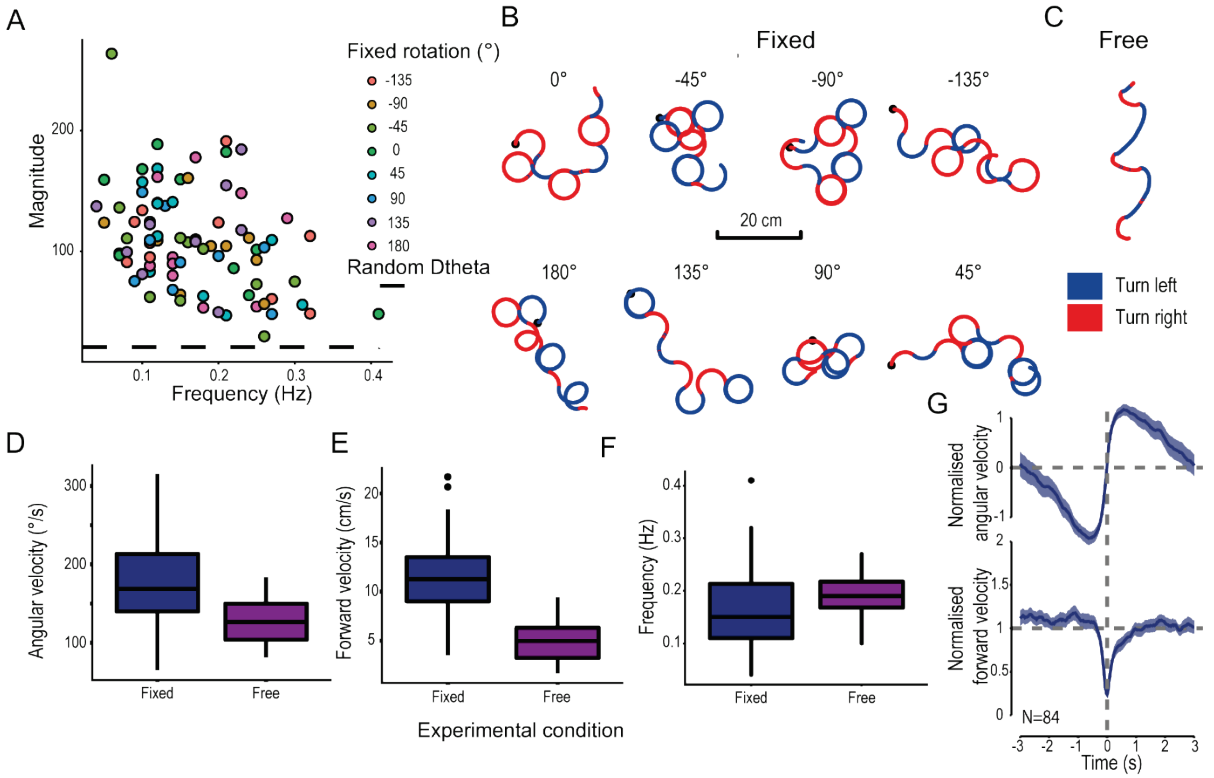

Figure 3. Ants still oscillate in the absence of rotational feedback. Zero-vector ants were tethered on the trackball in a way that prevented actual body rotation and tested in an unfamiliar environment. (A) Distribution of the individual Fourier dominant peak frequency and magnitude based on the angular velocity's spectral density time series (as in Figure 1D), method see Figures S2 B, C, D, E). High frequency indicates a fast-oscillatory rhythm, and a high magnitude indicates a strong presence of this oscillatory rhythm. The colour symbols represent the rotation relative to the theoretical nest direction (0°). The dashed black line represents the mean magnitude obtained from 200 Gaussian white noise signals (18.75). (B) Example paths of different individuals fixed in different orientations. (C) Example path from an ant that was free to rotate on the trackball, recorded in unfamiliar terrain in previous experiments. (B, C) In both situations, ants alternate regularly between right (blue) and left (red), but turns are sharper in the absence of rotational feedback. Peak of angular velocity (D), amplitude of forward velocity (E) and Frequency (F) of the individual's average oscillation cycle show that ants move faster, turn faster and slightly longer in the absence of rotation feedback. (G) Angular velocities (top-row) and forward velocities (bottom row) co-vary in a way that seem conserved across experimental conditions. Population cycles have been reconstructed by merging all rotational condition as there is no differences of amplitude of mean peak of angular velocity and mean forward amplitude cycles between rotational conditions (Anova: Df= $F_{7,84}$= 1.0103, $p \geq 0.432$). Each individual signal has been normalised before pooling. Coloured areas around mean curves represent the 95% confidence interval, based on the inter-individual variation. See also Figure S2 for methods.

The mean oscillation frequencies (mean±se: 0.17±0.007 Hz) were quite close to what we observed when these ants were free to rotate in an unfamiliar environment (Wilcoxon test for repeated measures: p=1, N=88, Figure 3F). Thus, ants can display regular turning oscillations without rotational feedback, whether as a result of optic flow or a change of orientation relative

to directional cues such as the visual panorama, wind, celestial compass cues or the magnetic field. Here again, the lateral oscillations displayed by the fixed ants showed the simultaneous variation of forward speed, as observed in the other conditions (Figure 3G). Consequently, we are left with the conclusion that these oscillatory dynamics are generated intrinsically.

Interestingly, the absence of rotational feedback led to higher angular velocities (mean: fixed=176 deg/s; free=128 deg/s; $p<0.001$), higher forward velocity (mean: fixed=11 cm/s; free=5 cm/s; $p<0.001$) and slightly slower turn alternation (i.e., lower frequency: fixed=0.16 Hz; free=0.19 Hz, $p=0.0189$) than ants that were free to physically rotate on the ball (Figures 3A-F). Rotational sensory feedback is thus involved in limiting the amplitude of the oscillations.

The observed movement signature emerges readily from a simple neural circuit.

Similarly to previous work[50,303], we designed a simplistic neural model based on the circuitry of the insect pre-motor area so-called lateral accessory lobes (LAL). The purpose of this model was not to match observed data quantitatively[294] but simply to test whether the co-varying relationship observed between angular and forward velocity could emerge from this type of circuit. Activation of the neurons in the left and right pre-motor areas are known to mediate left and right turns respectively in insects[50,227,228,304–306]. Furthermore, these left and right regions are known to reciprocally inhibit each other[50,227,228,305]. Modelling two reciprocally inhibiting neurons with internal feedback – that tries to maintain a basal activity – is sufficient to obtain the typical oscillatory activity between left and right LAL[50,227] (Figure 4) and thus provides an explanation for the regular oscillations between left and right turns observed in nsects. Interestingly, we show here that simply assuming that forward velocity is controlled by the sum of left and right output – while angular velocity results from their difference[50,229,294]– is sufficient for the covariation observed in ants to emerge (Figure 4). Bursts of forward speed appear when one side largely dominates over the other, that is when the ant is at the maximum speed of its angular sweep and thus roughly aligned with its overall direction of travel. Inversely, a break of forward speed occurs when the dominancy is reverted between LAL neurons, that is at the moment where ant reverts their turning direction (Figure 4). Importantly, the emergence of this particular relationship is robust to parameter change (Figure S5) and thus a stable feature of these types of circuits.

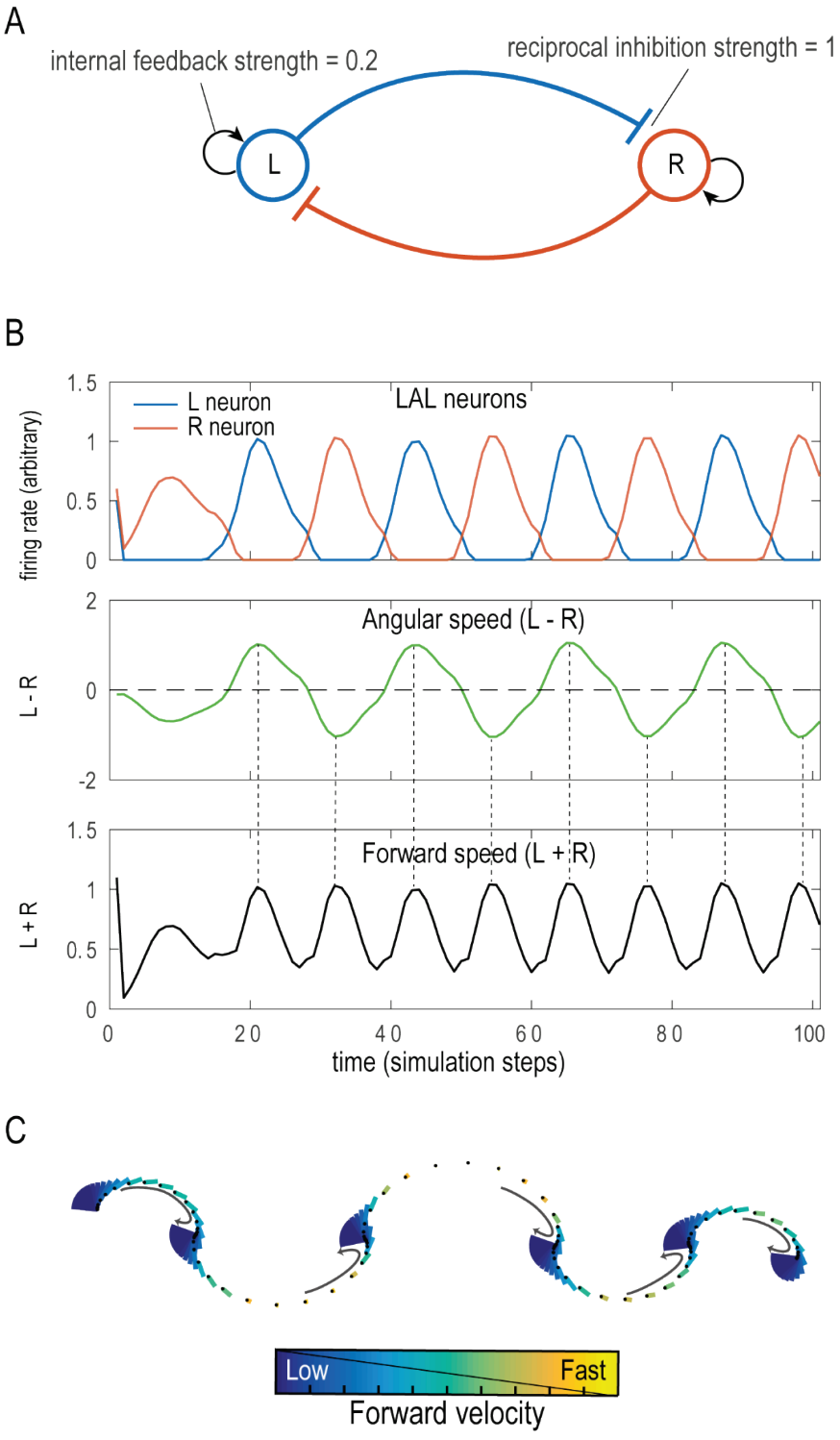

Figure 4. Reciprocal inhibition between two units produces the observed relationship between angular and forward velocity. Scheme of the model abstracted from the lateral accessory lobe (LAL). The Right (R) and Left (L) hemisphere neurons reciprocally inhibit each other (blue and red connection), while trying to sustain a basal firing rate through internal feedback (black arrow). (B) This results in the emergence of stable anti-phasic oscillatory activity between the R and L neurons (B, upper row). Assuming that angular velocity is controlled by the difference (B, middle row) – and forward speed by the sum (B, bottom row) – between left and right activation is sufficient to elicit the movement dynamics observed in ants (compare Figure 4C with Figure 2C). (C) Details of the dynamic of the path generated by the model. Colour indicates forward velocity (scales are arbitrary). Black dots indicate the successive positions of the agent and vectors indicate the current heading direction. Variation of forward velocities are indicated by both the colour and the length of the vectors (the longer the vector, the smaller the forward speed and thus the higher the time spent in this direction). As ants, the model results in a zigzagging path where velocity drops during turn reversal and increases when facing the overall direction of travel (Figures 2A, C, D). While the model enables the modulation of amplitude and frequency of the oscillations, the forward/angular velocities relationship is quite robust to parameter change (see Figure S5).

Discussion

An embedded solution for the compromise between exploration/exploitation

We recorded the detailed locomotor movements of two distantly related ant species – *M. croslandi* and *I. purpureus* – using a trackball-treadmill device directly in their natural environment. Despite that one species is a solitary visual navigator (*M. croslandi*) and the other (*I. purpureus*) uses pheromone trails and mass recruitment, we noticed a remarkable similar behavioural signature. Both species continuously display regular lateral oscillations with a synchronised burst of forward speed when facing the general direction of travel (Figures 1, 2A, C, S3). This pattern movement strongly optimises the overall ground distance covered while simultaneously enabling the ant to slow down when scanning to left and right directions, which may extend up to a full U-turn in some ants (Figures 2 C-F).

Previous observations assumed that ants accelerate when facing their goal direction as a response to the recognition of familiar views when aligned in this particular direction[71,75,165]. Here we show that this acceleration is the product of an endogenous process, as it is still expressed in unfamiliar terrain or when the ant body is artificially fixed on our trackball in a given orientation (Figure 3). This findings stresses the often disregarded importance of internally generated movement within the 'sensorimotor' loop[224,286,307–309].

The described internally generated movement dynamic provides an embedded solution for the compromise between exploration (looking on the side) and exploitation (covering ground in the desired direction). External visual cues can then modulate the exploration/exploitation balance to the task at hand by simply adjusting the amplitude of this endogenous dynamic. Higher amplitude oscillations optimise 'exploration' (higher amplitude scans) in an unfamiliar environment, while lower amplitudes favour 'exploitation' (straighter paths) on a familiar route (Figures 2, S3).

Interestingly, this movement signature is equally useful, and used, during the acquisition of learnt visual information, when naïve ants display their learning walk around the nest[148] (Figure S4). Optimising the learning of visual cues in naïve ants requires to bias the balance towards 'exploration' in the same manner as searching for familiar cues in an unfamiliar environment does in experienced ants; thus, it is not surprising to see here also high amplitude oscillations

(Figures 2A-D, S3). The apparent different needs for the acquisition of information on the one hand and the use of that information on the other hand, are thus solved with the same sensory-motor solution. The weaker modulation observed in *I. purpureus* (Figure S3) may be explained by their strong reliance on chemical trails[298], whose absence on the trackball may favour exploration in both visually familiar and unfamiliar conditions.

Finally, we see in both species that the internally generated oscillations can be strongly inhibited when not needed, such as when moving in the dark (Figures 1C, D, S3A, B). Indeed, oscillations are not always useful and it may be advantageous to repress them in situations like when inside the nest or when trying to escape an aversive situation. Thus, both the animal's internal state and the presence/absence of relevant contextual information – such as a visual panorama by opposition to no panorama at all – modulates the expression of the internally produced oscillations in a similar vein as the male fly's internal state continuously tunes up or down the gain of circuits promoting visual pursuit[199]. However, what specific type of visual information promotes the expression of oscillations remains to be seen.

Evolutionary consideration and neural Implementation.

Lateral oscillations around 0.3-1Hz are also observed in moths[51,53,292,310] *Drosophila* larvae[229], Colorado beetles[301], flying hymenopteran[41,296,311] and other insects[228], suggesting an ancestral way of moving, which predates at least the holometabolous insects' common ancestor (around 300 Myr ago).

In the insect brain, regular lateral oscillations seem to result from reciprocal contra-lateral inhibitions between left and right hemispheric premotor areas, so-called Lateral Accessory Lobes (LAL) an ancestral brain structure, highly conserved across insects[50,228,303]. These circuits – analogous to central pattern generators (CPG) – result in the internal production of asymmetrical and rhythmical excitation between left and right motor commands, so-called flip-flop neurons[50,227,228,304–306]. However, while CPG are well known to sustain a wide range of rhythmical limb movements[224,308,312,313], the LAL controls the displacement of the whole animal across space and thus directly contributes to the navigational task.

Some have suggested that neural systems evolved at first to coordinate movements endogenously[309,314] whereas the modulation of these movements by external sensory information originated only as a second step[314]. This view is supported by the current demonstration of an internally produced rhythm at the core of the navigational behaviour in

ants, as well as the observation that, across species, various multi-modal sensory cues converge to the same conserved region (the LAL) to produce the remarkable variety of navigational behaviours across species[50,52,228,303]. Modulation of oscillations by olfactory cues helps *Drosophila* larvae[229] to climb odour gradient, male moths to track pheromone plume[51–53,228,292] and ants to follow chemical trails[21]. Modulation of oscillations by vision for navigation, as observed in wasps[41,296] bumblebees[40] and ants[31,34,35,37,144,148] may have appeared later with the evolution of visual navigation in hymenopteran, through direct or indirect connections between the mushroom bodies – the seat of navigational visual memories[64,68,165] – and the LAL (Figure 4). Modulation of oscillations by re-afferent rotational visual cues, as we showed here in ants (Figure 3), might be ancestral to insects as we equally observe it in moths[52–54]. This likely evolved through connections between horizontal optic-flow detectors in the optic lobes[53,315] and the LAL (Figure 4), providing a useful feedback-control to calibrate the amplitude of turns, and more generally participating in the widespread opto-motor response[53].

The forward speed variation within the oscillation cycles presented here has not been reported in other insects' species and the fact that it is shared in two phylogenetically and ecologically distant ants (Figure S3) suggests that it is a shared feature in the ant family. This may be an adaptation for the use of vision while walking. Scanning multiple direction through body rotation is key for visual scene recognition in hymenopteran[141,316,317], and because ants are ground dwellers, they are reluctant to decouple their body orientation from their direction of travel; even though they can[318]. Ants thus benefit to pause when looking on the side, otherwise they would depart away from their general direction of travel. Conversely, the timely burst of forward speed when facing the overall direction of travel (Figures 2A, C, D) enables to stretch the oscillations and thus strongly improves the amount of ground covered (Figures 2 D-F). In addition, pausing when looking on the side must improve the efficiency of visual recognition due to gaze stabilization, which accommodates remarkably well the idea that views are learnt and recognized when oriented left and right – rather than towards and away – from the goal[41,63].

Interestingly, the efficient covariation between forward and angular velocity observed here in ants is captured by a model of the LAL by simply assuming that forward speed results from the summed excitation of both hemisphere motor commands, while turning velocities results from the difference between left and right excitation (Figure 4). Certainly, we do not exclude that more complex circuitry could produce other regimes of covariations, but our simple model shows that this particular relationship between forward and angular speed is robust to parameter change (Figure S5), and thus can readily emerge from the LAL. However, the oscillations'

amplitude and frequencies vary with parameter change, at least across a factor of 2 (Figure S5). Therefore, we can easily envision how various inputs into the LAL (such as pictured in Figure 5) could modulate the amplitude and frequency of the emerging oscillations, without altering the fundamental relationship between forward and angular velocities. For instance, inputs from the central complex such as PFL2 neurons project bilaterally to the LAL[47,130,319] and could thus promote the overall modulation of oscillations amplitude as shown here. Inversely, PFL3 neurons, which project unilaterally to the LAL, could mediate lateralised information, whether from memorised views [63] or path integration[133,134] to bias the oscillations toward one side[47]. Understanding precisely how such inputs interact with oscillations in insects opens the door to a complexity that would be too vast to tackle here, but given the rapid development of neurobiological tools and knowledge about the circuitry of the lateral accessory lobes, this may constitute a realistic endeavour in the near future.

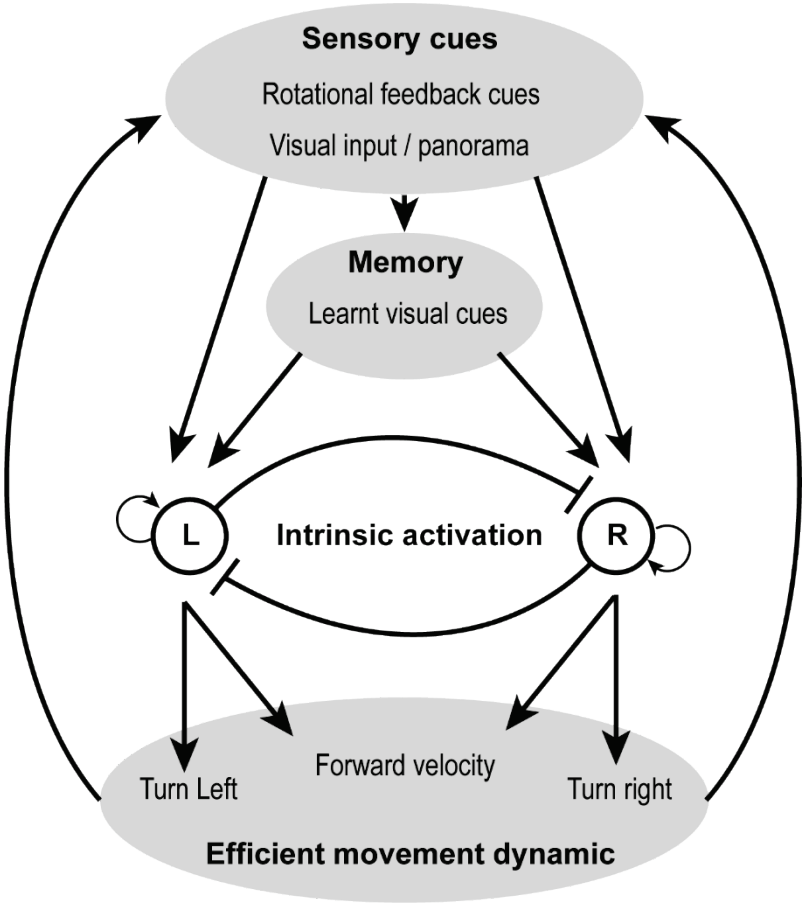

Figure 5. An intrinsic oscillator at the core of visual navigation. We propose a simple scheme to encompass our results. In this view, sensory input (in this case various innate and learnt visual information) act on behaviour only indirectly, through the systematic modulation of an intrinsic oscillator. The latter ensures that an efficient movement dynamic is preserved across navigational contexts, which would not necessarily be the case if various and potentially conflicting sensory information were directly modulating movement. This scheme also highlights the idea that action is not merely the product of perception. At the core of behaviour lies an intrinsic, self-generated dynamic, which are modulated, rather than controlled, by sensory perception.

STAR methods

Study Animal & Experimental site

All experiments took place within an open grassy woodland at the National Australian University, Canberra from Feb. to Mar. 2019. We had the opportunity to work with two Australian endemic ant species: *Myrmecia croslandi* and *Iridomyrmex purpureus*. *Myrmecia croslandi* workers are known to forage solitarily, with each individual either hunting on the ground in the vicinity of the nest or navigating routinely back and forth toward the same favorite foraging tree throughout her life span[149]. These ants rely mainly on learnt terrestrial visual cues to navigate but are also able to resort to PI when the visual environment does not provide guidance[148–150,297]. Eight nests of *M. croslandi,* that foraged on two distinct trees between 6.0 and 30.0 m away from the colony, were used in this study. *Iridomyrmex purpureus* ants form large colonies and forage along pheromone trails that lead to food patches. Despite employing pheromone trails for recruitment, this species also uses both learnt visual information and path integration for navigation[298]. We also performed navigational experiments with two *I. purpureus* nests to ensure that this species relies indeed on both learnt visual terrestrial cues and path integration, which they did surprisingly well (see Figure S1). For the main experiment, a feeder was placed 7.0 m away from the nest and foragers were free to familiarize themselves with the route for 72 h before being tested.

Trackball system and data extraction

During tests, ants were mounted on a trackball device[300]. This device consists of a polystyrene ball held in levitation in an aluminum cup by an air flow. The trackball has two sensors placed at 90° to the azimuth of the sphere, which record the movements of this sphere and translate them into X and Y data retracing the path of the ant. The X and Y acquisition of the trackball rotations happened at a 30 Hz frequency (i.e., 30 data points per second), enabling us to reconstruct the ant's movements with high precision. Additionally, a camera (640×480 pixels) recording from above provided details of the ant's body orientation, also at 30 Hz. We also

analyzed *M. croslandi* learning walks recorded directly on the natural ground. Head directions were obtained via video recordings at 25 Hz (provided by Jochen Zeil).

In this study, we used two different trackball configurations to record the ants' motor responses: further referred to as 'Free ant' and 'Fixed ant' experiments, respectively.

Free ant experiments: two small wheels prevented the polystyrene ball from rotating in the horizontal plane, however, all other degrees of freedom of the ball rotation were accessible (Figure S2 A; 'closed-loop'[300]). Ants were attached on top of the ball by putting magnetic paint on their thorax and a micro-magnet fixed at the bottom end of a single dental thread that was in turn attached to a 0. 5 mm pin. Crucially, the pin was placed within a glass capillary. This procedure enabled the ants to execute physical rotations on the ball (the ball is not rotating horizontally) but prevented any translational movement. Ants could thus execute body rotations and control the direction in which they faced but any attempt to go forward or backward resulted in ball rotations. We used the recorded videos to manually track the ants' body orientation through time using the free software Kinovea (v-0.9.1).

Fixed ant experiment: the two small wheels were no longer in place. Hence, the ball could now turn in any direction, including the horizontal plane (Figure S2B; 'open-loop'[300]). Ants were tethered directly to a needle with a micro magnet (glued at the end of the needle) and magnetic paint on their thorax. The top end of the needle was glued to a small piece of paper sheet (0.5×2.5 cm). Consequently, the fixed ant could no longer rotate, and the experimenter could choose in which direction individual was facing. Any attempt to move, including turning, by the ants resulted in ball rotations. This trackball configuration was only conducted with the more robust *M. croslandi*.

Free ant experiments: protocol

At the start of each test, the ant was mounted on the trackball device but surrounded by an opaque cylinder (30×30 cm) that prevented the ant from seeing any cues from the visual scenery around her. Once the ant was in place on the device, the whole apparatus was moved to the desired test location in the field. Afterward, the surrounding cylinder was removed, revealing the visual scenery to the ant and data recording began. To ensure a high level of homing motivation, only individuals who had previously received a 40% sucrose solution (for

M. croslandi) or a food item (for *I. purpureus*) were tested. The recording period was 3.5 min for the robust *M. croslandi* and 1.5 min for the flimsier *I. purpureus*.

To test the impact of terrestrial visual cues on the oscillation behavior, ants were tested under three distinct conditions.

Familiar (F): ants were tested along their habitual route, which therefore presents a familiar visual view.

Unfamiliar (U): ants were tested at least 50 m away from the habitual route, which therefore presents an unfamiliar panorama.

Dark (D): ants were tested in total darkness, within an opaque cylinder (30×30 cm) covered with a red Plexiglas plate that transmitted only the low red wavelengths, which ants cannot perceive[49,320].

To test the impact of PI on oscillation behavior, ants were tested as either full- or zero vector ants. Full vector (FV): ants were caught at the start of their inbound trip to the nest (i.e., at the foraging tree for *M. croslandi* and at the feeder for *I. purpureus*). FV ants have an informative homing PI vector, which points in the food-to-nest compass direction. Consequently, FV ants can rely on both PI vector and the learnt visual scenery while being tested. Zero vector (ZV): homing ants were captured just before entering the nest, that is, at the end of their inbound trip. Hence, their PI homing vector is reduced to zero and thus no longer directionally informative. Consequently, ZV ants can only rely on the learnt visual scenery while being tested. For each of the three visual conditions FV and ZV ants were tested, resulting in a total of six conditions.

For *I. purpureus*, at least 16 ants were tested in each of the six conditions (F: FV&ZV =16; U: FV&ZV =17; D: FV=16 & ZV=17). Since *I. purpureus* forms very populous colonies with an abundance of foragers, all individuals were tested only once, in one of the six conditions. The data obtained are therefore statistically independent. On the contrary, *M. croslandi* forms sparsely populated colonies and individuals usually make only one foraging trip per day[149]. Thus, it is time-consuming and challenging to capture, mark and follow individuals throughout foraging trips. Individuals were therefore captured (either at the foraging tree (FV) or before reaching their nest (ZV)) and tested successively in a pseudo-random order in all three visual panoramas: Familiar (F), Unfamiliar (U) and in the Dark (D). Both the sequence in which the visual conditions were experienced and the individuality were

included in the statistical models as it is likely that the state of the PI vector will be modified across successive tests. Overall, 32 *M. croslandi* ants were tested with some individuals tested as ZV or FV ants on two different days. At least 16 *M. croslandi* ants were tested in each of the six conditions (F: FV&ZV =17; U: FV&ZV =17; D: FV=17 & ZV =16). Overall, 101 recordings were obtained.

In the 'free ant' experiments, the ant's body axis can turn without the ball movement. We used the recorded videos to manually track the ants' body orientation through time using the free software Kinovea. We removed the first 3s of recording of each ant as the removal of the opaque ring may have disrupted the behavior. Overall, the analyzed recording length was 100s (except for two ants: 84 and 99s) for *M. croslandi* individuals and 50s (except for two ants: 49s) for *I. purpureus* ants. For details of the Fourier analysis (see below); nine paths of *I. purpureus* were discarded (F FV=1, U FV = 1, U ZV =2, D FV =2, D ZV = 3) as the ants displayed too many pauses.

Fixed ant experiments: protocol

To test if oscillations are due to an intrinsic oscillator or caused by the fact that ants try to keep a bearing toward an external stimulus, we conducted an additional experiment on *M. croslandi* ants. We recorded foragers without an informative integration vector (ZV) in the same unfamiliar environment (U) as before. Ants were tested in eight different fixed orientations, covering the 360° azimuth by bins of 45°; and with one direction corresponding to the food-to-nest compass direction. Each ant was tested in all eight orientations in a pseudo-random sequence. To change the ant's orientation, the experimenter would first place the opaque cylinder (30×30 cm) around the trackball system to prevent the ant from perceiving the visual panorama, then rotate the whole set-up (trackball and mounted ant) and finally remove the opaque cylinder to re-start data collection. Ants were recorded for at least 15s up to 20s in each orientation. Eleven ants were tested in all eight orientations. Since the ants were fixed, trackball rotations along the horizontal axis provided a direct measure of the angular velocity of the attempted turn generated by the ant. Angular velocity time series were then extracted from the trackball data. At the end, the available length of the recordings for the analysis had 512 frames (~17s) except for 5 individuals (294,394,456,474,494 frames). It should be noted here that prior to the Fourier analysis (see below) we added a series of 0s (zero padding) at the end of the time

series until it had a length of 3000 data points to match the same recording length obtained in the free ant experiment). This permits to increase the precision in the frequency range obtained from the Fourier analysis.

Quatification and statistical analysis

All statistical analyses have been run using the free software R (v 3.6.2. R Core Development Team). For all statistical tests, the p-values were compared to the critical alpha risk at 0.05, with the appropriate correction if needed. Statistical parameters mean and the associated standard error is given within the text and/or on figures: N represents the number of individuals (sample size).

Fourier analysis

To reveal the occurrence of regular lateral oscillations, we choose to focus on the angular velocity value (Figure S2C), which constitutes a direct reading from the left/right motor control. This time series was processed through three successive steps to obtain its 'spectral density', according to the Wiener-Khinchin theorem. First, the signal was parsimoniously smoothed with a moving median running of a length of five frames (0.17s) to reduce the influence of the recording noise (Figure S2D, dashed blue line). Then, the recorded time series was passed through an autocorrelation function (Figure S2D). Finally, a Fourier transform was performed on these autocorrelation coefficients, providing the power spectral density (Figure S2E). With this approach, the magnitudes obtained are independent from angular drift and amplitudes of the oscillations and thus can be directly compared across individuals. A high magnitude indicates a strong oscillation for a given frequency. For each individual, the dominant frequency (i.e., presenting the highest peak magnitude) and its magnitude were extracted (Figure S2E, dashed blue lines). To check whether these magnitudes indicate a significant regular oscillation, we compared them to the average spectral density magnitude resulting from 200 Gaussian white noise signals of the same length (within each species and experiment). Gaussian white noise signals were obtained by drawing a sequence of random values drawn from a normal law. These simulated signals were then processed through the exact same operations as the ants' angular velocity recording: namely smoothing,

autocorrelation, Fourier transformation and extraction of the highest peak magnitude. The mean of the 200 highest magnitudes obtained was then compared to the real ants' equivalent magnitudes with a Wilcoxon one-tail test. As each experimental group has been compared with this mean magnitude of the simulated angular velocity signal, the p-value is subsequently adjusted using the Bonferroni correction.

Average oscillatory cycle

To extract the average dynamics of an oscillation cycle, the mean cycles at the individual and population levels were reconstructed as follows. First, we smoothed the angular velocity time series of each individual by running twice a median with a window length of 31 frames for *M. croslandi* (for both free and fixed experiments), 25 frames for data during learning walks on the natural ground and seven frames for *I. purpureus*. This window length is much smaller than one oscillatory cycle and thus smoothens the data without altering the cycle general dynamics (Figure S2 F). Second, we indexed moments when the time series crosses 0 (from – to +) as t_0; and extracted data within a window of ±90 frames around the t_0 indices (±60 frames for *I. purpureus*; Figure S2 F). We then reconstructed a mean cycle for each individual by averaging the individual's extracted windows, aligned at t_0 (Figure S2 G). The individuals' average forward speed dynamics during one cycle was obtained in the same way by using the same indices t_0 obtained from the angular velocity data (Figure S2 H). For each ant, the mean angular velocity peak and amplitude of forward velocity cycles were extracted for analysis. Finally, we reconstructed the average cycle at the level of the population by averaging the mean cycle of all individuals. Note that to do so, each individual's mean cycle was first normalized to show similar amplitudes (mean_cycle_normalised = mean_cycle/mean|mean_cycle_values|). The goal was here to observe the cycle dynamics through time and not to estimate the inter-individual variation in amplitude, which was analyzed previously using the individual's mean cycle amplitude. Note that the criterion used to align the time series (the change from a left to a right turn) necessarily creates an artefact in the averaged angular velocity obtained. Namely, an average change from left turn to right turn at t_0. However, several factors indicate the relevance of such pooling at the population level: (1) the period of the average cycle corresponds to the mean frequency obtained from the Fourier transform. (2) we can observe a significant reversal of the angular velocity before and after the mean oscillation cycle. (3) the

associated forward velocities co-vary in a significant way, indicating the existence of conserved dynamics.

Analysis of the ants' direction of movement

We reconstructed the ant paths of time that derived from the trackball recording for a fixed period to determine the mean direction of movement (mu) as well as the mean circular vector length (r, a measure of dispersion) of each individual. The mean directions (mu) were analyzed using a Rayleigh test (from R package: Circular) that also includes a theoretical direction (analogous to the V-test). To test whether the angular data are distributed uniformly as a null hypothesis or if they are oriented toward the theoretical direction of the nest as indicated by the state of the PI or the familiar panorama, the average vectors lengths (r) were analyzed via a Wilcoxon-Mann-Whitney test with a Bonferroni correction for multiple testing.

Analysis of optimization

To investigate the benefit of variation of forward and angular velocities signal on the overall ground distance covered we reconstructed for each individual a fictive path where forward speed was maintained constant (we took the average forward speed, so that the total distance walked remain the same as in the original path). To estimate the overall ground distance covered for a given path, we computed a 'global trajectory' by smoothing the path with a sliding window, until effectively removing the oscillations component (Figure 4B grey paths). To estimate the actual benefit of variation of forward speed on the distance covered, we compared the length of the 'global trajectories' between the fictive path (with constant forward speed) and original path (Figure 2D, E). A ratio >1 mean that the original path covered more ground distance, and vice versa. Ratios were compared with Wilcoxon one-tail test to the threshold one.

To test for an effect of the familiarity and vector on the distance covered we calculated an 'Effectiveness ratio' for each individual as the ratio between the length of the 'global trajectory' / 'actual distance walked' on the original paths with oscillations (Figure 2D, F). To enable a fair comparison across individuals, we computed the "effectiveness ratio" on a 100s portion of paths, using an additive mixed model.

Statistical models

For the free ant experiment, two types of models were tested: the first considering the interaction between visual panorama and vector modalities, the second with simple additive effect. It should be noted here that in case of deviation of the residuals of these models from normality and or homoscedasticity, the response variables have been transformed. Only the model presenting the lowest Akaike information criterion was retained and subsequently analyzed via an analysis of variance (Anova), followed by a post-hoc analysis of Tukey's rank comparison. Finally, for *M. croslandi* whose individuals were tested across several conditions, the models are mixed models that controlled the sequence and the individuality effect as random variable. For some models, we removed the sequence effect because of a singularity problem of this factor (i.e., the information given by this variable is already contained in other variables). For fixed ant experiments (which were tested only as ZV ants in an unfamiliar environment), the model analyzed the effect of the condition of the subsequent rotations.

Computational model

The computational model presented in Figure 5 has been built and run using Matlab® R2016b. The code is open access and available at :
https://github.com/awystrac/Neural_oscillator

It is a step-based model (‘For loop’). Two neurons (Left and Right neurons) reciprocally inhibit each other, while trying to maintain a baseline activity through self-excitation and internal feedback.

Variable	Description
L	Left neuron activity
R	Right neuron activity
LNF	Left neuron internal feedback
RNF	Right neuron internal feedback

Parameters	Description
W	Reciprocal inhibition synaptic weight
Baseline	Firing rate of the oscillator neurons without any external modulation (default at 0.5)
Exhaust rate	Rate at which the negative internal feedback is modulated between each time step
Noise	Standard error of the normal distribution of the noise added to the activity of the neurons of the oscillator (default at 0.1)

Initialization

R_1= random (0to1)

L_1 = random (0to1)

$RNF_1 = 0$

$LNF_1 = 0$

At each time step

L and R neuron update their activity due to their self-excitation, internal feedback, inhibition from the other neuron, and noise.

$$L_{t+1} = L_t - LNF_t - (R_t \times W) + (random(-1\ to\ 1) \times noise)$$

$$R_{t+1} = R_t - RNF_t - (L_t \times W) + (random(-1\ to\ 1) \times noise)$$

Set a hard limit to the activity both neurons.

$$LM_{t+1} = \begin{cases} L_{t+1} & if\ L_{t+1} > 0 \\ 0 & if\ L_{t+1} \leq 0 \end{cases} \qquad RM_{t+1} = \begin{cases} RM_{t+1} & if\ R_{t+1} > 0 \\ 0 & if\ R_{t+1} \leq 0 \end{cases}$$

Update the internal negative feedback for the left and right motor neurons. The internal feedback changes proportionally to the difference between its own activity and the neuron activity (relative to the baseline activity)

$$\mathrm{RNF}_{t+1} = \mathrm{RNF}_t + \text{Exhaust rate} \times (\mathrm{R}_{t+1} - \mathrm{RNF}_t - \text{Baseline})$$

$$\mathrm{LNF}_{t+1} = \mathrm{LNF}_t + \text{Exhaust rate} \times (\mathrm{L}_{t+1} - \mathrm{LNF}_t - \text{Baseline})$$

Computation of the angular and forward velocities

Angular_velocity = R - L

Foward_velocity = R + L

Acknowledgments

We want to thank the Australian National University and particularly Jochen Zeil, Zoltán Kócsi and Trevor Murray for their advice and technical support. We also thank Hansjürgen Dahmen for providing us with the trackball system and Ajay Narendra for his incredible knowledge about the local Australian ants. We are grateful to all these people for their helpful advice. We also thank Jochen Zeil, Paul Graham and Michael Mangan for their helpful feedback on the manuscript. We are grateful Jochen Zeil to have provide the data about learning walk. Finally, we thank the ants tested in these experiments for their participation.

Funding:

European Research Council, Grant reference number: EMERG-ANT 759817, Author: Antoine Wystrach.

Supplemental information

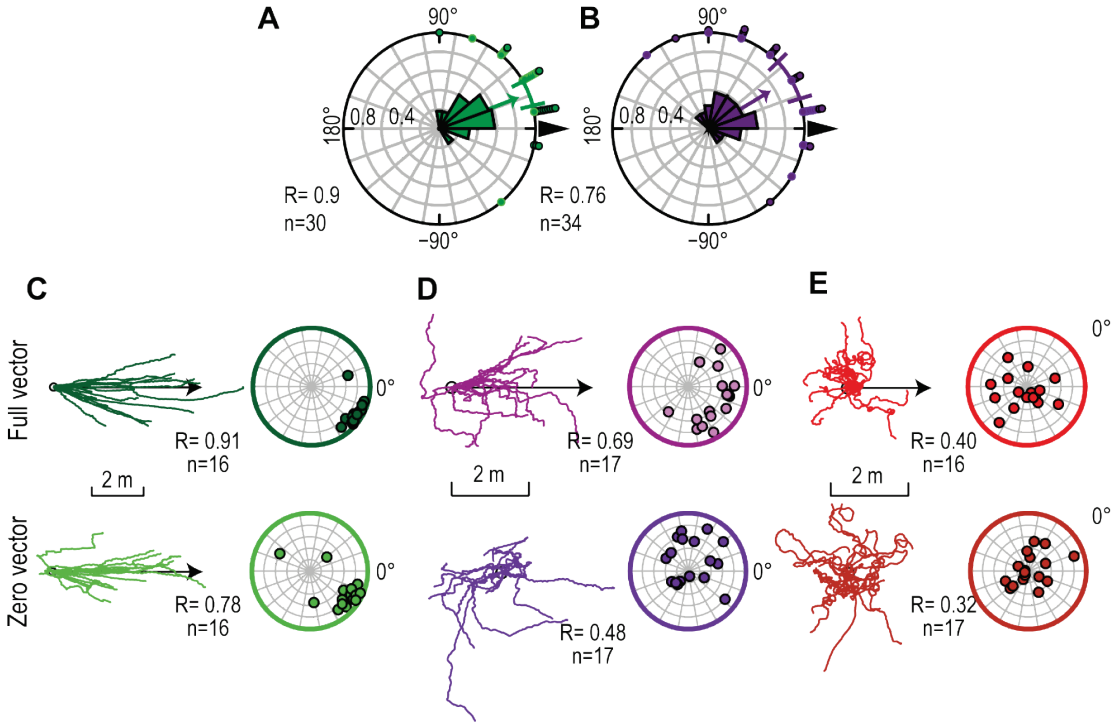

Figure S1: The meat ant *Iridomyrmex purpureus* uses both visual and celestial cues to navigate, related to Figures 1 A-C. (A-B) Ants were released at the center of a goniometer divided in 18 sectors (20° each) either in a familiar (green) or unfamiliar (purple) surroundings. The taken directions of the tested ants were recorded at two points. (A) Circular histogram depicting the directional decisions of tested zero-vector (ZV) ants (without informative integration vector) in presence of familiar surroundings. (B) Circular histogram depicting the directional decisions of tested full-vector (FV) ants (with informative integration vector) in unfamiliar surroundings. The arrow corresponds to the mean vector of the distribution. The 95% confidence interval of the mean is displayed as a coloured arc. Each dot corresponds to one corrected direction obtained from one individual. after several tested individuals, the goniometers were rotated (180°) to prevent the use of chemical trails. Dots with a black rim are data recorded before rotation of the goniometers and the dots without black rim after rotation. (C-E) Path of ant reconstructed over 25 s from the trackball, in a familiar ((C) green) or an unfamiliar panorama ((D) purple) and in the dark ((E) red). For each condition, individuals were tested either as FV- or ZV vector ant. The first column of each condition shows the paths oriented to the theoretical direction of the nest (arrow). In the second column, each dot indicates the average circular vector calculated over the entire path of an individual, showing the mean direction and the average vector length (i.e., a point closer to the periphery indicates straighter paths). The R values indicate the length of the average resulting vector of the population. In all graphs, the direction (in familiar terrain) or theoretical direction (for FV in unfamiliar terrain) of the nest is set at 0°. The results show that ants in presence of familiar panorama were oriented toward their nest irrespectively of the PI state (FV or ZV) (Rayleigh test: on goniometers (A): $p<0.001$; path displayed on the trackball (B): ps = FV & ZV < 0.001). Secondly, when tested in unfamiliar surroundings, FV ants followed their PI vector (Rayleigh test: on goniometers (B): $p<0.001$; path displayed on the trackball (D, first row): p = FV < 0.001). But ZV ants (Figure 1D second row) showed random orientations (Rayleigh test p: ZV=0.672). Finally, ants displayed randomly orientated paths in all darkness conditions (Figure 1E; Rayleigh test p: FV=0.213, ZV=0.866). Overall, these results demonstrate that this species use learnt terrestrial cues as well as their PI to navigate when released on the goniometers or mounted on the trackball system. Therefore, in both experiment this species does not only rely on chemical trails but also on the visual panorama and the path integration during foraging.

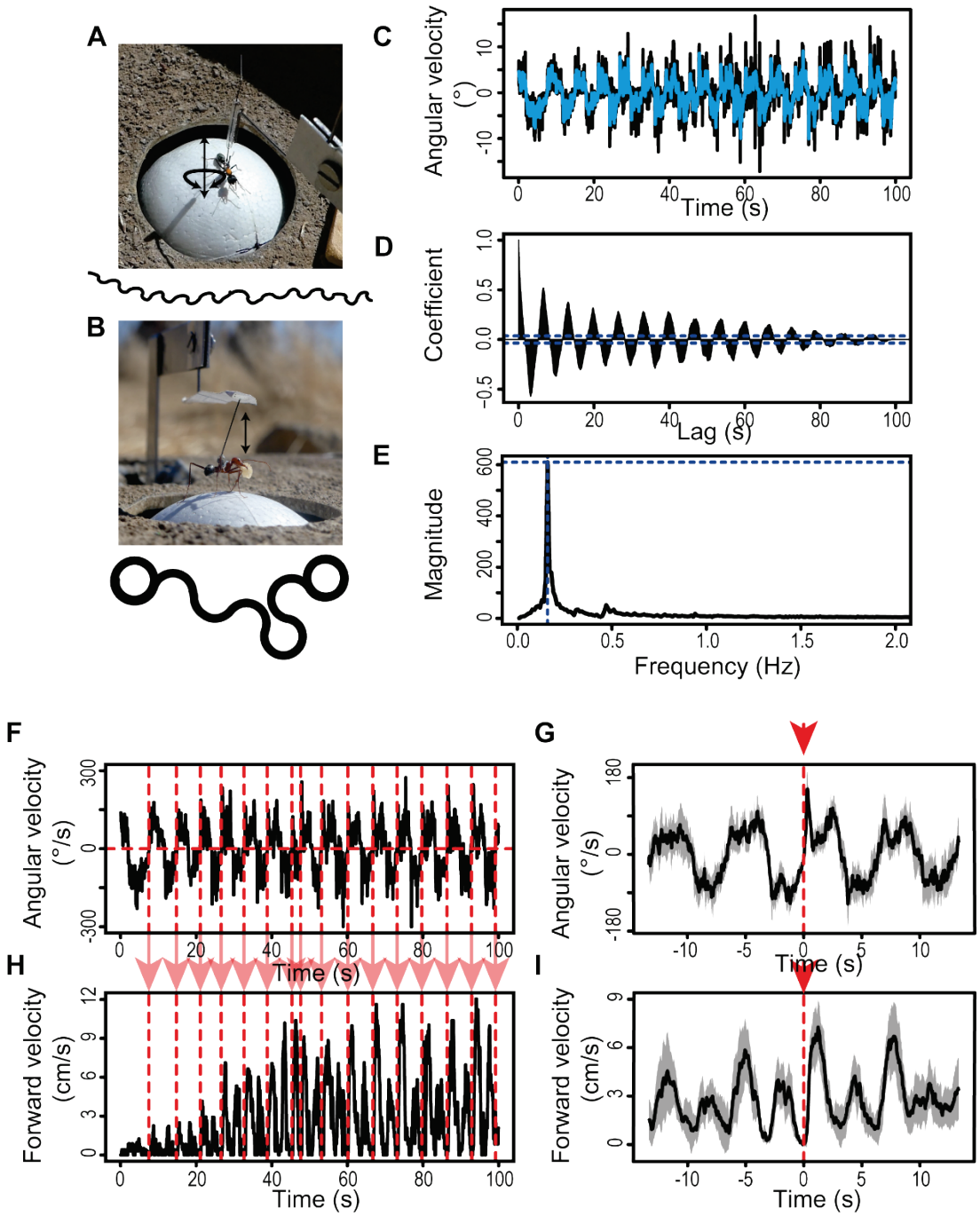

Figure S2: Trackball set-ups, recording and processing of the ants' trajectory, related to Figures 1-3 and STAR Methods. (A) Trackball set-up for 'free ant experiment' (top view). Two wheels prevent the sphere from rotating along the horizontal plane. Ants are free to rotate their body along the yaw axis to control in which direction they perceive the world. (B) Trackball set-up for 'fixed ant experiment' (side view). The two wheels have been removed, so the ball can turn in every direction. Ants are fixed in a way that prevent body rotations along the yaw axis, so they are forced to keep their bearing in the imposed direction. For A and B an example path has been plotted below the picture. (C) Angular velocity signal over time (recorded at 30 readings/s) in an individual of the species *M. croslandi* (black) with smoothed signal superimposed (blue). (D) Autocorrelation carried out on the entire smoothed angular velocity signal. (E) Fourier transformation of the autocorrelation coefficients signal (shown in

D) provides the ‘spectral density’. This approach has the advantage to provide magnitudes that are directly comparable between individuals. For each individual, the frequency peak with the highest magnitude was extracted, indicating a strong oscillation of the angular velocity signal at that frequency (dashed blue lines). F-I Methodology to obtain an average oscillation cycle. (F) We used the angular velocity signal to flag moments when the signal crosses 0 and goes up to positive angles (vertical dashed red lines). (G) We extracted portions of the signal of ±3s (large enough to contain a full oscillation cycle) around each of the flags, aligned them at flag = t_0 and averaged them to obtain the individual’s average cycle (±95% confidence interval in grey) of the angular velocity signal. (I) The individual’s average cycle for the forward velocity signal was achieved using the angular velocity flags (vertical dashed red lines as in F) on the forward velocities (H).

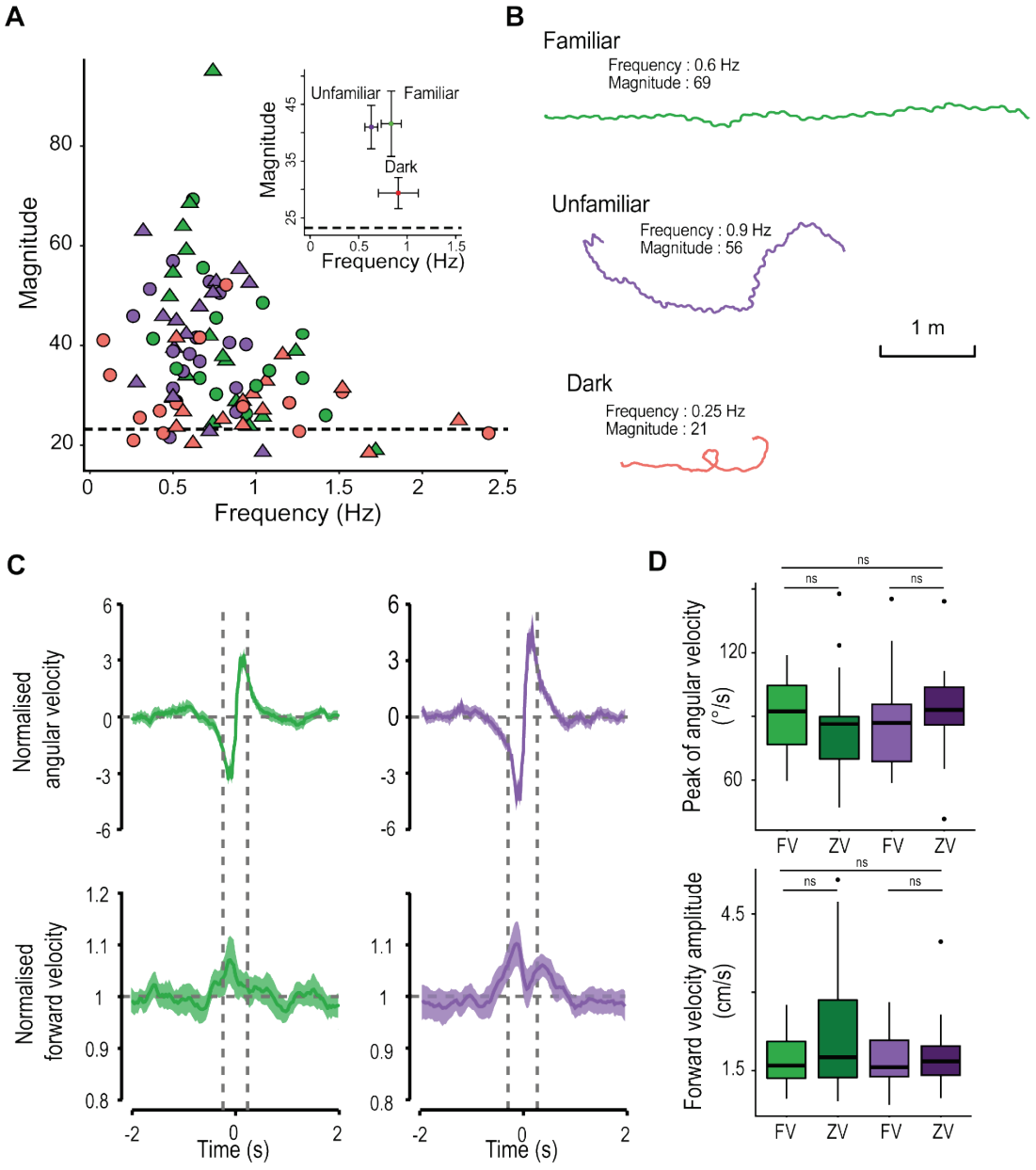

Figure S3: Oscillation characteristics across visual conditions, related to Figures 1-2. Individuals were tested within a familiar panorama (green), an unfamiliar panorama (purple) or in the dark (red). (A) shows the frequency and spectral density magnitude of the dominant oscillation (highest magnitude) (A) (for method see Star methods and Figures S2 F-I). High frequencies indicate a fast-oscillatory rhythm and high magnitudes indicate a strong presence of this oscillation. Symbols indicate whether the state of the path integration vector was full (round) or set to zero (triangles). Inserts show the mean frequency against the mean magnitude of each visual condition with the associated 95% confidence interval around the mean. The dashed black line represents the mean of the spectral density peak magnitudes resulting from 200 Gaussian white noise signals. Magnitudes were higher than those obtained with the spectral density of a Gaussian white noise ((A) dashed line; Wilcoxon one-tail test: ps≤0.01), showing that ants displayed lateral oscillations with a higher regularity than random. Analysis reveals that the regularity differ between visual panoramas with ants tested in familiar and unfamiliar terrain yield more regular oscillations than in the dark ((A) Anova: $F_{2,90}$=10.038, p < 0.001, F vs U = p>0.96, df=86, mean±se: $F_{(FV+ZV)}$ =41.59± 3; $U_{(FV+ZV)}$ =41±2 ; D vs U or F = p< 0.001,

mean±se: $D_{(FV+ZV)}$=29.4±×1.45). However, independent of the PI state, ants showed a tendency to oscillate quicker in familiar than in unfamiliar terrain (ps ≥ 0.180, mean±se: mean±se: F(FV+ZV) =0.83±0.056 Hz; U(FV+ZV) =0.63±0.037). (B) shows an example path for each condition across 83 s.(C) Population-average cycle (see Star methods and Figure S3) shows how angular and forward velocities co-vary. Angular velocities (top-row) and forward velocity (bottom row) co-vary in a way that is conserved across conditions: when on familiar route (green) or in unfamiliar terrain (purple). Population cycles have been reconstructed by merging full- (FV) and zero-vector (ZV) data and normalising the data amplitude within the individual's average cycle. Colour areas around the mean curves represent the 95% confidence interval, based on the inter-individual variation. Dashed lines represent the moment when the ants are facing their overall direction of travels. Angular velocities (top-row) and forward velocity (bottom row) co-varies in a way that seem conserved across experimental conditions and species (see Figure 3). (D) Boxplots show the actual distribution of the non-normalized mean peak of angular speed and forward velocity amplitude for the individuals' average cycle (FV on the left, ZV on the right, N : F=31 (FV = 15, ZV = 16); U =31 (FV = 16,U ZV =15). The mean peak of angular velocities and forward velocity amplitude underlying the oscillations are rather constant across navigational context ((D), (ps >0.05)). Therefore, there is no clear effect on the amplitude of oscillation display within the path (A, B).

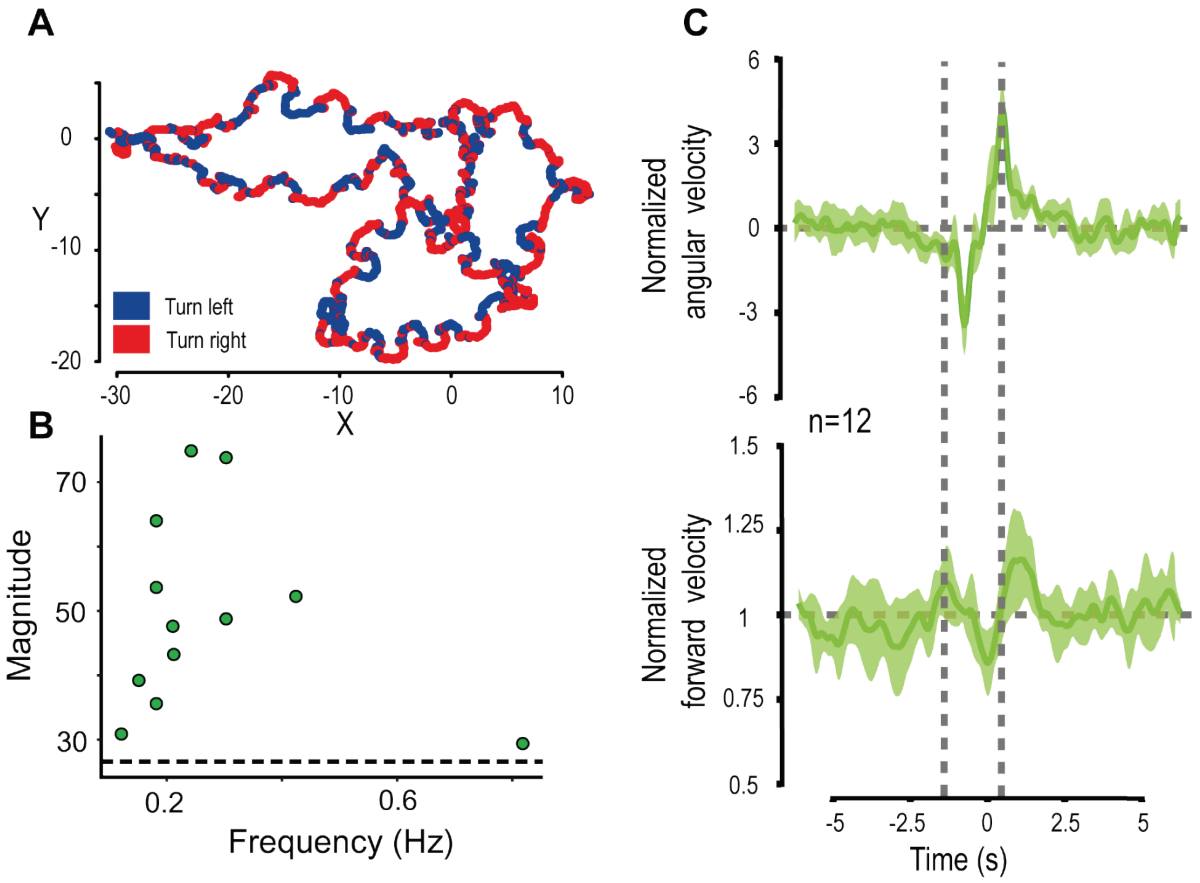

Figure S4. Ant learning walks show similar dynamics of oscillation, related to Figures 1-2. Ants path and head orientation were recorded (25 Hz) during their learning walks directly on the ground (courtesy of Jochen Zeil, see Jayatilaka et al, 2018). (A) Example path of an individual showing clear alternation between right (red) and left (blue) turn. (B) Frequency and spectral density magnitude of the dominant oscillation (highest magnitude) of angular velocities times series of 25s (for method see Star methods and Figures S2 F-I). Magnitudes were higher than those obtained with the spectral density of a Gaussian white noise ((A) dashed line; Wilcoxon one-tail test: $p \leq 0.001$). (C) Angular velocity (top-row) and forward velocity (bottom row) co-vary in a similar way than when recorded on the track ball (see Figure 3). Population cycles have been normalised by the data amplitude within the individuals mean cycle (see Figure S*3* for example). Colour areas around the mean curves represent the 95% confidence interval, based on the inter-individual variation. The natural learning walks showed regular oscillations as well as the same dynamical relationship between angular and forward velocities than trackball data. Ants walking on the ground also tend to increase their forward velocity when they are aligned with their general direction of travel.

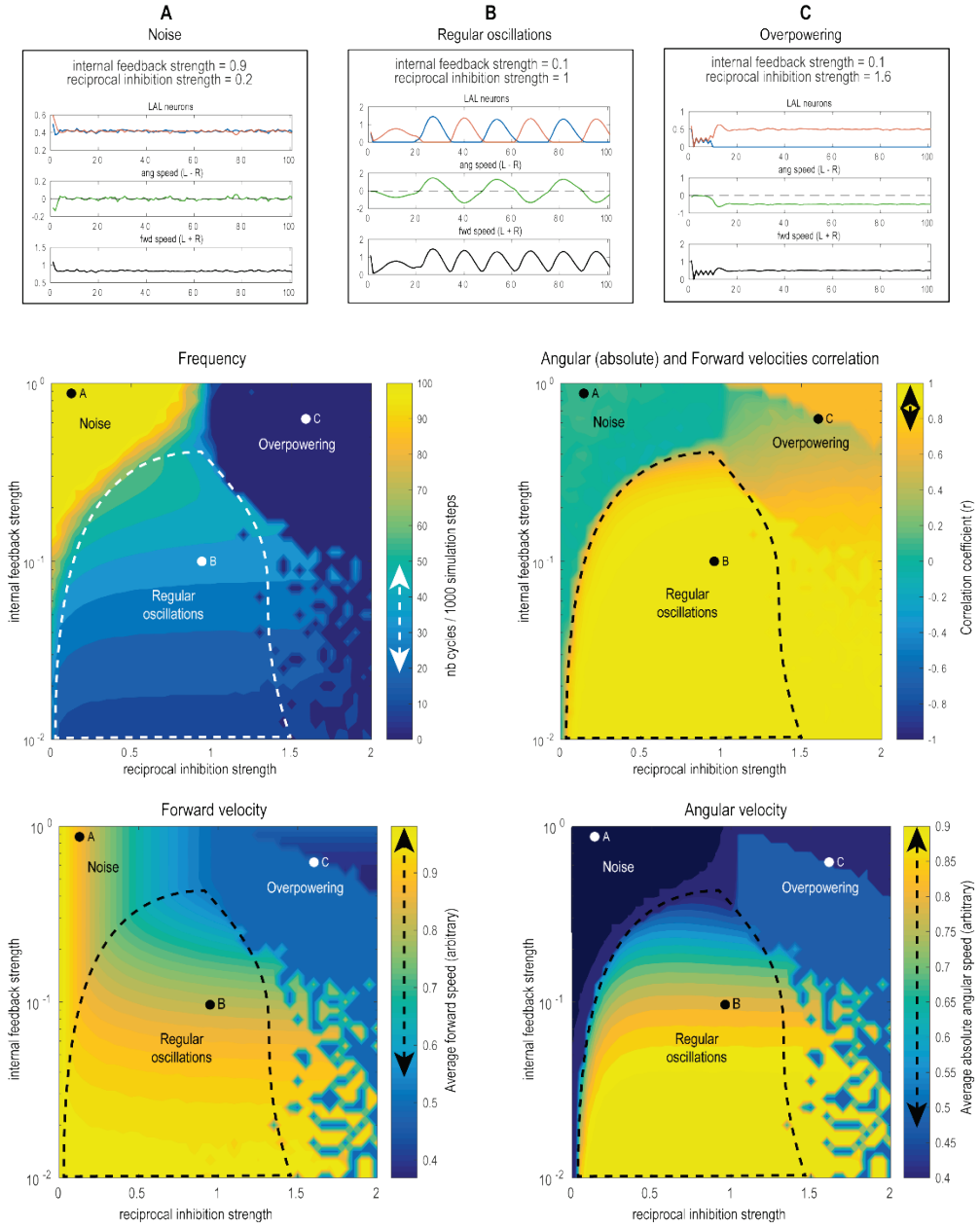

Figure S5. The covariation between angular and forward velocity is robust to parameter change, related to Figure 4. Exploration of our abstract LAL model's (Figure 4) sensitivity to change in the two free parameters (inhibition strength and internal feedback strength). Regular oscillations between LAL neurons emerge in a wide space of parameters (functional range delineated by the dashed line, an example for a given parameter set (dot) is shown in (B)). While frequencies (right of middle row), forward and angular velocities (bottom row) can vary roughly across a factor 2 across the functional parameter range, the correlation between absolute angular and forward velocity is constrained around 1 (dashed arrows in the colour bars indicate the variation in the functional range). This positive covariation indicates that the agent slows down (low forward velocity) when reversing turning direction (low absolute angular velocity) and accelerates (high forward velocity) in between, that is when sweeping past its general direction of travel. Outside of this functional range, regular oscillations disappear for extreme parameter sets. For instance, if one neuron overpowers the other due to too strong reciprocal inhibitory strength (C, overpowering); or inversely, due to the absence of reciprocal inhibition (strength <0.01) or a too strong internal adaptation preventing the neurons to modulate their baseline activity, and thus resulting in noise (A).

Chapter III

Is this scenery worth exploring? Insight into the visual encoding of navigating ants.

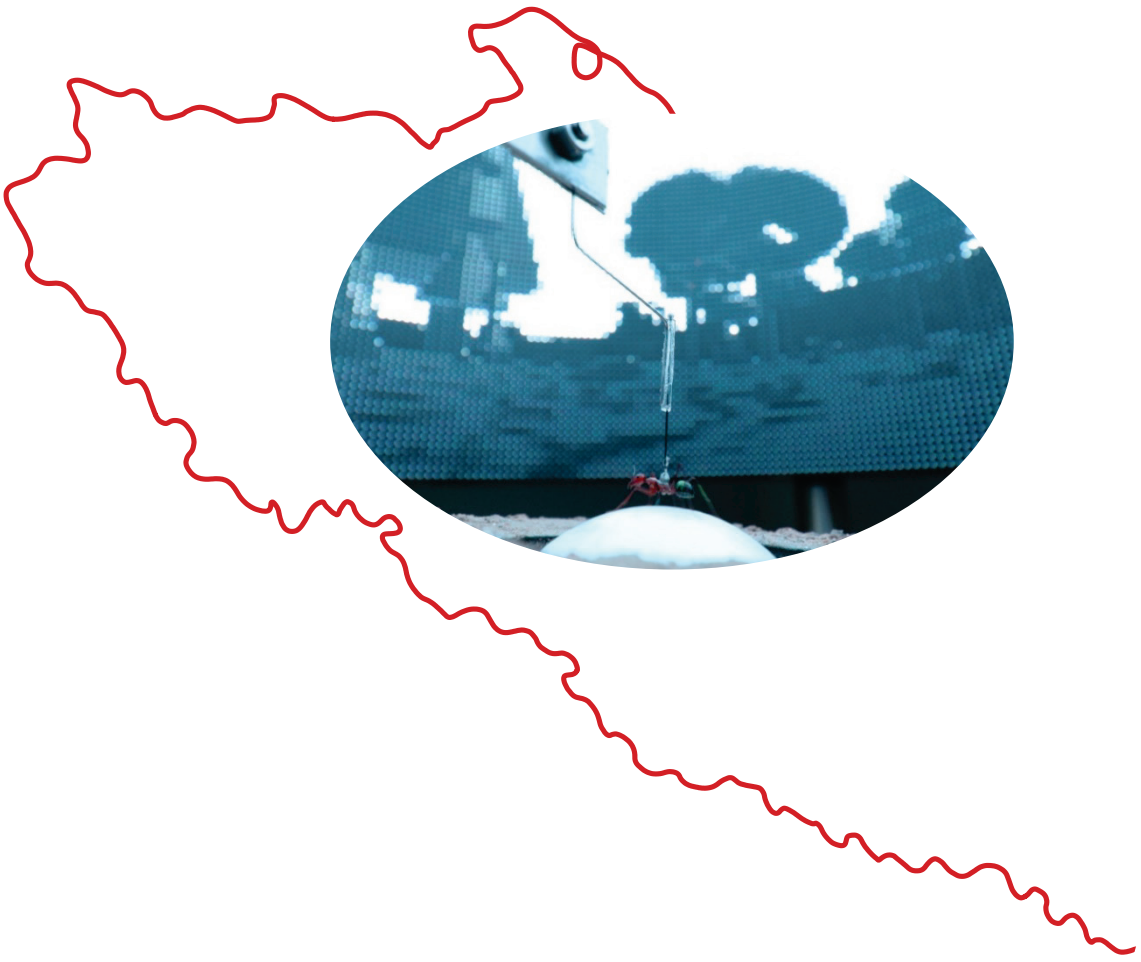

Is this scenery worth exploring? Insight into the visual encoding of navigating ants.

Leo Clement*, Sebastian Schwarz*, Blandine Mahot-Castaing* and Antoine Wystrach*

*Centre de Recherches sur la Cognition Animale, CNRS, Université Paul Sabatier, Toulouse 31062 cedex 09, France

Abstract

Solitary foraging insects rely heavily on vision to navigate in their environments. Despite evidence of ants' ability to learn visual scenes, it is unclear what cues they encode to decide whether a scene is worth exploring at the first place. We conducted experiments using a virtual reality setup to understand what visual cues motivate the ants to explore their visual surroundings. We recorded the motor behaviour of solitary foraging ants *Cataglyphis velox* navigating in a virtual reality setup. We measured the ants' lateral oscillations, which they naturally display while navigating, in response to different visual scenes in both closed-loop and open-loop. Results show that the presence or absence of translational optic flow and parallax movements resulting from the ants' movements in the world have little impact on the ants' oscillations, however, rotational optic flow is key to regulate the oscillations' amplitude. Interestingly, the actual production of oscillations is independent of such dynamic cues, but is strongly dependent on the visual structure of the environment. Ants' oscillations are disrupted if the scenery contains only horizontal, only vertical or no edges. Inversely, if the sceneries contain both types of edges (horizontal and vertical) the production of oscillations is similar to a naturalistic panorama. The actual quantity of edges, the heterogeneity of the visual pattern across azimuths, the overall light intensity or the elevation of bright regions does not impact the oscillations. We conclude that ants use a simple but efficient heuristic to decide whether a visual world is worth exploring. The latter seems to be a matched filter, enabling ants to detect the presence of at least two different edge orientations.

Introduction

Desert ants possess exceptional navigation abilities. They acquire knowledge of long foraging paths that wind through the trees and bushes of their native surroundings. Numerous studies have shown that these insects use vision to navigate [12,15,20,71,72,75,137,139,140,140–144,282] .This view-based navigation is based on encoding the panoramic scenery as a unified representation rather than extracting individual objects [20,69,71,72,75,141,143,163,279,282].

Insect visual systems extract specific features [234] such as boundaries/edges [16,56,234,235], relative brightness and color [230,231]. The ant's behaviour suggests that they rely greatly on global cues [20] such as information from the skyline – the line between terrestrial objects and the sky [12,15,208,236] and the position of the center of mass of dark areas [162,230–233]. Finally, in addition to these static cues, bees, and wasps can use dynamic cues like translational optic flow for guidance [163,285].

Most of these studies exploited the heading behaviour of insects to investigate which cues they rely on. Indeed, the learnt or innate position of these features on the insect retina allow them to maintain their course and heading. Here we did not investigate which features are important for heading control, but which features needs to be present in the visual scene for the ants to trigger an exploration behaviour at the first place. In other words, do insects possess a 'matched filter' [321,322] that indicates that the surrounding visual scenery is worth navigating in?

We used a virtual reality (VR) setup to record the detailed motor behaviour of solitary foraging ant *Cataglyphis velox* placed in various visual sceneries. We quantified the lateral oscillations, which ants spontaneously display when navigating in unfamiliar natural environment [34,35,37,209], as a proxy for the expression of exploration behaviour. Results highlight the importance of the presence of specific static features, notably a diversity of edge orientations, to triggers production of regular oscillations. Dynamic features, such as rotational optic flow, turn out to be important for the oscillation's amplitude control but not for their production. Our findings are discussed in the light of the ants' neural circuits and visual ecology.

Results

To determine whether ants display regular lateral oscillations – that is, alternate between left and right turns at a steady rhythm – we computed the power spectral density (PSD) analysis of the ants' angular velocity signals, indicating the presence of rhythmic patterns in the time series (see methods, Fig. S1). The magnitude of the PSD Fourier peak, which represented the most prominent rhythm in the signal, reflects the regularity of the oscillations for a given frequency, with higher magnitudes indicating a more consistent rhythm. We also measured the frequency and the clarity i.e., magnitude of the oscillations.

Do ants oscillate in the VR with a naturalistic reconstructed environment

We first investigated whether ants would display oscillations in a realistic VR environment consisting of distal (skyline) and proximal cues (bushes, trees, rocks …).

Ants recorded in this naturalistic environment displayed oscillation visible by the naked eyes (Fig1. A). The highest PSD magnitudes obtained from the ant's signal were greater than those obtained from randomly resampled signals (Wilcoxon one-tail test: v =15, $p<0.001$; mean±se: naturalistic panorama = 179.938± 13.53; resampled signal = 108.102±0.494), indicating that ants displayed lateral oscillations with a higher regularity than would be expected by chance.

The peak frequency fell within the expected range of 0.1 to 0.54 Hz (Fig. 1D, J), consistent with previous observations in other insect species [209,229,301]. Importantly, this rhythm is 10 to 50 times slower than the ants' typical stepping frequency [302], showing that it was not a by-product of their walking gait but must result from another oscillatory mechanism [209]. Overall, these results confirm that ants produce regular lateral oscillations in this in naturalistic-looking virtual environment.

Dynamic visual cues are involved in the control, but not the production, of oscillations

In the previous experiment, ants were tested in closed loop with the environment, that is, the ant's movement generated translational and rotational optic flow, as well as parallax movements of the objects.

We investigated whether these dynamic cues are necessary to trigger regular oscillation by recordings ants with a static image of the same realistic looking environment. By doing so, the ants still perceived rotational optic flow caused by their own rotation on the ball, but did no longer experienced translational optic flow or parallax movements. In this situation, ants still displayed clear oscillations (Wilcoxon one-tail test: v =305, $p<0.001$). Angular and forward velocities were not impacted by the absence of translation, but the regularity of the oscillation was slightly lower, albeit not significantly, than when in close-loop (Fig. 1C; $F_{1,132}= 2.2464$, $p>0.05$; mean±se: naturalistic = 180±12; naturalistic fixed= 158±4) and the oscillations' frequency was significantly higher (Fig. 1D; $F_{1,132}= 10.801$, $p<0.01$). Suggesting that translational optic flow is implicated in the timing of turn alternation rather than their regularity.

We then tested the impact of rotational optic flow (ROF) on oscillation behaviour by comparing the ant behaviour in abstract visual sceneries consisting either only of vertical (with ROF) or horizontal (without ROF) stripes (Fig; S1B last row). The latter producing no ROF as the ant turns. In these abstracts environments, ants still display regular oscillations visible by the naked eye (Fig.1G, H; Wilcoxon one-tail test = ps< 0.05; means±se: horizontal: 119.535 ± 5.37; vertical : 130.504± 5.54; resampled signal both group = 107.505 ±3.89). The absence of rotational optic flow (i.e., with horizontal edges) dramatically increased the angular velocity (Fig.1K; $F_{1,56}= 10.54$, $p<0.001$, mean±se : horizontal : 52.776±1.323 °/s; vertical : 47.876± 1.433 °/s) and reduced the forward speed (Fig.1L; $F_{1,56}= 26.74$, $p<0.001$, means±se : horizontal : 3.86± 2.312 cm/s; vertical 5.285 ±2.504 cm/s), leading the ants to often execute full loops (Fig.1H). This confirms that ROF is involved in limiting the amplitude of the oscillation, as previously suggested [209,323]. However, the oscillations regularity and frequency were not different between vertical or horizontal edges (Anova, magnitude: $F_{1,56}= 2.01$, $p= 0.155$; frequency: $F_{1,56}= 0.139$, $p=0.708$), showing that the presence or absence of ROF does not impact the production of oscillation.

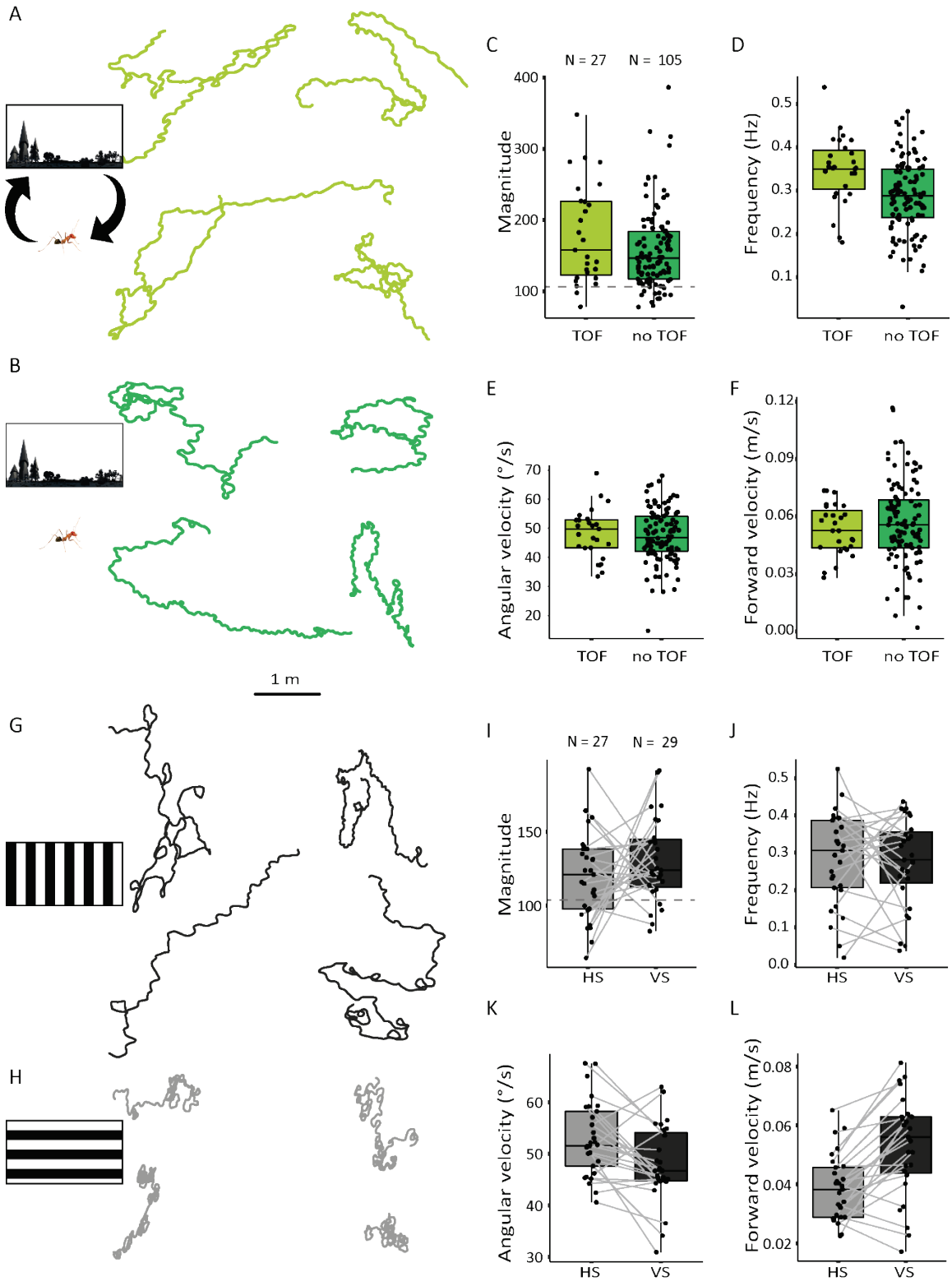

Figure 1. Ants do display regular oscillation in a naturalistic reconstructed environment. (A-B, G-H) Examples paths of four ants across 160 s recorded with translational optic flow (TOF; A, light green) and without TOF (B, green) or recorded in visual surrounding made of vertical (G, grey) and horizontal (B, light grey) stripes. (C-D; I-J) Distribution of the individual Fourier dominant peak obtained from angular velocities times series across 160s. High magnitudes indicate a strong presence of this oscillation. High frequencies indicate a fast-

oscillatory rhythm. The dashed black line represents the mean of the spectral density peak magnitudes resulting from 100 random resamples of the angular velocity time series (see methods). (C; I) Dominant frequency. (D; J) Highest peak magnitude. (E-F, K-L) Distribution of the angular (E; K) and forward velocities (F; L).

Overall, dynamic cues such as rotational and translational visual feedback are involved in the control of the oscillation amplitude and frequency, but not in their actual production.

Diversity of edges orientation impacts the production of oscillations.

Despite being tested within an abstract environment (only vertical or only horizontal edges), ants still displayed clear oscillations. However, these were less regular (Lower PSD magnitude) than in the naturalistic-looking environment (naturalistic with TOF= 180±12; naturalistic no TOF= 158±4; horizontal: 119.535 ± 5.37; vertical: 130.504± 5.54). We first hypothesized that this was due to the lack of heterogeneity in these abstract visual scenes presenting a regular pattern of stripes, which would inhibit the production of oscillation. Indeed, functionally, a visual environment presenting a homogeneous pattern across azimuths is less worth exploring than a heterogeneous one. To test for this, we recorded ants in visual sceneries presenting a same number and diversity of edges (both vertical and horizontal), but with either a homogeneous or heterogeneous distribution across azimuths (Fig.2 A). We found no effect on the regularity and frequency of the oscillations between these experimental conditions ($F_{1,59}$= 0.1253, $p>0.05$), showing that the homogeneity/heterogeneity of the visual scene had no impact on the production or control of oscillations.

Furthermore, the magnitude of oscillations in these conditions was close to the one recorded in a naturalistic visual scenery (mean±se: naturalistic = 180±12; naturalistic fixed= 158±4; Heterogeneous = 164±12; homogeneous: 165±9), suggesting that two edge orientations is sufficient for the ants to fully produced its oscillatory behaviour. Based on this, we put forth the hypothesis that the variety of edge orientations plays a role in the interpretation of a coherent natural panorama.

To test this idea, we analysed together the results of a series of experiments conducted with visual background that spanned from the complete absence of edges (uniform black or uniform white) to single edges orientation (multiple or single vertical or horizontal edges), two edges

orientation (both horizontal and vertical) or more edge orientation (natural looking panorama). Across these conditions, the number of edges orientation had a strong impact on the regularity of oscillations (Fig.2, $F_{3,547}$= 40.559, p<0.001, mean±se: zero = 133.22±3.483; one = 134.519±3.223; two= 167.4067±6.4; naturalistic: 161.4075±4.326,). Contrastingly, the actual quantity of edges across the scenery (Fig. S2B Anova: Edges length: p>0.05; Edges orientation: χ^2 = 25.925, ps<0.001), or overall brightness (Fig. S2A Anova: Brightness: χ^2 = 0.787, p> 0.05; Edges orientation: χ^2 = 19.050, ps<0.001) of the pattern had no significant effect.

Thus, for ants, the primary visual features that trigger the production of oscillations appears to be based on a sufficiently diverse edge orientation rather than on other parameters tested here (Fig. S2).

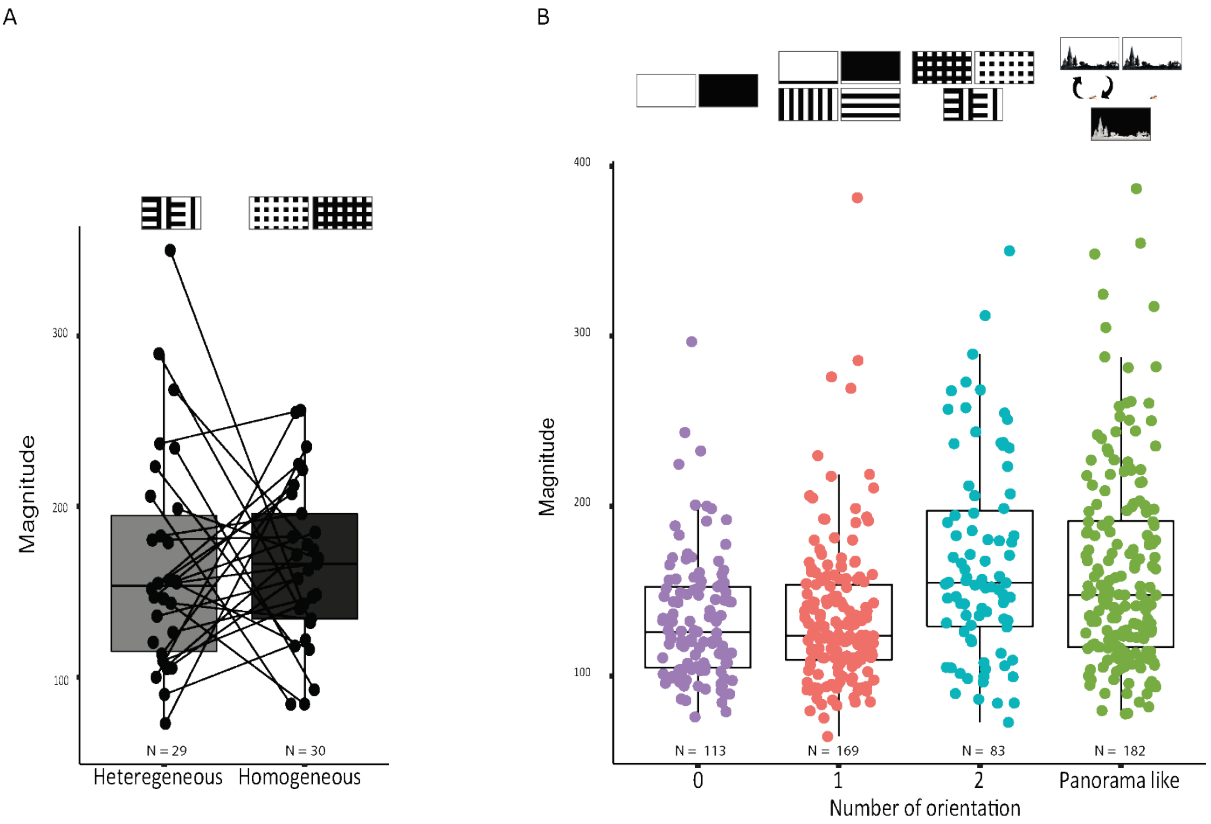

Figure 2. Ants do display regular oscillation in a naturalistic reconstructed environment. (A, B) Distribution of the individual Fourier dominant magnitudes obtained on angular velocities times series across 160 s. High magnitudes indicate a strong presence of this oscillation. (A) Ants recorded in heterogeneous (left) or homogeneous (right) background constitute of horizontal and vertical stripes. (B) We pooled together several experiments according to the number of edges orientation from absence of edges to several.

Discussion

We demonstrated that ants navigating in a virtual reality environment exhibit their natural oscillatory behaviour, with magnitudes and frequencies that closely resemble those observed in ants in the field [37,148,209]. Such oscillations reflect the activity of an intrinsic neural oscillator, widespread across species and serving various navigational context [50,209,227–229,301]. In ants, these oscillations are key to visual navigation as they optimize visual exploration and are amplified when the ant is in an unfamiliar visual environment [209]. Therefore, we reasoned that the production of such oscillations can serve as a proxy to quantify the ant's motivation at exploring a novel visual world. This provided us with a tool to investigate whether this motivation to explore depends on the visual structure of the surrounding and identifies which visual cues are key for the ant to consider a visual environment worth exploring.

Dynamic cues for the control of oscillations

The lateral oscillations and forward displacements of ants in the world generate a dynamic, re-afferent sensory feedback in the form of rotational and translational optic flow, respectively. Such dynamic cues are known to play a major role in insects for various tasks such as speed control [32,324–326], optomotor responses [38,327], distance estimation for landing [110,328–331] or the recognition of a familiar scenery itself [285,332]. Manipulating these dynamic cues in our virtual reality set-up did influence the dynamics of the oscillations. As previously shown [54,315,323,333], the absence of rotational optic flow led to a dramatic increase of the turns amplitude (Fig. 1H, K) confirming the role of rotational optic flow as negative feedback to control the extent of the current turn. Removing translational cues, such as translational optic flow and the parallax motion of the objects led to higher frequency (fig 1.D) but they do not impact the oscillations' regularity (Fig.1G-I).

Overall, this suggests that dynamic cues are involved in controlling the dynamics (amplitude and timing) of oscillation, but not involved in their actual production.

Static cues for the production of oscillations

Interestingly, presenting artificially impoverished visual sceneries disrupted the regular oscillatory rhythm of the ants (Fig. 2B), showing that the structure of the world perceived by the ants influences the production of oscillations. The crucial parameter to explain the presence of prominent, regular oscillations is the diversity of edge orientations (Fig.2B) rather than overall brightness or the quantity of edges in the scene (Fig.S2). For instance, oscillations are equally inhibited in a uniform background (black or white Fig. 2B), slightly more prominent in a scenery consisting of only one type of edge orientation (horizontal or vertical, and independently of the number of bars displayed), and fully reinstated in sceneries with a combination of at least two edge orientations (Fig.2B). The insect's visual system is known to extract edges to detect the boundaries of objects and surfaces [234,334–336]. Here we show that this feature, at least in *Cataglyphis* ants, is also important to trigger oscillations and thus a proper exploration of the scene.

Ants are well-known to use the skyline, to maintain their heading direction [12,15,236,282]. The skyline represents the boundary between the sky, on top, and the terrestrial objects, below. Given that in natural condition the sky is generally brighter than the ground, we could have expected that insect possess a 'matched filter' [321,322] to process preferentially scenery that are brighter in the upper part [24,282]. Perhaps surprisingly, inversions of the scenery contrast did not matter: ants displayed equally prominent oscillations whether the upper part of the scenery was bright or dark (Fig.S2 C). However, the scenery presented here were monochromatic (black and white) using LED with RGB wavelength, and thus lack UVs as well as light polarization. Arthropods eyes [22,102,337] and navigation behaviour [98,321,338–341] are sensitive to UV and light polarization. Hence, it remains possible that ants possess a match filter preferentially filtering in sceneries with UV and/or polarized light in the upper part of the visual field [22,24]. However, we show here that the position of brightness in the RGB range, which is picked up mainly by the ant's long-range visual receptor [320], does not matter to control the production of exploratory behaviours.

Functional considerations

Oscillations in ants are optimized for visual exploration [209]. Thus, it would be useless to perform such exploratory behaviours in structure-less sceneries with no diversity of edge orientation. Therefore, it makes functional sense that ants inhibit oscillations in such structure-less environments (Fig.1 G-H, Fig. 2 B). The fact that ants rely on the presence of a diversity of edges orientations – rather than brightness or the actual quantity of edges – to control the production of oscillations (Fig.S2), can be explained functionally. Indeed, relying on brightness or the overall amount of edges would lead ants to oscillate and explore differently in visually cluttered environments (dark but large quantity of edges) and visually poorer open environments (bright with little quantity of edges); even though both environments must be equally scanned across all azimuths to recall a proper heading [37,41,143]. Relying on the presence of at least two different edges orientations appears as a good proxy to recognize an environment worth exploring. The only natural landscapes that would not fit this criterion would be ones with a perfectly flat horizon (in which case there would be only one type of edge orientation: the horizon). Indeed, such flat sceneries provide no directional information and are thus not worth exploring visually. Furthermore, if such a scenario were to occur, ants would naturally fall back on their path integration mechanisms to navigate, and the latter would therefore not be hindered by the production of high amplitude lateral oscillations. As C.fortis, which lived in a featureless environment, relied more on their PI and had difficulties learning visual cues compared to M.bagoti, which thrived in a more structured environment [182].

Perhaps more surprisingly, ants produced equally regular and prominent oscillations in a natural-like scenery than in an artificial scenery consisting of the same repeated pattern across azimuths, as long as the latter presented both horizontal and vertical edges (Fig. 2B). Such patterns were directionally non-informative, and thus theoretically not worth exploring, contrary to what the ants did. This shows that ants pay no attention to whether the perceived scenery changes significantly across the heading direction; or at least this information is not used to control the production of oscillation. Nonetheless, it may seem irrelevant to explore a visual world that provides no directional information from an anthropomorphic perspective, however, such environments, consisting of a perfectly repeated pattern of at least two types of edge orientation are extremely unlikely to exist in natural condition. As often the case in ant navigation literature [137,219–223], we conclude that ants use a simple but efficient heuristic to decide whether a visual world is worth exploring. The latter seems to be a match filter, enabling

the ants to detect the presence of at least two different edge orientations. How similar or different such a match filter is in different ant species remains to be seen.

Neural considerations

It is still unclear which are the neuronal pathway that detect edges orientations and triggered oscillation. Are they processed beforehand in higher brain areas, such as the mushroom body of insects, or from early neuronal relay as the optics lobes.

Visual feature extractions can occur early in the visual processing. Notably, lateral inhibition between neighbouring ommatidia extract local edges, and these can then be integrated and summed in the optic lobes. From there, several pathways may convey various information to influence oscillations. Lateral oscillations in insects are likely produced in a pre-motor area called the Lateral Accessory Lobes (LAL), which receive multiple input from many brain regions [50,52,228,303,342,343].

Regarding the effect of dynamic visual cues, a recent work has shown that wide-field rotational optic flow computed in the optic lobes [54,315,333] is locally compared to efference copies of the motor signal, as well as proprioceptive feedback to form a prediction error signal that is sent to the LAL to modulate the oscillations [323]. This control operates via an asymmetrical activation of the LAL enhancing a left or a right turn, in order to reduce the computed error. This is in congruence with the high amplitude turns (looping behavior) observed in the absence of horizontal optic flow (Fig 1G-L), which must result in a prediction error that activates one side of the LAL to prolong the current turn.

Our work reveals the existence of another pathway, which conveys this time information about static features in the visual scene, and notably, the presence of at least two types of edge orientation. This pathway does not modulate the amplitude and frequency of oscillations but their actual presence, which could be simply achieved through bilateral and thus overall excitation or inhibition of the LAL production of rhythmical oscillations. However, through which relay this pathway operates remains unclear. Evidence suggests the existence of a direct pathway from the optic lobe to the Lateral Accessory Lobes (LAL) [50,52,303,343] providing a likely candidate to explain how the presence of a diversity of edge in the scene can modulate the activity of the LAL, and thus the production of regular oscillation. Alternatively, a parallel

pathway exists from the optics lobe to the Mushroom bodies (MBs) [65,344–346], which outputs information to the LAL [50,70,347,348]. The MBs are implicated in formation and retrieval of route memories in ants and can output a familiarity signal of the currently perceived scene [64,68,273,349], which we know can modulate the dynamics of oscillation [37,209]. Whether information about the static visual feature identified here are conveyed through the MBs remains however *a priori* less likely, given that it operates already during early exploration of novel environments, without the need for learning.

Ontogenetic considerations

Given that our experiments exclusively involved a single species raised in a similar environment, we cannot conclude whether the visual features identified here vary across species and whether they are constrained developmentally or modulated by early visual experience. Structural re-organization through synaptic change along the visual pathway is well known to occur during early exposition to light in hymenopteran [350–352]. Early visual experience and synaptic change could allow individuals to be best suited to their surroundings. Thus, the brain seems to adapt to their new visual environment. Additionally, early life adaptations are likely widespread throughout the animal kingdom, from invertebrates to vertebrates [350–355]. Manipulating the visual environment during early experiences, as well as comparative studies across different ant species in such VR system promises to shed light on the plasticity of the brain in interpreting a visual scenery.

Conclusion

We showed that ants adjust their visual exploration to the type of structure of the surrounding scenery. This control is based on an apparently simple heuristic or ‘matched filter’ [321,322], such as the detection of both vertical and horizontal edges of the scenery [335], which will in turn trigger the production of regular oscillations and thus expose the ant gaze in multiple direction. Dynamic cues, such as optic flow, are also picked up but used for a different purpose of controlling the amplitude of oscillations. How plastic and different across species this

heuristic is remains unknown, but the possibility to conduct experiments with navigating insects in VR systems promise to shed light onto how insects encode their visual natural environment, and thus further insight into their Umwelt [356].

Methodology

Study Animal

We used the thermophilic ants *Cataglyphis velox.* Workers, rather than using pheromone, are known to forage solitarily [357] relying mainly on learnt terrestrial visual cues and path integration vector (PI).

Three nests of the species *Cataglyphis velox,* originating from Seville in Spain and now maintained at the lab, were used in the experiments. These nests are in a room with controlled ventilation, temperature (24-30 °C), humidity (15-40%) and a natural 12-hour day-night light cycle including ultraviolet light. These colonies are underfed to ensure their motivation to search for food.

Trackball set up & VR

To record ants' movement, we mounted them on a trackball device [300]. This device consists of a polystyrene ball held in levitation in an aluminium cup by an air flow. The trackball has two sensors placed at 90° to the azimuth of the sphere, which record the movements of this sphere and translate them into X and Y data retracing the path of the ant. The X and Y acquisition of the trackball rotations happened at a 30 Hz frequency (i.e., 30 data points per second), enabling us to reconstruct the ant's movements with high precision. The polystyrene ball was prevented from rotating in the horizontal plane by two small wheels. Ants were attached to the top of the ball by applying magnetic paint to their thorax and placing a micro-magnet at the bottom of a dental thread. This thread was then attached to a 0.5 mm pin located within a glass capillary. This setup allowed the ants to rotate their bodies axis but prevented them from escaping forwards or backwards. As a result, the ants could control the direction in which they faced, but any attempts to move forwards or backwards resulted in rotations of the ball.

During experiments, ants on the trackball were placed at the centre of the virtual reality set up (Fig. S1 A). This device consists of a cylinder of 50 cm diameter and 76 cm high. The inner surface of the cylinder made of LED panels assembled to form a set of 73728 LEDs for a resolution of 0.94 degrees per pixel which exceeds the visual acuity of Cataglyphis ants' eyes, which is 2 degrees per pixel [173]. The LEDs are controlled through the computer and the virtual environment is managed using the freeware Unity 2020.1.

In this study, we used two different trackball/VR configurations to record the ants' motor responses: further referred to as 'open-loop' and 'closed-loop' experiments, respectively.

"Closed-loop": This dynamic configuration allows the actions of the ants to modify the virtual reality display, creating a feedback loop where the actions of the ants influence the display, and the display influences the actions of the ants.

"Open-loop": In this static configuration, ants' movement do not modify the virtual reality display.

Virtual environment & experiment

To identify key visual features that trigger navigation, we recorded ants in various environments, spanning from natural to abstract patterns (Fig.S1 B). Each ant was tested up to three visual conditions in a random order. Between each test, ants were released inside their nest for at least 3 minutes before being retrieved for another trial. Each individual was therefore placed in the VR up to three times but was only used once for each visual condition.

Data extraction and analysis.

All statistical analyses have been run using the free software R (v 3.6.2. R Core Development Team). For all statistical tests, the p-values were compared to the critical alpha risk at 0.05, with the appropriate correction if needed. The statistical parameter's mean and the associated standard error is given within the text and/or in figures: N represents the number of individuals.

To determine the presence of regular lateral oscillations, our focus was on the angular velocity, which is a direct measurement of the left/right motor control. We processed the time series data

through three successive steps to calculate its spectral density using the Wiener-Khinchin theorem. First, we smoothed the x, y path (Fig S1 A, red path) using a Savitzky-Golay filter (from R “trajr” package) with a window length of 2 seconds. Then, we extracted the angular velocity time series, which was smoothed twice: first with a moving median, then with a moving mean, both with a window length of 0.5s (Fig. S1C). Next, we conducted an autocorrelation function (Fig. S1D) on the smoothed time series, and performed a Fourier transform on the autocorrelation coefficients to obtain the power spectral density (Fig. S1E). For each individual, we extracted the dominant frequency, which was the frequency with the highest peak magnitude, and the corresponding magnitude (Fig. S1E). To determine if these magnitudes indicated a significant regular oscillation, we compared them to the average spectral density magnitude calculated from 100 resamples of the angular velocity time series. These resampled signals underwent the same processing as the original angular velocity time series data, including smoothing, autocorrelation, Fourier transform, and extraction of the highest peak magnitude. The average of the 100 highest magnitudes was then compared to the real ants' equivalent magnitudes using a Wilcoxon one-tail test for paired data.

Statistical models

To determine which key features as an impact on the oscillations' behaviour, we compared our condition using mixed models.

We conducted our analysis using two types of models: one that considers the interaction and the other with a simple additive effect. It's worth mentioning that if the residuals of these models deviated from normality and/or homoscedasticity, the response variables were transformed. The model was selected and further analysed through an analysis of variance (Anova), followed by a Tukey's rank comparison post-hoc analysis. Additionally, multiple independent experiments were performed, and each individual was tested across different conditions. As a result, the models were mixed models that controlled for the effects of the sequence and individual, as well as considering the set of experiments as a random variable.

Supplemental information

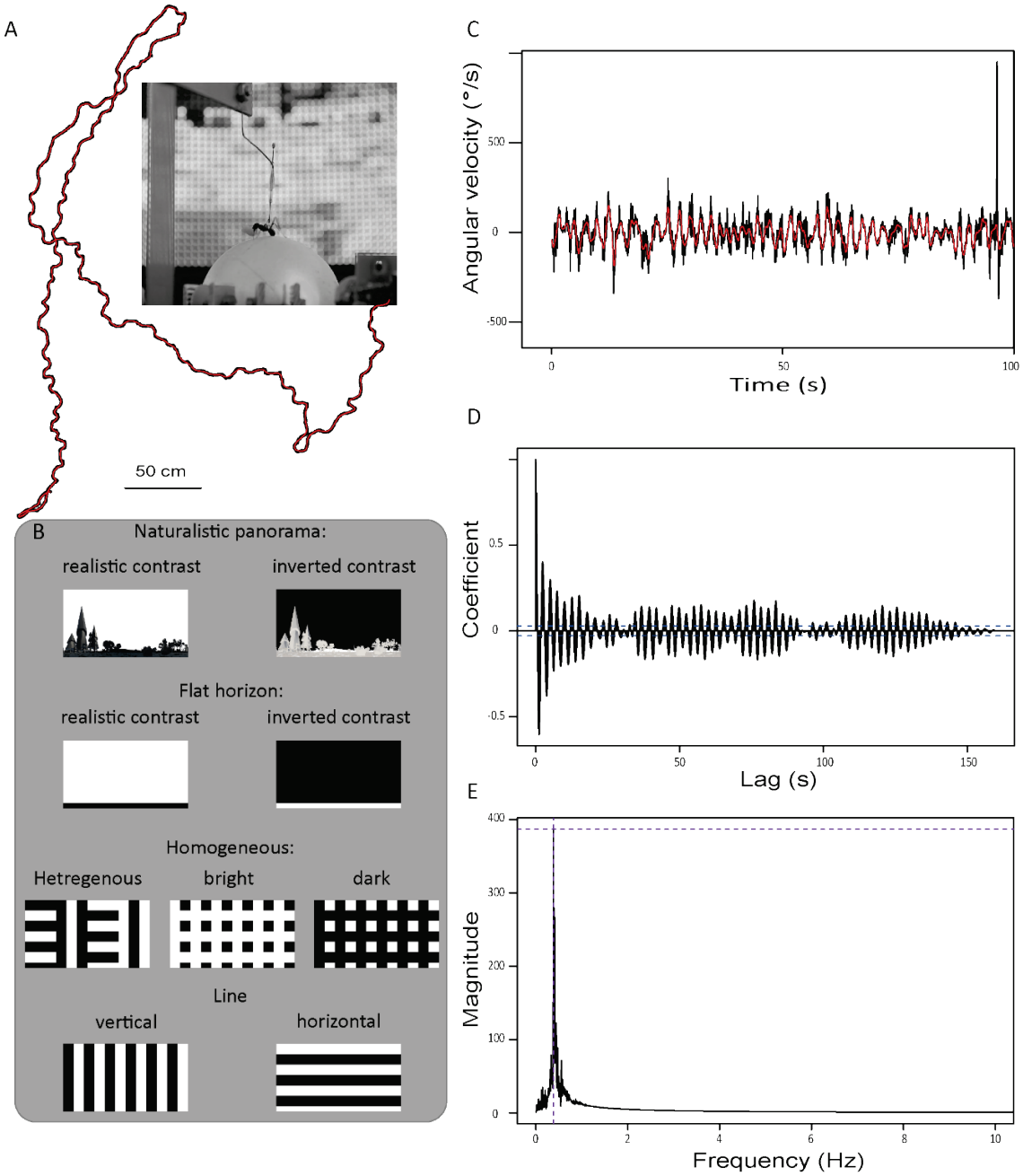

Figure S1: Trackball set-ups, recording and processing of the ants' trajectory. (A) Picture of the trackball within the virtual reality set-up (side view). Two wheels prevent the sphere from rotating along the horizontal plane. Ants are free to rotate their body along the yaw axis to control in which direction they perceive the world. The path shows an example path of ants recorded in a naturalistic environment (B) black path is the original recording, the overlay red path is the smoothed one (Savitzky-Golay filter of 2 seconds) (B) Background use during the experiment (C) Angular velocity signal over time of the example path (A) in an individual of the species with smoothed signal superimposed (red). (D) Autocorrelation carried out on the entire smoothed angular velocity signal. (E) Fourier transformation of the autocorrelation coefficients signal (shown in D) provides the 'power spectral density'. This approach has the advantage to provide magnitudes that are directly comparable between individuals. For each individual, the frequency peak with the highest magnitude was extracted, indicating a strong oscillation of the angular velocity signal at that frequency (dashed blue lines).

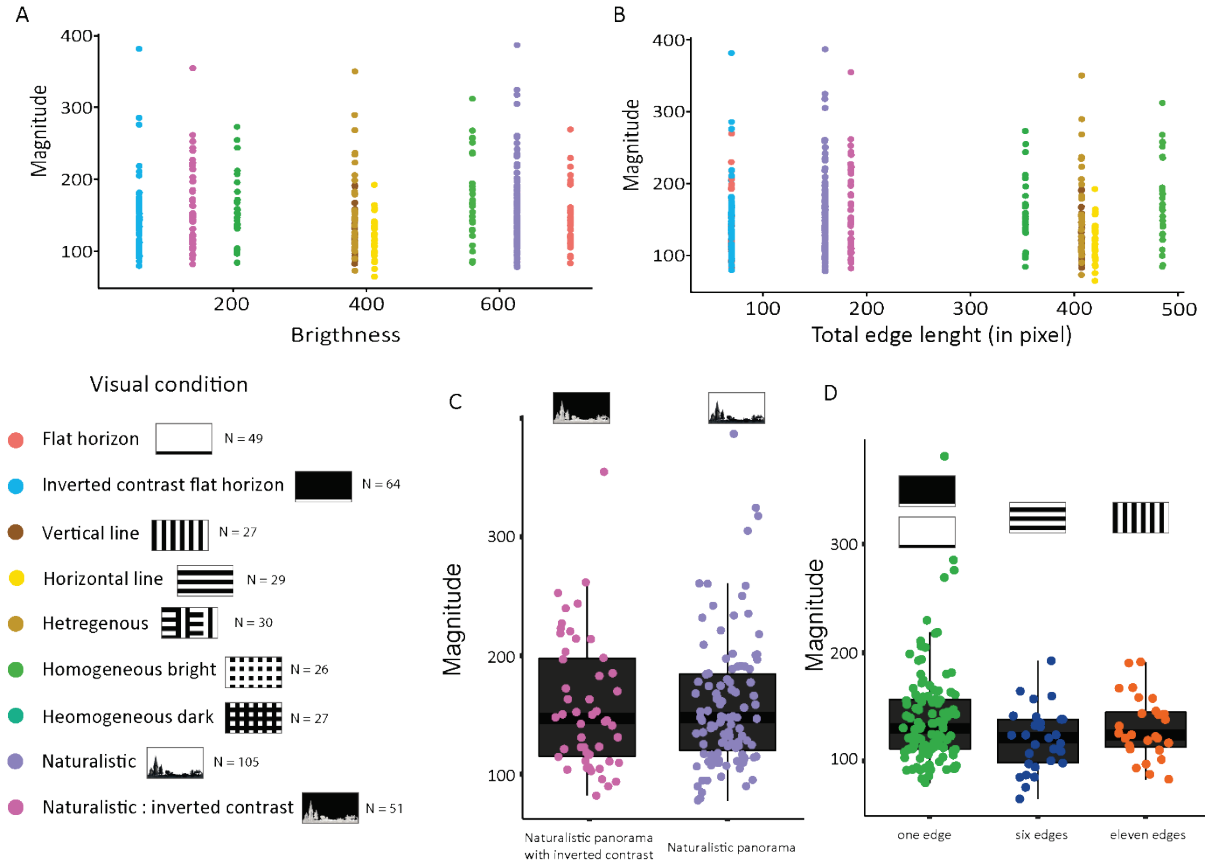

Figure S2: Ant's oscillation behaviour is triggers by the numbers of edges rather than other parameters. (A-D) Distribution of magnitudes according to (A) the brightness, (B) length of edges, (C) position of contrast and (D) number of stripes. For (A-B) the diversity of edges orientation significantly impacts the oscillation magnitude whereas the brightness (A) or the total edge length (B) didn't have an effect (Anova ps: edge orientation <0.05, other parameters > 0.05). For the position of contrast and number of edges, no effect had a significant impact on the magnitude of oscillation, i.e., their clarity (ps > 0.05).

Discussion

This thesis presents an integrative approach that combines behavioral experiments and computational modeling in order to gain a further understanding of the mechanisms of ant navigation. I recorded the ants' trajectories in great detail, both in natural environments and virtual reality setups, and conducted in-depth path analyses.

This research on ants has provided insights into several aspects of how behavior and intelligence emerge. Specifically, it explores how behaviors arise from a distributed flow of information between the brain, body, and environment, where endogenous movement plays a crucial role in this information flow. This endogenous production of movement is modulated by innate and learned factors to adapt to the task at hand in a continuous manner. It facilitates the acquisition and retrieval of route memory (Chapter 2) as well as the motivation to explore the world (Chapter 3). These findings suggest that the brain area responsible for the endogenous production of oscillation is at the core of motor controls and can be modulated in various ways (chapter 2, 3)

Our model shows, that simplicity can give rise to complexity through emergent properties, where discrete behaviors can be explained by continuous process rather than clear-cut decision. Additionally, I underlined several points suggesting that ants update egocentric route memories rather than reconstructing a map-like representation of the space around them (chapter 1).

Finally, my work also led me to reflect about epistemology, notably how scientific questions can be asked and answered. I will discuss these points in turns.

4.1. The brain, the body and the environment

In Chapter 3, emphasized the presence of recurrent pathways that may carry the same information to different brain areas. The parallels pathways are involved in spontaneous motor response, as well as in the context of learning. Interestingly, both learned and innate

components converge into an intrinsic oscillator: the lateral accessory lobes (LAL). Therefore, internally generated movement seems to be modulated by both pathways, this corroborates the view that the LAL, and thus this intrinsic oscillator, act as a bottleneck for sensory information [50,228]. In the following sections, I will first discuss how these multiple pathways in the brain form a parallel and modular system that is remarkably adaptative and flexible.

In addition to accommodating various sensory inputs, this oscillator actively participates in placing the animal's sensors in phase with its environment. Notably, the oscillations allow the ant to continuously scan her environment. These scans are ideal for egocentric recognition of the scene, as performed by its brain [71,141,152,282,316,317], so that ants can recover the direction of their route while avoiding the heavy cognitive burden of mentally rotating the scene or reconstructing complex space [152,316,317]. I will highlight the often-overlooked importance of internally generated movement within the 'sensorimotor' loop, as well as how simple heuristic mechanisms can replace more complex explanations of ant navigation. Overall, this places behavior as a product of the interaction between the brain, body, and environment, blurring the lines of what can be considered intelligence and decision-making.

4.1.1. Information flow

I demonstrated that behavior is not solely due to a unidirectional flow of information from sensory input to motor controls, but rather involves bidirectional and parallel flows across various brain areas. Indeed, by its fundamental place in the navigational task, this oscillator is not solely involved in the generation of movement but is rather multi-functional and multi-modal. Information is gathered actively through movement, rather than being solely triggered by sensory input[307] (Chapter 2). In this context, I will first discuss how the flow of information modulates the endogenous production of oscillations, and then, how the presence of intrinsic oscillators closes the loop between internal and external sources of information.

A. Parallel pathways from the eyes

In Chapter 2, I emphasized and discussed the coexistence of two early visual processing pathways from the eyes that converge to the LAL, which is responsible for the endogenous production of regular oscillations. I demonstrated that endogenous oscillations are modulated by innate cues, namely the dynamic optic flow and the static structure of the visual scenery (Chapters 2 and 3).

These features are extracted by the peripheral pathways and processed in the early neural relay known as the optic lobes [315,327,333,344,358–362]. First, lateral inhibition occurs between neighboring ommatidia[358,359], enabling the extraction of edge information. Signals from these early interactions between ommatidia are then integrated and summed in the optic lobes [358,359], allowing for more complex and dynamic feature extraction, including wide field optic flow [315,333,360–362]. From the optic lobes, a direct pathway exists toward the LAL [50,52,303,343], explaining how these visual features directly modulate oscillations (Chapter 3).

We showed that static cues such as the presence of at least two different edge orientation in the scene triggers the endogenous production of oscillations, i.e., their clarity, while dynamic cues such as optic flow modulate the turns and frequency of oscillations (chapter 3). The pathway, carrying information about the presence or absence of edges in the scenes because it affects the overall production of oscillations and do not favor left or right turns, likely connects and convey similar signal to both sides of the LAL. This modulation can either increase the activity, leading to the regular production of oscillations, or decrease the activity, thus inhibiting the oscillations (Fig. 1). Therefore, the presence of multiple of edges orientations, which indicate an exploitable visual scene for navigation, increases the overall intensity of oscillations and thus a proper exploration of the visual surroundings.

Contrastingly, optic flow does not trigger the oscillations' production, but does influence their dynamics (amplitude and frequency, chapter 3) by inciting the ant to turn left vs. right. This modulation thus must involve a differential control between the left and the right of the LAL (Fig. 1), which is further supported by both experimental and anatomical data [53,54,315,333]. Rather than triggering exploration, this fine sensory motor control regulates the extent of each left and right turns and ensure that the overall direction is rather straight. Indeed, as we showed, removing rotation optic flow led the ant to display full loops rather than covering ground (Chapter 3).

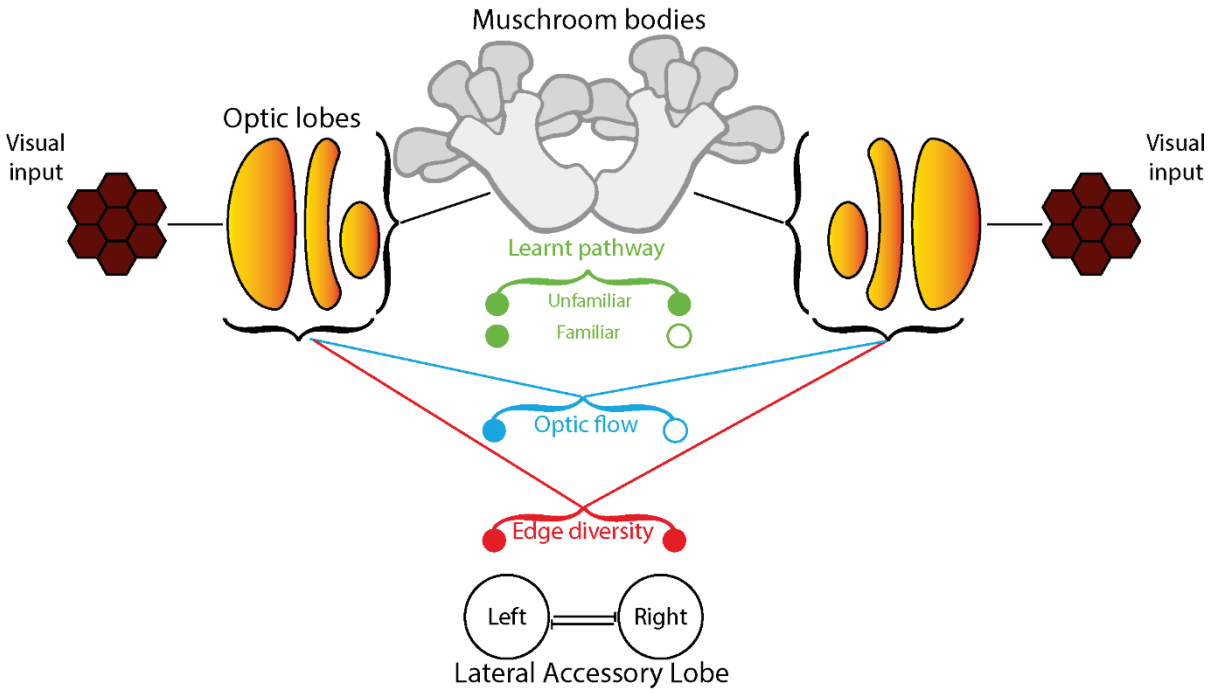

Figure 1 Multiple pathways conveying visual information to modulate oscillations. This figure illustrates neural pathways involved in the impact of visual information on the production of oscillation by the lateral accessory lobes (LAL). The pathway responsible for information about the presence of a diversity of edges orientation in the scenery (shown in red) likely connects to both sides of the LAL (2 filled dots) to regulate the overall activity of the LAL. This regulation can either enhance activity, resulting in regular oscillations to explore the environment, or suppress activity, inhibiting oscillations in a visually plain environment**.** Simultaneously, optic flow detectors in the optic lobes modulate the characteristics of oscillations, such as their amplitude and frequency (blue). This modulation must be lateralized (ipsilateral vs. contralateral, open vs. full dots) to regulate the amplitude of the left vs. right turns according to the direction of the optic flow. Additionally, there is a pathway from the optic lobes to the mushroom body (MB), which is believed to be involved in visual learning and recognition of the surrounding scene. From the mushroom body, several pathways connect to the LAL (shown in green), allowing information about the scene familiarity to modulate the oscillations. Unfamiliar visual scenes lead to increased oscillations (green, full symbol) and thus favour exploration, similarly to the pathway conveying information about the number of edge orientations. Conversely, familiar scenes reduce the oscillations' amplitudes, promoting exploitation of the environment and triggering left or right movements (green, open vs. full dots) to optimize forward motion and maintain a straighter path, similarly to the optic flow pathway.

In Chapter 3, I discussed the existence of a third pathway in insects that runs from the optic lobes to the mushroom body (MB), as further supported by anatomical data [65,344–346]. This pathway is thought to be involved in the context of visual learning, as the MB has been shown to be the substrate for learning and retrieval [64,65,68,70,164,165]. From the mushroom body

a direct pathway innervates the LAL [50,70,347,348]. Thus, through this pathway, learnt information can modulate the activity of the LAL, which is further supported by results of chapter 2, which show how learnt visual cues modulates the dynamics of the oscillations.

Interestingly, there is an analogy in the way innate and learnt information modulate oscillations (Fig. 1). Unfamiliar panoramas such as detected by the MB trigger higher oscillations (chapter 2), similarly to the pathway that conveys information about the numbers of edge orientations (chapter 3). Indeed, both sources of information indicate the need for exploration. Conversely, familiarity of the visual scene reduces the oscillation amplitude and triggers left vs. right movements optimizing forward movement and straighter path (chapter 2), similarly to the way optic flow pathway controls the dynamics of oscillations (chapter 3). Indeed, both sources of information favor the behavior of covering ground.

All in all, we can see how multiples pathway from the eyes to the brain, carrying innate and learned information, modulate the endogenous production of oscillations. These pathways serve multiple functions, such as biasing the overall exploration/exploitation balance (chapter 2) or fine-tuning of left and right turns to control the ant's direction (chapter 2 &3).

B. Oscillation at the core: an ancestral design

I presented evidence emphasizing the often-disregarded importance of internally generated movement within the 'sensorimotor' loop (chapter 2). This evidence highlights that exploration, memory acquisition, and retrieval, which are essential for navigation tasks, are all supported by endogenous production of oscillations (Chapter 2). This place internally generated action at the core of the navigational task, both regarding the acquisition of information through learning (exploration), and the use of this information for route following (exploitation).

According to some proposals [309,314], neural systems initially evolved to coordinate movements endogenously [307], indicating that the modulation of these movements by external sensory information emerged only as a secondary step. In the insect brain, the LAL is an ancestral brain area that appears to be the seat of such endogenous motor coordination[50,228,303,342], through the production of regular oscillations, Indeed, as this structure is widely preserved[50,228,303,347], intrinsic oscillators are not only at the core of navigation in ants

but seem to be an ancestral characteristic, found in most arthropod species. Therefore, we could imagine how various sensory modalities carrying navigational information came as a second step, by being 'plugged' onto this oscillator to serve various navigational purposes across species [50,228,301], such as chemotaxis through oscillations in crawling maggots [229] or pheromone plume tracking through oscillations in flying moths [51,54,228,292].

It is worth noting that oscillations are not always beneficial and may need to be suppressed in certain situations, such as when the organism is in its nest (chapter 2) or attempting to escape a threat. This is why the organism's inner state and the availability of contextual cues, such as the structure of the visual surroundings (chapter 3), must influence the expression of internally generated oscillations.

The diversity of information that can modulate oscillations depicts a modular design, where various sensory information can be ‘plugged’ to modulate oscillation. This allows to draw a possible evolutionary scenario. First, brain structures evolved to coordinate movement[307,309,314], providing a regular rhythm necessary for proper locomotion. Second, sensory information such as, visual, tactile, or olfactory cues, then came to modulate these lateral oscillations for guidance. Finally, more processed cues, such as the familiarity of the visual scene processed in the MB, also exploited this core oscillator for more sophisticated navigation, such as route following.

Overall, this diversity is a testament of the adaptability of such a modular design of insect brain -for navigation task-.

C. The oscillator closes the loop.

Up until now, I have presented evidence demonstrating a unidirectional flow of information through parallel pathways that modulate intrinsic oscillators. However, this flow appears to be bidirectional through both movement-related afferent signals and internal neural feedbacks (chapter 2). These dynamic re-afferent signals, both internal and external (Fig. 2), are key to the interaction between the brain, body, and environment.

First, the ants' lateral oscillations and forward displacements generate a dynamic, re-afferent sensory feedback through rotational and translational optic flow. Although optic flows are involved in controlling the amplitude and timing of oscillation, they do not contribute to their actual production (as discussed in Chapter 2 and 3). However, by moving, the ants are

continuously exploring the world, which enables them to modify their body orientation and close the sensory-motor feedback loop, thus resolving the question of "where to look" through this closed loop between the brain, the body, and the environment.

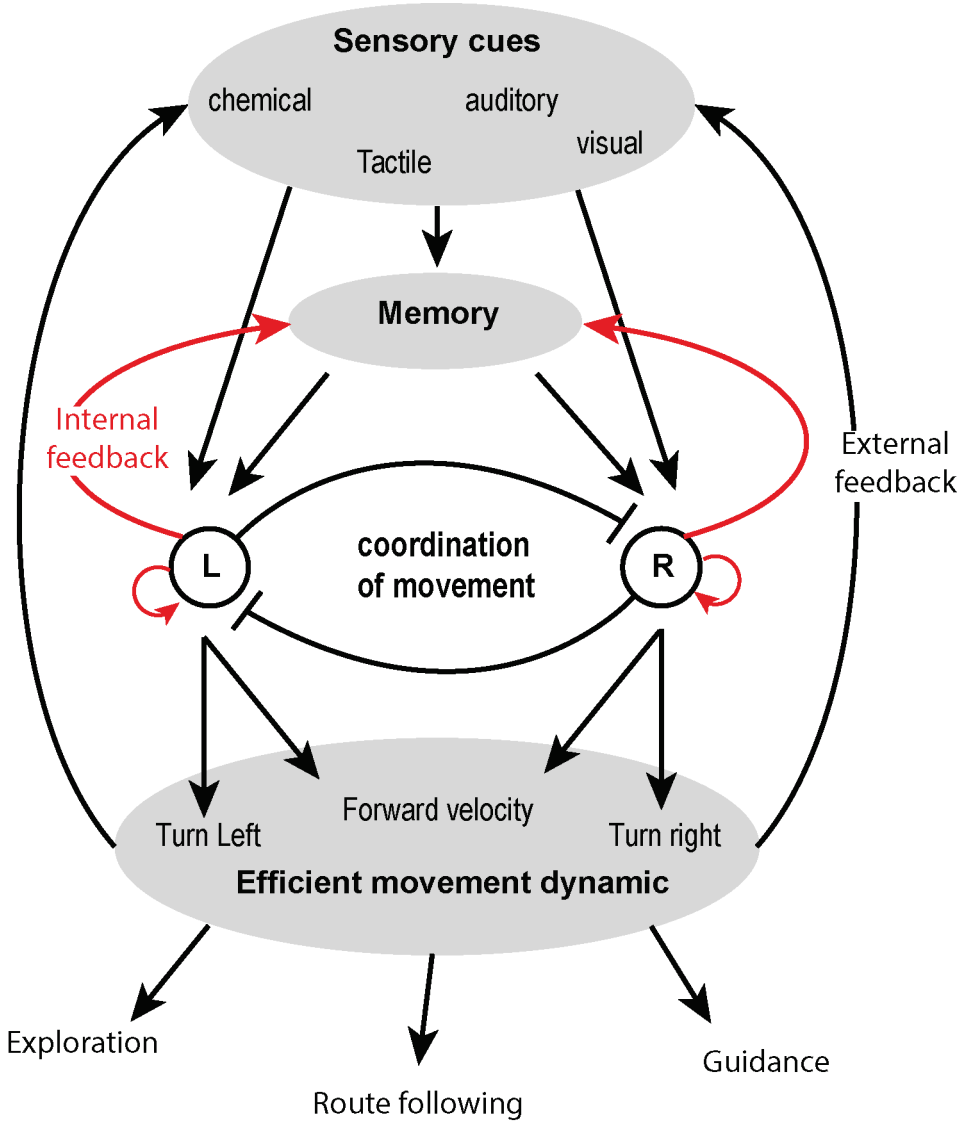

Figure 2: An intrinsic oscillator at the core of visual navigation. Simple scheme to encompass our results. In this view, sensory input (in this case various innate and learnt visual information) acts on behaviour only indirectly, through the systematic modulation of an intrinsic oscillator. The latter ensures that an efficient movement dynamic is preserved across navigational contexts, which would not necessarily be the case if various and potentially conflicting sensory information were directly modulating movement. This scheme also highlights the idea that action is not merely the product of perception. At the core of behaviour lies an intrinsic, self-generated dynamic, which is modulated, rather than controlled, by sensory perception. Finally, the oscillator coordinates movement but also produces both internal (red) and external afferences feeding the sensory motor loop, as well as likely sustain continuous memory formation.

Second, regarding memory formation and retrieval, the mushroom body has been recognized as a substrate for route memory [64,68–70,164,165,165,166]. However, how memory is orchestrated during learning is unclear. In Chapter 1, I presented evidence suggesting that memory is updated in a continuous manner. Several cues suggest that such a continuous learning also relies on the oscillation behaviour. At the start of the ant foraging life, oscillations are involved in learning as ants - as other insect such as wasp[41] and bumblebees[40] - displayed regular oscillations during learning walk[31,145,148] (Chapter 2) or flight as in other insect such as wasp and bumblebees . In addition, neuroanatomical data has shown that this endogenous oscillator is connected via dopaminergic neurons to the memory centre: the MB [363]. One possibility is that the intrinsic oscillator continuously sends internal feedback signals to orchestrate continuous learning into the MB[273]. Thus, in addition to solve 'where to look', the display of regular oscillations may well equally solve the problem of 'when to learn' during the navigation task.

On the one hand, the Mushroom Body modulates the oscillations according to the familiarity of the scene, and on the other hand, the oscillator modulates learning through both internal and external re-afference. As a result, it is impossible to deduce whether the ants oscillate to learn or learn because they oscillate. This highlights the importance of considering the embodied nature of perception and action, rather than considering them as separate processes.

4.1.2. Emergence of behaviour

In chapter 1 and 2 I showed that apparent and distinct behaviours could be solved by a same mechanism. For instance, early learning walks and later route following both relied on the display of regular oscillation (chapter2). I also underlined how behaviour can result from the continuous interaction between brain, body, and environment. Due to this interaction, behaviour is modulated moment to moment and allowed to adjustment and diversity of behaviour. I will now discuss how apparently distinct behaviours that are adapted to a given situation that we -humans- would qualify as intelligent decisions, may arise from the emergent properties of distributed interactions.

A. Deciding whether to scan or not

When ants are in an unfamiliar area or are engaged in learning walk, they are known to occasionally display an apparently discrete behaviour: "scanning " [31,146,148,161,297,317,364]. The ants stop and turn on the spot facing multiple directions in a sequence [31,146,148,161,297,317,364–366]. These scanning behaviours appear, at first, ideally suited to scan the scene when in need of information. This could be interpreted as resulting from an 'informed decision' triggered by the knowledge of the current directional uncertainty[317,367]. However, assuming that angular velocity and forward speed are under the control of the LAL (chapter 2), we can understand how a scan would naturally emerge under certain 'distributed' circumstances: notably when the environment appears unfamiliar as during learning walks or in novel environment, that is when scan often occurs[31,148,297,317,365–367]. Indeed, in these situations the LAL is strongly activated by the unfamiliarity of the scene, triggering exceedingly large turns as during scanning (chapter 1). Based on this idea, a recent study [364] as demonstrated that indeed, the successive turning directions effected during scans are under the control of the oscillator, and that the successive pauses observed result from a random, Poisson-like process[364], which likelihood simply increases in an unfamiliar environment. Thus, this apparently distinct and intelligent behaviour appears to emerge from mechanisms that are continuously operant during the navigation task, rather than an informed -clear-cut- decision where ants somehow decide to stop and look.

B. Deciding whether to Search, Dash or Explore

In Chapter 2, I showed that the apparent discrepancy between the need for information acquisition (i.e., sampling) on the one hand and the use of that information (i.e., goal directed behaviour) on the other hand is continuously resolved by modulating the activity of an intrinsic oscillator using the same embodied sensory-motor solution. For instance, route following, and goal pinpointing seem to be separate behaviours resulting from distinct mechanisms: the first looks like a directed straight path [20,26–28,149–152,368], whereas the second looks like a sinuous path [30,255–257]. This range of behaviour encompasses various contexts and functions, such as exploring an unfamiliar world, searching in an unfamiliar environment[254,255,369], and searching with a familiar environment for the nest exact location[30,257]. One might assume that the production of between these behaviours and their orchestration require complex decision-making based on context. However, simple distributed, and continuous mechanisms can account for all these behaviours and their transitions over time.

First, when an ant is exploring the world where everything is unfamiliar in all directions, their memories do not trigger left vs right commands, but rather enhance the overall oscillator activity. Triggering, wide oscillation amplitude, as shown in Chapter 2, as experienced ant typically displays such exploratory path in an unfamiliar panorama [254,255,369]. Once familiar with a particular route, this familiarity decreases the activity of the oscillators, thus decreasing the amplitude of oscillation and thus favouring forward movement (chapter 2). However, and perhaps surprisingly, when an experienced ant arrives near her nest, oscillation amplitude increase again as in an unfamiliar environment[37], even though the environment must appear familiar. Rather than a complex decision or recognition of the nest area, this can be simply explained by the presence of opponent memories banks: one attractive -facing the nest direction- and one repulsive – facing away from the nest [37,62]. Close to the nest, attractive and repulsive memories acquired during the sinuous learning walks are close to each other's and recognised whatever the direction faced. Both opponent familiarity signal, therefore cancel each other, thus triggering big oscillations amplitude as the one recorded in unfamiliar terrain [37,62].

Thus searching, dashing, or exploring can be explained both by interacting memory banks as well as how their output modulates the intrinsic production of oscillation without involving any clear-cut decision. Behaviours, rather than being a set of discrete decisions based on an integrated knowledge of the current situation, are likely to be a continuous process involving the same underlying distributed mechanisms (chapter 2, 3).

C. Deciding when it is time to quit

In chapter 1, I underlined a very similar opponent process at another level. The dynamics between two memory banks - one persistent and one labile (transient) –interacting with each other before modulating behaviour, also explain both search and route-following paths (chapter 1). Also, it was observed that ants that learned a looping sinuous path during the first trial would repeat portions of the path in subsequent trials but eventually ignore their route, and thus never get stuck. This behaviour does not result from a distinct decision where ants make a conscious choice to stop repeating a same portion of a route again and again. Instead, a growing inhibition of the expression of one memory bank onto the other leads ants to increasingly ignore repeated segments and therefore no longer recapitulate them (chapter 1).

Here again, this a continuous and antagonistic process between neurons is sufficient to explain the transition between behaviours without involving any other decision-making mechanism.

These two interacting memory banks provide a simple and parsimonious solution for continuous learning, where apparently distinct behaviours can emerge from the same mechanism.

D. Intelligence: an emerging property

From an anthropomorphic perspective, we could say that ants exhibit intelligence as they balance their behaviour optimally to exploit and achieve their goals. Contrastingly, observing an ant repeatedly following the same useless path portion despite having their goal in plain sight (chapter 1), could be assumed as a 'non-intelligent' behaviour.

I showed that a distributed system may not necessarily require a high level of information integration to produce an efficient behaviour based on an apparent decision-making. However, it's important to recognize that this does not imply that the system is not intelligent. In fact, intelligence is a complex and multifaceted concept that can manifest in various ways, some of which may not involve clear-cut decision-making processes. Therefore, it is useful to acknowledge that the definition of intelligence is not always clear-cut and that different perspectives exist regarding what constitutes intelligence. Intelligence can be seen as the result of the complex interactions and reverberation of information within the brain, allowing for the continuous modulation of behaviour to suit the task at hand.
Thus, navigation through simple mechanism working in parallels form an embodied intelligence allowing to spare the problem what, when, and where to look during navigation task.
Thus, this form of an embodied intelligence allow to be 'blind' to the rest of the world.

4.1.3. Casting doubt on the cognitive map

Throughout my thesis work, I have demonstrated that ants (insects) behaviour emerges from the distributed interaction of information among the brain, the body and the environment

rather than being centralized in a specific brain area. As a result, the use of moment-to-moment information enables the emergence of a variety and remarkably efficient navigation behaviours without mentally reconstructing the spatial environment, planning, and 'deciding' what action to execute.

A. A killjoy explanation

Our experiments on ant behaviour revealed that they possess the ability to learn continuously, as in the so-called 'latent learning[243–245]. Interestingly, in the vertebrate literature, latent learning is commonly believed to involve the reconstruction of map-like representations of space [246]. But does latent learning *'fundamentally'* requires such a map-like reconstruction is unclear, and such representation in insects is much debated [137,196,218–223].

I have demonstrated that ants rely on their egocentric route memories, even if it causes them to walk in circles during experiments, without making any progress between trials, despite the goal being in clear sight (chapter 1). This strange and ineffective behaviour contradicts the notion that ants construct a comprehensive representation of their surroundings. With such a reconstruction of space, ants would be able to deduce the spatial organization of the environment and therefore optimize their path towards their goal, at least across trials.

Instead, the ants' behaviour revealed the heuristics at play: homing ants continuously learn to associate the egocentric visual scenery perceived with the motor command performed, even if the movements effected lead to nowhere (chapter 1). This heuristic leads the ants to walk along useless loops repeatedly, a non-functional behaviour, only as a consequence of our non-natural experimental displacements. In natural conditions, this heuristic is perfectly functional, as path integration ensures that the early motor command effected leads the naïve insect to its nest, thus acting as a scaffold to guide the visual learning of routes that do lead to the goal[28,153].

Previous research suggests that a unified representation of space may not be necessary to explain the wide variety of behaviours observed in navigating insects [60,63,68,69,69,76,133,281]. Furthermore, it is unclear how a map-like representation could be implemented in insect neural circuits [45,166,170,280]. Contrastingly, the heuristic we put forward fits well with the insect's known circuitry. Parallel egocentric memory bank [66,261–263], with different time dynamics, can be

straightforwardly encoded by parallel Mushroom bodies output neurons (MBONs) [62,68,259–261,263–266,268], and their interaction can be mediated by the known lateral inhibition between such MBONs [264,272].

Taken together, both behavioural evidence, and neural explanation seem to favour the use of such heuristics rather than the reconstruction of the space.

4.2. How to unravel mechanisms: an attempt to epistemology.

This thesis employs an integrative approach that combines behavioural experiments and computational modelling to gain a deeper understanding of the mechanisms of ant navigation. I was able to draw general conclusions that extend beyond the field of ant navigation, such as the ubiquitous involvement of intrinsic actions at the core of the information flow. Furthermore, this integrative approach has also transformed my vision of a scientific inquiry. Although some of my work has been unsuccessful and remains an ongoing process, it has helped me refine my approach regarding how to ask and answer scientific questions.

4.2.1. Insight to the scientific process: lesson from my experience

I employed various approaches, some successful, some failing, but both shared the advantage to give rise to new questions. For instance, during my initial field season, I had the chance to observe *Cataglyphis velox* displaying a peculiar behaviour: oscillations. Witnessing this unexpected behaviour immediately sparked numerous questions that I attempted to address in Chapter 2. However, the worked I realized also gave rise to new mysteries.

Thus, I will now present some outstanding questions that remain in my mind as well as a model that is still an ongoing work but illustrates specific errors that can occur during modelling efforts.

A. My outstanding questions

Here, I present the main questions and associated predictions that arose from the different work I performed - hopefully these will inspire future work.

- Does the fact that search patterns typically extend over time result from interacting memory banks? In Chapter 1, I demonstrated that continuous learning relies on the simultaneous recall of competitive memory banks, which allow for the emergence of a variety of behaviours, from route following to search paths. The discovery that ants learn continuously has raised further questions, such as whether the growing inhibitory memory (transient) can actually become repulsive and therefore responsible for the extension of search patterns[255–257,370] over time (i.e., by repulsing the ant from the already explored areas). This could be straightforwardly tested by modifying my models to include repulsive transient memory and deriving testable predictions from this model.

- Does the ant visual system extract specific spatial frequencies? It is unlikely that edge orientations are the only parameters triggering oscillations and participating in memory formation. The extraction of spatial frequencies appears to be widespread in vertebrates, and modelling studies have shown that this capability could provide a significant advantage for navigating insects [174,371]. By performing Fourier transformations on the images displayed in the virtual reality environment, it is possible to manipulate the spatial frequencies that ants perceive. I predict that ants encode specific visual frequencies and predominantly rely on those with very large wavelengths (large feature in the panorama). Through modelling, we can investigate whether the large receptive field described in the insect optic lobes can provide such an encoding of spatial frequencies. Determining if ants do indeed rely on large spatial wavelengths will enable us to improve our virtual navigating agents and explore the perceptual experience of insects.

- Is the phase of oscillations linked to continuous learning? I have demonstrated that ants do oscillate during the learning stage. Moreover, there are similarities between the shape of the learning walk and the subsequent approach to the nest[40,41,148], suggesting a close connection between the phase of oscillations and learning. By studying these sensory-motor rules, we can establish a link between the intrinsic oscillation phase (as presented in Chapter 2) and its role in supporting continuous learning (Chapter 1) through internal re-afferent signals, (as suggested by Wystrach 2023[177]). By coupling VR experiments with systematic rotations of the panorama, it should be possible to determine whether reorientations resulting from rotation depend on the phases of these oscillations or can occur at any time. Additionally, this gives an insight into the sensory motor rules of ants during both learning and route following. Helping to significantly enhance our ant-agent models by incorporating more sophisticated sensory-to-motor components.

- What is the plasticity of the ant's representation of a natural scene? Although feature extraction may occur early in their visual system (as discussed in Chapter 3), this does not rule out the possibility of some plasticity in the interpretation of navigable scenery. In fact, there are significant synaptic changes and structural reorganization in the brains of foraging hymenopterans early in their careers [170,350,352], indicating that the brain may adapt to new visual environments and experiences. This plasticity is likely widespread across the animal kingdom, from invertebrates to vertebrates, as demonstrated by the famous Blakemore cat experiments [353]. Investigating synaptic changes in the early life of hymenopterans in relation to their environment could provide insight into how ants perceive the world as a result of filters set during both ontogeny (plasticity) and phylogeny.

- How learnt components are integrated into the brain for navigation? Although memory was previously thought to be independent of the temporality of views along the route[71,72,143,297], I participated in a study suggesting that there is a temporal component to memory retrieval. Indeed, disrupting the sequence of views during homing triggers a typical behaviour expressing directional uncertainty: scanning [213,372]. This highlights the fact that the field of insect navigation still has much to uncover about how views are encoded based on temporality and lateralization of the brain. In general, much remains to know how the MB encodes view and how its input is integrated into the CX [60,68,202] and the intrinsic oscillator (chapter 2).

B. An ongoing model

In the context of modelling, there are two types of mistakes that can occur: legislative errors and ontological errors. Legislative errors can occur due to incorrect assumptions or axioms of the model, in which case the latter should be rejected. Ontological errors, on the other hand, can arise from a mistake in the underlying conceptual framework or the neglect of certain parameters, but the assumptions and operation of the model may remain plausible. Both types of errors can lead to failure in capturing the behavioural signatures we wish to understand, however, models should be rejected only in the first case. Therefore, it is essential for researchers to carefully consider whether model’s mis-predictions are due to an ontological or legislative error.

My first model - still an ongoing work-is typically an illustration of an ontological error, at least as far as our current knowledge goes. The goal of this model was to obtain testable behavioural predictions and see how visual information can be processed/memorized and how

motor action can be conducted accordingly. Currently, the prevailing idea suggests that during the learning phase, navigating insects memorize the visual panorama when they are precisely oriented in the direction of their nest [71,72,141,152]. Then, upon returning to the nest, individuals compare the current views with those in memory to follow their route [71,72,141,152].

I designed an agent able to navigate using known navigation strategies (path integration and visual navigation). But I attempted to integrate three recent notions of visual learning in ants: 1- left vs. right lateralized memory banks [63] ; 2- attractive vs. aversive memory banks [37,62,74] and 3- the time wise retrospective, trace-like, aspect of learning[74].

Recent papers combining experimental and modelling approaches suggest that ants can build a lateralized memory bank [63]. Ants are able to recognize their route irrespective of their body orientation by categorizing views as left or right of their goal and, by later, recognizing these views[63]. Thus, insects can determine whether the route direction lies to their left or right. Additionally, when a new ditch or obstacle is placed along a well-known foraging route, ants can anticipate the trap and avoid it before it is even visible. The negative event of falling in the pit is not associated with the current view within the pit, but with the view experienced a few moments before. This suggests that previous views have been associated as repulsive, and shows that ants update memory retrospectively [74,241].

By unifying these three notions within the same model, it is possible to derive a clear prediction: if a turn in one direction leads to an obstacle, then the view associated with this turn becomes aversive, and then, during the next trip, recognizing this view should henceforth lead the ant to turn in the opposite direction, which would effectively lead her away from the trap. By modelling these rules, I showed that an agent would successfully learn a route and avoid a trap (unpublished data), producing remarkably similar paths as ants do [74,241].

We performed a preliminary experiment to test our model. We divided our test subjects into two groups: a naïve group and an experienced group. The naïve group consisted of ants that had no prior knowledge of the route when they experienced the pitfall, while the experienced group had already learned the route several times before we introduced the pitfall. Our ant agent models were able to explain the data from the naïve group effectively but failed to explain the results from the experienced group. This revealed suggests an ontological error, as where I neglected to account for the effect of previous experience on the formation of aversive memory. Therefore, while the model of lateralized memory bank and retrospective memory construction remains relevant and plausible, it requires some adjustments to explain the effect of previous

experience on behaviour, and I hope to make these corrections and test the model experimentally in the future.

4.2.2. How to ask, predict and answer questions

In the scientific process, questions play a crucial role. While objectivity is vital in science, our questions are rooted in our subjectivity, which is formed by our prior research and knowledge, and even our failures. Tinbergen's four questions provide a framework for our research, dividing the study of animal behaviour into four perspectives which I tackled in my work: "mechanism" (chapter 2 and 3), "ontogeny" (chapter 1), "function"(chapter 1,2 & 3), and "phylogeny" (chapter 2) (Tinbergen, 1963[373]). Conducting experiments with ants provided an opportunity to observe unexpected behaviours, which, in turn, led to new questions and avenues for exploration (as shown previously). Tinbergen's work demonstrated the value of observing animals in their natural environment, as it often generates insightful questions and even uncovers unexpected answers.

But this framework is inherently connected with our own experience in the way we ask and answer questions. During my PhD I tried to use a multi-level approach, coupling experimentation and modelling, as well as advanced statistics; keeping in mind that I am not objective but rather subjective: notably I tend to perceive this insects' beaviour through the belief of simplicity.

A. Considering the animal's umwelt

Conducting experiments is a challenging and ongoing process, where even failure can be an opportunity to learn and gain new insights. Two errors of the opposite kind gave me novel insight. During my first VR experiment designed to study learning mechanism, I put all my effort into trying to make ants learn a route in the VR, which resulted in a failure. Ants would never learn in the VR. Conversely, in the field, I put all my efforts into trying to impair ants' route learning in their natural environment, but I never succeeded. In a natural environment, ants always learn, even without a reward. However, this failure inspired me to explore the learning strategies and mechanism of navigating ants (chapter 1). These paradoxical results, highlight the importance of being in tune with the ecological world of animals, their

umwelt[356], in order to investigate the mechanisms underlying behaviour. If we are not in phase with the umwelt, the question we asked might make no sense to the animal and, worst, the conclusion that we draw could be totally aberrant. In the case of the VR, failure is probably due to the lack of UV light, which induces important synaptic change in the ant brain [170,352,374], and which is an important component of the insect's visual repertoire[339].

Animals have their own specific way of perceiving and interacting with the environment. In my attempt to understand behaviour, I embarked on an approach that, unfortunately, failed due to a lack of synchronization with their sensory experiences. But, for me, failure is key to scientific progress, not only because it rejects wrong theory[375], but also through a more constructive aspect: by providing insight for novel hypothesis.

B. The case of the cognitive map

Navigation is a ubiquitous task that we encounter in our daily lives, making it challenging to generate hypotheses that are dissociated from our own experiences and perceptions of the world. In addition, both vertebrates (including us humans) and invertebrates rely on similar strategies for navigating their complex environments, such as learned terrestrial cues and vector based navigation[78,248,376]. Vertebrates appear to use these sources of information to construct a mental representation of their surroundings known as a cognitive map[248–250]. The prevalence of this task and strategy, combined with our own experiences, can have an impact on the study of navigation. For instance, it is still widely debated whether insects, such as bees, also build a similar centralized representation of space [137,196,218–223], a hypothesis that surely is rooted in our human introspection.

The evidence argued over is whether the behaviours observed in insects form a positive proof for the existence of cognitive map or can be explained by lower-level heuristics mechanisms [137,218–223]. However, as achieved before with ants [196], we presented here (chapter 1) behaviours that are incongruent with a map-like representation, and thus provide convincing evidence for its absence. Such an approach (i.e., testing for the absence rather than the presence of a map-like representation) or at least seeking for more parsimonious hypothesis is a key to answering questions that are still much debated. Thus, it may be more efficient in resolving the current debate regarding the use of map-like representations, especially in bees, to design protocol putting forward behaviours that at odds with the use of cognitive map, rather than

trying to prove the existence of such a complex representation of space. As we did in chapter 1, such incongruent behaviours enabled us to dig into a simpler explanation, where continuous learning is based on the interaction of two memory banks.

This approach does not completely solve the issues that arise from our own subjectivity, but by looking in both directions (search for congruent and incongruent proofs) we can try to seek for more parsimonious hypotheses and explanations.

C. The pro and cons of modelling

In addition to considering the animal's umwelt and Tinbergen's framework, one can consider the use of the neuroanatomy to try to ask and answer questions more objectively. A way to link behaviour and neuroanatomy is to use a modelling approach[68,76].

Models allow to simplify reality and understand how behaviour emerges from the interactions between multiple components. These models allow us to ask questions about the mechanisms and possible implementations in relation to the insect's neuroanatomy. By creating models, we can explore how a behaviour could be implemented based on our underlying hypotheses and knowledge of the insect's neuroanatomy[37,62,63,65,68,71,132,205,264]. By doing so, we can make predictions about the insect's behaviour and use these predictions as a basis for experimentation. Despite the abstraction involved in creating models, we may be amazed by how these models can help identify behavioural signatures that have not yet been explained in the literature (chapter 1 & 2).

I'm still amazed at how complex behaviour can emerge from simplicity. Even from the simple models (but still biologically plausible as presented here chapter 1&2). Thus, for me, simplicity and plausibility are necessary conditions to avoid falling into too complex and incongruent models. Behavioural mathematical models use equations to represent and summarize the output, as quantified in specific assays, but they do not necessarily explain the underlying mechanisms that give rise to the behaviour. Instead, they compress the behavioural output into an equation, thus they describe the product rather than explain its emergence. By modelling the final product, mathematical models may have hidden assumptions about availability of world parameters to the system. When it comes to unravel mechanisms, models should benefit from constraints such as neurobiological plausibility, ecological function and obviously experimentation (chapter 1&2). On the other hand, as new experimental or neural

results emerge, our models can be further refined, creating a positive feedback loop towards achieving a more comprehensive, multi-level understanding of navigation in natural environments. Most importantly, neural models, by asking which structure are involved and how it could be implemented, allow us to give testable predictions both at the behavioural and neural level, which can be thus tested with either with behavioural or neurobiological approaches.

However, creating models involves simplification, one could argue that by doing so, we inevitably remove the inherent complexity for behaviour to emerge. But models, despite their simplicity, allow us to explore emergent properties and provide testable predictions to fuel experiments targeted at demonstrating how behaviour fundamentally emerges from interacting modules. In other words, they enable us to understand how brains body and environment interact. Thus, I am now convinced that models are a powerful but dangerous tool to both ask and answer questions.

"All models are wrong, but some are useful."[377]

George E.P. Box

To sum up, questions in science are inherently connected to past research and current observations, forming a continuous cycle of interaction between answers, failures, successes, and subjectivity. This dynamic process allows for new discoveries and a deeper understanding of the natural behaviour. Modelling, experimentation, and neurobiological approaches all serve multiple purposes, including the exploration -raising questions- and dissecting the intricate interactions among the brain, environment, and body, thereby enabling us to understand the underlying mechanics of behaviour through the generation of testable predictions.

Ultimately, it can be challenging to separate the processes which enable us to ask questions, make predictions, and provide answers. All these aspects must be in alignment with the animal's umwelt, ensuring ecological relevance. While questions should strive for objectivity, it is important to recognize that our own subjectivity, existing knowledge, and personal interests shape the questions we ask. One of a way to control our own experiences is by using various frameworks, such as the use of anatomically constrained model or Tinbergen's four questions that offer avenues to address different levels of inquiry. However, it is through the process of answering questions that we can actively control and maintain objectivity.

Conclusion

This work has employed a multi-level approach to investigate how behaviour arises from the brain's interaction with the internal and external environment. The integrative approach has revealed that the core of higher-level processes in ant navigation mechanisms is a basic and ancestral component. This work presents evidence that contradicts the prevalent 'sensorimotor' view suggesting that animals passively await a stimulus to trigger a response, characterizing them as inactive until external stimuli switch their state to an active one. I emphasized the significance of internally generated movements, putting forward an active-dynamic view of animals that actively move around their environment to gather and process information. This perspective acknowledges that external stimuli can modulate behaviour but also recognizes the significant role played by internal states and motivation, underlying that navigation behaviour emerges from the interactions between the brain, body, and environment, where the distinction between internal and external information sources is blurred. The non-linear dynamic created by the interaction between distributed sources of information is key for discrete behaviour to emerge from continuous mechanism. Thus, and perhaps paradoxically, richly connected neural networks suggest higher intelligence, but provide a perfect ground for decisions to emerge from distributed interactions, without the need for centralizing information in one place to form ‘informed’ decision-making. One could define intelligence as the faculty of using previous knowledge to adapt decisions in novel contexts involving high-level processes and top-down decisions. However, intelligence can also be seen as an emergent property of such a modular and distributed system.

In conclusion, this work contributes to unravel how behaviour arises from continuous multi-level interactions. Stressing the importance of embodiment mechanisms that free the organism from the need of centralizing information and forming higher levels representations. Thus, the definition of intelligence can’t be as clear-cut as a wise decision-making process, emphasizing the need for a distributed approach to get a better understanding of behaviour.

I hope that this work will contribute to the further advancement of our understanding of mechanisms underlying visual navigation, while also providing new tools for their study. Despite considering insects from a belief of simplicity, their behaviour is paradoxically sophisticated and complex because simplicity can give rise to emergent properties.

The lesson is, always try.

References

1. Pfeffer, S., and Wolf, H. (2020). Arthropod spatial cognition. Anim Cogn *23*, 1041–1049. 10.1007/s10071-020-01446-4.

2. Scudder, G.G.E. (2017). The Importance of Insects. In Insect Biodiversity, R. G. Foottit and P. H. Adler, eds. (John Wiley & Sons, Ltd), pp. 9–43. 10.1002/9781118945568.ch2.

3. Stork, N.E. (2018). How Many Species of Insects and Other Terrestrial Arthropods Are There on Earth? Annu. Rev. Entomol. *63*, 31–45. 10.1146/annurev-ento-020117-043348.

4. Wilson, E.O. (1987). The Little Things That Run the world* (The Importance and Conservation of Invertebrates). Conservation Biology *1*, 344–346. 10.1111/j.1523-1739.1987.tb00055.x.

5. Bar-On, Y.M., Phillips, R., and Milo, R. (2018). The biomass distribution on Earth. Proc. Natl. Acad. Sci. U.S.A. *115*, 6506–6511. 10.1073/pnas.1711842115.

6. Descartes, R. (1637). Discours de la méthode.

7. Platt, M.L., and Spelke, E.S. (2009). What can developmental and comparative cognitive neuroscience tell us about the adult human brain? Current Opinion in Neurobiology *19*, 1–5. 10.1016/j.conb.2009.06.002.

8. Fabre, J.-H. (1879). Souvenirs entomologiques.

9. Freeman, R. (1968). Charles Darwin on the routes of male humble bees.

10. Buehlmann, C., Mangan, M., and Graham, P. (2020). Multimodal interactions in insect navigation. Anim Cogn *23*, 1129–1141. 10.1007/s10071-020-01383-2.

11. Collett, T.S. (1992). Landmark learning and guidance in insects. Phil. Trans. R. Soc. Lond. B *337*, 295–303. 10.1098/rstb.1992.0107.

12. Collett, T.S., Graham, P., and Harris, R.A. (2007). Novel landmark-guided routes in ants. Journal of Experimental Biology *210*, 2025–2032. 10.1242/jeb.000315.

13. Dacke, M., Baird, E., Byrne, M., Scholtz, C.H., and Warrant, E.J. (2013). Dung Beetles Use the Milky Way for Orientation. Current Biology *23*, 298–300. 10.1016/j.cub.2012.12.034.

14. Fleischmann, P.N., Grob, R., Müller, V.L., Wehner, R., and Rössler, W. (2018). The Geomagnetic Field Is a Compass Cue in Cataglyphis Ant Navigation. Current Biology *28*, 1440-1444.e2. 10.1016/j.cub.2018.03.043.

15. Graham, P., and Cheng, K. (2009). Ants use the panoramic skyline as a visual cue during navigation. Current Biology *19*, R935–R937. 10.1016/j.cub.2009.08.015.

16. Harris, R.A., Graham, P., and Collett, T.S. (2007). Visual Cues for the Retrieval of Landmark Memories by Navigating Wood Ants. Current Biology *17*, 93–102. 10.1016/j.cub.2006.10.068.

17. Müller, M., and Wehner, R. (2007). Wind and sky as compass cues in desert ant navigation. Naturwissenschaften *94*, 589–594. 10.1007/s00114-007-0232-4.

18. Wehner, R., and Muller, M. (2006). The significance of direct sunlight and polarized skylight in the ant's celestial system of navigation. Proceedings of the National Academy of Sciences *103*, 12575–12579. 10.1073/pnas.0604430103.

19. Willis, MarkA., and Arbas, EdmundA. (1991). Odor-modulated upwind flight of the sphinx moth, Manduca sexta L. J Comp Physiol A *169*. 10.1007/BF00197655.

20. Wystrach, A., Beugnon, G., and Cheng, K. (2011). Landmarks or panoramas: what do navigating ants attend to for guidance? Front Zool *8*, 21. 10.1186/1742-9994-8-21.

21. Hangartner, W. (1967). Spezifit/it und Inaktivierung des Spurphcromons yon Lasius fuliginosus Latr. und Orientierung der Arbeiterinnen im Duftfeld. Springer *57*, 34. 10.1007/BF00303068.

22. Labhart, T., and Meyer, E.P. (2002). Neural mechanisms in insect navigation: polarization compass and odometer. Current Opinion in Neurobiology *12*, 707–714. 10.1016/S0959-4388(02)00384-7.

23. Labhart, T., and Meyer, E.P. (1999). Detectors for polarized skylight in insects: a survey of ommatidial specializations in the dorsal rim area of the compound eye. Microsc. Res. Tech. *47*, 368–379. 10.1002/(SICI)1097-0029(19991215)47:6<368::AID-JEMT2>3.0.CO;2-Q.

24. Möller, R. (2002). Insects Could Exploit UV–Green Contrast for Landmark Navigation. Journal of Theoretical Biology *214*, 619–631. 10.1006/jtbi.2001.2484.

25. Wittlinger, M., Wehner, R., and Wolf, H. (2007). The desert ant odometer: a stride integrator that accounts for stride length and walking speed. Journal of Experimental Biology *210*, 198–207. 10.1242/jeb.02657.

26. Kohler, M., and Wehner, R. (2005). Idiosyncratic route-based memories in desert ants, Melophorus bagoti: How do they interact with path-integration vectors? Neurobiology of Learning and Memory *83*, 1–12. 10.1016/j.nlm.2004.05.011.

27. Mangan, M., and Webb, B. (2012). Spontaneous formation of multiple routes in individual desert ants (Cataglyphis velox). Behavioral Ecology *23*, 944–954. 10.1093/beheco/ars051.

28. Müller, M., and Wehner, R. (2010). Path Integration Provides a Scaffold for Landmark Learning in Desert Ants. Current Biology *20*, 1368–1371. 10.1016/j.cub.2010.06.035.

29. Schatz, B., Chameron, S., Beugnon, G., and Collett, T.S. (1999). The use of path integration to guide route learning in ants. Nature *399*, 769–772. 10.1038/21625.

30. Schultheiss, P., Cheng, K., and Reynolds, A.M. (2015). Searching behavior in social Hymenoptera. Learning and Motivation *50*, 59–67. 10.1016/j.lmot.2014.11.002.

31. Zeil, J., and Fleischmann, P.N. (2019). The learning walks of ants (Hymenoptera: Formicidae). 10.25849/MYRMECOL.NEWS_029:093.

32. Baird, E., Srinivasan, M.V., Zhang, S., and Cowling, A. (2005). Visual control of flight speed in honeybees. Journal of Experimental Biology *208*, 3895–3905. 10.1242/jeb.01818.

33. Boeddeker, N., and Hemmi, J.M. (2010). Visual gaze control during peering flight manoeuvres in honeybees. Proc. R. Soc. B. *277*, 1209–1217. 10.1098/rspb.2009.1928.

34. Lent, D.D., Graham, P., and Collett, T.S. (2013). Phase-Dependent Visual Control of the Zigzag Paths of Navigating Wood Ants. Current Biology *23*, 2393–2399. 10.1016/j.cub.2013.10.014.

35. Lent, D.D., Graham, P., and Collett, T.S. (2010). Image-matching during ant navigation occurs through saccade-like body turns controlled by learned visual features. Proceedings of the National Academy of Sciences *107*, 16348–16353. 10.1073/pnas.1006021107.

36. Lent, D.D., Graham, P., and Collett, T.S. (2009). A Motor Component to the Memories of Habitual Foraging Routes in Wood Ants? Current Biology *19*, 115–121. 10.1016/j.cub.2008.11.060.

37. Murray, T., Kócsi, Z., Dahmen, H., Narendra, A., Le Möel, F., Wystrach, A., and Zeil, J. (2020). The role of attractive and repellent scene memories in ant homing (*Myrmecia croslandi*). J Exp Biol *223*, jeb210021. 10.1242/jeb.210021.

38. Nityananda, V., Tarawneh, G., Errington, S., Serrano-Pedraza, I., and Read, J. (2017). The optomotor response of the praying mantis is driven predominantly by the central visual field. J Comp Physiol A *203*, 77–87. 10.1007/s00359-016-1139-3.

39. Nuutila, J., Honkanen, A.E., Heimonen, K., and Weckström, M. (2020). The effect of vertical extent of stimuli on cockroach optomotor response. Journal of Experimental Biology, jeb.204768. 10.1242/jeb.204768.

40. Philippides, A., de Ibarra, N.H., Riabinina, O., and Collett, T.S. (2013). Bumblebee calligraphy: the design and control of flight motifs in the learning and return flights of Bombus terrestris. Journal of Experimental Biology *216*, 1093–1104. 10.1242/jeb.081455.

41. Stürzl, W., Zeil, J., Boeddeker, N., and Hemmi, J.M. (2016). How Wasps Acquire and Use Views for Homing. Current Biology *26*, 470–482. 10.1016/j.cub.2015.12.052.

42. el Jundi, B., Pfeiffer, K., Heinze, S., and Homberg, U. (2014). Integration of polarization and chromatic cues in the insect sky compass. J Comp Physiol A. 10.1007/s00359-014-0890-6.

43. el Jundi, B., Pfeiffer, K., and Homberg, U. (2011). A Distinct Layer of the Medulla Integrates Sky Compass Signals in the Brain of an Insect. PLoS ONE *6*, e27855. 10.1371/journal.pone.0027855.

44. el Jundi, B., and Homberg, U. (2012). Receptive field properties and intensity-response functions of polarization-sensitive neurons of the optic tubercle in gregarious and solitarious locusts. Journal of Neurophysiology *108*, 1695–1710. 10.1152/jn.01023.2011.

45. Habenstein, J., Amini, E., Grübel, K., el Jundi, B., and Rössler, W. (2020). The brain of Cataglyphis ants: Neuronal organization and visual projections. J Comp Neurol *528*, 3479–3506. 10.1002/cne.24934.

46. Hardcastle, B.J., Omoto, J.J., Kandimalla, P., Nguyen, B.-C.M., Keleş, M.F., Boyd, N.K., Hartenstein, V., and Frye, M.A. (2021). A visual pathway for skylight polarization processing in Drosophila. eLife *10*, e63225. 10.7554/eLife.63225.

47. Hulse, B.K., Haberkern, H., Franconville, R., Turner-E, D., Dreher, M., Dan, C., Parekh, R., Hermundstad, A.M., Rubin, G.M., and Jayaraman, V. (2021). A connectome of the Drosophila

central complex reveals network motifs suitable for flexible navigation and context--dependent action selection. Elife, 180.

48. Kim, A.J., Fitzgerald, J.K., and Maimon, G. (2015). Cellular evidence for efference copy in Drosophila visuomotor processing. Nat Neurosci *18*, 1247–1255. 10.1038/nn.4083.

49. Ogawa, Y., Falkowski, M., Narendra, A., Zeil, J., and Hemmi, J.M. (2015). Three spectrally distinct photoreceptors in diurnal and nocturnal Australian ants. Proc. R. Soc. B. *282*, 20150673. 10.1098/rspb.2015.0673.

50. Steinbeck, F., Adden, A., and Graham, P. (2020). Connecting brain to behaviour: a role for general purpose steering circuits in insect orientation? J Exp Biol *223*, jeb212332. 10.1242/jeb.212332.

51. Kanzaki, R., Sugi, N., and Shibuya, T. (1992). Self-generated Zigzag Turning of Bombyx mori Males during Pheromone-mediated Upwind Walking(Physology). Zoological science. *9*, 515–527.

52. Namiki, S., Iwabuchi, S., Pansopha Kono, P., and Kanzaki, R. (2014). Information flow through neural circuits for pheromone orientation. Nat Commun *5*, 5919. 10.1038/ncomms6919.

53. Olberg, R.M. (1983). Pheromone-triggered flip-flopping interneurons in the ventral nerve cord of the silkworm moth,Bombyx mori. J. Comp. Physiol. *152*, 297–307. 10.1007/BF00606236.

54. Pansopha, P., Ando, N., and Kanzaki, R. (2014). Dynamic use of optic flow during pheromone tracking by the male silkmoth, Bombyx mori. Journal of Experimental Biology *217*, 1811–1820. 10.1242/jeb.090266.

55. Seelig, J.D., and Jayaraman, V. (2015). Neural dynamics for landmark orientation and angular path integration. Nature *521*, 186–191. 10.1038/nature14446.

56. Seelig, J.D., and Jayaraman, V. (2013). Feature detection and orientation tuning in the Drosophila central complex. Nature *503*, 262–266. 10.1038/nature12601.

57. Beetz, M.J., Kraus, C., and el Jundi, B. (2022). Neural representation of goal direction in the monarch butterfly brain (Neuroscience) 10.1101/2022.10.15.512348.

58. Beetz, M.J., Kraus, C., Franzke, M., and Dreyer, D. (2021). State-dependent egocentric and allocentric heading representation in the monarch butterfly brain. 34.

59. el Jundi, B., Baird, E., Byrne, M.J., and Dacke, M. (2019). The brain behind straight-line orientation in dung beetles. Journal of Experimental Biology *222*, jeb192450. 10.1242/jeb.192450.

60. Honkanen, A., and Adden, A. (2019). The insect central complex and the neural basis of navigational strategies. Journal of Experimental Biology, 15.

61. Kim, S.S., Hermundstad, A.M., Romani, S., Abbott, L.F., and Jayaraman, V. (2019). Generation of stable heading representations in diverse visual scenes. Nature *576*, 126–131. 10.1038/s41586-019-1767-1.

62. Le Möel, F., and Wystrach, A. (2020). Opponent processes in visual memories: A model of attraction and repulsion in navigating insects' mushroom bodies. PLoS Comput Biol *16*, e1007631. 10.1371/journal.pcbi.1007631.

63. Wystrach, A., Le Moël, F., Clement, L., and Schwarz, S. (2020). A lateralised design for the interaction of visual memories and heading representations in navigating ants (Animal Behavior and Cognition) 10.1101/2020.08.13.249193.

64. Buehlmann, C., Wozniak, B., Goulard, R., Webb, B., Graham, P., and Niven, J.E. (2020). Mushroom Bodies Are Required for Learned Visual Navigation, but Not for Innate Visual Behavior, in Ants. Current Biology *30*, 3438-3443.e2. 10.1016/j.cub.2020.07.013.

65. Heisenberg, M. (2003). Mushroom body memoir: from maps to models. Nat Rev Neurosci *4*, 266–275. 10.1038/nrn1074.

66. Izquierdo, I., Medina, J.H., Vianna, M.R.M., Izquierdo, L.A., and Barros, D.M. (1999). Separate mechanisms for short- and long-term memory. Behavioural Brain Research *103*, 1–11. 10.1016/S0166-4328(99)00036-4.

67. Menzel, R. (2014). The insect mushroom body, an experience-dependent recoding device. Journal of Physiology-Paris *108*, 84–95. 10.1016/j.jphysparis.2014.07.004.

68. Webb, B., and Wystrach, A. (2016). Neural mechanisms of insect navigation. Current Opinion in Insect Science *15*, 27–39. 10.1016/j.cois.2016.02.011.

69. Ardin, P., Peng, F., Mangan, M., Lagogiannis, K., and Webb, B. (2016). Using an Insect Mushroom Body Circuit to Encode Route Memory in Complex Natural Environments. PLoS Comput Biol *12*, e1004683. 10.1371/journal.pcbi.1004683.

70. Aso, Y., Hattori, D., Yu, Y., Johnston, R.M., Iyer, N.A., Ngo, T.-T., Dionne, H., Abbott, L., Axel, R., Tanimoto, H., et al. (2014). The neuronal architecture of the mushroom body provides a logic for associative learning. eLife *3*, e04577. 10.7554/eLife.04577.

71. Baddeley, B., Graham, P., Husbands, P., and Philippides, A. (2012). A Model of Ant Route Navigation Driven by Scene Familiarity. PLoS Comput Biol *8*, e1002336. 10.1371/journal.pcbi.1002336.

72. Baddeley, B., Graham, P., Philippides, A., and Husbands, P. (2011). Holistic visual encoding of ant-like routes: Navigation without waypoints. Adaptive Behavior *19*, 3–15. 10.1177/1059712310395410.

73. Hattori, D., Aso, Y., Swartz, K.J., Rubin, G.M., Abbott, L.F., and Axel, R. (2017). Representations of Novelty and Familiarity in a Mushroom Body Compartment. Cell *169*, 956-969.e17. 10.1016/j.cell.2017.04.028.

74. Wystrach, A., Buehlmann, C., Schwarz, S., Cheng, K., and Graham, P. (2020). Rapid Aversive and Memory Trace Learning during Route Navigation in Desert Ants. Current Biology *30*, 1927-1933.e2. 10.1016/j.cub.2020.02.082.

75. Wystrach, A., Mangan, M., Philippides, A., and Graham, P. (2013). Snapshots in ants? New interpretations of paradigmatic experiments. Journal of Experimental Biology *216*, 1766–1770. 10.1242/jeb.082941.

76. Le Moël, F., and Wystrach, A. (2020). Towards a multi-level understanding in insect navigation. Current Opinion in Insect Science *42*, 110–117. 10.1016/j.cois.2020.10.006.

77. Pritchard, D.J., and Healy, S.D. (2018). Taking an insect-inspired approach to bird navigation. Learn Behav *46*, 7–22. 10.3758/s13420-018-0314-5.

78. Wang, R.F., and Spelke, E.S. (2002). Human spatial representation: insights from animals. Trends in Cognitive Sciences *6*, 376–382. 10.1016/S1364-6613(02)01961-7.

79. Wystrach, A., and Graham, P. (2012). What can we learn from studies of insect navigation? Animal Behaviour *84*, 13–20. 10.1016/j.anbehav.2012.04.017.

80. Dupeyroux, J., Diperi, J., Boyron, M., Viollet, S., and Serres, J. (2017). A bio-inspired celestial compass applied to an ant-inspired robot for autonomous navigation. In 2017 European Conference on Mobile Robots (ECMR) (IEEE), pp. 1–6. 10.1109/ECMR.2017.8098680.

81. Franz, M.O., and Mallot, H.A. (2000). Biomimetic robot navigation &. Robotics and Autonomous Systems.

82. Lambrinos, D., Möller, R., Labhart, T., Pfeifer, R., and Wehner, R. (2000). A mobile robot employing insect strategies for navigation. Robotics and Autonomous Systems *30*, 39–64. 10.1016/S0921-8890(99)00064-0.

83. Srinivasan, M.V. (2011). Visual control of navigation in insects and its relevance for robotics. Current Opinion in Neurobiology *21*, 535–543. 10.1016/j.conb.2011.05.020.

84. Webb, B. (2020). Robots with insect brains. Science *368*, 244–245. 10.1126/science.aaz6869.

85. Ruffier, F., Viollet, S., Amic, S., and Franceschini, N. (2003). Bio-inspired optical flow circuits for the visual guidance of micro air vehicles. In Proceedings of the 2003 International Symposium on Circuits and Systems, 2003. ISCAS '03. (IEEE), pp. III-846-III–849. 10.1109/ISCAS.2003.1205152.

86. Gattaux, G., Vimbert, R., Wystrach, A., Serres, J.R., and Ruffier, F. (2023). Antcar: Simple Route Following Task with Ants-Inspired Vision and Neural Model. hal.

87. Serres, J.R., and Ruffier, F. (2017). Optic flow-based collision-free strategies: From insects to robots. Arthropod Structure & Development *46*, 703–717. 10.1016/j.asd.2017.06.003.

88. Franceschini, N., Ruffier, F., and Serres, J. (2007). A Bio-Inspired Flying Robot Sheds Light on Insect Piloting Abilities. Current Biology *17*, 329–335. 10.1016/j.cub.2006.12.032.

89. Wehner, R. (2016). Early ant trajectories: spatial behaviour before behaviourism. J Comp Physiol A *202*, 247–266. 10.1007/s00359-015-1060-1.

90. Santschi, F. (1911). Obervations et remarques critiques sur le mécanisme de l'orientation chez les fourmis.

91. Von Frisch, K. (1949). Die Polarisation des Himmelslichtes als orientierender Faktor bei den Tänzen der Bienen. Experientia, 142–148.

92. Cornetz, V. (1910). Album faisant suite aux Trajets de fourmis et retours au nid.pdf.

93. Von Frish, K. (1914). Der farbensinn und Formensinn der Biene.

94. Tinbergen, N., and Kruyt, W. (1938). Über die Orientierung des Bienenwolfes (Philanthus triangulum Fabr.). Z vergl Physiol *25*, 292–334.

95. Tinbergen, N. (1951). The Study of Instinct.

96. Brun, R. (1916). Weitere Untersuchungen über die Fernorientierung der Ameisen.

97. Wehner, R. (2008). The architecture of the desert ant's navigational toolkit (Hymenoptera: Formicidae). Myrmecol. News, 85–96.

98. Muller, M., and Wehner, R. (1988). Path integration in desert ants, Cataglyphis fortis. Proceedings of the National Academy of Sciences *85*, 5287–5290. 10.1073/pnas.85.14.5287.

99. Heinze, S., Narendra, A., and Cheung, A. (2018). Principles of Insect Path Integration. Current Biology *28*, R1043–R1058. 10.1016/j.cub.2018.04.058.

100. Zeil, J., Ribi, W.A., and Narendra, A. (2014). Polarisation Vision in Ants, Bees and Wasps. In Polarized Light and Polarization Vision in Animal Sciences, G. Horváth, ed. (Springer Berlin Heidelberg), pp. 41–60. 10.1007/978-3-642-54718-8_3.

101. Pomozi, I., HorvÁth, G., and Wehner, R. (2001). Polarization of cloudy skies and animal navigation. J Exp Biol.

102. Aepli, F., Labhart, T., and Meyer, E.P. (1985). Structural specializations of the cornea and retina at the dorsal rim of the compound eye in hymenopteran insects. Cell Tissue Res. *239*, 19–24. 10.1007/BF00214897.

103. Wolf, H., and Wehner, R. (2000). Pinpointing food sources: olfactory and anemotactic orientation in desert ants, Cataglyphis fortis. 10.5167/UZH-636.

104. Wystrach, A., and Schwarz, S. (2013). Ants use a predictive mechanism to compensate for passive displacements by wind. Current Biology *23*, R1083–R1085. 10.1016/j.cub.2013.10.072.

105. Fleischmann, P.N., Grob, R., and Rössler, W. (2021). Magnetosensation during re-learning walks in desert ants (Cataglyphis nodus). J Comp Physiol A *208*, 125–133.

106. Riveros, A.J., and Srygley, R.B. (2008). Do leafcutter ants, Atta colombica, orient their path-integrated home vector with a magnetic compass? Animal Behaviour *75*, 1273–1281. 10.1016/j.anbehav.2007.09.030.

107. Dacke, M., Byrne, M.J., Scholtz, C.H., and Warrant, E.J. (2004). Lunar orientation in a beetle. Proc. R. Soc. Lond. B *271*, 361–365. 10.1098/rspb.2003.2594.

108. Collett, T.S., and Collett, M. (2000). Path integration in insects. Current Opinion in Neurobiology.

109. Srinivasan, M.V. (2014). Going with the flow: a brief history of the study of the honeybee's navigational 'odometer.' J Comp Physiol A *200*, 563–573. 10.1007/s00359-014-0902-6.

110. Srinivasan, M.V., Zhang, S., Altwein, M., and Tautz, J. (2000). Honeybee Navigation: Nature and Calibration of the "Odometer." Science *287*, 851–853. 10.1126/science.287.5454.851.

111. Pfeffer, S.E., and Wittlinger, M. (2016). Optic flow odometry operates independently of stride integration in carried ants. Science *353*, 1155–1157. 10.1126/science.aaf9754.

112. Ronacher, B., and Wehner, R. (1995). Desert ants Cataglyphislot fortis use self-induced optic flow to measure distances travelled. J Comp Physiol A *177*.

113. Wolf, H. (2011). Odometry and insect navigation. Journal of Experimental Biology *214*, 1629–1641. 10.1242/jeb.038570.

114. Beugnon, G., and Campan, R. (1989). Homing in the field cricket,Gryllus campestris. J Insect Behav *2*, 187–198. 10.1007/BF01053291.

115. Durier, V., and Rivault, C. (1999). Path integration in cockroach larvae,Blattella germanica (L.) (insect: Dictyoptera): Direction and distance estimation. Animal Learning & Behavior *27*, 108–118. 10.3758/BF03199436.

116. Hironaka, M., Filippi, L., Nomakuchi, S., Horiguchi, H., and Hariyama, T. (2007). Hierarchical use of chemical marking and path integration in the homing trip of a subsocial shield bug. Animal Behaviour *73*, 739–745. 10.1016/j.anbehav.2006.06.009.

117. Kim, I.S., and Dickinson, M.H. (2017). Idiothetic Path Integration in the Fruit Fly Drosophila melanogaster. Current Biology *27*, 2227-2238.e3. 10.1016/j.cub.2017.06.026.

118. Sergi, C.M., Antonopoulos, T., and Rodríguez, R.L. (2021). Black widow spiders use path integration on their webs. Behav Ecol Sociobiol *75*, 73. 10.1007/s00265-021-03009-0.

119. Patel, R.N., and Cronin, T.W. (2020). Mantis Shrimp Navigate Home Using Celestial and Idiothetic Path Integration. Current Biology *30*, 1981-1987.e3. 10.1016/j.cub.2020.03.023.

120. Dacke, M., el Jundi, B., Gagnon, Y., Yilmaz, A., Byrne, M., and Baird, E. (2020). A dung beetle that path integrates without the use of landmarks. Anim Cogn *23*, 1161–1175. 10.1007/s10071-020-01426-8.

121. Homberg, U. (2008). Evolution of the central complex in the arthropod brain with respect to the visual system. Arthropod Structure & Development *37*, 347–362. 10.1016/j.asd.2008.01.008.

122. Lyu, C., Abbott, L.F., and Maimon, G. (2020). A neuronal circuit for vector computation builds an allocentric traveling-direction signal in the *Drosophila* fan-shaped body (Neuroscience) 10.1101/2020.12.22.423967.

123. Green, J., Vijayan, V., Mussells Pires, P., Adachi, A., and Maimon, G. (2018). Walking *Drosophila* aim to maintain a neural heading estimate at an internal goal angle (Neuroscience) 10.1101/315796.

124. Green, J., Adachi, A., Shah, K.K., Hirokawa, J.D., Magani, P.S., and Maimon, G. (2017). A neural circuit architecture for angular integration in Drosophila. Nature *546*, 101–106. 10.1038/nature22343.

125. Green, J., and Maimon, G. (2018). Building a heading signal from anatomically defined neuron types in the Drosophila central complex. Current Opinion in Neurobiology *52*, 156–164. 10.1016/j.conb.2018.06.010.

126. Heinze, S., and Homberg, U. (2007). Maplike Representation of Celestial *E* -Vector Orientations in the Brain of an Insect. Science *315*, 995–997. 10.1126/science.1135531.

127. Heinze, S., and Reppert, S.M. (2011). Sun Compass Integration of Skylight Cues in Migratory Monarch Butterflies. Neuron *69*, 345–358. 10.1016/j.neuron.2010.12.025.

128. Homberg, U. (2004). In search of the sky compass in the insect brain. Naturwissenschaften *91*, 199–208. 10.1007/s00114-004-0525-9.

129. Kathman, N.D., Kesavan, M., and Ritzmann, R.E. (2014). Encoding wide-field motion and direction in the central complex of the cockroach, *Blaberous discoidalis*. Journal of Experimental Biology, jeb.112391. 10.1242/jeb.112391.

130. Sayre, M.E., Templin, R., Chavez, J., Kempenaers, J., and Heinze, S. (2021). A projectome of the bumblebee central complex. eLife *10*, e68911. 10.7554/eLife.68911.

131. Turner-Evans, D.B., and Jayaraman, V. (2016). The insect central complex. Current Biology *26*, R453–R457. 10.1016/j.cub.2016.04.006.

132. Adden, A., Stewart, T.C., Webb, B., and Heinze, S. (2022). A Neural Model for Insect Steering Applied to Olfaction and Path Integration. Neural Computation *34*, 2205–2231. 10.1162/neco_a_01540.

133. Le Moël, F., Stone, T., Lihoreau, M., Wystrach, A., and Webb, B. (2019). The Central Complex as a Potential Substrate for Vector Based Navigation. Front. Psychol. *10*, 690. 10.3389/fpsyg.2019.00690.

134. Stone, T., Webb, B., Adden, A., Weddig, N.B., Honkanen, A., Templin, R., Wcislo, W., Scimeca, L., Warrant, E., and Heinze, S. (2017). An Anatomically Constrained Model for Path Integration in the Bee Brain. Current Biology *27*, 3069-3085.e11. 10.1016/j.cub.2017.08.052.

135. Bolek, S., Wittlinger, M., and Wolf, H. (2012). Establishing food site vectors in desert ants. Journal of Experimental Biology *215*, 653–656. 10.1242/jeb.062406.

136. Collett, M., Collett, T.S., and Wehner, R. (1999). Calibration of vector navigation in desert ants. Current Biology *9*, 1031-S1. 10.1016/S0960-9822(99)80451-5.

137. Menzel, R., Greggers, U., Smith, A., Berger, S., Brandt, R., Brunke, S., Bundrock, G., Hülse, S., Plümpe, T., Schaupp, F., et al. (2005). Honey bees navigate according to a map-like spatial memory. Proc. Natl. Acad. Sci. U.S.A. *102*, 3040–3045. 10.1073/pnas.0408550102.

138. Wehner, R., Harkness, R.D., and Schmid-Hempel, P. (1983). Foraging Strategies in Individually Searching Ants (Stuttgart: Fisher).

139. Collett, T.S., and Cartwright, B.A. (1983). Eidetic images in insects: their role in navigation. Trends in Neurosciences *6*, 101–105. https://doi.org/10.1016/0166-2236(83)90048-6.

140. Hoinville, T., and Wehner, R. (2018). Optimal multiguidance integration in insect navigation. Proc. Natl. Acad. Sci. U.S.A. *115*, 2824–2829. 10.1073/pnas.1721668115.

141. Zeil, J. (2012). Visual homing: an insect perspective. Current Opinion in Neurobiology *22*, 285–293. 10.1016/j.conb.2011.12.008.

142. Wehner, R., and Räber, F. (1979). visual spatial memory in desert ants,Cataglyphis bicolor (Hymenoptera: Formicidae). experientia *35*, 1569–1571. doi.org/10.1007/BF01953197.

143. Zeil, J., Hofmann, M.I., and Chahl, J.S. (2003). Catchment areas of panoramic snapshots in outdoor scenes. J. Opt. Soc. Am. A, JOSAA *20*, 450–469. 10.1364/JOSAA.20.000450.

144. Graham, P., and Collett, T.S. (2002). View-based navigation in insects: how wood ants (*Formica rufa* L.) look at and are guided by extended landmarks. Journal of Experimental Biology *205*, 2499–2509. 10.1242/jeb.205.16.2499.

145. Collett, T.S., and Zeil, J. (2018). Insect learning flights and walks. Current Biology *28*, R984–R988. 10.1016/j.cub.2018.04.050.

146. Fleischmann, P.N., Rössler, W., and Wehner, R. (2018). Early foraging life: spatial and temporal aspects of landmark learning in the ant Cataglyphis noda. J Comp Physiol A *204*, 579–592. 10.1007/s00359-018-1260-6.

147. Fleischmann, P.N., Christian, M., Müller, V.L., Rössler, W., and Wehner, R. (2016). Ontogeny of learning walks and the acquisition of landmark information in desert ants, *Cataglyphis fortis*. Journal of Experimental Biology, jeb.140459. 10.1242/jeb.140459.

148. Jayatilaka, P., Murray, T., Narendra, A., and Zeil, J. (2018). The choreography of learning walks in the Australian jack jumper ant *Myrmecia croslandi*. J Exp Biol *221*, jeb185306. 10.1242/jeb.185306.

149. Jayatilaka, P., Raderschall, C.A., Narendra, A., and Zeil, J. (2013). Individual foraging patterns of the jack jumper ant Myrmecia croslandi (Hymenoptera: Formicidae). Myrmecological News *19*, 75–83.

150. Narendra, A., Gourmaud, S., and Zeil, J. (2013). Mapping the navigational knowledge of individually foraging ants, *Myrmecia croslandi*. Proc. R. Soc. B *280*, 20130683. 10.1098/rspb.2013.0683.

151. Wehner, R., Boyer, M., Loertscher, F., Sommer, S., and Menzi, U. (2006). Ant Navigation: One-Way Routes Rather Than Maps. Current Biology *16*, 75–79. 10.1016/j.cub.2005.11.035.

152. Wystrach, A., Beugnon, G., and Cheng, K. (2012). Ants might use different view-matching strategies on and off the route. Journal of Experimental Biology *215*, 44–55. 10.1242/jeb.059584.

153. Collett, T.S., Graham, P., and Durier, V. (2003). Route learning by insects. Current Opinion in Neurobiology *13*, 718–725. 10.1016/j.conb.2003.10.004.

154. Narendra, A., Si, A., Sulikowski, D., and Cheng, K. (2007). Learning, retention and coding of nest-associated visual cues by the Australian desert ant, Melophorus bagoti. Behav Ecol Sociobiol *61*, 1543–1553. 10.1007/s00265-007-0386-2.

155. Åkesson, S., and Wehner, R. (2002). Landmark navigation in desert ants. J Exp Biol.

156. Cartwright, B.A., and Collett, T.S. (1983). Landmark learning in bees: Experiments and models. J. Comp. Physiol. *151*, 521–543. 10.1007/BF00605469.

157. Durier, V., Graham, P., and Collett, T.S. (2003). Snapshot Memories and Landmark Guidance in Wood Ants. Current Biology *13*, 1614–1618. 10.1016/j.cub.2003.08.024.

158. Graham, P., Fauria, K., and Collett, T.S. (2003). The influence of beacon-aiming on the routes of wood ants. Journal of Experimental Biology *206*, 535–541. 10.1242/jeb.00115.

159. Judd, S.P.D., and Collett, T.S. (1998). Multiple stored views and landmark guidance in ants. Nature *392*, 710–714. 10.1038/33681.

160. Graham, P., and Philippides, A. (2017). Vision for navigation: What can we learn from ants? Arthropod Structure & Development *46*, 718–722. 10.1016/j.asd.2017.07.001.

161. Wystrach, A., Schwarz, S., Schultheiss, P., Beugnon, G., and Cheng, K. (2011). Views, landmarks, and routes: how do desert ants negotiate an obstacle course? J Comp Physiol A *197*, 167–179. 10.1007/s00359-010-0597-2.

162. Buehlmann, C., Woodgate, J.L., and Collett, T.S. (2016). On the Encoding of Panoramic Visual Scenes in Navigating Wood Ants. Current Biology *26*, 2022–2027. 10.1016/j.cub.2016.06.005.

163. Stürzl, W., Cheung, A., Cheng, K., and Zeil, J. (2008). The information content of panoramic images I: The rotational errors and the similarity of views in rectangular experimental arenas. Journal of Experimental Psychology: Animal Behavior Processes *34*, 1–14. 10.1037/0097-7403.34.1.1.

164. Heinze, S. (2020). Visual Navigation: Ants Lose Track without Mushroom Bodies. Current Biology *30*, R984–R986. 10.1016/j.cub.2020.07.038.

165. Kamhi, J.F., Barron, A.B., and Narendra, A. (2020). Vertical Lobes of the Mushroom Bodies Are Essential for View-Based Navigation in Australian Myrmecia Ants. Current Biology *30*, 3432-3437.e3. 10.1016/j.cub.2020.06.030.

166. Mizunami, M., Weibrecht, J.M., and Strausfeld, N.J. (1998). Mushroom bodies of the cockroach: Their participation in place memory. J. Comp. Neurol. *402*, 520–537. 10.1002/(SICI)1096-9861(19981228)402:4<520::AID-CNE6>3.0.CO;2-K.

167. Kenyon, F.C. (1896). The brain of the bee. A preliminary contribution to the morphology of the nervous system of the arthropoda. J. Comp. Neurol. *6*, 133–210. 10.1002/cne.910060302.

168. Grob, R., Holland Cunz, O., Grübel, K., Pfeiffer, K., Rössler, W., and Fleischmann, P.N. (2022). Rotation of skylight polarization during learning walks is necessary to trigger neuronal plasticity in *Cataglyphis* ants. Proc. R. Soc. B. *289*, 20212499. 10.1098/rspb.2021.2499.

169. Grob, R., Fleischmann, P.N., Grübel, K., Wehner, R., and Rössler, W. (2017). The Role of Celestial Compass Information in Cataglyphis Ants during Learning Walks and for Neuroplasticity in the Central Complex and Mushroom Bodies. Front. Behav. Neurosci. *11*, 226. 10.3389/fnbeh.2017.00226.

170. Rössler, W. (2019). Neuroplasticity in desert ants (Hymenoptera: Formicidae) – importance for the ontogeny of navigation. 10.25849/MYRMECOL.NEWS_029:001.

171. Stieb, S.M., Hellwig, A., Wehner, R., and Rössler, W. (2012). Visual experience affects both behavioral and neuronal aspects in the individual life history of the desert ant Cataglyphis fortis. Devel Neurobio *72*, 729–742. 10.1002/dneu.20982.

172. Schwarz, S., Narendra, A., and Zeil, J. (2011). The properties of the visual system in the Australian desert ant Melophorus bagoti. Arthropod Structure & Development *40*, 128–134. 10.1016/j.asd.2010.10.003.

173. Zollikofer, C.P.E., Wehner, R., and Fukushi, T. (1995). Optical Scaling in Conspecific Cataglyphis Ants. J. Exp. Biol. *198*, 1637–1646. 10.1242/jeb.198.8.1637.

174. Stürzl, W., and Mallot, H.A. (2006). Efficient visual homing based on Fourier transformed panoramic images. Robotics and Autonomous Systems *54*, 300–313. 10.1016/j.robot.2005.12.001.

175. Wystrach, A., Dewar, A., Philippides, A., and Graham, P. (2016). How do field of view and resolution affect the information content of panoramic scenes for visual navigation? A computational investigation. J Comp Physiol A *202*, 87–95. 10.1007/s00359-015-1052-1.

176. Goulard, R., Buehlmann, C., Niven, J.E., Graham, P., and Webb, B. (2021). A unified mechanism to support innate and learned use of visual landmark guidance in insects (Animal Behavior and Cognition) 10.1101/2021.01.28.428620.

177. Wystrach, A. (2023). Neurons from pre-motor areas to the Mushroom bodies can orchestrate latent visual learning in navigating insects (Neuroscience) 10.1101/2023.03.09.531867.

178. Loesel, R., and Heuer, C.M. (2010). The mushroom bodies – prominent brain centres of arthropods and annelids with enigmatic evolutionary origin. Acta Zoologica *91*, 29–34. 10.1111/j.1463-6395.2009.00422.x.

179. Beugnon, G., Lachaud, J.-P., and Chagné, P. (2005). Use of Long-Term Stored Vector Information in the Neotropical Ant Gigantiops destructor. J Insect Behav *18*, 415–432. 10.1007/s10905-005-3700-8.

180. Bühlmann, C., Cheng, K., and Wehner, R. (2011). Vector-based and landmark-guided navigation in desert ants inhabiting landmark-free and landmark-rich environments. Journal of Experimental Biology *214*, 2845–2853. 10.1242/jeb.054601.

181. Cheng, K., Schultheiss, P., Schwarz, S., Wystrach, A., and Wehner, R. (2014). Beginnings of a synthetic approach to desert ant navigation. Behavioural Processes *102*, 51–61. 10.1016/j.beproc.2013.10.001.

182. Schwarz, S., and Cheng, K. (2010). Visual associative learning in two desert ant species. Behav Ecol Sociobiol *64*, 2033–2041. 10.1007/s00265-010-1016-y.

183. Cheng, K., Narendra, A., Sommer, S., and Wehner, R. (2009). Traveling in clutter: Navigation in the Central Australian desert ant Melophorus bagoti. Behavioural Processes *80*, 261–268. 10.1016/j.beproc.2008.10.015.

184. Cheng, K., Narendra, A., and Wehner, R. (2006). Behavioral ecology of odometric memories in desert ants: acquisition, retention, and integration. Behavioral Ecology *17*, 227–235. 10.1093/beheco/arj017.

185. Sommer, S., and Wehner, R. (2004). The ant's estimation of distance travelled: experiments with desert ants, Cataglyphis fortis. Journal of Comparative Physiology A: Sensory, Neural, and Behavioral Physiology *190*, 1–6. 10.1007/s00359-003-0465-4.

186. Schwarz, S., Wystrach, A., and Cheng, K. (2017). Ants' navigation in an unfamiliar environment is influenced by their experience of a familiar route. Sci Rep *7*, 14161. 10.1038/s41598-017-14036-1.

187. Buehlmann, C., D. Fernandes, A.S., and Graham, P. (2017). The interaction of path integration and terrestrial visual cues in navigating desert ants: what can we learn from path characteristics? Journal of Experimental Biology, jeb.167304. 10.1242/jeb.167304.

188. Wystrach, A., Mangan, M., and Webb, B. (2015). Optimal cue integration in ants. Proc. R. Soc. B *282*, 20151484. 10.1098/rspb.2015.1484.

189. Legge, E.L.G., Wystrach, A., Spetch, M.L., and Cheng, K. (2014). Combining sky and earth: desert ants (Melophorus bagoti) show weighted integration of celestial and terrestrial cues. Journal of Experimental Biology *217*, 4159–4166. 10.1242/jeb.107862.

190. Collett, M. (2014). A desert ant's memory of recent visual experience and the control of route guidance. Proc. R. Soc. B. *281*, 20140634. 10.1098/rspb.2014.0634.

191. Wystrach, A., Schwarz, S., Graham, P., and Cheng, K. (2019). Running paths to nowhere: repetition of routes shows how navigating ants modulate online the weights accorded to cues. Anim Cogn *22*, 213–222. 10.1007/s10071-019-01236-7.

192. Cheng, K., Srinivasan, M.V., and Zhang, S.W. (1999). Error is proportional to distance measured by honeybees: Webers law in the odometer. Animal Cognition *2*, 11–16. 10.1007/s100710050020.

193. Merkle, T., Knaden, M., and Wehner, R. (2006). Uncertainty about nest position influences systematic search strategies in desert ants. Journal of Experimental Biology *209*, 3545–3549. 10.1242/jeb.02395.

194. Merkle, T., and Wehner, R. (2009). How flexible is the systematic search behaviour of desert ants? Animal Behaviour *77*, 1051–1056. 10.1016/j.anbehav.2009.01.006.

195. Merkle, T., and Wehner, R. (2009). Repeated training does not improve the path integrator in desert ants. Behav Ecol Sociobiol *63*, 391–402. 10.1007/s00265-008-0673-6.

196. Andel, D., and Wehner, R. (2004). Path integration in desert ants, Cataglyphis : how to make a homing ant run away from home. Proc. R. Soc. Lond. B *271*, 1485–1489. 10.1098/rspb.2004.2749.

197. Wehner, R., Hoinville, T., Cruse, H., and Cheng, K. (2016). Steering intermediate courses: desert ants combine information from various navigational routines. J Comp Physiol A *202*, 459–472. 10.1007/s00359-016-1094-z.

198. Artiushin, G., and Sehgal, A. (2017). The Drosophila circuitry of sleep–wake regulation. Current Opinion in Neurobiology *44*, 243–250. 10.1016/j.conb.2017.03.004.

199. Hindmarsh Sten, T., Li, R., Otopalik, A., and Ruta, V. (2021). Sexual arousal gates visual processing during Drosophila courtship. Nature *595*, 549–553. 10.1038/s41586-021-03714-w.

200. Buehlmann, C., Dell-Cronin, S., Diyalagoda Pathirannahelage, A., Goulard, R., Webb, B., Niven, J.E., and Graham, P. (2023). Impact of central complex lesions on innate and learnt visual navigation in ants. J Comp Physiol A. 10.1007/s00359-023-01613-1.

201. Ofstad, T.A., Zuker, C.S., and Reiser, M.B. (2011). Visual place learning in Drosophila melanogaster. Nature *474*, 204–207. 10.1038/nature10131.

202. Collett, M., and Collett, T.S. (2018). How does the insect central complex use mushroom body output for steering? Current Biology *28*, R733–R734. 10.1016/j.cub.2018.05.060.

203. Heinze, S., and Pfeiffer, K. (2018). Editorial: The Insect Central Complex—From Sensory Coding to Directing Movement. Front. Behav. Neurosci. *12*, 156. 10.3389/fnbeh.2018.00156.

204. Nguyen, T.A.T., Beetz, M.J., Merlin, C., Pfeiffer, K., and el Jundi, B. (2022). Weighting of Celestial and Terrestrial Cues in the Monarch Butterfly Central Complex. Front. Neural Circuits *16*, 862279. 10.3389/fncir.2022.862279.

205. Sun, X., Yue, S., and Mangan, M. (2020). A decentralised neural model explaining optimal integration of navigational strategies in insects. eLife *9*, e54026. 10.7554/eLife.54026.

206. Schwarz, S., Mangan, M., Zeil, J., Webb, B., and Wystrach, A. (2017). How Ants Use Vision When Homing Backward. Current Biology *27*, 401–407. 10.1016/j.cub.2016.12.019.

207. Buehlmann, C., Aussel, A., and Graham, P. (2020). Dynamic multimodal interactions in navigating wood ants: What do path details tell us about cue integration? Journal of Experimental Biology, jeb.221036. 10.1242/jeb.221036.

208. Reid, S.F., Narendra, A., Hemmi, J.M., and Zeil, J. (2011). Polarised skylight and the landmark panorama provide night-active bull ants with compass information during route following. Journal of Experimental Biology *214*, 363–370. 10.1242/jeb.049338.

209. Clement, L., Schwarz, S., and Wystrach, A. (2023). An intrinsic oscillator underlies visual navigation in ants. Current Biology *33*, 411-422.e5. 10.1016/j.cub.2022.11.059.

210. Haalck, L., Mangan, M., Wystrach, A., Clement, L., Webb, B., and Risse, B. (2023). CATER: Combined Animal Tracking & Environment Reconstruction. SCIENCE ADVANCES.

211. Kócsi, Z., Murray, T., Dahmen, H., Narendra, A., and Zeil, J. (2020). The Antarium: A Reconstructed Visual Reality Device for Ant Navigation Research. Front. Behav. Neurosci. *14*, 599374. 10.3389/fnbeh.2020.599374.

212. Risse, B., Mangan, M., Stürzl, W., and Webb, B. (2018). Software to convert terrestrial LiDAR scans of natural environments into photorealistic meshes. Environmental Modelling & Software *99*, 88–100. 10.1016/j.envsoft.2017.09.018.

213. Schwarz, S., Mangan, M., Webb, B., and Wystrach, A. (2020). Route-following ants respond to alterations of the view sequence. Journal of Experimental Biology, jeb.218701. 10.1242/jeb.218701.

214. Adel, M., and Griffith, L.C. (2021). The Role of Dopamine in Associative Learning in Drosophila: An Updated Unified Model. Neurosci. Bull. *37*, 831–852. 10.1007/s12264-021-00665-0.

215. Giurfa, M. (2013). Cognition with few neurons: higher-order learning in insects. Trends in Neurosciences *36*, 285–294. 10.1016/j.tins.2012.12.011.

216. Thiagarajan, D., and Sachse, S. (2022). Multimodal Information Processing and Associative Learning in the Insect Brain. Insects *13*, 332. 10.3390/insects13040332.

217. Tully, T., and Quinn, W.G. (1985). Classical conditioning and retention in normal and mutantDrosophila melanogaster. J. Comp. Physiol. *157*, 263–277. 10.1007/BF01350033.

218. Cheeseman, J.F., Millar, C.D., Greggers, U., Lehmann, K., Pawley, M.D.M., Gallistel, C.R., Warman, G.R., and Menzel, R. (2014). Way-finding in displaced clock-shifted bees proves bees use a cognitive map. Proceedings of the National Academy of Sciences *111*, 8949–8954. 10.1073/pnas.1408039111.

219. Cheung, A., Collett, M., Collett, T.S., Dewar, A., Dyer, F., Graham, P., Mangan, M., Narendra, A., Philippides, A., Stürzl, W., et al. (2014). Still no convincing evidence for cognitive map use by honeybees. Proc. Natl. Acad. Sci. U.S.A. *111*. 10.1073/pnas.1413581111.

220. Cruse, H., and Wehner, R. (2011). No Need for a Cognitive Map: Decentralized Memory for Insect Navigation. PLoS Comput Biol *7*, e1002009. 10.1371/journal.pcbi.1002009.

221. Menzel, R., and Muller, U. (1996). Learning and Memory in Honeybees: From Behavior to Neural Substrates. Annu Rev Neurosci, 379–404. 10.1146/annurev.ne.19.030196.002115.

222. Wehner, R. (2003). Desert ant navigation: how miniature brains solve complex tasks. Journal of Comparative Physiology A: Sensory, Neural, and Behavioral Physiology *189*, 579–588. 10.1007/s00359-003-0431-1.

223. Wehner, R., and Menzel, R. (1990). Do Insects Have Cognitive Maps? Annu. Rev. Neurosci. *13*, 43–414.

224. Wolf, S., Dubreuil, A.M., Bertoni, T., Böhm, U.L., Bormuth, V., Candelier, R., Karpenko, S., Hildebrand, D.G.C., Bianco, I.H., Monasson, R., et al. (2017). Sensorimotor computation underlying phototaxis in zebrafish. Nat Commun *8*, 651. 10.1038/s41467-017-00310-3.

225. DeBose, J.L., and Nevitt, G.A. (2008). The use of Odors at Different Spatial Scales: Comparing Birds with Fish. J Chem Ecol *34*, 867–881. 10.1007/s10886-008-9493-4.

226. Freas, C.A., and Cheng, K. (2022). The Basis of Navigation Across Species. Annu. Rev. Psychol. *73*, 217–241. 10.1146/annurev-psych-020821-111311.

227. Iwano, M., Hill, E.S., Mori, A., Mishima, T., Mishima, T., Ito, K., and Kanzaki, R. (2010). Neurons associated with the flip-flop activity in the lateral accessory lobe and ventral protocerebrum of the silkworm moth brain. J. Comp. Neurol. *518*, 366–388. 10.1002/cne.22224.

228. Namiki, S., and Kanzaki, R. (2016). The neurobiological basis of orientation in insects: insights from the silkmoth mating dance. Current Opinion in Insect Science *15*, 16–26. 10.1016/j.cois.2016.02.009.

229. Wystrach, A., Lagogiannis, K., and Webb, B. (2016). Continuous lateral oscillations as a core mechanism for taxis in Drosophila larvae. eLife *5*, e15504. 10.7554/eLife.15504.

230. Ernst, R., and Heisenberg, M. (1999). The memory template in Drosophila pattern vision at the flight simulator. Vision Research *39*, 3920–3933. 10.1016/S0042-6989(99)00114-5.

231. Horridge, G.A. (2005). Recognition of a familiar place by the honeybee (Apis mellifera). J Comp Physiol A *191*, 301–316. 10.1007/s00359-004-0592-6.

232. Lent, D.D., Graham, P., and Collett, T.S. (2013). Visual Scene Perception in Navigating Wood Ants. Current Biology *23*, 684–690. 10.1016/j.cub.2013.03.016.

233. Woodgate, J.L., Buehlmann, C., and Collett, T.S. (2016). When navigating wood ants use a shape's centre of mass to extract directional information from a panoramic skyline. Journal of Experimental Biology, jeb.136697. 10.1242/jeb.136697.

234. Horridge, A. (2009). What does an insect see? Journal of Experimental Biology *212*, 2721–2729. 10.1242/jeb.030916.

235. O'Carroll, D. (1993). Feature-detecting neurons in dragonflies. Nature *362*, 541–543. 10.1038/362541a0.

236. Fukushi, T. (2001). Homing in wood ants. J. Exp. Biol. *204*.

237. Woodgate, J.L., Buehlmann, C., and Collett, T.S. (2016). When navigating wood ants use a shape's centre of mass to extract directional information from a panoramic skyline. Journal of Experimental Biology, jeb.136697. 10.1242/jeb.136697.

238. Wei, C., Rafalko, S., and Dyer, F. (2002). Deciding to learn: modulation of learning flights in honeybees, Apis mellifera. Journal of Comparative Physiology A: Sensory, Neural, and Behavioral Physiology *188*, 725–737. 10.1007/s00359-002-0346-2.

239. Gauthier, J.L., and Tank, D.W. (2018). A Dedicated Population for Reward Coding in the Hippocampus. Neuron *99*, 179-193.e7. 10.1016/j.neuron.2018.06.008.

240. Bar, A., Marom, C., Zorin, N., Gilad, T., Subach, A., Foitzik, S., and Scharf, I. (2022). Desert Ants Learn to Avoid Pitfall Traps While Foraging. Biology *11*, 897. 10.3390/biology11060897.

241. Freas, C.A., Wystrach, A., Schwarz, S., and Spetch, M.L. (2022). Aversive view memories and risk perception in navigating ants. Sci Rep *12*, 2899. 10.1038/s41598-022-06859-4.

242. Tolman, E.C. (1948). Cognitive maps in rats and men. Psychol Rev *55*, 189–208. doi:10.1037/h0061626.

243. Gaskin, S., and White, N.M. (2007). Unreinforced spatial (latent) learning is mediated by a circuit that includes dorsal entorhinal cortex and fimbria fornix. Hippocampus *17*, 586–594. 10.1002/hipo.20295.

244. Stouffer, E.M., and White, N.M. (2006). Neural circuits mediating latent learning and conditioning for salt in the rat. Neurobiology of Learning and Memory *86*, 91–99. 10.1016/j.nlm.2005.12.006.

245. White, N.M. (2004). The role of stimulus ambiguity and movement in spatial navigation: A multiple memory systems analysis of location discrimination. Neurobiology of Learning and Memory *82*, 216–229. 10.1016/j.nlm.2004.05.004.

246. Behrens, T.E.J., Muller, T.H., Whittington, J.C.R., Mark, S., Baram, A.B., Stachenfeld, K.L., and Kurth-Nelson, Z. (2018). What Is a Cognitive Map? Organizing Knowledge for Flexible Behavior. Neuron *100*, 490–509. 10.1016/j.neuron.2018.10.002.

247. Cartwright, B.A., and Collett, T.S. (1987). Landmark maps for honeybees. Biol. Cybern. *57*, 85–93. 10.1007/BF00318718.

248. McNaughton, B.L., Battaglia, F.P., Jensen, O., Moser, E.I., and Moser, M.-B. (2006). Path integration and the neural basis of the “cognitive map.” Nat Rev Neurosci *7*, 663–678. 10.1038/nrn1932.

249. Samsonovich, A., and McNaughton, B.L. (1997). Path Integration and Cognitive Mapping in a Continuous Attractor Neural Network Model. J. Neurosci. *17*, 5900–5920. 10.1523/JNEUROSCI.17-15-05900.1997.

250. Wang, R.F. (2016). Building a cognitive map by assembling multiple path integration systems. Psychon Bull Rev *23*, 692–702. 10.3758/s13423-015-0952-y.

251. Collett, M., and Collett, T.S. (2017). Path Integration: Combining Optic Flow with Compass Orientation. Current Biology *27*, R1113–R1116. 10.1016/j.cub.2017.09.004.

252. Rozhok, A. (2008). Orientation and navigation in vertebrates (Springer).

253. Wehner, R. (1979). Department of Zoology, Universityof Zurich, Winterthurerstrasse190, CH-8057 Zurich (Switzerland),30 September 1979. 3.

254. Wehner, R., Michel, B., and Antonsen, P. (1996). Visual navigation in insects: coupling of egocentric and geocentric information. Journal of Experimental Biology *199*, 129–140.

255. Schultheiss, P., and Cheng, K. (2011). Finding the nest: inbound searching behaviour in the Australian desert ant, Melophorus bagoti. Animal Behaviour *81*, 1031–1038. 10.1016/j.anbehav.2011.02.008.

256. Benhamou, S. (1994). Spatial memory and searching efficiency. Animal Behaviour *47*.

257. Wehner, R., and Srinivasan, M.V. (1981). Searching behaviour of desert ants, genusCataglyphis (Formicidae, Hymenoptera). J. Comp. Physiol. *142*, 315–338. 10.1007/BF00605445.

258. Collett, M., Chittka, L., and Collett, T.S. (2013). Spatial Memory in Insect Navigation. Current Biology *23*, R789–R800. 10.1016/j.cub.2013.07.020.

259. Aso, Y., and Rubin, G.M. (2016). Dopaminergic neurons write and update memories with cell-type-specific rules. eLife *5*, e16135. 10.7554/eLife.16135.

260. Bouzaiane, E., Trannoy, S., Scheunemann, L., Plaçais, P.-Y., and Preat, T. (2015). Two Independent Mushroom Body Output Circuits Retrieve the Six Discrete Components of Drosophila Aversive Memory. Cell Reports *11*, 1280–1292. 10.1016/j.celrep.2015.04.044.

261. Blum, A.L., Li, W., Cressy, M., and Dubnau, J. (2009). Short- and Long-Term Memory in Drosophila Require cAMP Signaling in Distinct Neuron Types. Current Biology *19*, 1341–1350. 10.1016/j.cub.2009.07.016.

262. Trannoy, S., Redt-Clouet, C., Dura, J.-M., and Preat, T. (2011). Parallel Processing of Appetitive Short- and Long-Term Memories In Drosophila. Current Biology *21*, 1647–1653. 10.1016/j.cub.2011.08.032.

263. Yamagata, N., Ichinose, T., Aso, Y., Plaçais, P.-Y., Friedrich, A.B., Sima, R.J., Preat, T., Rubin, G.M., and Tanimoto, H. (2015). Distinct dopamine neurons mediate reward signals for short- and long-term memories. Proc. Natl. Acad. Sci. U.S.A. *112*, 578–583. 10.1073/pnas.1421930112.

264. Aso, Y., Sitaraman, D., Ichinose, T., Kaun, K.R., Vogt, K., Belliart-Guérin, G., Plaçais, P.-Y., Robie, A.A., Yamagata, N., Schnaitmann, C., et al. (2014). Mushroom body output neurons encode valence and guide memory-based action selection in Drosophila. eLife *3*, e04580. 10.7554/eLife.04580.

265. Schleyer, M., Weiglein, A., Thoener, J., Strauch, M., Hartenstein, V., Kantar Weigelt, M., Schuller, S., Saumweber, T., Eichler, K., Rohwedder, A., et al. (2020). Identification of Dopaminergic Neurons That Can Both Establish Associative Memory and Acutely Terminate Its Behavioral Expression. J. Neurosci. *40*, 5990–6006. 10.1523/JNEUROSCI.0290-20.2020.

266. Schroll, C., Riemensperger, T., Bucher, D., Ehmer, J., Völler, T., Erbguth, K., Gerber, B., Hendel, T., Nagel, G., Buchner, E., et al. (2006). Light-Induced Activation of Distinct Modulatory Neurons Triggers Appetitive or Aversive Learning in Drosophila Larvae. Current Biology *16*, 1741–1747. 10.1016/j.cub.2006.07.023.

267. Waddell, S. (2013). Reinforcement signalling in Drosophila; dopamine does it all after all. Current Opinion in Neurobiology *23*, 324–329. 10.1016/j.conb.2013.01.005.

268. Waddell, S. (2010). Dopamine reveals neural circuit mechanisms of fly memory. Trends in Neurosciences *33*, 457–464. 10.1016/j.tins.2010.07.001.

269. Cohn, R., Morantte, I., and Ruta, V. (2015). Coordinated and Compartmentalized Neuromodulation Shapes Sensory Processing in Drosophila. Cell *163*, 1742–1755. 10.1016/j.cell.2015.11.019.

270. Krashes, M.J., DasGupta, S., Vreede, A., White, B., Armstrong, J.D., and Waddell, S. (2009). A Neural Circuit Mechanism Integrating Motivational State with Memory Expression in Drosophila. Cell *139*, 416–427. 10.1016/j.cell.2009.08.035.

271. Krashes, M.J., and Waddell, S. (2008). Rapid Consolidation to a *radish* and Protein Synthesis-Dependent Long-Term Memory after Single-Session Appetitive Olfactory Conditioning in *Drosophila*. J. Neurosci. *28*, 3103–3113. 10.1523/JNEUROSCI.5333-07.2008.

272. Cognigni, P., Felsenberg, J., and Waddell, S. (2018). Do the right thing: neural network mechanisms of memory formation, expression and update in Drosophila. Current Opinion in Neurobiology *49*, 51–58. 10.1016/j.conb.2017.12.002.

273. Wystrach, A. (2023). Neurons from pre-motor areas to the Mushroom bodies can orchestrate latent visual learning in navigating insects (Neuroscience) 10.1101/2023.03.09.531867.

274. de Cothi, W., Nyberg, N., Griesbauer, E.-M., Ghanamé, C., Zisch, F., Lefort, J.M., Fletcher, L., Newton, C., Renaudineau, S., Bendor, D., et al. (2022). Predictive maps in rats and humans for spatial navigation. Current Biology *32*, 3676-3689.e5. 10.1016/j.cub.2022.06.090.

275. Roberts, W.A., Cruz, C., and Tremblay, J. (2007). Rats take correct novel routes and shortcuts in an enclosed maze. Journal of Experimental Psychology: Animal Behavior Processes *33*, 79–91. 10.1037/0097-7403.33.2.79.

276. Rodriguez, F., Duran, E., Vargas, J.P., Torres, B., and Salas, C. (1994). Performance of goldfish trained in allocentric and egocentric maze procedures suggests the presence of a cognitive mapping system in fishes. Animal Learning & Behavior *22*, 409–420. 10.3758/BF03209160.

277. Tolman, E.C., Ritchie, B.F., and Kalish, D. (1946). Studies in Spatial Learning. I. Orientation and the Short-Cut. J. Exp. Psychol, 13–24.

278. Macquart, D., Garnier, L., Combe, M., and Beugnon, G. (2006). Ant navigation en route to the goal: signature routes facilitate way-finding of Gigantiops destructor. J Comp Physiol A *192*, 221–234. 10.1007/s00359-005-0064-7.

279. Wystrach, A., Cheng, K., Sosa, S., and Beugnon, G. (2011). Geometry, features, and panoramic views: Ants in rectangular arenas. Journal of Experimental Psychology: Animal Behavior Processes *37*, 420–435. 10.1037/a0023886.

280. Groh, C., and Rössler, W. (2020). Analysis of Synaptic Microcircuits in the Mushroom Bodies of the Honeybee. Insects *11*, 43. 10.3390/insects11010043.

281. Webb, B. (2019). The internal maps of insects. Journal of Experimental Biology *222*, jeb188094. 10.1242/jeb.188094.

282. Philippides, A., Baddeley, B., Cheng, K., and Graham, P. (2011). How might ants use panoramic views for route navigation? Journal of Experimental Biology *214*, 445–451. 10.1242/jeb.046755.

283. Stürzl, W., and Zeil, J. (2007). Depth, contrast and view-based homing in outdoor scenes. Biol Cybern *96*, 519–531. 10.1007/s00422-007-0147-3.

284. Hoinville, T., and Wehner, R. (2018). Optimal multiguidance integration in insect navigation. Proc Natl Acad Sci USA *115*, 2824–2829. 10.1073/pnas.1721668115.

285. Dittmar, L., Stürzl, W., Baird, E., Boeddeker, N., and Egelhaaf, M. (2010). Goal seeking in honeybees: matching of optic flow snapshots? Journal of Experimental Biology *213*, 2913–2923. 10.1242/jeb.043737.

286. Gomez-Marin, A., Stephens, G.J., and Louis, M. (2011). Active sampling and decision making in Drosophila chemotaxis. Nat Commun *2*, 441. 10.1038/ncomms1455.

287. Lehrer, M. (1996). SMALL-SCALE NAVIGATION IN THE HONEYBEE: ACTIVE ACQUISITION OF VISUAL INFORMATION ABOUT THE GOAL. The Journal of Experimental Biology *199*, 253–261.

288. Dawkins, M.S., and Woodington, A. (2000). Pattern recognition and active vision in chickens. Nature *403*, 652–655. 10.1038/35001064.

289. Otero-Millan, J., Troncoso, X.G., Macknik, S.L., Serrano-Pedraza, I., and Martinez-Conde, S. (2008). Saccades and microsaccades during visual fixation, exploration, and search: Foundations for a common saccadic generator. Journal of Vision *8*, 21–21. 10.1167/8.14.21.

290. Wachowiak, M. (2011). All in a Sniff: Olfaction as a Model for Active Sensing. Neuron *71*, 962–973. 10.1016/j.neuron.2011.08.030.

291. Wesson, D.W., Donahou, T.N., Johnson, M.O., and Wachowiak, M. (2008). Sniffing Behavior of Mice during Performance in Odor-Guided Tasks. Chemical Senses *33*, 581–596. 10.1093/chemse/bjn029.

292. Kuenen, L.P.S., and Baker, T.C. (1983). A non-anemotactic mechanism used in pheromone source location by flying moths. Physiol Entomol *8*, 277–289. 10.1111/j.1365-3032.1983.tb00360.x.

293. Izquierdo, E.J., and Lockery, S.R. (2010). Evolution and Analysis of Minimal Neural Circuits for Klinotaxis in Caenorhabditis elegans. Journal of Neuroscience *30*, 12908–12917. 10.1523/JNEUROSCI.2606-10.2010.

294. Adden, A., Stewart, T.C., Webb, B., and Heinze, S. (2020). A neural model for insect steering applied to olfaction and path integration (Neuroscience) 10.1101/2020.08.25.266247.

295. Kodzhabashev, A., and Mangan, M. (2015). Route Following Without Scanning. In Biomimetic and Biohybrid Systems, S. P. Wilson, P. F. M. J. Verschure, A. Mura, and T. J. Prescott, eds. (Springer International Publishing), pp. 199–210. 10.1007/978-3-319-22979-9_20.

296. Voss, R., and Zeil, J. (1998). Active vision in insects: an analysis of object-directed zig-zag flights in wasps (Odynerus spinipes ?, Eumenidae). Journal of Comparative Physiology A: Sensory, Neural, and Behavioral Physiology *182*, 377–387. 10.1007/s003590050187.

297. Zeil, J., Narendra, A., and Stürzl, W. (2014). Looking and homing: how displaced ants decide where to go. Phil. Trans. R. Soc. B *369*, 20130034. 10.1098/rstb.2013.0034.

298. Card, A., McDermott, C., and Narendra, A. (2016). Multiple orientation cues in an Australian trunk-trail-forming ant, Iridomyrmex purpureus. Aust. J. Zool. *64*, 227. 10.1071/ZO16046.

299. Collett, T.S., and Cartwright, B.A. (1983). Eidetic images in insects: their role in navigation.

300. Dahmen, H., Wahl, V.L., Pfeffer, S.E., Mallot, H.A., and Wittlinger, M. (2017). Naturalistic path integration of *Cataglyphis* desert ants on an air-cushioned lightweight spherical treadmill. J Exp Biol *220*, 634–644. 10.1242/jeb.148213.

301. Lonnendonker, U. (1991). DYNAMIC PROPERTIES OF ORIENTATION TO A VISUALLY FIXATED TARGET BY WALKING COLORADO BEETLES. Journal of Experimental Biology *158*, 16.

302. Zollikofer, C.P.E. (1994). STEPPING PATTERNS IN ANTS. Journal of Experimental Biology *192*, 107–118.

303. Namiki, S., and Kanzaki, R. (2016). Comparative Neuroanatomy of the Lateral Accessory Lobe in the Insect Brain. Front. Physiol. *7*. 10.3389/fphys.2016.00244.

304. Berni, J. (2015). Genetic Dissection of a Regionally Differentiated Network for Exploratory Behavior in Drosophila Larvae. Current Biology *25*, 1319–1326. 10.1016/j.cub.2015.03.023.

305. Berni, J., pulver, S.R., Griffith, L.C., and Bate, M. (2012). Autonomous Circuitry for Substrate Exploration in Freely Moving Drosophila Larvae. Current Biology *22*, 10.

306. Kanzaki, R. (2005). Neural Basis of Odor-source Searching Behavior in Insect Brain Systems Evaluated with a Mobile Robot. Chemical Senses *30*, i285–i286. 10.1093/chemse/bjh226.

307. Brembs, B. (2021). The brain as a dynamically active organ. Biochemical and Biophysical Research Communications *564*, 55–69. 10.1016/j.bbrc.2020.12.011.

308. Schroeder, C.E., Wilson, D.A., Radman, T., Scharfman, H., and Lakatos, P. (2010). Dynamics of Active Sensing and perceptual selection. Current Opinion in Neurobiology *20*, 172–176. 10.1016/j.conb.2010.02.010.

309. Yuste, R., MacLean, J.N., Smith, J., and Lansner, A. (2005). The cortex as a central pattern generator. Nat Rev Neurosci *6*, 477–483. 10.1038/nrn1686.

310. Kanzaki, R., and Mishima, T. (1996). Pheromone-Triggered 'Fiipflopping' Neural Signals Correlate with Activities of Neck Motor Neurons of a Male Moth, Bombyx mori. Zoological Science *13*, 79–87. 10.2108/zsj.13.79.

311. Egelhaaf, M., Boeddeker, N., Kern, R., Kurtz, R., and Lindemann, J.P. (2012). Spatial vision in insects is facilitated by shaping the dynamics of visual input through behavioral action. Front. Neural Circuits *6*. 10.3389/fncir.2012.00108.

312. Marder, E., and Calabrese, R.L. (1996). Principles of rhythmic motor pattern generation. Physiological Reviews *76*, 687–717. 10.1152/physrev.1996.76.3.687.

313. McAuley, J.H., Rothwell, J.C., and Marsden, C.D. (1999). Human anticipatory eye movements may reflect rhythmic central nervous activity. Neuroscience *94*, 339–350. 10.1016/S0306-4522(99)00337-1.

314. Keijzer, F., van Duijn, M., and Lyon, P. (2013). What nervous systems do: early evolution, input–output, and the skin brain thesis. Adaptive Behavior *21*, 67–85. 10.1177/1059712312465330.

315. Busch, C., Borst, A., and Mauss, A.S. (2018). Bi-directional Control of Walking Behavior by Horizontal Optic Flow Sensors. Current Biology *28*, 4037-4045.e5. 10.1016/j.cub.2018.11.010.

316. Wystrach, A. (2021). Movements, embodiment and the emergence of decisions. Insights from insect navigation. Biochemical and Biophysical Research Communications, S0006291X21007348. 10.1016/j.bbrc.2021.04.114.

317. Wystrach, A., Philippides, A., Aurejac, A., Cheng, K., and Graham, P. (2014). Visual scanning behaviours and their role in the navigation of the Australian desert ant Melophorus bagoti. J Comp Physiol A *200*, 615–626. 10.1007/s00359-014-0900-8.

318. Schwarz, S., Clement, L., Gkanias, E., and Wystrach, A. (2019). How do backward walking ants (*Cataglyphis velox*) cope with navigational uncertainty? (Animal Behavior and Cognition) 10.1101/2019.12.16.877704.

319. Heinze, S., Florman, J., Asokaraj, S., el Jundi, B., and Reppert, S.M. (2013). Anatomical basis of sun compass navigation II: The neuronal composition of the central complex of the monarch butterfly. J. Comp. Neurol. *521*, 267–298. 10.1002/cne.23214.

320. Aksoy, V., and Camlitepe, Y. (2018). Spectral sensitivities of ants – a review. Animal Biol. *68*, 55–73. 10.1163/15707563-17000119.

321. Cheng, K., and Freas, C.A. (2015). Path integration, views, search, and matched filters: the contributions of Rüdiger Wehner to the study of orientation and navigation. J Comp Physiol A *201*, 517–532. 10.1007/s00359-015-0984-9.

322. Wehner, R. (1987). 'Matched filters'-neural models of the external world. J. Comp. Physiol. *161*, 511–531. 10.1007/BF00603659.

323. Dauzere-Peres, O., and Wystrach, A. (2023). Ants integrate proprioception, visual context and efference copies to make robust predictions (Animal Behavior and Cognition) 10.1101/2023.03.29.534571.

324. Baird, E., Kornfeldt, T., and Dacke, M. (2010). Minimum viewing angle for visually guided ground speed control in bumblebees. Journal of Experimental Biology *213*, 1625–1632. 10.1242/jeb.038802.

325. Barron, A., and Srinivasan, M.V. (2006). Visual regulation of ground speed and headwind compensation in freely flying honey bees (*Apis mellifera* L.). Journal of Experimental Biology *209*, 978–984. 10.1242/jeb.02085.

326. Portelli, G., Ruffier, F., Roubieu, F.L., and Franceschini, N. (2011). Honeybees' Speed Depends on Dorsal as Well as Lateral, Ventral and Frontal Optic Flows. PLoS ONE *6*, e19486. 10.1371/journal.pone.0019486.

327. Krapp, H.G. (2000). Neuronal Matched Filters for Optic Flow Processing in Flying Insects. In International Review of Neurobiology (Elsevier), pp. 93–120. 10.1016/S0074-7742(08)60739-4.

328. Lehrer, M., Srinivasan, M.V., Zhang, S.W., and Horridge, G.A. (1988). Motion cues provide the bee's visual world with a third dimension. Nature *332*, 356–357. 10.1038/332356a0.

329. Ruffier, F., Portelli, G., Serres, J., Raharijaona, T., and Franceschini, N. (2019). From bees' surface following to lunar landing. hal.

330. Srinivasan, M.V., Zhang, S.W., Lehrer, M., and Collett, T.S. (1996). Honeybee Navigation *En Route* to the Goal: Visual Flight Control and Odometry. Journal of Experimental Biology *199*, 237–244. 10.1242/jeb.199.1.237.

331. Srinivasan, M.V., Lehrer, M., Zhang, S.W., and Horridge, G.A. (1989). How honeybees measure their distance from objects of unknown size. J. Comp. Physiol. *165*, 605–613. 10.1007/BF00610992.

332. Zeil, J. (1993). Orientation flights of solitary wasps (Cerceris; Spheeidae; Hymenoptera). J Comp Physiol A.

333. Egelhaaf, M. (2023). Optic flow based spatial vision in insects. J Comp Physiol A. 10.1007/s00359-022-01610-w.

334. Buehlmann, C., and Graham, P. (2022). Innate visual attraction in wood ants is a hardwired behavior seen across different motivational and ecological contexts. Insect. Soc. *69*, 271–277. 10.1007/s00040-022-00867-3.

335. Grabowska, M.J., Steeves, J., Alpay, J., van de Poll, M., Ertekin, D., and van Swinderen, B. (2018). Innate visual preferences and behavioral flexibility in *Drosophila*. Journal of Experimental Biology, jeb.185918. 10.1242/jeb.185918.

336. Maimon, G., Straw, A.D., and Dickinson, M.H. (2008). A Simple Vision-Based Algorithm for Decision Making in Flying Drosophila. Current Biology *18*, 464–470. 10.1016/j.cub.2008.02.054.

337. Mote, M.I., and Wehner, R. (1980). Functional characteristics of photoreceptors in the compound eye and ocellus of the desert ant,Cataglyphis bicolor. J. Comp. Physiol. *137*, 63–71. 10.1007/BF00656918.

338. Rossel, S., and Wehner, R. (1986). Polarization vision in bees. Nature *323*, 128–131. 10.1038/323128a0.

339. Schultheiss, P., Wystrach, A., Schwarz, S., Tack, A., Delor, J., Nooten, S.S., Bibost, A.-L., Freas, C.A., and Cheng, K. (2016). Crucial role of ultraviolet light for desert ants in determining direction from the terrestrial panorama. Animal Behaviour *115*, 19–28. 10.1016/j.anbehav.2016.02.027.

340. Wehner, R. (1976). Polarized-Light Navigation by Insects. Sci Am *235*, 106–115. 10.1038/scientificamerican0776-106.

341. Wystrach, A., Schwarz, S., Schultheiss, P., Baniel, A., and Cheng, K. (2014). Multiple sources of celestial compass information in the Central Australian desert ant Melophorus bagoti. J Comp Physiol A *200*, 591–601. 10.1007/s00359-014-0899-x.

342. Chiang, A.-S., Lin, C.-Y., Chuang, C.-C., Chang, H.-M., Hsieh, C.-H., Yeh, C.-W., Shih, C.-T., Wu, J.-J., Wang, G.-T., Chen, Y.-C., et al. (2011). Three-Dimensional Reconstruction of Brain-wide Wiring Networks in Drosophila at Single-Cell Resolution. Current Biology *21*, 1–11. 10.1016/j.cub.2010.11.056.

343. Namiki, S., and Kanzaki, R. (2018). Morphology of visual projection neurons supplying premotor area in the brain of the silkmoth Bombyx mori. Cell Tissue Res *374*, 497–515. 10.1007/s00441-018-2892-0.

344. Ehmer, B., and Gronenberg, W. (2002). Segregation of visual input to the mushroom bodies in the honeybee (Apis mellifera). J. Comp. Neurol. *451*, 362–373. 10.1002/cne.10355.

345. Gronenberg, W. (2001). Subdivisions of hymenopteran mushroom body calyces by their afferent supply. J. Comp. Neurol. *435*, 474–489. 10.1002/cne.1045.

346. Paulk, A.C., and Gronenberg, W. (2008). Higher order visual input to the mushroom bodies in the bee, Bombus impatiens. Arthropod Structure & Development *37*, 443–458. 10.1016/j.asd.2008.03.002.

347. Manjila, S.B., Kuruvilla, M., Ferveur, J.-F., Sane, S.P., and Hasan, G. (2019). Extended Flight Bouts Require Disinhibition from GABAergic Mushroom Body Neurons. Current Biology *29*, 283-293.e5. 10.1016/j.cub.2018.11.070.

348. Scaplen, K.M., Talay, M., Fisher, J.D., Cohn, R., Sorkaç, A., Aso, Y., Barnea, G., and Kaun, K.R. (2021). Transsynaptic mapping of Drosophila mushroom body output neurons. eLife *10*, e63379. 10.7554/eLife.63379.

349. Kamhi, J.F., Barron, A.B., and Narendra, A. (2020). Vertical Lobes of the Mushroom Bodies Are Essential for View-Based Navigation in Australian Myrmecia Ants. Current Biology *30*, 3432-3437.e3. 10.1016/j.cub.2020.06.030.

350. Cabirol, A., Cope, A.J., Barron, A.B., and Devaud, J.-M. (2018). Relationship between brain plasticity, learning and foraging performance in honey bees. PLoS ONE *13*, e0196749. 10.1371/journal.pone.0196749.

351. Rössler, W. (2019). Neuroplasticity in desert ants (Hymenoptera: Formicidae) – importance for the ontogeny of navigation. Myrmecological News. 10.25849/MYRMECOL.NEWS_029:001.

352. Rössler, W., and Groh, C. (2012). Plasticity of Synaptic Microcircuits in the Mushroom-Body Calyx of the Honey Bee. In Honeybee Neurobiology and Behavior, C. G. Galizia, D. Eisenhardt, and M. Giurfa, eds. (Springer Netherlands), pp. 141–153. 10.1007/978-94-007-2099-2_12.

353. Blakemore, C., and Cooper, G.F. (1970). Development of the Brain depends on the Visual Environment. Nature *228*, 477–478. 10.1038/228477a0.

354. Gu, J., and Kanai, R. (2014). What contributes to individual differences in brain structure? Front. Hum. Neurosci. *8*. 10.3389/fnhum.2014.00262.

355. Voss, P., Thomas, M.E., Cisneros-Franco, J.M., and de Villers-Sidani, É. (2017). Dynamic Brains and the Changing Rules of Neuroplasticity: Implications for Learning and Recovery. Front. Psychol. *8*, 1657. 10.3389/fpsyg.2017.01657.

356. von Uexküll, J. (1934). Mondes Animaux Et Monde Humain Bibliothèque Médiations-Éditions Denoël.

357. Cerdá, X., and Retana, J. (2000). Alternative strategies by thermophilic ants to cope with extreme heat: individual versus colony level traits. Oikos *89*, 155–163. 10.1034/j.1600-0706.2000.890117.x.

358. Bolzon, D.M., Nordström, K., and O'Carroll, D.C. (2009). Local and Large-Range Inhibition in Feature Detection. J. Neurosci. *29*, 14143–14150. 10.1523/JNEUROSCI.2857-09.2009.

359. Srinivasan, M., Laughlin, S.B., and Dubs, A. (1982). Predictive coding: a fresh view of inhibition in the retina. Proc. R. Soc. Lond. B. *216*, 427–459. 10.1098/rspb.1982.0085.

360. Borst, A. (2014). Fly visual course control: behaviour, algorithms and circuits. Nat Rev Neurosci *15*, 590–599. 10.1038/nrn3799.

361. Egelhaaf, M., Kern, R., and Lindemann, J.P. (2014). Motion as a source of environmental information: a fresh view on biological motion computation by insect brains. Front. Neural Circuits *8*. 10.3389/fncir.2014.00127.

362. Mauss, A.S., and Borst, A. (2019). Motion Vision in Arthropods. In The Oxford Handbook of Invertebrate Neurobiology, J. H. Byrne, ed. (Oxford University Press), pp. 318–344. 10.1093/oxfordhb/9780190456757.013.14.

363. Wendt, B., and Homberg, U. (1992). Immunocytochemistry of dopamine in the brain of the locustSchistocerca gregaria. J. Comp. Neurol. *321*, 387–403. 10.1002/cne.903210307.

364. Deeti, S., Cheng, K., Graham, P., and Wystrach, A. (2023). Scanning behaviour in ants: an interplay between random-rate processes and oscillators. J Comp Physiol A. 10.1007/s00359-023-01628-8.

365. Narendra, A., and Ramirez-Esquivel, F. (2017). Subtle changes in the landmark panorama disrupt visual navigation in a nocturnal bull ant. Phil. Trans. R. Soc. B *372*, 20160068. 10.1098/rstb.2016.0068.

366. Islam, M., Deeti, S., Mahmudah, Z., Kamhi, J.F., and Cheng, K. (2021). Detour learning ability and the effect of novel sensory cues on learning in Australian bull ants, *Myrmecia midas* (Animal Behavior and Cognition) 10.1101/2021.01.25.428158.

367. Islam, M., Freas, C.A., and Cheng, K. (2020). Effect of large visual changes on the navigation of the nocturnal bull ant, Myrmecia midas. Anim Cogn *23*, 1071–1080. 10.1007/s10071-020-01377-0.

368. Collett, T.S. (1996). Insect Navigation *En Route* to the Goal: Multiple Strategies for the Use of Landmarks. Journal of Experimental Biology *199*, 227–235. 10.1242/jeb.199.1.227.

369. Schultheiss, P., Wystrach, A., Legge, E.L.G., and Cheng, K. (2012). Information content of visual scenes influences systematic search of desert ants. Journal of Experimental Biology, jeb.075077. 10.1242/jeb.075077.

370. Bovet, P., and Benhamou, S. (1988). Spatial analysis of animals' movements using a correlated random walk model. Journal of Theoretical Biology *131*, 419–433. 10.1016/S0022-5193(88)80038-9.

371. Stone, T., Mangan, M., Wystrach, A., and Webb, B. (2018). Rotation invariant visual processing for spatial memory in insects. Interface Focus. *8*, 20180010. 10.1098/rsfs.2018.0010.

372. Graham, P., and Mangan, M. (2015). Insect navigation: do ants live in the now? Journal of Experimental Biology *218*, 819–823. 10.1242/jeb.065409.

373. Tinbergen, N. (1963). On aims and methods of ethology.

374. Scholl, C., Wang, Y., Krischke, M., Mueller, M.J., Amdam, G.V., and Rössler, W. (2014). Light exposure leads to reorganization of microglomeruli in the mushroom bodies and influences juvenile hormone levels in the honeybee: Synaptic Reorganization after Light Exposure. Devel Neurobio *74*, 1141–1153. 10.1002/dneu.22195.

375. Popper, K. (1935). Karl Popper: The Logic of Scientific Discovery.

376. Cerritelli, G., Benhamou, S., and Luschi, P. (2021). Evaluating vector navigation in green turtles migrating in a dynamic oceanic environment. Ethology Ecology & Evolution *33*, 290–306. 10.1080/03949370.2021.1878281.

377. Curchoe, C.L. (2020). All Models Are Wrong, but Some Are Useful. J Assist Reprod Genet *37*, 2389–2391. 10.1007/s10815-020-01895-3.

Appendix I:
the formatted publication of chapter II

Article

Current Biology

An intrinsic oscillator underlies visual navigation in ants

Graphical abstract

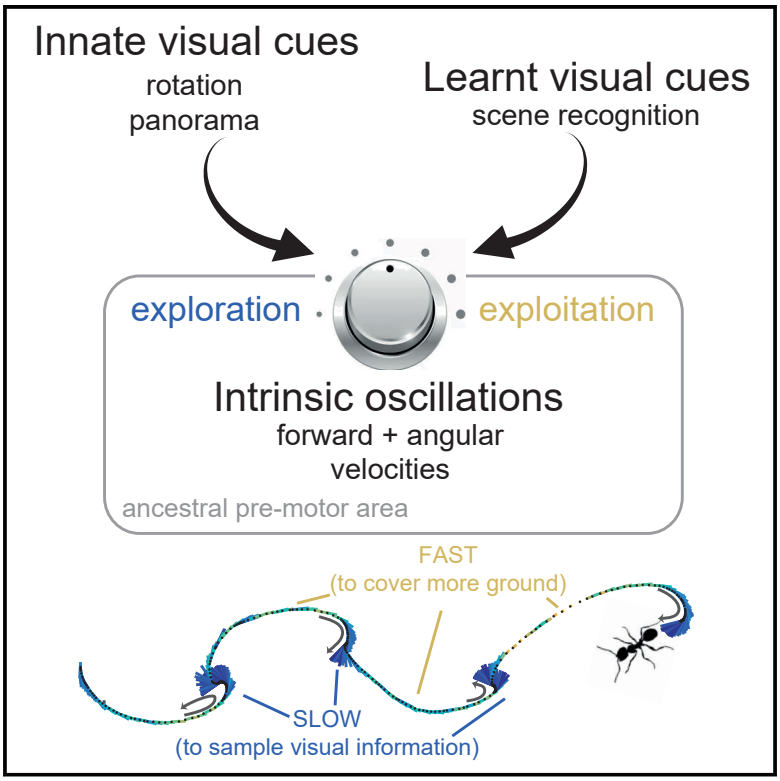

Authors

Leo Clement, Sebastian Schwarz, Antoine Wystrach

Correspondence

clement.leo@univ-tlse3.fr

In brief

Clement et al. reveal a fine-tuned movement dynamic, generated intrinsically and rhythmically in navigating ants. This lower-level motor pattern optimizes both the information sampling and the distance covered and drastically reduces the degree of freedom needed for higher-level strategies to control behavior.

Highlights

- Navigating ants display regular oscillations that are produced intrinsically
- The movement dynamic optimizes the exploration and exploitation trade-off
- Visual cues adjust the trade-off by simply modulating the oscillations' amplitude
- The intrinsic movement emerges readily from an ancestral brain area

Clement et al., 2023, Current Biology *33*, 411–422
February 6, 2023
https://doi.org/10.1016/j.cub.2022.11.059

CellPress

Current Biology

CellPress

Article

An intrinsic oscillator underlies visual navigation in ants

Leo Clement,[1,2,*] Sebastian Schwarz,[1] and Antoine Wystrach[1]
[1]Centre de Recherches sur la Cognition Animale, CBI, CNRS, Université Paul Sabatier, 31062 Toulouse Cedex 09, France
[2]Lead contact
*Correspondence: clement.leo@univ-tlse3.fr
https://doi.org/10.1016/j.cub.2022.11.059

SUMMARY

Many insects display lateral oscillations while moving, but how these oscillations are produced and participate in visual navigation remains unclear. Here, we show that visually navigating ants continuously display regular lateral oscillations coupled with variations of forward speed that strongly optimize the distance covered while simultaneously enabling them to scan left and right directions. This pattern of movement is produced endogenously and conserved across navigational contexts in two phylogenetically distant ant species. Moreover, the oscillations' amplitude can be modulated by both innate or learnt visual cues to adjust the exploration/exploitation balance to the current need. This lower-level motor pattern thus drastically reduces the degree of freedom needed for higher-level strategies to control behavior. The observed dynamical signature readily emerges from a simple neural circuit model of the insect's conserved pre-motor area known as the lateral accessory lobe, offering a surprisingly simple but effective neural control and endorsing oscillation as a core, ancestral way of moving in insects.

INTRODUCTION

Navigating through space implies both to acquire information (exploration) and to use this information to move in the correct direction (exploitation). A way to acquire information is to sample the environment by actively moving. Such ''active sampling'' is common across the animal kingdom, encompassing both invertebrates[1–3] and vertebrates.[4–8] However, active sampling entails movements that are typically different than moving toward the goal and thus requires the animal to solve a trade-off. Achieving a balance between sampling actions (exploration) and goal-directed actions (exploitation) lies at the core of the behavioral control, but how it is achieved and how it evolved in animals remains unclear.

A way of sampling the world is through the production of regular alternations between left and right turns along the path: lateral oscillations. Lateral oscillations are observed in wide range of taxa (vertebrates,[8,9] invertebrates[10–14]) and have been mainly studied in the context of olfactory behaviors, such as plume following in moths,[12,15–17] trail following in ants,[18] or odor gradient climbing in *Drosophila* larvae[14] and *Caenorhabditis elegans*.[19] The intrinsic production of oscillations enables an efficient sampling of odor across locations, and models show that oscillations modulated by odor perception provide a remarkably effective way of reaching the source.[14,19,20]

Modeling studies have shown that lateral oscillations can also be useful for visual navigation. For instance, having the amplitude of oscillation modulated by the familiarity of the perceived visual scenes can produce robust visual navigational behaviors, such as route-following[21] or homing,[22] and captures particular behavioral signatures observed in ants.[23] Moreover, visually guided insects such as ants,[23–28] wasps,[29,30] or bumblebees[31] do display oscillations whose expression appears to be coupled with visual perceptual cues. But whether or not these lateral oscillations are produced internally, how exactly they interact with visual cues and how they participate in the visual navigational task remains unclear.

We focused on the expression of oscillations in two ecologically and phylogenetically distant ant species: *Myrmecia croslandi*, which are solitary foragers relying heavily on vision;[23,27,32–34] and *Iridomyrmex purpureus*, which uses mass recruitment and pheromone trials as well as other modalities for navigation.[35] The replication of the experiments in two distant species enables us to discern whether the observed signatures are species-specific or shared across ants.

As most central place foragers, these ants species are known to rely on two main strategies to guide their foraging journeys.[33,35] The first strategy, commonly called path integration (PI), allows individuals to continuously estimate the distance and compass direction that separates them from their nest (or other starting point) during their foraging trip.[36–38] The second, commonly called view-based navigation, involves the learning and subsequent recognition of the learnt visual panorama.[38–40] To see how these navigational strategies interact with oscillations, we mounted ants on a spherical treadmill device[41] (see STAR Methods), directly in their natural environment. This device enables the recording of the ants' motor behavior in detail, without the interference of the uneven ground, while facilitating the control of the surrounding visual cue perceived. We characterized whether the obtained trajectories show a regular oscillatory pattern of movement and how these patterns are influenced by the presence or absence of: (1) visual input, (2) learnt visual terrestrial cues, (3) PI

homing vector, and (4) rotational visual feedback. In both species, our results revealed the presence of a conserved pattern of oscillations generated intrinsically, which comprises both angular and forward velocity components. This pattern of movement provides a remarkable trade-off between exploration and exploitation, and the amplitude of the oscillations can be flexibly adjusted by visual information in a way that is adapted to the navigational tasks at hand. Finally, we propose a simple neural circuit model of reciprocal inhibition between left and right pre-motor areas to explore how these movement dynamics could be produced.

RESULTS

Ants mounted on the trackball display their natural navigational behavior

We first investigated whether ants mounted on the trackball display their natural navigational behaviors across different experimental conditions. When released on the ground in their natural environment, both species studied here (*Myrmecia croslandi* and *Iridomyrmex purpureus*; see Figure S1) are known to rely on learnt terrestrial cues as well as, to a lesser extent, on PI.[23,33–35] We first tethered ants and placed them on top of the trackball in a way that enabled them to physically rotate and control their actual body orientation[41] (Figure S2A). The trackball was placed in three distinct visual conditions: (1) along the individual ant's familiar route (F) and, therefore, in presence of familiar terrestrial cues; (2) in an unfamiliar location (U) 50 m away from their usual route; or (3) without any visual input, in complete darkness (D). For each of these visual conditions, ants were tested either with (full-vector [FV] ants) or without (zero-vector [ZV] ants) PI information. While FV ants were captured at their feeding place and thus possessed a PI homing vector pointing in the food-to-nest compass direction, ZV ants were caught just before entering their nest and thus no longer possessed a PI homing vector.

Irrespectively of the PI state (FV or ZV), ants mounted on the trackball within their familiar visual route (i.e., in the presence of learnt terrestrial cues) displayed paths that were oriented toward the nest direction (Figure 1A; Rayleigh test with nest as theoretical direction ps: FV and ZV < 0.001), proving that they recognized and used the familiar terrestrial cues to orient, even without PI information (ZV). When tested in unfamiliar surroundings, FV ants were oriented toward the theoretical direction of the nest, as indicated by their PI (Figure 1B first row; Rayleigh test with PI as theoretical direction p: FV < 0.001), but ZV ants (Figure 1B second row) showed random orientations (Rayleigh test p: ZV = 0.443). This confirms that the distant release points were indeed unfamiliar to the ants and that the ants relied on their PI when tested as FV ants. When tested in total darkness, ants displayed randomly oriented paths in all conditions (Figure 1C; Rayleigh test p: FV = 0.354; ZV = 0.360), showing that the chosen dark condition was effective in preventing the ants from using either terrestrial or celestial cues for orientation. Overall, these results demonstrate that *M. croslandi* foragers rely on learnt terrestrial cues as well as their PI to navigate when mounted on the trackball system (Figure 1).

We then looked at the individual's path straightness (R values in Figure 1 that indicate whether the ant's travel directions were constant across time [R = 1] or not [R = 0]). Independent of the PI state, the ants' paths were straighter in familiar terrain as compared with the other conditions (Figure 1; familiar versus unfamiliar and familiar versus dark: ps < 0.001), showing that the recognition of learnt terrestrial cues was most effective at helping the ant to maintain a constant direction of travel. With regard to the effect of the PI state, there was no difference in the path straightness within each visual condition (FV versus ZV; ps < 0.1, Figure 1).

Overall, these results show that *M. croslandi* rely greatly on learnt visual cues and to a lesser extent on their PI. The latter still enables them to guide their general direction in unfamiliar terrain but has only a limited impact on their path's straightness. Qualitatively similar results were obtained with our second species, *I. purpureus* (see Figure S1). These results are consistent with what is observed in these species when navigating in their natural environment.[33,35]

Ants display regular lateral oscillations

To determine whether ants display regular lateral oscillations—that is, alternate between left and right turns at a steady rhythm—we first used our video recordings to track the ant's change in body orientation when mounted on the trackball. The body angular velocity signal is independent of the ant's actual forward movement and, thus, a direct reading of its motor control for turning. We conducted a Fourier analysis on autocorrelation coefficients of the angular velocity time series to obtain a "power spectral density" (PSD) (see Figures S2C–S2E for detailed method). This PSD provides information about the regularity and frequency of oscillation, with higher magnitude values (y axis; Figure S2E) indicating more regular oscillation at the corresponding frequency (x axis; Figure S2E). For each ant, we selected the frequency corresponding to the highest magnitude (peak), that is, the most salient rhythm in the signal. In all experimental conditions, the obtained peak fell in the expected range of 0.2–1.5 Hz, as observed in other insect species.[14,42] It should be noted that this rhythm is 10–50 times slower than ants' typical stepping frequency[43] and, thus, is not the consequence of their rhythmic walking gait but more likely the product of a different oscillatory mechanism. For both species, the highest PSD magnitudes obtained with the ant's signal were higher than the ones obtained with a Gaussian white noise (Figure 1D dashed line; Wilcoxon one-tail test: $p \leq 0.001$, see Figures S3A and S3C for *I. purpureus*), showing that ants displayed lateral oscillations with a higher regularity than random. We also replicated the same analysis using tracks of *M. croslandi* ants recorded directly on the ground while displaying learning walks around their nest (Figure S4), which confirms that these regular oscillations are not a consequence of being mounted on the trackball setup.

The navigational context modifies the regularity and frequency of oscillations

We tested whether the visual condition and the state of the path integrator influenced how regular the oscillations were, which can be measured with the magnitude of the individuals' PSD peak (see Figures S2C–S2E for individual example and STAR Methods) (Figures 1D and 1E). The statistical model revealed no interaction between both effects (Akaike Information Criterion [AIC] = −198.8, $F_{2,101} = 0.434$, p = 0.647); however, the additive model (i.e., without interaction AIC = −215.8) explains the variation of the magnitude peaks relatively well (R^2 marginal = 56% and conditional = 67%). The PI state did not affect the regularity

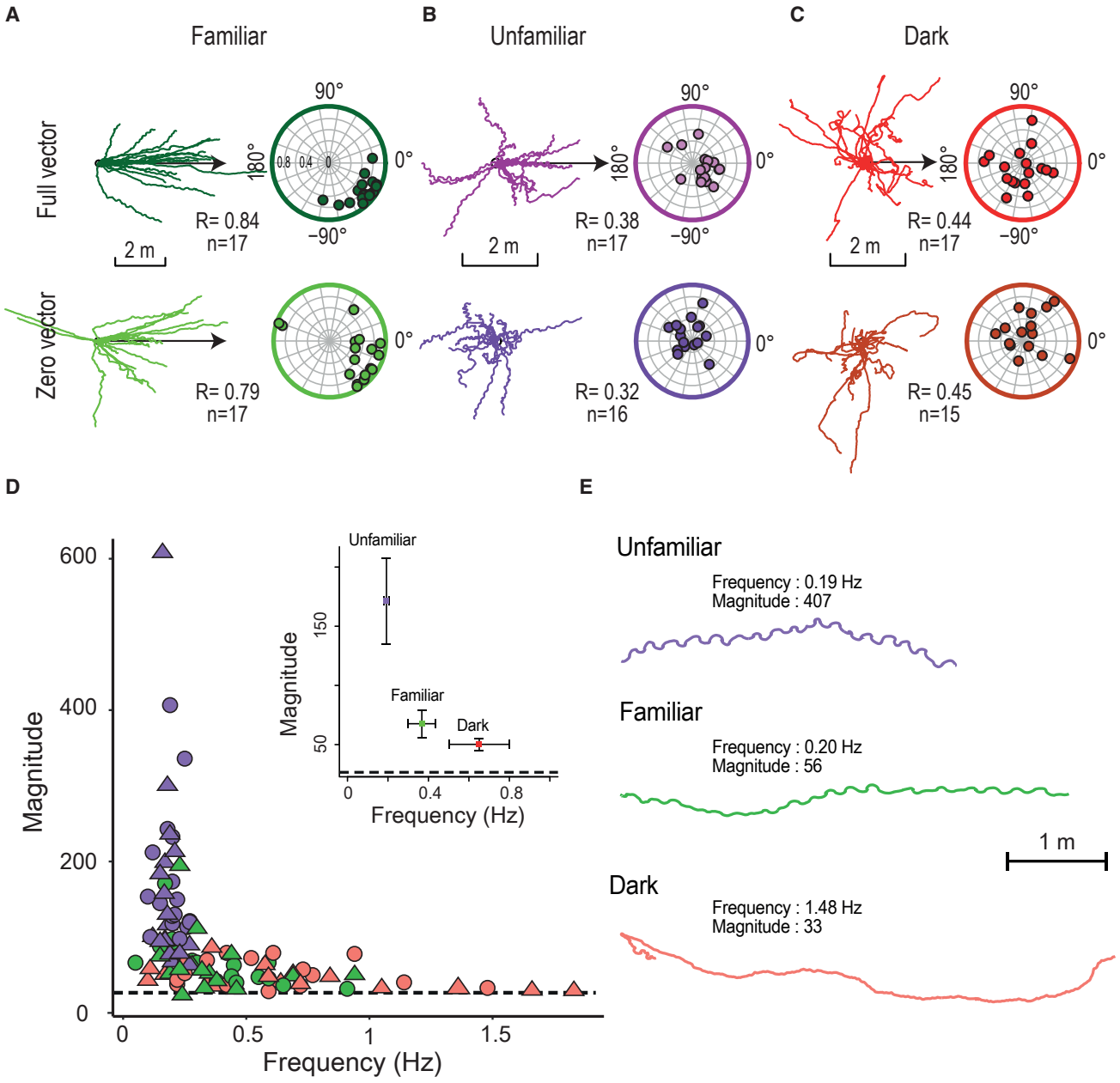

Figure 1. Oscillation characteristics vary across visual conditions

(A–C) Trajectories of *M. croslandi* tested on the trackball in a familiar panorama along their known route (A, green), an unfamiliar panorama (B, purple), or in the dark (C, red). For each condition, individuals were tested either with (full-vector, top row) or without (zero-vector, bottom row) path integration information. Reconstructed paths over 60 s are displayed relative to the real (in familiar) or theoretical (in full-vector) direction of the nest (arrow). In the circular plots, each dot indicates the average circular vector calculated over the entire path of an individual, showing the mean direction and the average vector length (i.e., a point closer to the periphery indicates straighter paths). The R values ("straightness" between 0 and 1) indicate the length of the average resulting vector of the population. The direction (in familiar terrain) or theoretical direction (for FV in unfamiliar terrain) of the nest is 0°.

(D) The graphs show the frequency and spectral density magnitude of the dominant oscillation (highest magnitude) for method (see Figure S2 and STAR Methods). High frequencies indicate a fast oscillatory rhythm and high magnitudes indicate a strong presence of this oscillation. Individuals were tested within a familiar panorama (green), an unfamiliar panorama (purple), or in the dark (red). Symbols indicate whether the state of the path integration vector was full (round) or zero (triangles) at the beginning of the experiment. Inserts show the mean frequency against the mean magnitude of each visual condition, with the associated 95% confidence interval around the mean. The dashed black line represents the mean of the spectral density peak magnitudes resulting from 200 Gaussian white noise signals.

(E) Example path for each condition for *M. croslandi* across 100 s. For similar results on *M. croslandi* recorded directly on the ground and on our second species, *I. purpureus*, see also Figures S1, S3 and S4. See also Figure S2 for methods.

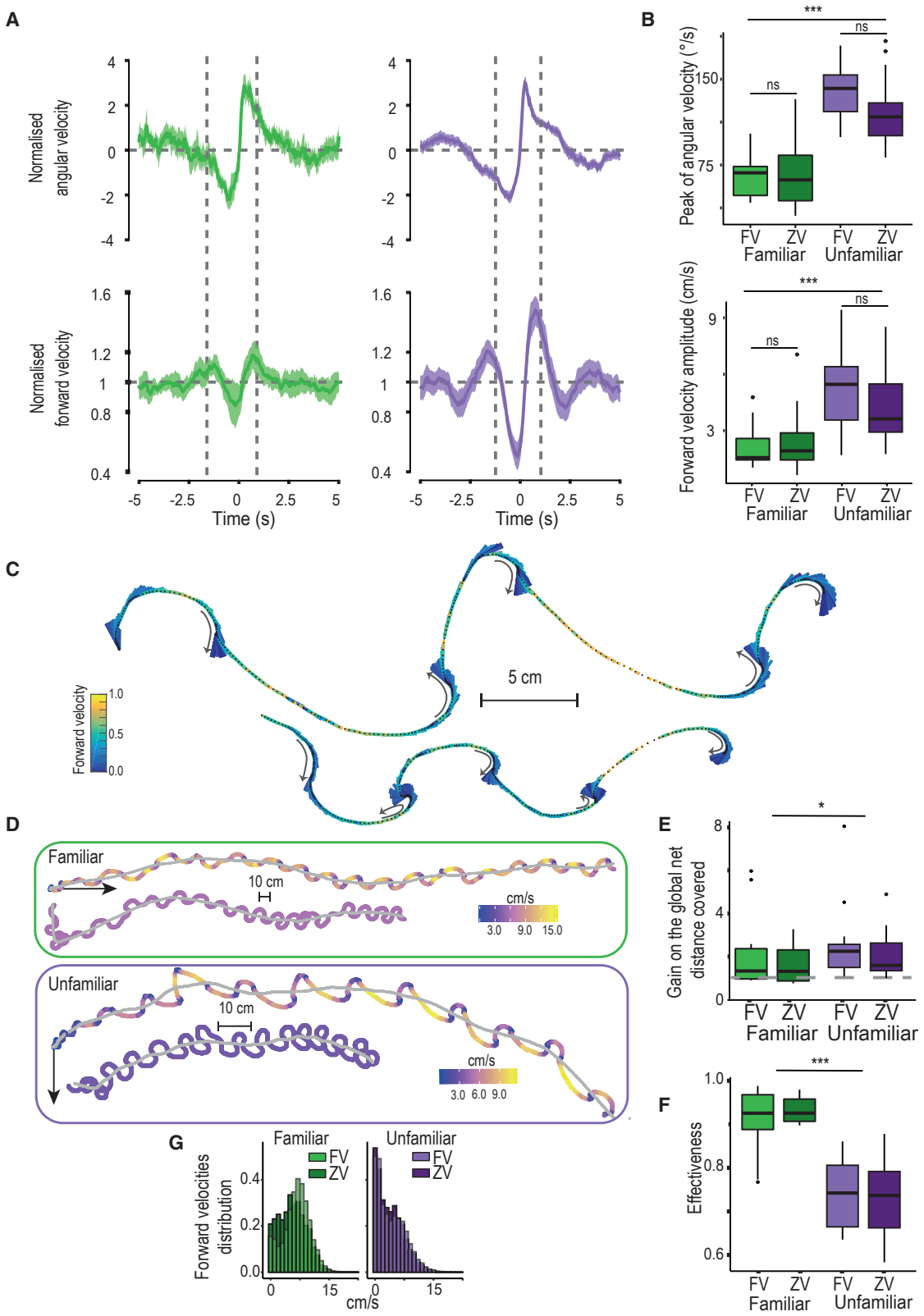

Figure 2. Co-variation of forward velocity and angular velocities optimize the distance covered and visual exploration

(A) Angular velocities (top row) and forward velocity (bottom row) co-vary in a way that seem conserved across visual conditions (on familiar route [green, n = 12] or in unfamiliar terrain [purple, n = 34]). Population cycles have been reconstructed by merging full-vector (FV) and zero-vector (ZV) data and normalizing the data

(legend continued on next page)

of oscillations (PSD peak magnitudes [Figure 1D; ANOVA: vector effect: $F_{1,101} = 1.291$, $p > 0.200$]), however, the three visual conditions did (Figure 1D; ANOVA: visual condition effect: $F_{2,101} = 83.663$, $p < 0.001$; post hoc: F versus U: $p < 0.001$; F versus D: $p = 0.016$; U versus D: $p < 0.001$): oscillations were most regular in unfamiliar terrain, intermediate in a familiar environment, and least regular in the dark (Figures 1D and 1E; mean ± SE: $U_{(FV+ZV)} = 171 \pm 19$; $F_{(FV+ZV)} = 68 \pm 6$; $D_{(FV+ZV)} = 50 \pm 3$). The effect of individuality is significant ($p = 0.015$), indicating that some individuals show more regular oscillations than others, across conditions.

We then investigated whether our different conditions influenced the oscillations' frequencies (Figure 1D, x axis), which indicates how quickly the turn alternation happens. Here, again, the PI state had no observable effect (Wilcoxon test for repeated measures; F: FV versus ZV $p = 0.635$; U: FV versus ZV $p = 0.343$, mean ± SE in F: FV = 0.38 ± 0.05 Hz, ZV = 0.34 ± 0.04 Hz; U: FV = 0.19 ± 0.01 Hz, ZV = 0.18 ± 0.0009 Hz; Figure 1D); however, independent of the PI state, the oscillatory frequencies were significantly higher in a familiar (F) than in an unfamiliar (U) visual panorama ($p = 0.023$, mean ± SE: $F_{(FV+ZV)} = 0.37 \pm 0.036$ Hz; $U_{(FV+ZV)} = 0.19 \pm 0.008$ Hz; Figure 1D). Thus, the presence of familiar visual cues tends to increase the frequency of oscillations.

In the dark, however, peak magnitudes are significantly weaker, closer to Gaussian noise and with a wider frequency range, suggesting that the PSD peak in some individuals may result from noise (Figures 1D and 1E). Oscillations seems to persist in the dark; however, their expression is greatly inhibited, suggesting that visual input is important for the expression of oscillation (Figure 1).

Overall, these results confirm the existence of regular oscillations and that their expression is influenced by the perceived familiarity of the visual surrounding, with slower and most regular oscillations being expressed in unfamiliar terrain (Figures 1D, 1E, and S4A). The second ant species, *I. purpureus*, also showed significantly regular oscillations, with the same tendency to produce slower oscillation in visually unfamiliar terrain and to inhibit their expression when in the dark (Figure S3).

The navigational context modulates the angular and forward velocity of oscillations

To investigate the dynamics of the ant oscillatory movements in more details, we combined for each ant its body angular velocity signal—obtained from video recording—with the forward movement signal—obtained from the trackball movements. We reconstructed "average cycles" for each individual by pooling the angular and forward velocity recordings 3 s before and 3 s after the moments when ants switch from a left to a right turn (i.e., when the time series of the angular velocity crosses zero, from negative to positive; see Figures S2F–S2I). That way, we can quantify each individual's average dynamic of angular and forward velocity and compare them across conditions.

The visual surrounding had a strong effect ($p < 0.001$): ants displayed higher peaks of angular velocity (Figure 2B, upper row; mean ± SE: $U_{(FV+ZV)} = 129 \pm 4.8$ deg/s; $F_{(FV+ZV)} = 67.5 \pm 4.4$ deg/s) and higher forward velocity amplitudes (Figure 2B, second row, mean ± SE: $U_{(FV+ZV)} = 4.8 \pm 0.34$ cm/s; $F_{(FV+ZV)} = 2.3 \pm 0.2$ cm/s) in an unfamiliar environment. There was, however, neither an effect of the PI state on turn or forward velocity ($p > 0.05$) nor an interaction between the visual surroundings and the PI state (mean peak of angular velocity model: AIC = 160.9, interaction $p > 0.05$; amplitude of forward velocity model: AIC = 109.9, interaction $p = 0.22$). Therefore, the amplitude of lateral oscillations within the path are larger in an unfamiliar panorama than in a familiar one, independent of the PI state (Figure 1E).

Lateral oscillations are combined with specific forward velocity variations

To test for the existence of conserved oscillatory dynamics across individuals, each individual's average cycle (Figures S2F–S2I for method example) was normalized and averaged to obtain a cycle at the population level. To ensure that we pooled ants oscillating in similar frequency ranges, we separated data from familiar and unfamiliar terrain and selected only individuals showing a peak frequency within 0.1–0.27 Hz for *M. croslandi* (n = 12). These frequency ranges correspond to high magnitudes, ensuring that they are not a consequence of noise. The emerging population-averaged oscillation patterns show the existence of movement dynamics that are consistent across individuals, for both familiar and unfamiliar environments (Figure 2A). Forward velocity covaries with angular velocity in a particular way. Forward velocity is quite low when the ants reverse their turning direction (i.e., when angular velocity crosses zero). In contrast, we observe significant peaks of forward velocity, which happen briefly (up to 1 s), while the ant is sweeping to the left or right (Figure 2A).

amplitude within the individual's average cycle (Figures S2F–S2I). Colored areas around the mean curves represent the 95% confidence interval, based on the inter-individual variation. Dashed lines represent the moment when the ants are facing their overall direction of travel.

(B) Boxplots show the actual distribution of the non-normalized mean peak of angular speed (top row) and forward velocity amplitude (bottom row) for the individuals' average cycle (FV on the left, ZV on the right).

(C) Details of paths (12 s) displayed by two different individuals in unfamiliar terrain. Black dots indicate the successive positions of the animal and vectors indicate the current heading direction. Variations of forward velocities are indicated by both the color and the length of the vectors (the longer the vector, the smaller the forward speed and thus the greater the time spent in this direction). Gray arrows emphasize the directions of turns.

(D) Reconstructed path (100 s) of two individuals recorded in a familiar (green panel) and in an unfamiliar (purple panel) panorama. Each path has been either reconstructed with the actual forward velocity signal of the ant (top path) or with a constant speed (mean of the individual's forward velocity signal, bottom path). Color scales indicate the forward velocity. For each path, the global trajectory is shown in gray (i.e., path smoothed to remove the lateral oscillations). Straight black arrows indicate the direction of the nest.

(E–G) Population statistics across conditions. (E) Ratio of the effective distance covered (length of gray path in D) between the reconstructed path with variation speed against path with constant speed for the different conditions. A ratio >1 (dashed gray line) indicates that the effective distance covered is longer with forward speed variation than without. (F) Ratio between the effective distance covered (length of gray path in D) and the actual distance walked. (G) Distribution of the forward velocity in cm/s for each condition. Stars show the levels of significance.

(B and E–G) n = 17 for each condition. For similar results on *M. croslandi* recorded directly on the ground and on our second species, *I. purpureus*, see also Figures S1, S3, and S4. See also Figure S2 for methods.

Remarkably, these peaks coincide well with the moment when the ant's body orientation is aligned with its overall direction of travel (Figure 2A, dashed lines), even though during these moments the ant's angular velocity is quite high. The same co-variation is present in our second species, *I. purpureus* (Figures S3C and S3D), showing that this signature is not specific to *M. croslandi*.

We replicated the same analysis using tracks of *M. croslandi* ants, recorded directly on the ground while displaying learning walks around their nest, and observed the same relationship between forward and angular speed (Figure S4), which confirms that these dynamics are not a consequence of being mounted on the trackball setup.

Thus, ants (Figures 2, S3, and S4) display large sweeps from one side to the other and therefore spend a minimal amount of time facing their goal direction (i.e., the middle of the sweep), as angular speed is high at this moment. However, they produce a burst of forward velocity during this moment—that is, when aligned with their direction of travel (Figures 2A, 2C, and 2D). In contrast, they slow down, and sometimes even pause, at the end of each left and right sweep, that is, when their body is facing away from their overall direction of travel (Figures 2A, 2C, 2D, and 2G).

The dynamics of lateral oscillations optimize the distance covered

To investigate the benefit of such regular variations of forward movement within the oscillations' cycle, we compared the ant's real paths with reconstructed versions of their paths, where we kept the original angular speed signal but averaged the forward speed so that it became constant (Figure 2D). By doing so, the actual distance walked remains identical but, remarkably, the effective ground distance covered (length of the gray paths in Figure 2D) by the original paths (with forward speed variation) increased by up to a factor of 8 (median = 1.5; 25/75 percentiles = 1.08/2.5) compared with the paths with constant speed. This positive gain concerns 81% of our individuals and is significant in all our conditions (ratio above 1: ps < 0.009, Figure 2E).

We then looked at the ratio between the effective ground distance covered (length of the gray path in Figure 2F) and the actual distance walked, across conditions. The smaller the ratio the more local oscillations impeded the ant's ability to cover ground effectively (a ratio of 1 indicates a straight path, without local oscillations). Such an "effectiveness ratio" is impacted by the presence of familiar visual surrounding but not by the PI state (panorama effect: $F_{1,101} = 142.090$, $p < 0.001$; PI effect: $F_{1,101} = 0.683$, $p = 0.407$). Paths displayed when on familiar terrain are more effective to cover ground than in an unfamiliar environment (post hoc, Figures 2D and 2F versus U: $p < 0.001$). This is in line with the fact that ants displayed smaller amplitudes of oscillation in the presence of a familiar panorama (Figures 2A and 2B). In addition, we observed that ants in a familiar environment displayed less pauses (Figure 2G) and higher forward velocities (n = 34, $p < 0.001$, mean ± SE: F = 6.087 ± 0.336, U = 3.961 ± 0.182 cm/s).

Oscillations are modulated by rotational feedback

To test whether oscillations result from an intrinsic oscillator rather than a control mechanism based on an external directional reference (i.e., servo-mechanism), we investigated whether ants deprived of rotational feedback (either via optic-flow or compass cues) would still oscillate. To do so, ants were mounted on the trackball in a way that prevented them from physically rotating their body on the ball: when the ant tries to turn, it is the ball that counterturns. In other words, the fixed ant experiences neither a change of body orientation nor visual rotational feedback when trying to turn (see Figure S2B). For this experiment, we recorded *M. croslandi* ants in unfamiliar terrain as this condition had produced the clearest oscillations in our previous experiments (Figure 1D). To control for the potential effects of facing directions (depending on celestial or terrestrial visual cues), we tested each ant fixed in eight subsequent different orientations with a 45° rotational shift.

Despite the absence of visual rotational feedback, the obtained peak magnitudes of the angular velocity PSD (see STAR Methods) were much higher than expected from a Gaussian white noise ($p < 0.001$), clearly showing the presence of a regular alternation between left and right turns (Figures 3A and 3B). The ant's body orientation relative to the world had no effect on the magnitudes (orientation: $F_{7,83} = 0.3729$, $p = 0.914$), nor did the other random parameters (individual $p = 0.933$, sequence $p = 0.473$). The mean oscillation frequencies (mean ± SE: 0.17 ± 0.007 Hz) were quite close to what we observed when these ants were free to rotate in an unfamiliar environment (Wilcoxon test for repeated measures: p = 1, n = 88, Figure 3F). Thus, ants can display regular turning oscillations without rotational feedback, whether as a result of optic flow or a change of orientation relative to directional cues such as the visual panorama, wind, celestial compass cues, or the magnetic field. Here, again, the lateral oscillations displayed by the fixed ants showed the simultaneous variation of forward speed, as observed in the other conditions (Figure 3G). Consequently, we are left with the conclusion that these oscillatory dynamics are generated intrinsically.

Interestingly, the absence of rotational feedback led to higher angular velocities (mean: fixed = 176 deg/s; free = 128 deg/s; $p < 0.001$), higher forward velocities (mean: fixed = 11 cm/s; free = 5 cm/s; $p < 0.001$), and slightly slower turn alternations (i.e., lower frequency: fixed = 0.16 Hz; free = 0.19 Hz, $p = 0.0189$) than those observed in ants that were free to physically rotate on the ball (Figures 3A–3F). Rotational sensory feedback is thus involved in limiting the amplitude of the oscillations.

The observed movement signature emerges readily from a simple neural circuit

Similar to previous work,[44,45] we designed a simplistic neural model based on the circuitry of the insect's pre-motor area—the so-called lateral accessory lobes (LALs). The purpose of this model was not to match observed data quantitatively[20] but simply to test whether the co-varying relationship observed between angular and forward velocity could emerge from this type of circuit. Activation of the neurons in the left and right pre-motor areas are known to mediate left and right turns, respectively, in insects.[11,13,45–48] Furthermore, these left and right regions are known to reciprocally inhibit each other.[11,13,45,47] Modeling two reciprocally inhibiting neurons with internal feedback—that tries to maintain a basal activity—is sufficient to obtain the typical oscillatory activity between left and right LAL[11,45] (Figure 4) and thus provides

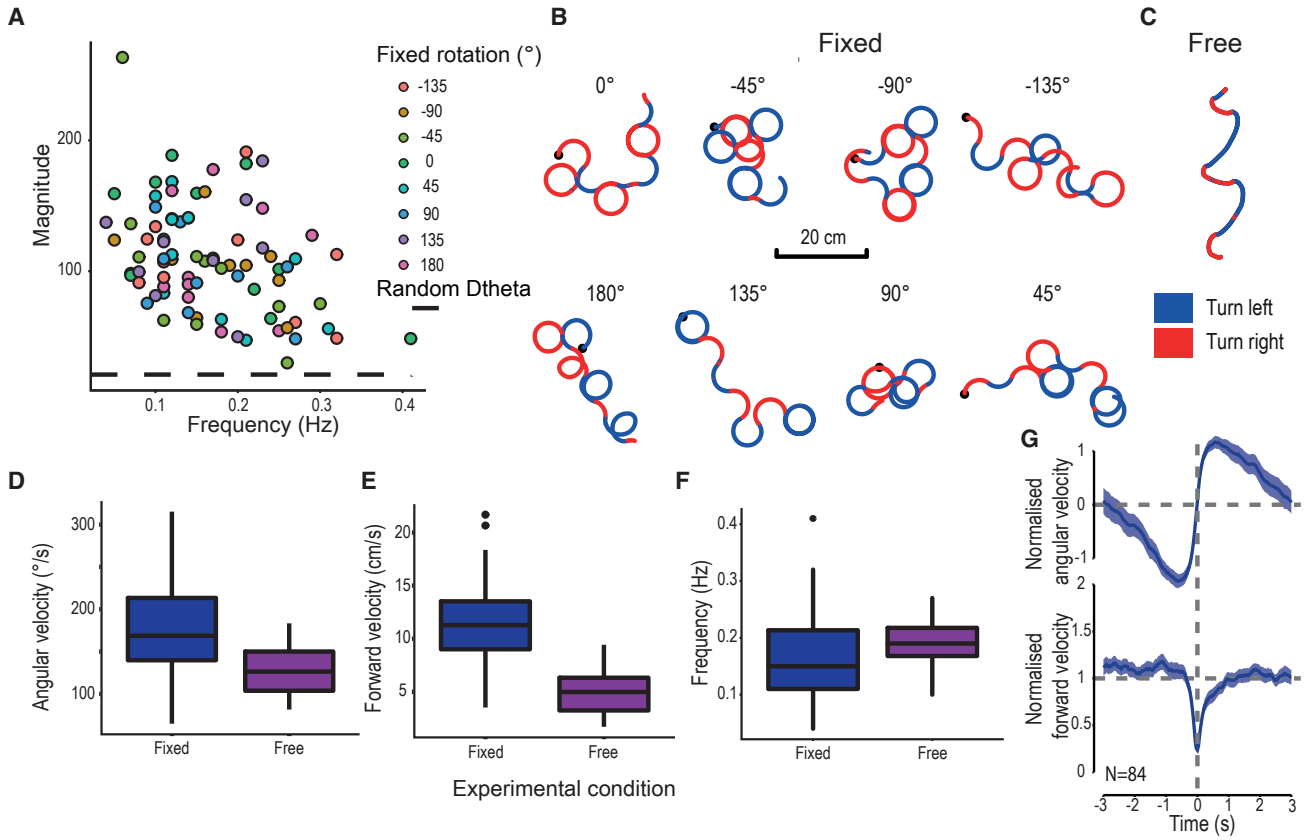

Figure 3. Ants still oscillate in the absence of rotational feedback

Zero-vector ants were tethered on the trackball in a way that prevented actual body rotation and were then tested in an unfamiliar environment.

(A) Distribution of the individual Fourier dominant peak frequency and magnitude, based on the angular velocity's spectral density time series (as in Figure 1D) (STAR Methods; see Figures S2B–S2E). High frequency indicates a fast oscillatory rhythm, and a high magnitude indicates a strong presence of this oscillatory rhythm. The color symbols represent the rotation relative to the theoretical nest direction (0°). The dashed black line represents the mean magnitude obtained from 200 Gaussian white noise signals (18.75).

(B) Example paths of different individuals fixed in different orientations.

(C) Example path from an ant that was free to rotate on the trackball, recorded in unfamiliar terrain in previous experiments. (B and C) In both situations, ants alternate regularly between right (blue) and left (red), but turns are sharper in the absence of rotational feedback.

(D–F) Peak of angular velocity (D), amplitude of forward velocity (E), and frequency (F) of the individual's average oscillation cycle show that ants move faster and turn faster and slightly longer in the absence of rotation feedback.

(G) Angular velocities (top row) and forward velocities (bottom row) co-vary in a way that seems conserved across experimental conditions. Population cycles have been reconstructed by merging all rotational conditions as there is no difference in amplitude of mean peaks of angular velocity and mean forward amplitude cycles between rotational conditions (ANOVA: Df = $F_{7,84}$ = 1.0103, $p \geq 0.432$). Each individual signal has been normalized before pooling. Colored areas around mean curves represent the 95% confidence interval, based on the inter-individual variation. See also Figure S2 for methods.

an explanation for the regular oscillations between left and right turns observed in insects. Interestingly, we show here that simply assuming that forward velocity is controlled by the sum of left and right output—while angular velocity results from their difference[14,20,45]—is sufficient for the co-variation observed in ants to emerge (Figure 4). Bursts of forward speed appear when one side largely dominates the other, that is, when the ant is at the maximum speed of its angular sweep and thus roughly aligned with its overall direction of travel. Conversely, a break in forward speed occurs when the dominance is reversed between LAL neurons, that is, at the moment the ant switches its turning direction (Figure 4). Importantly, the emergence of this particular relationship is robust to parameter change (Figure S5) and is thus a stable feature of these types of circuits.

DISCUSSION

An embedded solution for the compromise between exploration/exploitation

We recorded the detailed locomotor movements of two distantly related ant species—*M. croslandi* and *I. purpureus*—using a trackball-treadmill device directly in their natural environments. Despite one species being a solitary visual navigator (*M. croslandi*) and the other (*I. purpureus*) using pheromone trails and mass recruitment, we noticed a remarkably similar behavioral signature. Both species continuously display regular lateral oscillations with a synchronized burst of forward speed when facing the general direction of travel (Figures 1, 2A, 2C, and S3). This pattern of movement strongly optimizes the overall ground distance covered while simultaneously enabling the ant

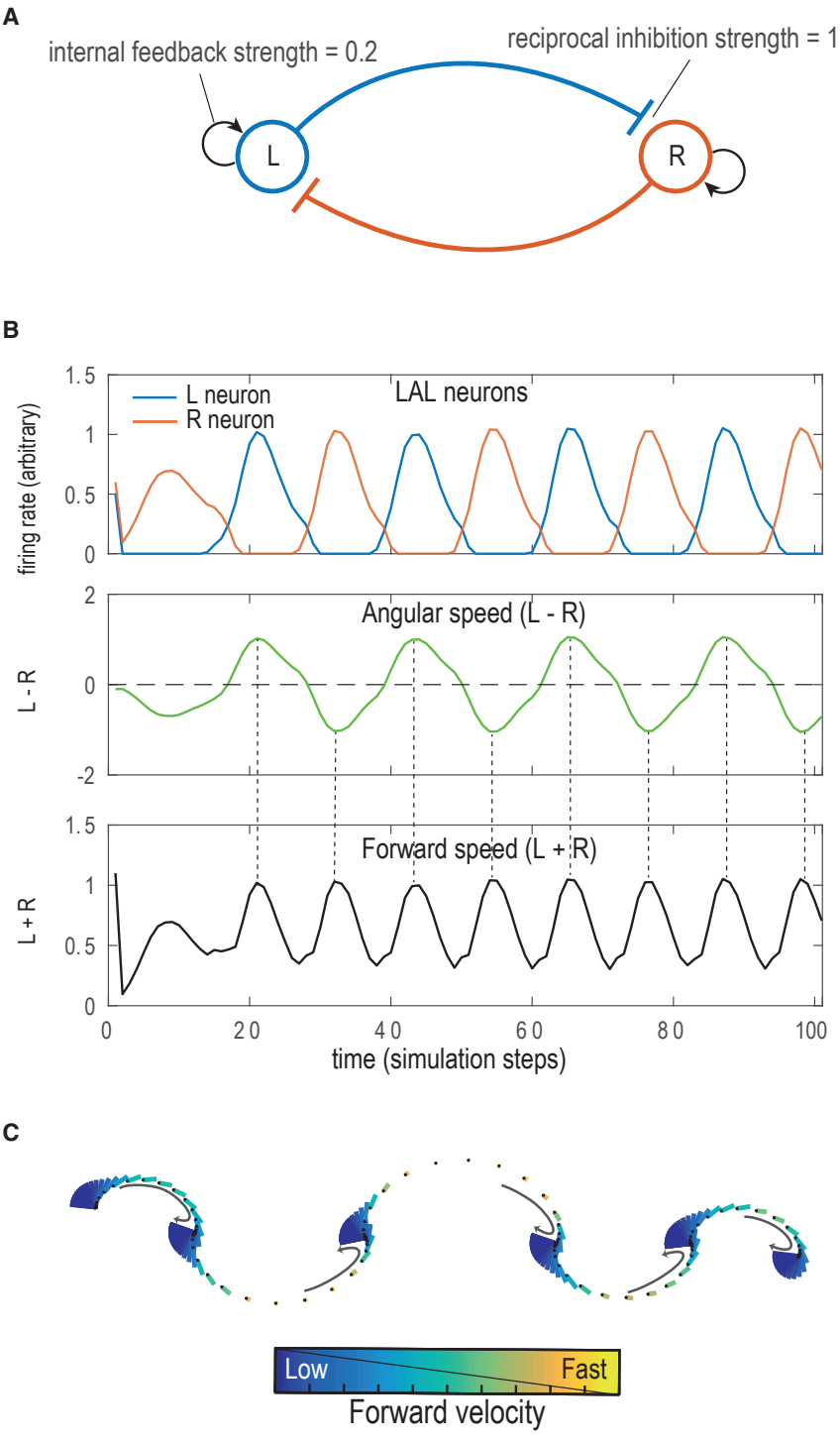

Figure 4. Reciprocal inhibition between two units produces the observed relationship between angular and forward velocity

(A) Scheme of the model abstracted from the lateral accessory lobe (LAL). The right (R) and left (L) hemisphere neurons reciprocally inhibit each other (blue and red connection), while trying to sustain a basal firing rate through internal feedback (black arrow).

(B) This results in the emergence of stable antiphasic oscillatory activity between the R and L neurons (B, upper row). Assuming that angular velocity is controlled by the difference (B, middle row)—and forward speed by the sum (B, bottom row)—between left and right activation is sufficient to elicit the movement dynamics observed in ants (compare Figure 4C with Figure 2C).

(C) Details of the dynamics of the path generated by the model. Color indicates forward velocity (scales are arbitrary). Black dots indicate the successive positions of the agent and vectors indicate the current heading direction. Variation of forward velocities are indicated by both the color and the length of the vectors (the longer the vector, the smaller the forward speed and thus the greater the time spent in this direction). As with ants, the model results in a zigzagging path where velocity drops during turn reversal and increases when facing the overall direction of travel (Figures 2A, 2C, and 2D). Although the model enables the modulation of amplitude and frequency of the oscillations, the forward/angular velocities' relationship is quite robust to parameter change (see Figure S5).

to slow down when scanning left and right directions, which may extend up to a full U-turn in some ants (Figures 2C–2F).

Previous observations assumed that ants accelerate when facing their goal direction as a response to the recognition of familiar views.[49–51] Here, we show that this acceleration is the product of an endogenous process, as it is still expressed in unfamiliar terrain or when the ant's body is artificially fixed on our trackball in a given orientation (Figure 3). This findings stresses the often disregarded importance of internally generated movement within the "sensorimotor" loop.[2,8,52–54]

The described internally generated movement dynamic provides an embedded solution for the compromise between exploration (looking to the side) and exploitation (covering ground in the desired direction). External visual cues can then modulate the exploration/exploitation balance to the task at hand by simply adjusting the amplitude of this endogenous dynamic. Higher amplitude oscillations optimize "exploration" (higher amplitude scans) in an unfamiliar environment, while lower amplitudes favor "exploitation" (straighter paths) on a familiar route (Figures 2 and S3).

Interestingly, this movement signature is equally useful—and used—during the acquisition of learnt visual information, when naive ants display their learning walk around the nest[27] (Figure S4). Optimizing the learning of visual cues in naive ants requires biasing the balance toward exploration in the same manner as searching for familiar cues in an unfamiliar environment does in experienced ants; thus, it is not surprising to also see high amplitude oscillations here (Figures 2A–2D and S3). The apparently different needs for the

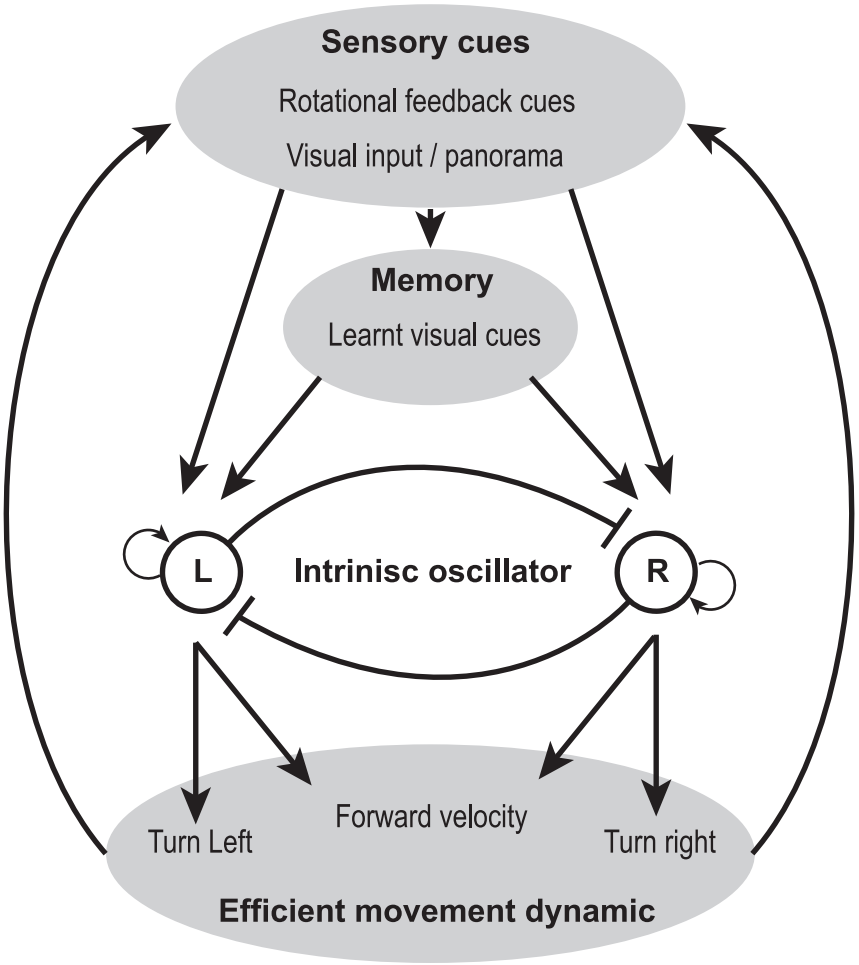

Figure 5. An intrinsic oscillator at the core of visual navigation

We propose a simple scheme to encompass our results. In this view, sensory input (in this case various innate and learnt visual information) acts on behavior only indirectly, through the systematic modulation of an intrinsic oscillator. The latter ensures that an efficient movement dynamic is preserved across navigational contexts, which would not necessarily be the case if various and potentially conflicting sensory information was directly modulating movement. This scheme also highlights the idea that action is not merely the product of perception. At the core of behavior lies an intrinsic, self-generated dynamic, which is modulated, rather than controlled, by sensory perception.

acquisition of information on the one hand and the use of that information on the other hand are thus solved with the same sensory-motor solution. The weaker modulation observed in *I. purpureus* (Figure S3) may be explained by their strong reliance on chemical trails,[35] whose absence on the trackball may favor exploration in both visually familiar and unfamiliar conditions.

Finally, we see in both species that the internally generated oscillations can be strongly inhibited when not needed, such as when moving in the dark (Figures 1C, 1D, S3A, and S3B). Indeed, oscillations are not always useful, and it may be advantageous to repress them in particular scenarios, such as when inside the nest or when trying to escape an aversive situation. Thus, both the animal's internal state and the presence/absence of relevant contextual information—such as a visual panorama opposed to no panorama at all—modulates the expression of the internally produced oscillations in a similar manner in which the male fly's internal state continuously tunes up or down the gain of circuits promoting visual pursuit.[55] However, what specific types of visual information promote the expression of oscillations remains to be seen.

Evolutionary consideration and neural implementation

Lateral oscillations of around 0.3–1 Hz are also observed in moths,[12,15,16,56] *Drosophila* larvae,[14] Colorado beetles,[42] flying hymenopteran,[29,30,57] and other insects,[13] suggesting an ancestral way of moving that predates at least the holometabolous insects' common ancestor (around 300 mya).

In the insect brain, regular lateral oscillations seem to result from reciprocal contra-lateral inhibitions between left and right hemispheric premotor areas—the so-called LAL, which is an ancestral brain structure highly conserved across insects.[13,44,45] These circuits—analogous to central pattern generators (CPGs)—result in the internal production of asymmetrical and rhythmical excitation between left and right motor commands, the so-called "flip-flop" neurons.[11,13,45–48] However, while CPGs are known to sustain a wide range of rhythmical limb movements,[8,53,58,59] the LAL controls the displacement of the whole animal across space and thus directly contributes to the navigational task.

Some have suggested that neural systems evolved at first to coordinate movements endogenously,[54,60] whereas the modulation of these movements by external sensory information originated only as a second step.[60] This view is supported by the current demonstration of an internally produced rhythm at the core of navigational behavior in ants, as well as the observation that, across species, various multi-modal sensory cues converge to the same conserved region (the LAL) to produce the remarkable variety of navigational behaviors across species.[13,17,44,45] Modulation of oscillations by olfactory cues helps *Drosophila* larvae[14] to climb odor gradients, male moths to track pheromone plumes,[12,13,15–17] and ants to follow chemical trails.[18] Modulation of oscillations by vision for navigation, as observed in wasps,[29,30] bumblebees,[31] and ants,[23–28] may have appeared later with the evolution of visual navigation in hymenopteran, through direct or indirect connections between the mushroom bodies—the seat of navigational visual memories[50,61,62]—and the LAL (Figure 4). The modulation of oscillations by re-afferent rotational visual cues, as we showed here in ants (Figure 3), might be ancestral to insects, as we equally observe it in moths.[16,17,63] This likely evolved through connections between horizontal optic-flow detectors in the optic

lobes[16,64] and the LAL (Figure 4), providing a useful feedback-control to calibrate the amplitude of turns and, more generally, participating in the widespread opto-motor response.[16]

The forward speed variation within the oscillation cycles presented here has not been reported in other insect species, and the fact that it is shared in two phylogenetically and ecologically distant ants (Figure S3) suggests that it is a shared feature in the ant family. This may be an adaptation for the use of vision while walking. Scanning multiple direction through body rotation is key for visual scene recognition in hymenopteran,[40,65,66] and because ants are ground dwellers, they are reluctant to decouple their body orientation from their direction of travel, even though they can.[67] Ants thus benefit from pausing when looking to the side; otherwise, they would depart from their general direction of travel. Conversely, the timely burst of forward speed when facing the overall direction of travel (Figures 2A, 2C, and 2D) enables the stretching of the oscillations and thus strongly increases the amount of ground covered (Figures 2D–2F). In addition, pausing when looking to the side must improve the efficiency of visual recognition due to gaze stabilization, which accommodates remarkably well the idea that views are learnt and recognized when oriented left and right—rather than toward and away—from the goal.[29,68]

Interestingly, the efficient co-variation between forward and angular velocity observed here in ants is captured by a model of the LAL by simply assuming that forward speed results from the summed excitation of both hemispheres' motor commands, while turning velocities results from the difference between left and right excitation (Figure 4). Certainly, we do not exclude the idea that more complex circuitry could produce other regimes of covariations, but our simple model shows that this particular relationship between forward and angular speed is robust to parameter change (Figure S5), and thus can readily emerge from the LAL. However, the oscillations' amplitude and frequency vary with parameter change, at least across a factor of 2 (Figure S5). Therefore, we can easily envision how various inputs into the LAL (such as pictured in Figure 5) could modulate the amplitude and frequency of the emerging oscillations without altering the fundamental relationship between forward and angular velocities. For instance, inputs from the central complex, such as PFL2 neurons, project bilaterally to the LAL[69–71] and could thus promote the overall modulation of oscillation amplitude, as shown here. Conversely, PFL3 neurons, which project unilaterally to the LAL, could mediate lateralized information, whether from memorized views[68] or PI,[72,73] to bias the oscillations toward one side.[71] Understanding precisely how such inputs interact with oscillations in insects opens the door to a complexity that would be too vast to tackle here, but given the rapid development of neurobiological tools and knowledge of the circuitry of the LALs, this may constitute a realistic endeavor in the near future.

STAR★METHODS

Detailed methods are provided in the online version of this paper and include the following:

- KEY RESOURCES TABLE
- RESOURCE AVAILABILITY
  - Lead contact
  - Materials availability
  - Data and code availability
- EXPERIMENTAL MODEL AND SUBJECT DETAILS
  - Study Animal & Experimental site
- METHOD DETAILS
  - Trackball system and data extraction
  - Free ant experiments: protocol
  - Fixed ant experiments: protocol
- QUANTIFICATION AND STATISTICAL ANALYSIS
  - Fourier analysis
  - Average oscillatory cycle
  - Analysis of the ants' direction of movement
  - Analysis of optimization
  - Statistical models
- COMPUTATIONAL MODEL
  - Initialization
  - At each time step
  - Computation of the angular and forward velocities

SUPPLEMENTAL INFORMATION

Supplemental information can be found online at https://doi.org/10.1016/j.cub.2022.11.059.

ACKNOWLEDGMENTS

We want to thank the Australian National University and, particularly, Jochen Zeil, Zoltán Kócsi, and Trevor Murray for their advice and technical support. We also thank Hansjürgen Dahmen for providing us with the trackball system and Ajay Narendra for his incredible knowledge of the local Australian ants. We are grateful to all these people for their helpful advice. We also thank Jochen Zeil, Paul Graham, and Michael Mangan for their helpful feedback on the manuscript. We are grateful to Jochen Zeil for having provided the data on the learning walk. Finally, we thank the ants tested in these experiments for their participation. Funding: European Research Council, grant reference number: EMERG-ANT 759817, author: A.W.

AUTHOR CONTRIBUTIONS

Conception and design of the experiment, data collection, analysis and interpretation of data, drafting and revising the article, L.C.; conception and design of the experiment, data collection, drafting and revising the article, S.S.; conception and design of the experiment, data collection, analysis and interpretation of data, conception and design of the computational model, drafting and revising the article, supervision of project, A.W.

DECLARATION OF INTERESTS

The authors declare no competing interests.

Received: September 7, 2022
Revised: November 6, 2022
Accepted: November 24, 2022
Published: December 19, 2022

REFERENCES

1. Dittmar, L., Stürzl, W., Baird, E., Boeddeker, N., and Egelhaaf, M. (2010). Goal seeking in honeybees: matching of optic flow snapshots? J. Exp. Biol. *213*, 2913–2923. https://doi.org/10.1242/jeb.043737.
2. Gomez-Marin, A., Stephens, G.J., and Louis, M. (2011). Active sampling and decision making in Drosophila chemotaxis. Nat. Commun. *2*, 441. https://doi.org/10.1038/ncomms1455.

3. Lehrer, M. (1996). Small-scale navigation in the honeybee: active acquisition of visual information about the goal. J. Exp. Biol. *199*, 253–261.
4. Dawkins, M.S., and Woodington, A. (2000). Pattern recognition and active vision in chickens. Nature *403*, 652–655. https://doi.org/10.1038/35001064.
5. Otero-Millan, J., Troncoso, X.G., Macknik, S.L., Serrano-Pedraza, I., and Martinez-Conde, S. (2008). Saccades and microsaccades during visual fixation, exploration, and search: foundations for a common saccadic generator. J. Vision *8*. 21.1–2118. https://doi.org/10.1167/8.14.21.
6. Wachowiak, M. (2011). All in a sniff: olfaction as a model for active Sensing. Neuron *71*, 962–973. https://doi.org/10.1016/j.neuron.2011.08.030.
7. Wesson, D.W., Donahou, T.N., Johnson, M.O., and Wachowiak, M. (2008). Sniffing behavior of mice during performance in odor-guided tasks. Chem. Senses *33*, 581–596. https://doi.org/10.1093/chemse/bjn029.
8. Wolf, S., Dubreuil, A.M., Bertoni, T., Böhm, U.L., Bormuth, V., Candelier, R., Karpenko, S., Hildebrand, D.G.C., Bianco, I.H., Monasson, R., et al. (2017). Sensorimotor computation underlying phototaxis in zebrafish. Nat. Commun. *8*, 651. https://doi.org/10.1038/s41467-017-00310-3.
9. DeBose, J.L., and Nevitt, G.A. (2008). The use of odors at different spatial scales: comparing birds with fish. J. Chem. Ecol. *34*, 867–881. https://doi.org/10.1007/s10886-008-9493-4.
10. Freas, C.A., and Cheng, K. (2022). The basis of navigation across species. Annu. Rev. Psychol. *73*, 217–241. https://doi.org/10.1146/annurev-psych-020821-111311.
11. Iwano, M., Hill, E.S., Mori, A., Mishima, T., Mishima, T., Ito, K., and Kanzaki, R. (2010). Neurons associated with the flip-flop activity in the lateral accessory lobe and ventral protocerebrum of the silkworm moth brain. J. Comp. Neurol. *518*, 366–388. https://doi.org/10.1002/cne.22224.
12. Kanzaki, R., Sugi, N., and Shibuya, T. (1992). Self-generated zigzag turning of Bombyx mori Males during pheromone-mediated upwind walking(physology). Zool. Sci. *9*, 515–527.
13. Namiki, S., and Kanzaki, R. (2016). The neurobiological basis of orientation in insects: insights from the silkmoth mating dance. Curr. Opin. Insect Sci. *15*, 16–26. https://doi.org/10.1016/j.cois.2016.02.009.
14. Wystrach, A., Lagogiannis, K., and Webb, B. (2016). Continuous lateral oscillations as a core mechanism for taxis in Drosophila larvae. eLife *5*, e15504. https://doi.org/10.7554/eLife.15504.
15. Kuenen, L.P.S., and Baker, T.C. (1983). A non-anemotactic mechanism used in pheromone source location by flying moths. Physiol. Entomol. *8*, 277–289. https://doi.org/10.1111/j.1365-3032.1983.tb00360.x.
16. Olberg, R.M. (1983). Pheromone-triggered flip-flopping interneurons in the ventral nerve cord of the silkworm moth,Bombyx mori. J. Comp. Physiol. *152*, 297–307. https://doi.org/10.1007/BF00606236.
17. Namiki, S., Iwabuchi, S., Pansopha Kono, P., and Kanzaki, R. (2014). Information flow through neural circuits for pheromone orientation. Nat. Commun. *5*, 5919. https://doi.org/10.1038/ncomms6919.
18. Hangartner, W. (1967). Spezifit/it und Inaktivierung des Spurphcromons yon Lasius fuliginosus Latr. und Orientierung der Arbeiterinnen im Duftfeld. Z. vergl. Physiol. *57*, 34. https://doi.org/10.1007/BF00303068.
19. Izquierdo, E.J., and Lockery, S.R. (2010). Evolution and analysis of minimal neural circuits for klinotaxis in Caenorhabditis elegans. J. Neurosci. *30*, 12908–12917. https://doi.org/10.1523/JNEUROSCI.2606-10.2010.
20. Adden, A., Stewart, T.C., Webb, B., and Heinze, S. (2020). A neural model for insect steering applied to olfaction and path integration. Neural Comput. *7*, 34. https://doi.org/10.1101/2020.08.25.266247.
21. Kodzhabashev, A., and Mangan, M. (2015). Route following without scanning. In Biomimetic and Biohybrid Systems, P.F.M.J. Verschure, A. Mura, and T.J. Prescott, eds. (Springer International Publishing), pp. 199–210. https://doi.org/10.1007/978-3-319-22979-9_20.
22. Le Möel, F., and Wystrach, A. (2020). Opponent processes in visual memories: A model of attraction and repulsion in navigating insects' mushroom bodies. PLoS Comput. Biol. *16*, e1007631. https://doi.org/10.1371/journal.pcbi.1007631.
23. Murray, T., Kócsi, Z., Dahmen, H., Narendra, A., Le Möel, F., Wystrach, A., and Zeil, J. (2020). The role of attractive and repellent scene memories in ant homing (*Myrmecia croslandi*). J. Exp. Biol. *223*, jeb210021. https://doi.org/10.1242/jeb.210021.
24. Graham, P., and Collett, T.S. (2002). View-based navigation in insects: how wood ants (*Formica rufa* L.) look at and are guided by extended landmarks. J. Exp. Biol. *205*, 2499–2509. https://doi.org/10.1242/jeb.205.16.2499.
25. Lent, D.D., Graham, P., and Collett, T.S. (2013). Phase-dependent visual control of the zigzag paths of navigating wood ants. Curr. Biol. *23*, 2393–2399. https://doi.org/10.1016/j.cub.2013.10.014.
26. Lent, D.D., Graham, P., and Collett, T.S. (2010). Image-matching during ant navigation occurs through saccade-like body turns controlled by learned visual features. Proc. Natl. Acad. Sci. USA *107*, 16348–16353. https://doi.org/10.1073/pnas.1006021107.
27. Jayatilaka, P., Murray, T., Narendra, A., and Zeil, J. (2018). The choreography of learning walks in the Australian jack jumper ant *Myrmecia croslandi*. J. Exp. Biol. *221*, jeb185306. https://doi.org/10.1242/jeb.185306.
28. Zeil, J., and Fleischmann, P.N. (2019). The learning walks of ants (Hymenoptera: Formicidae). NEWS_029:093. https://doi.org/10.25849/MYRMECOL.
29. Stürzl, W., Zeil, J., Boeddeker, N., and Hemmi, J.M. (2016). How wasps acquire and use views for homing. Curr. Biol. *26*, 470–482. https://doi.org/10.1016/j.cub.2015.12.052.
30. Voss, R., and Zeil, J. (1998). Active vision in insects: an analysis of object-directed zig-zag flights in wasps (Odynerus spinipes?, Eumenidae). J. Comp. Physiol. A *182*, 377–387. https://doi.org/10.1007/s003590050187.
31. Philippides, A., de Ibarra, N.H., Riabinina, O., and Collett, T.S. (2013). Bumblebee calligraphy: the design and control of flight motifs in the learning and return flights of Bombus terrestris. J. Exp. Biol. *216*, 1093–1104. https://doi.org/10.1242/jeb.081455.
32. Jayatilaka, P., Raderschall, C.A., Narendra, A., and Zeil, J. (2013). Individual foraging patterns of the jack jumper ant Myrmecia croslandi (Hymenoptera: Formicidae). Myrmecol. News *19*, 75–83.
33. Narendra, A., Gourmaud, S., and Zeil, J. (2013). Mapping the navigational knowledge of individually foraging ants, *Myrmecia croslandi*. Proc. Biol. Sci. *280*, 20130683. https://doi.org/10.1098/rspb.2013.0683.
34. Zeil, J., Narendra, A., and Stürzl, W. (2014). Looking and homing: how displaced ants decide where to go. Philos. Trans. R. Soc. Lond. B Biol. Sci. *369*, 20130034. https://doi.org/10.1098/rstb.2013.0034.
35. Card, A., McDermott, C., and Narendra, A. (2016). Multiple orientation cues in an Australian trunk-trail-forming ant, Iridomyrmex purpureus. Aust. J. Zool. *64*, 227. https://doi.org/10.1071/ZO16046.
36. Collett, M., and Collett, T.S. (2017). Path integration: combining optic flow with compass orientation. Curr. Biol. *27*, R1113–R1116. https://doi.org/10.1016/j.cub.2017.09.004.
37. Heinze, S., Narendra, A., and Cheung, A. (2018). Principles of insect path integration. Curr. Biol. *28*, R1043–R1058. https://doi.org/10.1016/j.cub.2018.04.058.
38. Müller, M., and Wehner, R. (1988). Path integration in desert ants, Cataglyphis fortis. Proc. Natl. Acad. Sci. USA *85*, 5287–5290. https://doi.org/10.1073/pnas.85.14.5287.
39. Collett, T.S., and Cartwright, B.A. (1983). Eidetic images in insects: their role in navigation. Trends in Neurosciences *6*, 101–105.
40. Zeil, J. (2012). Visual homing: an insect perspective. Curr. Opin. Neurobiol. *22*, 285–293. https://doi.org/10.1016/j.conb.2011.12.008.
41. Dahmen, H., Wahl, V.L., Pfeffer, S.E., Mallot, H.A., and Wittlinger, M. (2017). Naturalistic path integration of *Cataglyphis* desert ants on an air-cushioned lightweight spherical treadmill. J. Exp. Biol. *220*, 634–644. https://doi.org/10.1242/jeb.148213.
42. Lönnendonker, U. (1991). Dynamic properties of orientation to a visually fixated target by walking Colorado beetles. J. Exp. Biol. *158*, 149–164.

43. Zollikofer, C.P.E. (1994). Stepping patterns in ants – INFLUENCE OF BODY MORPHOLOGY. J. Exp. Biol. *192*, 107–118.

44. Namiki, S., and Kanzaki, R. (2016). Comparative neuroanatomy of the lateral accessory lobe in the insect brain. Front. Physiol. *7*, 244. https://doi.org/10.3389/fphys.2016.00244.

45. Steinbeck, F., Adden, A., and Graham, P. (2020). Connecting brain to behaviour: a role for general purpose steering circuits in insect orientation? J. Exp. Biol. *223*, jeb212332. https://doi.org/10.1242/jeb.212332.

46. Berni, J. (2015). Genetic dissection of a regionally differentiated network for exploratory behavior in drosophila larvae. Curr. Biol. *25*, 1319–1326. https://doi.org/10.1016/j.cub.2015.03.023.

47. Berni, J., Pulver, S.R., Griffith, L.C., and Bate, M. (2012). Autonomous circuitry for substrate exploration in freely moving *Drosophila* larvae. Curr. Biol. *22*, 10.

48. Kanzaki, R., Nagasawa, S., and Shimoyama, I. (2005). Neural basis of odor-source searching behavior in insect brain systems evaluated with a mobile robot. Chem. Senses *30*, i285–i286. https://doi.org/10.1093/chemse/bjh226.

49. Baddeley, B., Graham, P., Husbands, P., and Philippides, A. (2012). A model of ant route navigation driven by scene familiarity. PLoS Comput. Biol. *8*, e1002336. https://doi.org/10.1371/journal.pcbi.1002336.

50. Kamhi, J.F., Barron, A.B., and Narendra, A. (2020). Vertical lobes of the mushroom bodies are essential for view-based navigation in Australian Myrmecia Ants. Curr. Biol. *30*, 3432–3437.e3. https://doi.org/10.1016/j.cub.2020.06.030.

51. Wystrach, A., Mangan, M., Philippides, A., and Graham, P. (2013). Snapshots in ants? New interpretations of paradigmatic experiments. J. Exp. Biol. *216*, 1766–1770. https://doi.org/10.1242/jeb.082941.

52. Brembs, B. (2021). The brain as a dynamically active organ. Biochem. Biophys. Res. Commun. *564*, 55–69. https://doi.org/10.1016/j.bbrc.2020.12.011.

53. Schroeder, C.E., Wilson, D.A., Radman, T., Scharfman, H., and Lakatos, P. (2010). Dynamics of Active Sensing and perceptual selection. Curr. Opin. Neurobiol. *20*, 172–176. https://doi.org/10.1016/j.conb.2010.02.010.

54. Yuste, R., MacLean, J.N., Smith, J., and Lansner, A. (2005). The cortex as a central pattern generator. Nat. Rev. Neurosci. *6*, 477–483. https://doi.org/10.1038/nrn1686.

55. Hindmarsh Sten, T., Li, R., Otopalik, A., and Ruta, V. (2021). Sexual arousal gates visual processing during Drosophila courtship. Nature *595*, 549–553. https://doi.org/10.1038/s41586-021-03714-w.

56. Kanzaki, R., and Mishima, T. (1996). Pheromone-triggered 'Fiipflopping' neural signals correlate with activities of neck motor neurons of a male moth, Bombyx mori. Zool. Sci. *13*, 79–87. https://doi.org/10.2108/zsj.13.79.

57. Egelhaaf, M., Boeddeker, N., Kern, R., Kurtz, R., and Lindemann, J.P. (2012). Spatial vision in insects is facilitated by shaping the dynamics of visual input through behavioral action. Front. Neural Circuits *6*, 108. https://doi.org/10.3389/fncir.2012.00108.

58. Marder, E., and Calabrese, R.L. (1996). Principles of rhythmic motor pattern generation. Physiol. Rev. *76*, 687–717. https://doi.org/10.1152/physrev.1996.76.3.687.

59. McAuley, J.H., Rothwell, J.C., and Marsden, C.D. (1999). Human anticipatory eye movements may reflect rhythmic central nervous activity. Neuroscience *94*, 339–350. https://doi.org/10.1016/S0306-4522(99)00337-1.

60. Keijzer, F., van Duijn, M., and Lyon, P. (2013). What nervous systems do: early evolution, input–output, and the skin brain thesis. Adaptive Behavior *21*, 67–85. https://doi.org/10.1177/1059712312465330.

61. Buehlmann, C., Wozniak, B., Goulard, R., Webb, B., Graham, P., and Niven, J.E. (2020). Mushroom bodies are required for learned visual navigation, but not for innate visual behavior, in ants. Curr. Biol. *30*, 3438–3443.e2. https://doi.org/10.1016/j.cub.2020.07.013.

62. Webb, B., and Wystrach, A. (2016). Neural mechanisms of insect navigation. Curr. Opin. Insect Sci. *15*, 27–39. https://doi.org/10.1016/j.cois.2016.02.011.

63. Pansopha, P., Ando, N., and Kanzaki, R. (2014). Dynamic use of optic flow during pheromone tracking by the male silkmoth, Bombyx mori. J. Exp. Biol. *217*, 1811–1820. https://doi.org/10.1242/jeb.090266.

64. Busch, C., Borst, A., and Mauss, A.S. (2018). Bi-directional control of walking behavior by horizontal optic flow sensors. Curr. Biol. *28*, 4037–4045.e5. https://doi.org/10.1016/j.cub.2018.11.010.

65. Wystrach, A. (2021). Movements, embodiment and the emergence of decisions. Insights from insect navigation. Biochem. Biophys. Res. Commun. *564*, 70–77. https://doi.org/10.1016/j.bbrc.2021.04.114.

66. Wystrach, A., Philippides, A., Aurejac, A., Cheng, K., and Graham, P. (2014). Visual scanning behaviours and their role in the navigation of the Australian desert ant Melophorus bagoti. J. Comp. Physiol. A Neuroethol. Sens. Neural Behav. Physiol. *200*, 615–626. https://doi.org/10.1007/s00359-014-0900-8.

67. Schwarz, S., Clement, L., Gkanias, E., and Wystrach, A. (2019). How do backward walking ants (*Cataglyphis velox*) cope with navigational uncertainty? Preprint at bioRxiv. https://doi.org/10.1101/2019.12.16.877704.

68. Wystrach, A., Le Moël, F., Clement, L., and Schwarz, S. (2020). A lateralised design for the interaction of visual memories and heading representations in navigating ants (Animal Behavior and Cognition). Preprint at bioRxiv. https://doi.org/10.1101/2020.08.13.249193.

69. Heinze, S., Florman, J., Asokaraj, S., el Jundi, B., and Reppert, S.M. (2013). Anatomical basis of sun compass navigation II: The neuronal composition of the central complex of the monarch butterfly. J. Comp. Neurol. *521*, 267–298. https://doi.org/10.1002/cne.23214.

70. Sayre, M.E., Templin, R., Chavez, J., Kempenaers, J., and Heinze, S. (2021). A projectome of the bumblebee central complex. eLife *10*, e68911. https://doi.org/10.7554/eLife.68911.

71. Hulse, B.K., Haberkern, H., Franconville, R., Turner-Evans, D., Takemura, S., Wolff, T., Noorman, M., Dreher, M., Dan, C., Parekh, R., et al. A connectome of the Drosophila central complex reveals network motifs suitable for flexible navigation and context– dependent action selection. eLife 10, e66039.

72. Stone, T., Webb, B., Adden, A., Weddig, N.B., Honkanen, A., Templin, R., Wcislo, W., Scimeca, L., Warrant, E., and Heinze, S. (2017). An anatomically constrained model for path integration in the bee brain. Curr. Biol. *27*, 3069–3085.e11. https://doi.org/10.1016/j.cub.2017.08.052.

73. Le Moël, F., Stone, T., Lihoreau, M., Wystrach, A., and Webb, B. (2019). The central complex as a potential substrate for vector based navigation. Front. Psychol. *10*, 690. https://doi.org/10.3389/fpsyg.2019.00690.

74. Aksoy, V., and Camlitepe, Y. (2018). Spectral sensitivities of ants – a review. Anim. Biol. *68*, 55–73. https://doi.org/10.1163/15707563-17000119.

75. Ogawa, Y., Falkowski, M., Narendra, A., Zeil, J., and Hemmi, J.M. (2015). Three spectrally distinct photoreceptors in diurnal and nocturnal Australian ants. Proc. Biol. Sci. *282*, 20150673. https://doi.org/10.1098/rspb.2015.0673.

STAR★METHODS

KEY RESOURCES TABLE

REAGENT or RESOURCE	SOURCE	IDENTIFIER
Deposited data		
Raw data and second order data	https://github.com/ClementLe0/Data-Clement-et-al.-An-intrinsic-oscillator-underlies-visual-navigation-in-ants-Current-Biology-2022	N/A
Experimental models: Organisms/strains		
Myrmecia croslandi	N/A	N/A
Iridomyrmex purpureus	N/A	N/A
Software and algorithms		
Analysis software	R studio: https://rstudio.com/	version 3.6.2.
Model generation	Matlab® https://www.mathworks.com/	R2016b
Data extraction	Kinovea: https://www.kinovea.org/	Version -0.9.1
Other		
Computational model	https://github.com/awystrac/Neural_oscillator	N/A

RESOURCE AVAILABILITY

Lead contact

Further information and requests for resources and reagents should be directed to and will be fulfilled by the lead contact, Leo Clement (clement.leo@univ-tlse3.fr).

Materials availability

As experiments took place in the natural environment this study did not generate new unique reagents.

Data and code availability

Any data or code information required to generate this results paper is available from the lead contact upon request.

- Raw and second order data have been deposited at https://github.com/ClementLe0/Data-Clement-et-al.-An-intrinsic-oscillator-underlies-visual-navigation-in-ants-Current-Biology-2022 and are publicly available as of the date of publication. DOIs are listed in the key resources table
- All original code has been deposited at: https://github.com/awystrac/Neural_oscillator and is publicly available as of the date of publication.
- Any additional information required to reanalyze the data reported in this paper is available from the lead contact upon request.

EXPERIMENTAL MODEL AND SUBJECT DETAILS

Study Animal & Experimental site

All experiments took place within an open grassy woodland at the National Australian University, Canberra from Feb. to Mar. 2019. We had the opportunity to work with two Australian endemic ant species: *Myrmecia croslandi* and *Iridomyrmex purpureus*. *Myrmecia croslandi* workers are known to forage solitarily, with each individual either hunting on the ground in the vicinity of the nest or navigating routinely back and forth toward the same favorite foraging tree throughout her life span.[32] These ants rely mainly on learnt terrestrial visual cues to navigate but are also able to resort to PI when the visual environment does not provide guidance.[27,32–34] Eight nests of *M. croslandi*, that foraged on two distinct trees between 6.0 and 30.0 m away from the colony, were used in this study. *Iridomyrmex purpureus* ants form large colonies and forage along pheromone trails that lead to food patches. Despite employing pheromone trails for recruitment, this species also uses both learnt visual information and path integration for navigation.[35] We also performed navigational experiments with two *I. purpureus* nests to ensure that this species relies indeed on both learnt visual

terrestrial cues and path integration, which they did surprisingly well (see Figure S1). For the main experiment, a feeder was placed 7.0 m away from the nest and foragers were free to familiarize themselves with the route for 72 h before being tested.

METHOD DETAILS

Trackball system and data extraction

During tests, ants were mounted on a trackball device.[41] This device consists of a polystyrene ball held in levitation in an aluminum cup by an air flow. The trackball has two sensors placed at 90° to the azimuth of the sphere, which record the movements of this sphere and translate them into X and Y data retracing the path of the ant. The X and Y acquisition of the trackball rotations happened at a 30 Hz frequency (i.e., 30 data points per second), enabling us to reconstruct the ant's movements with high precision. Additionally, a camera (640×480 pixels) recording from above provided details of the ant's body orientation, also at 30 Hz. We also analyzed *M. croslandi* learning walks recorded directly on the natural ground. Head directions were obtained via video recordings at 25 Hz (provided by Jochen Zeil).

In this study, we used two different trackball configurations to record the ants' motor responses: further referred to as 'Free ant' and 'Fixed ant' experiments, respectively.

Free ant experiments: two small wheels prevented the polystyrene ball from rotating in the horizontal plane, however, all other degrees of freedom of the ball rotation were accessible (Figure S2A; 'closed-loop[41]'). Ants were attached on top of the ball by putting magnetic paint on their thorax and a micro-magnet fixed at the bottom end of a single dental thread that was in turn attached to a 0.5 mm pin. Crucially, the pin was placed within a glass capillary. This procedure enabled the ants to execute physical rotations on the ball (the ball is not rotating horizontally) but prevented any translational movement. Ants could thus execute body rotations and control the direction in which they faced but any attempt to go forward or backward resulted in ball rotations. We used the recorded videos to manually track the ants' body orientation through time using the free software Kinovea (v-0.9.1).

Fixed ant experiment: the two small wheels were no longer in place. Hence, the ball could now turn in any direction, including the horizontal plane (Figure S2B; 'open-loop[41]'). Ants were tethered directly to a needle with a micro magnet (glued at the end of the needle) and magnetic paint on their thorax. The top end of the needle was glued to a small piece of paper sheet (0.5×2.5 cm). Consequently, the fixed ant could no longer rotate, and the experimenter could choose in which direction individual was facing. Any attempt to move, including turning, by the ants resulted in ball rotations. This trackball configuration was only conducted with the more robust *M. croslandi*.

Free ant experiments: protocol

At the start of each test, the ant was mounted on the trackball device but surrounded by an opaque cylinder (30×30 cm) that prevented the ant from seeing any cues from the visual scenery around her. Once the ant was in place on the device, the whole apparatus was moved to the desired test location in the field. Afterward, the surrounding cylinder was removed, revealing the visual scenery to the ant and data recording began. To ensure a high level of homing motivation, only individuals who had previously received a 40% sucrose solution (for *M. croslandi*) or a food item (for *I. purpureus*) were tested. The recording period was 3.5 min for the robust *M. croslandi* and 1.5 min for the flimsier *I. purpureus*.

To test the impact of terrestrial visual cues on the oscillation behavior, ants were tested under three distinct conditions.

Familiar (F): ants were tested along their habitual route, which therefore presents a familiar visual view.

Unfamiliar (U): ants were tested at least 50 m away from the habitual route, which therefore presents an unfamiliar panorama.

Dark (D): ants were tested in total darkness, within an opaque cylinder (30×30 cm) covered with a red Plexiglas plate that transmitted only the low red wavelengths, which ants cannot perceive.[74,75]

To test the impact of PI on oscillation behavior, ants were tested as either full- or zero vector ants. Full vector (FV): ants were caught at the start of their inbound trip to the nest (i.e., at the foraging tree for *M. croslandi* and at the feeder for *I. purpureus*). FV ants have an informative homing PI vector, which points in the food-to-nest compass direction. Consequently, FV ants can rely on both PI vector and the learnt visual scenery while being tested. Zero vector (ZV): homing ants were captured just before entering the nest, that is, at the end of their inbound trip. Hence, their PI homing vector is reduced to zero and thus no longer directionally informative. Consequently, ZV ants can only rely on the learnt visual scenery while being tested. For each of the three visual conditions FV and ZV ants were tested, resulting in a total of six conditions.

For *I. purpureus*, at least 16 ants were tested in each of the six conditions (F: FV&ZV =16; U: FV&ZV =17; D: FV=16 & ZV=17). Since *I. purpureus* forms very populous colonies with an abundance of foragers, all individuals were tested only once, in one of the six conditions. The data obtained are therefore statistically independent. On the contrary, *M. croslandi* forms sparsely populated colonies and individuals usually make only one foraging trip per day.[32] Thus, it is time-consuming and challenging to capture, mark and follow individuals throughout foraging trips. Individuals were therefore captured (either at the foraging tree (FV) or before reaching their nest (ZV)) and tested successively in a pseudo-random order in all three visual panoramas: Familiar (F), Unfamiliar (U) and in the Dark (D). Both the sequence in which the visual conditions were experienced and the individuality were included in the statistical models as it is likely that the state of the PI vector will be modified across successive tests. Overall, 32 *M. croslandi* ants were tested with some individuals tested as ZV or FV ants on two different days. At least 16 *M. croslandi* ants were tested in each of the six conditions (F: FV&ZV =17; U: FV&ZV =17; D: FV=17 & ZV =16). Overall, 101 recordings were obtained.

In the 'free ant' experiments, the ant's body axis can turn without the ball movement. We used the recorded videos to manually track the ants' body orientation through time using the free software Kinovea. We removed the first 3s of recording of each ant as the removal of the opaque ring may have disrupted the behavior. Overall, the analyzed recording length was 100s (except for two ants: 84 and 99s) for *M. croslandi* individuals and 50s (except for two ants: 49s) for *I. purpureus* ants. For details of the Fourier analysis (see below); nine paths of *I. purpureus* were discarded (F FV=1, U FV = 1, U ZV =2, D FV =2, D ZV = 3) as the ants displayed too many pauses.

Fixed ant experiments: protocol

To test if oscillations are due to an intrinsic oscillator or caused by the fact that ants try to keep a bearing toward an external stimulus, we conducted an additional experiment on *M. croslandi* ants. We recorded foragers without an informative integration vector (ZV) in the same unfamiliar environment (U) as before. Ants were tested in eight different fixed orientations, covering the 360° azimuth by bins of 45°; and with one direction corresponding to the food-to-nest compass direction. Each ant was tested in all eight orientations in a pseudo-random sequence. To change the ant's orientation, the experimenter would first place the opaque cylinder (30×30 cm) around the trackball system to prevent the ant from perceiving the visual panorama, then rotate the whole set-up (trackball and mounted ant) and finally remove the opaque cylinder to re-start data collection. Ants were recorded for at least 15s up to 20s in each orientation. Eleven ants were tested in all eight orientations. Since the ants were fixed, trackball rotations along the horizontal axis provided a direct measure of the angular velocity of the attempted turn generated by the ant. Angular velocity time series were then extracted from the trackball data. At the end, the available length of the recordings for the analysis had 512 frames (~17s) except for 5 individuals (294,394,456,474,494 frames). It should be noted here that prior to the Fourier analysis (see below) we added a series of 0s (zero padding) at the end of the time series until it had a length of 3000 data points to match the same recording length obtained in the free ant experiment). This permits to increase the precision in the frequency range obtained from the Fourier analysis.

QUANTIFICATION AND STATISTICAL ANALYSIS

All statistical analyses have been run using the free software R (v 3.6.2. R Core Development Team). For all statistical tests, the p-values were compared to the critical alpha risk at 0.05, with the appropriate correction if needed. Statistical parameters mean and the associated standard error is given within the text and/or on figures: n represents the number of individuals (sample size).

Fourier analysis

To reveal the occurrence of regular lateral oscillations, we choose to focus on the angular velocity value (Figure S2C), which constitutes a direct reading from the left/right motor control. This time series was processed through three successive steps to obtain its 'spectral density', according to the Wiener-Khinchin theorem. First, the signal was parsimoniously smoothed with a moving median running of a length of five frames (0.17s) to reduce the influence of the recording noise (Figure S2D, dashed blue line). Then, the recorded time series was passed through an autocorrelation function (Figure S2D). Finally, a Fourier transform was performed on these autocorrelation coefficients, providing the power spectral density (Figure S2E). With this approach, the magnitudes obtained are independent from angular drift and amplitudes of the oscillations and thus can be directly compared across individuals. A high magnitude indicates a strong oscillation for a given frequency. For each individual, the dominant frequency (i.e., presenting the highest peak magnitude) and its magnitude were extracted (Figure S2E, dashed blue lines). To check whether these magnitudes indicate a significant regular oscillation, we compared them to the average spectral density magnitude resulting from 200 Gaussian white noise signals of the same length (within each species and experiment). Gaussian white noise signals were obtained by drawing a sequence of random values drawn from a normal law. These simulated signals were then processed through the exact same operations as the ants' angular velocity recording: namely smoothing, autocorrelation, Fourier transformation and extraction of the highest peak magnitude. The mean of the 200 highest magnitudes obtained was then compared to the real ants' equivalent magnitudes with a Wilcoxon one-tail test. As each experimental group has been compared with this mean magnitude of the simulated angular velocity signal, the p-value is subsequently adjusted using the Bonferroni correction.

Average oscillatory cycle

To extract the average dynamics of an oscillation cycle, the mean cycles at the individual and population levels were reconstructed as follows. First, we smoothed the angular velocity time series of each individual by running twice a median with a window length of 31 frames for *M. croslandi* (for both free and fixed experiments), 25 frames for data during learning walks on the natural ground and seven frames for *I. purpureus*. This window length is much smaller than one oscillatory cycle and thus smoothens the data without altering the cycle general dynamics (Figure S2F). Second, we indexed moments when the time series crosses 0 (from – to +) as t_0; and extracted data within a window of ±90 frames around the t_0 indices (±60 frames for *I. purpureus*; Figure S2F). We then reconstructed a mean cycle for each individual by averaging the individual's extracted windows, aligned at t_0 (Figure S2G). The individuals' average forward speed dynamics during one cycle was obtained in the same way by using the same indices t_0 obtained from the angular velocity data (Figure S2H). For each ant, the mean angular velocity peak and amplitude of forward velocity cycles were extracted for analysis. Finally, we reconstructed the average cycle at the level of the population by averaging the mean cycle of all individuals. Note that to do so, each individual's mean cycle was first normalized to show similar amplitudes (mean_cycle_normalised = mean_cycle/mean|mean_cycle_values|). The goal was here to observe the cycle dynamics through time and not to estimate the inter-individual variation in amplitude, which was analyzed previously using the individual's mean cycle amplitude. Note that the criterion used to align the time series (the

change from a left to a right turn) necessarily creates an artefact in the averaged angular velocity obtained. Namely, an average change from left turn to right turn at t_0. However, several factors indicate the relevance of such pooling at the population level: (1) the period of the average cycle corresponds to the mean frequency obtained from the Fourier transform. (2) we can observe a significant reversal of the angular velocity before and after the mean oscillation cycle. (3) the associated forward velocities co-vary in a significant way, indicating the existence of conserved dynamics.

Analysis of the ants' direction of movement

We reconstructed the ant paths of time that derived from the trackball recording for a fixed period to determine the mean direction of movement (mu) as well as the mean circular vector length (r, a measure of dispersion) of each individual. The mean directions (mu) were analyzed using a Rayleigh test (from R package: Circular) that also includes a theoretical direction (analogous to the V-test). To test whether the angular data are distributed uniformly as a null hypothesis or if they are oriented toward the theoretical direction of the nest as indicated by the state of the PI or the familiar panorama, the average vectors lengths (r) were analyzed via a Wilcoxon-Mann-Whitney test with a Bonferroni correction for multiple testing.

Analysis of optimization

To investigate the benefit of variation of forward and angular velocities signal on the overall ground distance covered we reconstructed for each individual a fictive path where forward speed was maintained constant (we took the average forward speed, so that the total distance walked remain the same as in the original path). To estimate the overall ground distance covered for a given path, we computed a 'global trajectory' by smoothing the path with a sliding window, until effectively removing the oscillations component (Figure 4B grey paths). To estimate the actual benefit of variation of forward speed on the distance covered, we compared the length of the 'global trajectories' between the fictive path (with constant forward speed) and original path (Figures 2D and 2E). A ratio >1 mean that the original path covered more ground distance, and vice versa. Ratios were compared with Wilcoxon one-tail test to the threshold one.

To test for an effect of the familiarity and vector on the distance covered we calculated an 'Effectiveness ratio' for each individual as the ratio between the length of the 'global trajectory' / 'actual distance walked' on the original paths with oscillations (Figures 2D and 2F). To enable a fair comparison across individuals, we computed the ''effectiveness ratio'' on a 100s portion of paths, using an additive mixed model.

Statistical models

For the free ant experiment, two types of models were tested: the first considering the interaction between visual panorama and vector modalities, the second with simple additive effect. It should be noted here that in case of deviation of the residuals of these models from normality and or homoscedasticity, the response variables have been transformed. Only the model presenting the lowest Akaike information criterion (AIC) was retained and subsequently analyzed via an analysis of variance (Anova), followed by a post-hoc analysis of Tukey's rank comparison. Finally, for *M. croslandi* whose individuals were tested across several conditions, the models are mixed models that controlled the sequence and the individuality effect as random variable. For some models, we removed the sequence effect because of a singularity problem of this factor (i.e., the information given by this variable is already contained in other variables). For fixed ant experiments (which were tested only as ZV ants in an unfamiliar environment), the model analyzed the effect of the condition of the subsequent rotations.

COMPUTATIONAL MODEL

The computational model presented in Figure 5 has been built and run using Matlab® R2016b. The code is open access and available at: https://github.com/awystrac/Neural_oscillator

It is a step-based model ('For loop'). Two neurons (Left and Right neurons) reciprocally inhibit each other, while trying to maintain a baseline activity through self-excitation and internal feedback.

Variable	Description
L	Left neuron activity
R	Right neuron activity
LNF	Left neuron internal feedback
RNF	Right neuron internal feedback

Parameters	Description
W	Reciprocal inhibition synaptic weight
Baseline	Firing rate of the oscillator neurons without any external modulation (default at 0.5)

(*Continued on next page*)

Continued

Parameters	Description
Exhaust rate	Rate at which the negative internal feedback is modulated between each time step
Noise	Standard error of the normal distribution of the noise added to the activity of the neurons of the oscillator (default at 0.1)

Initialization

$RNF_1 = 0$
$LNF_1 = 0$

At each time step

$$L_{t+1} = L_t - LNF_t - (R_t \times W) + (random(-1 \text{ to } 1) \times noise)$$

$$R_{t+1} = R_t - RNF_t - (L_t \times W) + (random(-1 \text{ to } 1) \times noise)$$

Set a hard limit to the activity both neurons

$$R_1 = \text{random (0to1)}$$

$$L_1 = \text{random (0to1)}$$

L and R neuron update their activity due to their self-excitation, internal feedback, inhibition from the other neuron, and noise.

$$LM_{t+1} = \begin{cases} L_{t+1} & \text{if } L_{t+1} > 0 \\ 0 & \text{if } L_{t+1} \leq 0 \end{cases} \quad RM_{t+1} = \begin{cases} RM_{t+1} & \text{if } R_{t+1} > 0 \\ 0 & \text{if } R_{t+1} \leq 0 \end{cases}$$

Update the internal negative feedback for the left and right motor neurons. The internal feedback changes proportionally to the difference between its own activity and the neuron activity (relative to the baseline activity)

$$RNF_{t+1} = RNF_t + \text{Exhaust rate} \times (R_{t+1} - RNF_t - \text{Baseline})$$

$$LNF_{t+1} = LNF_t + \text{Exhaust rate} \times (L_{t+1} - LNF_t - \text{Baseline})$$

Computation of the angular and forward velocities

$$\text{Angular\_velocity} = R - L$$

$$\text{Foward\_velocity} = R + L$$

Appendix II: Other formatted publication which I contributed.

Compensation to visual impairments and behavioral plasticity in navigating ants

Sebastian Schwarz[1], Leo Clement[1], Lars Haalck[2], Benjamin Risse[2] and Antoine Wystrach[1]

[1]Centre de Recherches sur la Cognition Animale, CNRS, Université Paul Sabatier, Toulouse 31062 cedex 09, France

[2]Institute for Informatics, Computer Vision and Machine Learning Systems, University of Münster, 48149 Münster, Germany

Address of correspondence:
Sebastian Schwarz
Université Paul Sabatier
Centre de Recherches sur la Cognition Animale, CNRS
31062 Toulouse
Email: sebastian.schwarz@gmail.com
Phone: +33561558444

Keywords: compound eye; desert ants; insect vision; monocular; navigation; orientation; route-following

Abstract

Desert ants are known to rely heavily on vision while venturing for food and returning to the nest. During these foraging trips, ants memorize and recognize their visual surroundings, which enables them to recapitulate individually learnt routes in a fast and effective manner. The compound eyes are crucial for such visual navigation; however, it remains unclear how information from both eyes are integrated and how ants cope with visual impairment. Here we manipulated the ants' visual system by covering one of the two compound eyes and analyzed their ability to recognize familiar views in various situations. Monocular ants showed an immediate disruption of their ability to recapitulate their familiar route. However, they were able to compensate for the visual impairment in a few hours by restarting a route-learning ontogeny, as naïve ants do. This re-learning process with one eye forms novel memories, without erasing the previous memories acquired with two eyes. Additionally, ants having learnt a route with one eye only are unable to recognize it with two eyes, even though more information is available. Together, this shows that visual memories are encoded and recalled in an egocentric and fundamentally binocular way, where the visual input as a whole must be matched to enable recognition. We show how this kind of visual processing fits with their neural circuitry.

Significance Statement

If humans look at the world with both eyes, they have no problem to then recognize it with one eye only, and vice-versa. Thus, our way of encoding the world is robust to changes of the visual field. Yet ants do so very differently. Views learnt with two eyes can only be recognized with two eyes, and views learnt with one eye can only be recognized with one eyes (the same eye). However, this rigidity is compensated by a remarkable behavioral flexibility. Upon covering one eye, ants – which can no longer recognize their familiar surroundings – will restart a learning process to store these novel visual inputs in a parallel memory and resume their normal foraging activity.

Introduction

Self-organized living beings and engineered machines are both able to fulfill their tasks reliably. However, living organisms show flexibility in the way they achieve their functions and can often compensate for unexpected impairments, whereas machines cannot (1). The aptitude for compensation has been well-studied in human with regards to impairments such as cognitive

pathologies, aging or brain damage (2, 3), and is evident after morphological impairments, such as when one manages to achieve with one hand what one used to do with two. These forms of compensations require time and likely involve neural rewiring, so-called structural or network plasticity (4, 5)

In insects, which are often assumed to be less versatile than vertebrates (6, 7), the ability to compensate for impairments is usually studied as an instantaneous response and viewed as the product of the evolved natural redundancy and robustness of these systems, rather than the result of neural plasticity through a life time. For instance, the instantaneous change in gait following a single our double leg amputation may be interpreted as a robust and 'spontaneous' response of the neural machinery governing leg coordination (e.g., in ants (8), cockroaches (9), stick-insects (10) and other arthropods like crabs (11)). Robustness through redundancy in insects is also well-appreciated in the context of navigation. For instance, representation of directions is based on the integration of a vast array of sensory cues such as visual terrestrial cues (12-15), multiple celestial cues (16-20), olfactory cues (21, 22), wind cues (23, 24), magnetic cues (25, 26) and also self-motion cues (27). Hence, depriving a navigating insect from one modality – or all modalities but one – does not necessarily disrupt their ability to orient. Unilateral suppression of one eye input, however, has a direct impact on the navigational performance of ants (28, 29). Monocular ants may still show evidence of recognition of learnt terrestrial cues but their navigational behavior is drastically affected, revealing an intriguing mix between flexibility and rigidity (28, 29). For instance, monocular desert ants that have learnt a landmark array with one eye only are incapable of recognizing it if the eye cap has been swapped to the other eye, suggesting that there is no inter-ocular transfer of visual terrestrial cues (28). Here again, these studies focused on the insects' response that immediately follows the manipulation. But whether some plastic, compensatory mechanisms are at play, and given time, can enable a recovery of a functional behavior remains unknown.

Here, we investigated this question by conducting various eye-capping manipulations on visually navigating desert ants (*Cataglyphis velox*). Both, their immediate response as well as the potential compensatory effects emerging after a longer period of time were observed and analyzed. The results show that visual manipulations via eye-capping caused substantial impairments that disrupt the ant's ability to home. However, a few hours upon the visual impairment, ants recovered a functional navigation behavior, indicating the existence of a profound plasticity and behavioral flexibility. We explored the mechanisms underlying this plasticity and, as a corollary, gained insight into the way visual information is stored in their brain.

Results and Discussion

One-eye-capping disrupt learnt route-following. Iberian desert ants (*Cataglyphis velox*) were individually marked and let free to navigate back and forth along an 8.0 m long route between their nest and a feeder (Fig. 1A). The surrounding natural landscape provided plenty of visual information and the route floor was covered with a 1.2 m wide wooden board ensuring an even substrate for the navigating ants. Once experienced to the route (after at least 10 foraging trips), ants were captured at the feeder one by one for the eye-cap treatment: either their left or right compound eye was covered with opaque paint. The eye-capped ant was then provided with a food item, released near the feeder and her homing path was recorded. Regardless of the side of the eye cap, ants failed to navigate directly toward their nest. Instead, their initial direction showed a bias toward the side opposite to the eye cover (Fig. 1B) as previously reported in Tunisian desert ants (28). All eye-capped ants (10 out of 10) veered sidewise and fell off their usual route corridor, defined by the wood plank on the floor (Fig. 1A). To enable them to reach home, ants falling off the wood boards were systematically captured and re-released back onto the route beeline (Fig. 1A, dashed line) where path recording resumed. Eye-capped ants veered off the boards 3.42 times on average before reaching their nest surrounding, where recording was stopped (Fig. 1A, Fig. SI1). The difficulty to head home was obvious along the complete homing path (Fig. 1A). By comparison, Sham ants, which received a paint mark on the head but untouched compound eyes and ocelli, showed clearly oriented (Fig. 1B) and much straighter paths (Fig. 1A, Fig. SI1) and almost never left their route corridor (1 out of 17 ants fell one time, so a probability of 0.06 time/ants on average). Thus, covering one compound eye drastically affects navigation in homing ants.

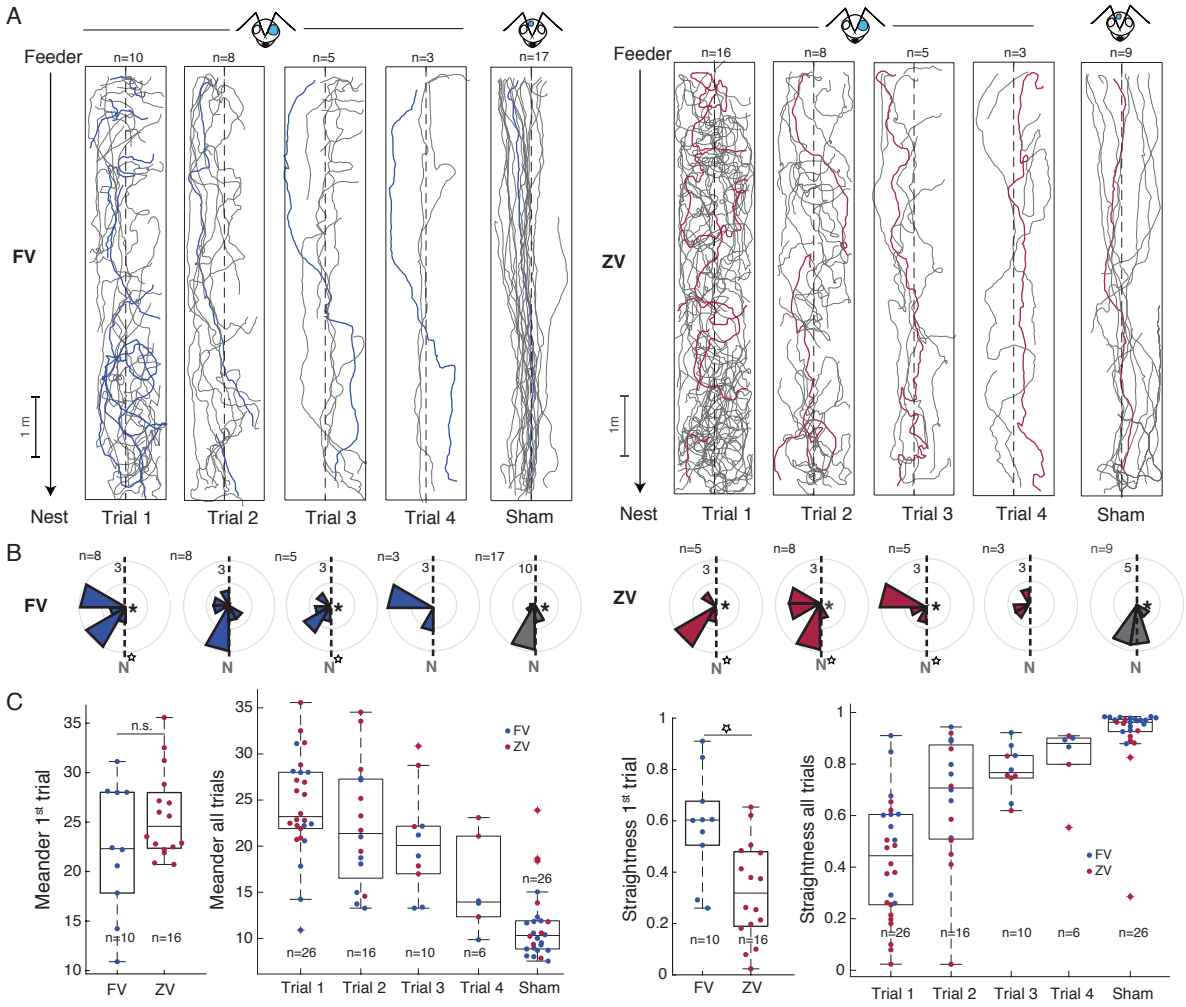

Fig. 1. Initial side biases of homing paths in eye capped ants. Black arrows: travel direction of eye capped ants from feeder to nest along a straight foraging route; dashed line: middle of the foraging route; grey lines: ant paths, gaps between paths occurred when ants ran off the board and were re-released in the middle of the homing route; ant head sketch: eye cap condition (this applies to all other Figures). Left- (LEC) and right (REC) eye capped ants were pooled. Paths of REC ants were mirrored and depicted as LEC ants (painted blue eye in ant head). (A) Homing paths from trial 1 to 4 in full vector- (FV) and zero vector ants (ZV) together with homing paths of Sham ants with uncovered eyes. Side biases in paths are visible in both FV (blue example paths) and ZV (red example paths) ants but not in Sham controls. (B) Dashed line: feeder nest direction; number at the outer rim of diagrams: number of ants per sector. Circular histograms depicting directional distribution of ant's paths after 0.2 m of travel across trials and condition. Significant differences from random distributions are indicated with a star (Rayleigh test) at the center of the diagrams and significant differences from the nest direction (N) are indicated with and open star (S-test, for statistical details see Table S1). (C) Meander and straightness of ant paths across trails and condition. FV and ZV vector ants differ significantly in the level of straightness in their first homing path but not in the level of meander. With increasing trial number both FV and ZV paths resemble more Sham paths with low meander and high level of straightness.

The compound eyes of ants extract information from both, celestial compass cues — which are key for path integration (PI) — and terrestrial cues — which are key for learnt views during route-following (30). To test whether the behavioral defect observed in eye-capped ant is due to a disruption of the PI system or the use of learnt views, the experiment was repeated by using this time so-called zero-vector (ZV) ants. While full-vector (FV) ants are captured at the feeder, ZV ants were captured on their way home just before entering their nest, then received an eye-cap and were released with their food item right near the feeder. The PI vector of a ZV ant does no longer point toward the nest; hence the ant can solely rely on learnt terrestrial cues for homing (31).

As for FV ants, covering one eye of ZV ants strongly disrupted their ability to navigate home (Fig.1A). Their initial directions were also biased toward the open eye side (Fig. 1B) and all of them (16 out of 16) repeatedly ran off their usual route corridor (4.43 times/ant on average) to the contrary of ZV sham ants (0.33 times/ant on average). Their overall paths were significantly less straight (Anova: $F_{1,24} = 10.7$, $P = 0.003$) but only marginally more meandrous (Anova: $F_{1,24} = 2.42$, $P = 0.133$; Fig.1C) than eye-capped FV ants. Consequently, eye capping strongly impairs the use of learnt terrestrial cues and the directional input provided by the PI is helping only slightly the FV eye-capped ants to maintain straighter paths. This is in line with previous evidence that information based on celestial but not terrestrial compass cues undergoes inter-ocular transfer (28).

Eye-capped ants spontaneously recover their route-following behavior. Surprisingly, within a few hours, some of the tested eye-capped ants reoccurred at the feeder again, which provided the opportunity to record their subsequent homebound trips. With increasing homing trials, eye-capped ants gradually recovered their navigational efficiency (Fig. 1). To ensure this recovery was not simply due to an increased reliance on PI, eye-capped ants reaching their nest were captured as ZV ants and released again at the feeder for a second run home. Whether as FV- or ZV ants, their initial direction upon release still tended to be biased toward the open eye side until the 3rd homing trial (Fig. 1B; see Table S1 for circular statistics). However, both FV- and ZV paths showed progressively less local meander (Anova: $F_{0.1,49.4} = 25.170$, $P < 0.001$) and more overall straightness (Anova: $F_{1.1,51.3} = 32.52$, $P < 0.001$; Fig. 1C). During the 4th homing trial the path straightness of eye-capped ants resembled the one from the sham ants (Anova: $F_{1,30} = 2.68$, $P = 0.112$), and even though they still showed slightly more local meandering (Anova: $F_{1,30} = 5.39$, $P = 0.027$; Fig. 1C), most eye-capped foragers (5 out of 6) managed to home while no-longer exiting their route corridor. Within a relatively short time period, eye-capped ants

can thus recover the ability to follow their familiar route again, using terrestrial cues. These insects are therefore able to compensate impressively fast the strong impairment caused by losing the visual input of one eye, showing a remarkable plasticity in their navigational capacities.

Eye-capped ants show a persistent lateralized sensory-motor defect. The fact that the initial direction of both FV- and ZV ants upon eye-covering was biased toward the open eye side as compared to the correct route direction (Fig. 1B) provides two insights. First, because ZV ants did not head randomly (or backtracked) like they do on visually unfamiliar terrain ((32), Fig. 2B), freshly eye-capped ants must still be able to derive some information from their visual route memory. Second, because the side of the directional bias depends purely on the side of the capped eye (Fig. 2A, C), a lateralized sensory-motor defect caused by losing one-eye input might be at play.

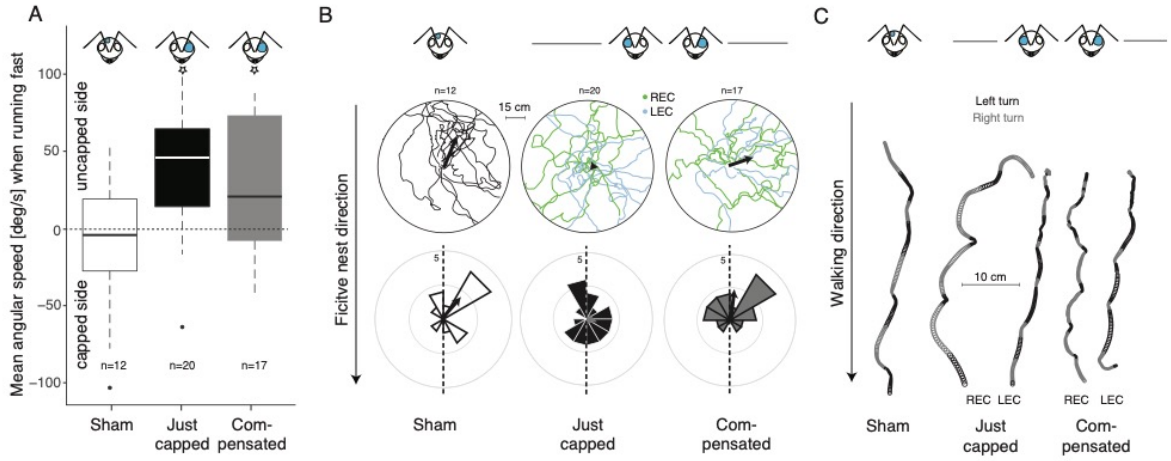

Fig. 2. Initial side bias in eye-capped ants released in unfamiliar surroundings. (A) Distribution of side preferences of ants with just capped eyes (Just capped) and ants that had compensated (Compensated) for the visual impairment in their familiar foraging route. The characteristic motor deficit, displayed by capped ants toward the side bias of the uncapped eye is evident in Just capped ants, as represented by the higher mean angular speed when turning to the uncapped eye side. Compensated ants show a lower side bias and resemble more the even distribution of Sham ants. Stars indicates significant difference to random, one-sided Wilcoxon test (see text for details). (B) Tracked paths of Sham, Just capped and Compensated ants (upper panels) and initial (60 cm radius) heading directions (lower panels). Black arrows depict mean heading directions. (C) Example paths of ants with (Just capped, Compensated) and without (Sham) the characteristic motor deficit caused by eye-capping.

To investigate this lateralized sensory-motor defect independently of the expression of the recognition of visual memories, freshly eye-capped ants were released in unfamiliar surroundings and their behavior was analyzed based on video recordings. Eye-capped ants tended to regularly alternate between brief bursts of speed when turning toward the open eye

side and pauses by rotating on the spot toward the covered eye side (Fig. 2C). This can be simply quantified by assessing whether turning direction is biased on one side when the ants forward speed is above the individual's average. While sham ants with both eyes open showed no bias (Sham ants: one-sided Wilcoxon test: V = 32, P = 0.715, Fig. 2A) freshly one-eye capped ant turned more toward the open eye when walking fast (Just-capped ants: one-sided Wilcoxon test: V = 188, P = 0.001; Fig. 2A).

To test whether the observed recovery of route-following behavior is due to a compensation over time of such a lateralized sensory-motor defect, we tested whether the bias persisted in ants after they had recovered their route-following behavior with one eye. Eye-capped ants that had recovered their route still displayed the lateralized defect on unfamiliar terrain (Compensated ants: one-sided Wilcoxon test: V = 113, P = 0.044, Fig. 2). We noted that, given longer period of time with the eye cap, this bias eventually tended to fade (data in preparation) showing the ability of experienced ants to also correct for such a sensory-motor defect. However, the persistence of the lateralized bias here (Fig. 1, 2) shows that the ant's route recovery is due to a process that is quicker and different from overcoming such a sensori-motor defect. Also, this longer lasting sensori-motor defect may explain why one-eye ants having just recovered their route still showed more meandering than sham ants (Figure 1).

Eye-capped ants compensate by re-engaging in a new route ontogeny. We next investigated whether the recovery of route-following behavior in eye-capped ants is based on the ability to eventually recall previous binocular memories, or alternatively, based on the formation of novel, monocular route memories. To do so, we covered the left or right eye of a new cohort of experienced, individually marked ants, and released them back to their nest. Their behavior was recorded once they emerged outdoors again. Upon leaving their nest entrance these freshly eye-capped ants behaved remarkably similar to naïve foragers exiting their nest for the first time: they displayed typical learning walks (Fig. 3). These convoluted paths and pirouettes enable them to expose their gaze in multiple directions for visual learning (33). Learning walks are likely a consequence of perceiving an unfamiliar scenery when leaving the nest. Indeed, experienced ants may also display a few zigzags and pirouettes upon departure if an alteration of the visual surrounding has occurred around the nest; but in general, they rapidly scoot along their familiar outbound route again (33, 34). Here, the eye-capped ants remained at first very close to the nest and re-entered their colony often, like naïve ants do (Fig. 3C). They displayed on average more than 15 subsequent learning trips before reaching the familiar feeder located 5.0 m away (Fig. 3A, B) supporting the idea that the scenery appeared strongly unfamiliar to

these eye-capped ants. Interestingly and contrary to naïve ants, learning walks of freshly eye-capped ants were biased toward the feeder direction (Fig. 3A); this was true from the first learning walks onward (Fig. 3C, One-tailed T-test: $P = 0.019$) indicating that previous memory of the feeder direction persisted despite the eye-cover. Whether this directional memory was due to remnant memories of terrestrial cues learnt with both eyes, or the expression of a stored food-ward celestial compass vector (35, 36) could not be disentangle here.

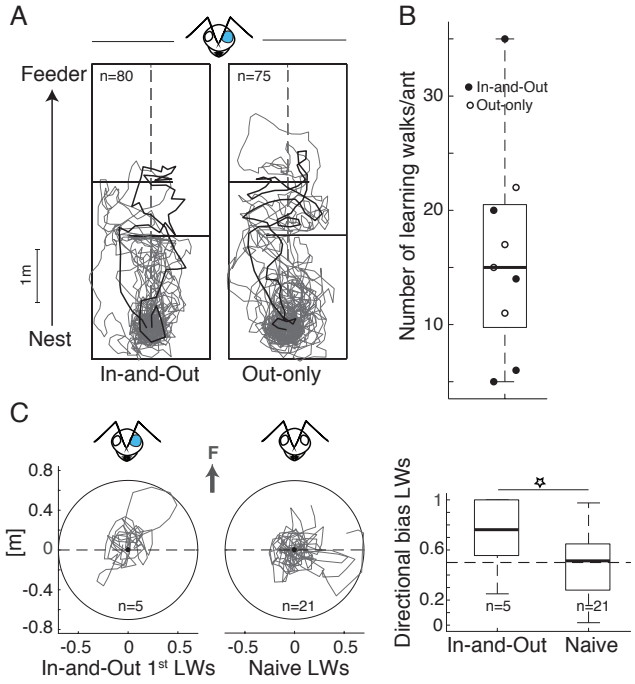

Fig. 3. Learning walks (LWs) in eye capped ants. Horizontal lines: one-way baffles on the foraging route that could be traversed during outbound trips but had to be negotiated during inbound trips (this also applies for Figs. 4 and 5). (A) LWs displayed by In-and-Out and Out-only ants during training. Black bold lines: example paths. (B) Distribution of the number of LWs in In-and-Out and Out-only ants. (C) Comparison between directional path bias of first LWs in In-and-Out and naïve ants. In-and-Out ants show a significantly higher bias toward the feeder direction (grey arrow) than naïve ants.

The subsequent out- and inbound (i.e., homing) trips of these eye-cap ants were also recorded, which, as expected, showed gradual improvements (Fig. SI3 and SI4). After 8 successful trips between the nest and feeder, all the recorded eye-capped ants (In-and-Out) had fully recovered their ability to run between the nest and the feeder without colliding into baffles (Fig. 4A). Tested as ZV ants, these individuals could home equally well, (Fig. 4A) showing as previously, that they used terrestrial cues.

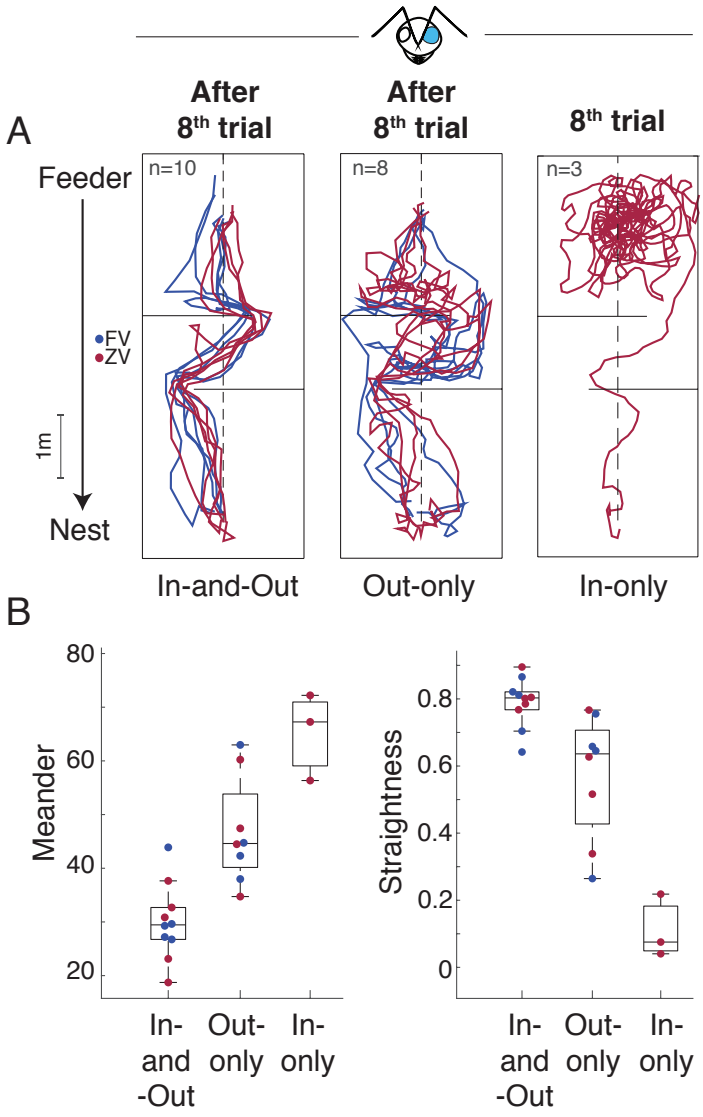

Fig. 4. Paths and path characteristics of eye capped ants after compensation with in and outbound trip (In-and-Out), no inbound trip (Out-only) and no outbound trip (In-only). (A) Paths of homing ants after 8 training trials. All In-and-Out and Out-only ants were able to home whereas In-only ants struggled and only one individual succeeded. (B) Meander and straightness of homing paths after 8 training trials. In-and-Out ants displayed paths with the lowest meander (Anova: In-and-Out vs. Out-only: $F_{0.29,0.07} = 4.122$, $P = 0.001$; In-and-Out vs. In-only: $F_{0.63,0.11} = 5.981$, $P < 0.001$) and highest level of straightness (Anova: In-and-Out vs. Out-only: $F_{-0.02,0.06} = -3.436$, $P = 0.003$, In-and-Out vs. In-only: $F_{-0.69,0.09} = -7.327$, $P < 0.001$), followed by Out-only and In-Only ants.

To ensure that this recovery was actually due to performing learning walks, and not simply due to the time passed while navigating outdoors, the experiment was replicated by using two additional cohorts of freshly eye-capped ants that had previous experience (with both eyes) of the route. In one group (In-only), eye-capped ants were systematically captured upon exiting the nest and released at the feeder for homing, preventing them to display learning walks around the nest and outbound trips to the feeder. In the other group (Out-only), eye-capped ants

were free to display learning walks but upon reaching the feeder, these ants were systematically captured and released inside their nest entrance, preventing them to perform their homing runs (inbound trips). This latter group of ants (Out-only) displayed similar learning walks than the previous condition (Fig. 3), and after 8 successful outbound trials up to the feeder, foragers were able to home quite well, albeit not as successful as ants that had experienced both out- and inbound trips (Fig.4 and Fig. SI3). This shows that inbound trips are helpful but not crucial for route recovery. Contrastingly, ants deprived of learning walks (In-only) showed no improvement in their homing ability despite spending a long time navigating outdoor (Fig. 4). On the contrary, they showed a decrease in homing performance across trials (Fig. SI3), suggesting again that freshly eye-capped ants have strongly impaired but remnant binocular visual memories of the route, but that subsequent experience outdoor does not enable to re-access them, or form new functional ones. Note that In-only ants, as being transferred from the nest to the feeder, could not rely upon path integration. After eight attempts of homing without learning walks, these ants searched at length around the release point (feeder) and only one individual eventually managed to home (Fig. 4). It was rather difficult to conduct this condition, as In-only ants mostly failed to reach their nest during training. After 10 min of search and an unsuccessful inbound trip the foragers had to be put back manually to the nest. Unfortunately, many of those individuals stopped their foraging activity and hence could not be tested anymore.

In sum, performing learning walks and outbound trips is crucial for eye-capped ants to recover their route. This echoes what is observed in naïve ants with untouched eyes, for whom learning walks and outbound trips are key for learning an inbound route, while inbound experience may help but seems to be insufficient on its own (37-41). Together, this suggests that eye-capped ants cannot recognize the learnt route with both eyes to full capacity and thus perceive at first the world as quite unfamiliar. This unfamiliarity triggers learning walks upon leaving their nest, which enables them to form novel memories of the terrestrial cues and eventually re-learn the route monocularly. Therefore, ants with previous experience possess the flexibility to recapitulate the natural ontogeny of route learning for a second time.

Ants learn binocular visual memories. Previous behavioral work in ants and bees has shown that visual memories learnt with one eye cannot be retrieved using the other eye, suggesting that these insects form two separated visual memories for each eye, with an absence of inter-ocular transfer between these visual memories (28, 42). The current study revealed that visual memories acquired with both eyes cannot be retrieved with one eye. Rather than two separated

visual memories for each eye, one possible explanation is that visual memories are fundamentally binocular, that is, their recall implies the correct and simultaneous combination of both left and right visual input. Indeed, neurobiological studies show that each eye sends bilateral visual projections to the Kenyon cells (KCs) in both the left and right hemispheres of the mushroom bodies (MBs)(43), where visual memories for route-following are formed (44-46). What's more, visual projection to the KCs are pseudo-random, therefore, it seems quite likely that individual KCs, whether in the left or right hemisphere, receives input from both eyes, and thus must receive the correct bilateral input to be activated (Fig. 6). If this hypothesis is correct, it predicts, rather counterintuitively, that memories acquired with one eye could not be retrieved with both eyes.

To test this prediction, a novel cohort of ants from a new nest was eye-capped either on the left or the right eye. Crucially, the training to the foraging route and the transformation of the visual scenery by clearing the floor and altering the natural bushes and other terrestrial cues around the route was done afterward. The set-up was similar to the former experiment: a 5.0 m long route containing two baffles in the middle and one feeder at the end. These ants had binocular memories of the previous natural surroundings but experienced the foraging route and its novel surroundings only with an eye-cap (i.e., monocular). After a few hours, the eye-capped ants were familiarized with the new surroundings, discovered the feeder and learnt to home successfully along the novel route (Fig. 5A). When captured at the nest and released again as ZV ants near the feeder, these now experienced eye-capped foragers had no difficulties to recapitulate the route, confirming that they had formed (monocular) visual memories of the terrestrial cues (Fig. 5A, left panel). However, when uncapped, that is, when exposed for the first time to this particular route with two eyes, the ants struggled immensely to home (Fig. 5A, right panel). All uncapped ants searched predominantly in the upper section of their foraging route incapable of negotiating the baffles, only 2 out of 10 eventually managed to reach the nest entrance (Fig. 5A, right panel). Even when some (5 out of 10) of these ants were re-released beyond the baffles, closer to the nest, they were not able to home successfully and wandered around seemingly without purposeful orientation (paths not shown). Thus, ants with two eyes were unable to recognize the route learnt with one eye. In other words, adding the visual input of the second eye prevents the access to the visual memories acquired with one eye only. Therefore, when it comes to navigation, visual memories are binocular.

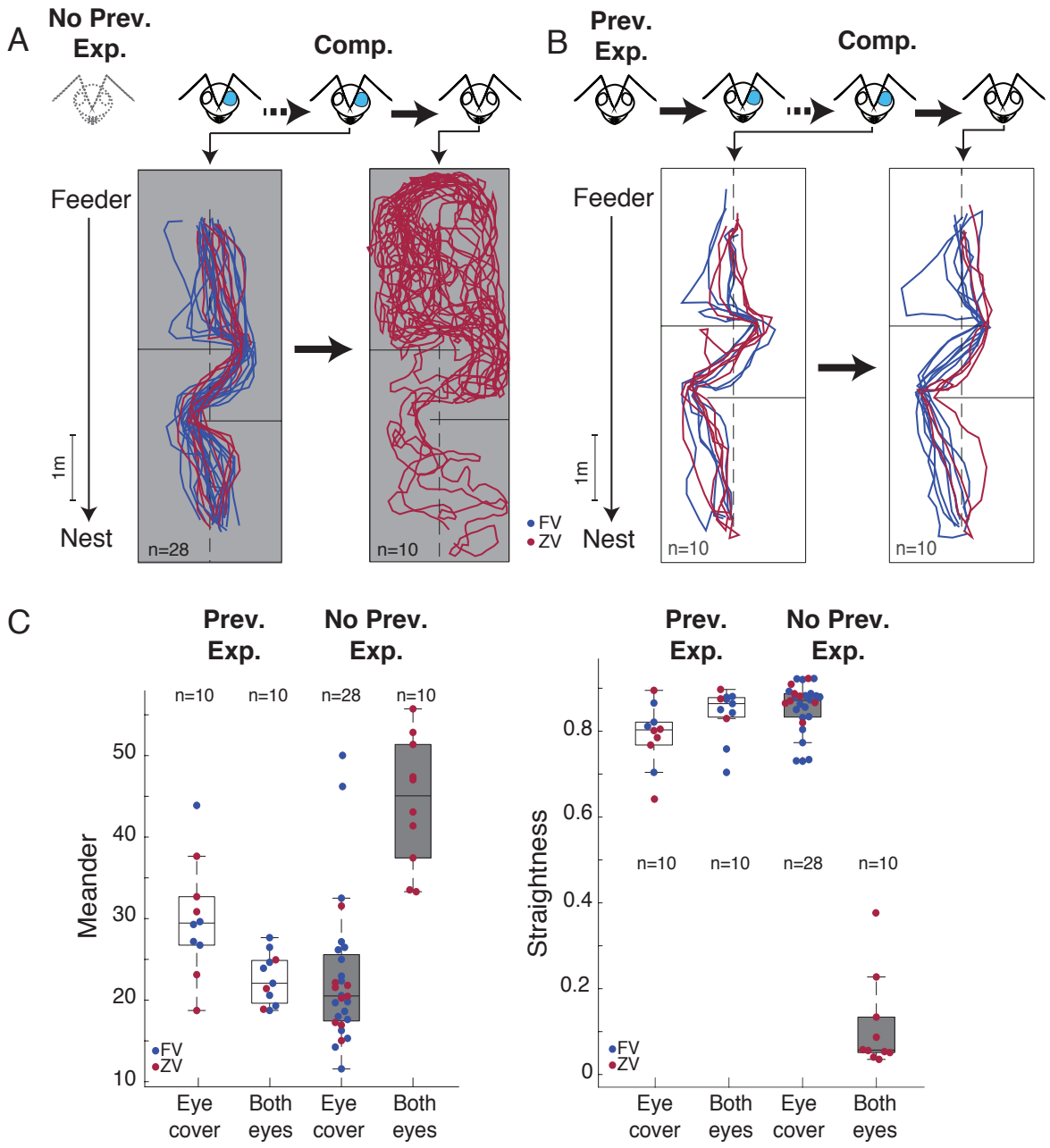

Fig. 5. Visual impairment before route learning. (A) Ants that learnt the route with one eye covered, hence no previous experience (no prev. exp.) of the route with uncovered eyes. After compensation (comp.) and reaching the feeder, homing paths are displayed with the eye cap still in place (left panel) and with uncapped eyes (right panel). Ants without previous experience of the route struggle to find back to the nest once the eye cap is removed. (B) Ants that learnt the route with both eyes, hence previous experience (prev. exp.) of the route before eye capping. After eye capping and reaching the feeder, homing paths are displayed with the eye cap still in place (left panel) and the eye cap removed (right panel). Ants with previous experience of the route have no difficulties to find back to the nest. (C) Path characteristics of ants with and without previous experience of the route before eye capping. Ant with previous experience show paths with low meander and high level of straightness after eye cap was removed whereas ants without previous experience of the route show paths with high meander and low level of straightness with both eyes uncovered (Anova meander: $F_{-0.13,0.05} = -2.487$, $P = 0.018$, Anova straightness: $F_{0.07,0.02} = 3.281$, $P = 0.002$).

In terms of neural implementation, this supports the idea that many KCs in the MB receive input from both eyes simultaneously (Fig. 6). It remains likely however that some KCs receive input from one eye only, which could explain why some freshly eye-capped ants, or freshly uncapped ants, even though strongly impaired, could still derive a rough estimation of the nest direction, as if they recognized the scene only partially or sporadically. The variation in homing performance observed across individuals may be explained, at least in part, by the more or less fortunate random connectivity in their mushroom body.

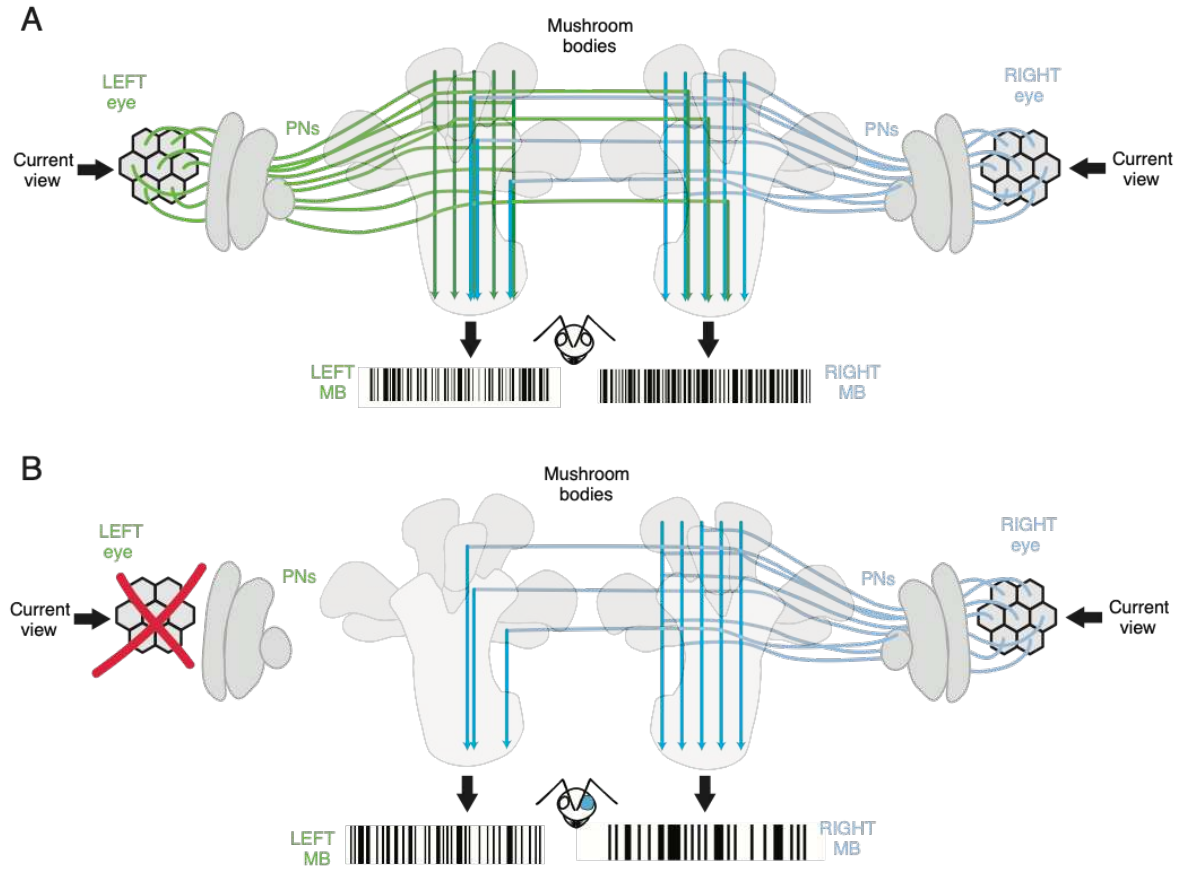

Fig. 6. Simplified model depicting neurobiological implications. (A) Both compound eyes feed into both Mushroom Bodies and elicit via projection neurons (PN) a certain set of Kenyon cells for each perceived view along a familiar route. (B) If the left eye is impaired (eye cap) the patterns of Kenyon cells are disrupted as they perceive only input from the uncapped right eye. Hence, the familiarity of the visual scenery is altered and homing ants need to compensate for the lack of visual information by relearning the surrounding scenery. The different bar codes represent different activated sets of Kenyon cells for a given view, for each compound eye.

Eye-cap ants do not forget past binocular memories. To control whether the visual impairment observed with freshly uncapped ants (Fig. 5A, right panel) was indeed due to an inability to access visual memories sorted with one eye and not just an inherent consequence of the recent recovery of bilateral visual input, the previous experiment was re-run with a cohort

of ants that, this time, had previous two-eyed experience of the route. These ants were eye-caped, let free to re-learn the route with one eye, then 'uncapped' and tested. Contrary to the previous cohort of ants with no previous experience of the route, these foragers did not struggle whatsoever to home toward the nest with uncapped eyes, even when tested as ZV ant (Fig. 5B). This shows that uncapping the ants bears no inherent issue and thus confirms that memories acquired with one eye are no longer accessible with two eyes (Fig. 5A). In addition, it shows that the latter cohort of ants had not forgotten their former visual memories of the route acquired with two eyes. Learning the route anew with one eye does not override the memories of the previous two-eye memories.

In neurobiological terms, one-eyed memories and two-eyed memories are likely to recruit different set of KCs in both hemispheres, with perhaps a certain amount of overlap between them (Fig. 6). This can be viewed as learning and remembering two different routes, which desert ants can also do (47). Indeed, ants possess hundreds of thousands of KCs (43) and models of the MBs show that this offers memory space for recognizing a large amount of visual sceneries (48, 49); enough to remember views around the nest, along multiple routes or as shown here, along the same route but with monocular and binocular inputs.

Conclusion

The response of navigating ants to visual impairments shows a surprising mix between rigidity and flexibility. Rigidity in the sense that the recognition of visual memories is not robust to changes in the visual field, highlighting a fundamental difference with the way human encode the visual world. Flexibility in the sense that experienced ants manage to compensate such a deficit by re-engaging a route learning process in a similar way than naïve ants do at the onset of their foraging ontogeny. With time, ants re-learn and recognize a route with ease, and the newly acquired memory does not override previous ones. Investigating the plastic neural mechanisms underlying these feats will form a great agenda for future research.

Material and Methods

Experiments took place during June and July 2017-19 on a plain open field with grassy vegetation close to the harbor in the metropolitan area of Seville, South of Spain. Three different nests of the Iberian desert ant *Cataglyphis velox* were used for training and testing. Workers exhibit behaviors typical for solitary foraging ants that venture out of the nest to find food

without the help of pheromone trails (50). Instead their navigational guidance is primarily based on visual input derived from celestial and terrestrial sensory cues (51).

General experimental set-up

All set-ups shared a similar basic design, which is described in the following while specific differences were appropriately mentioned above. Ants were trained to follow a route from the nest to a feeder that provided food *ad libitum* in form of a variety of buttery, sweet biscuit crumbs. Nests were enclosed with thin white plastic planks, a smooth material, too slippery for the tarsi of the ants and hence preventing them to forage elsewhere. A square plastic bowl was sunk into the ground and served as feeder. The walls of the feeder were covered with fluon to prevent ants from climbing out. During training ants dropped into the feeder and could return to the nest via a small wooden ramp that led the ants out of the feeder onto the foraging route. Training continued until the ants familiarized with the foraging route and scuttled fast and straight forward between the nest and the feeder at least five times. For tests, ants were either caught at the feeder or close to the nest entrance. Ants caught at the feeder have both the familiar visual scenery and the homing vector of their path integrator as scaffold for homing: hence full-vector ants (FV). Ants caught close to the nest ran off their homing vector and can solely rely on the familiar visual scenery during homing: hence zero-vector ants (ZV). All tested ants were subjected to an eye-cap procedure, which was non-invasive and reversible. For that foragers were manually caught and the first two pair of legs including one of the antenna were carefully fixed between two fingertips. Thus, the head of the ant was immobile and one of the compound eyes could be covered with a drop of opaque enamel paint (Tamiya). The tip of a thin pin acted as brush and painted ants were subsequently checked for an even and complete cover of the targeted eye with the help of a 10× magnifying glass. Afterward ants were transferred into a small plastic vial and tested as soon as the foragers held on to a crumb. Paths of tested ants were recorded with pen and paper and the help of a square grid (0.5×0.5 m) made of string and tent pegs mounted on the ground. Paths were digitized with GraphClick (Arizona Software) and statistical analyses were calculated with Matlab (Mathworks, Matick, MA, U.S.A.).

Paths in the unfamiliar environment (Sham, Just capped and Compensated ants) were recorded with a Panasonic Lumix camera (DMC FZ200) fixed on a tripod, digitized via a novel video tracker system of the Risse group at the University of Münster (52, 53) and analyzed with R studio. LEC and REC ants were pooled by mirroring paths of REC ants to LEC. Differences in their tendency to turn left or right were determined by comparing the angular velocity via a calculation of Dtheta and forward velocity. The X and Y values of the paths were smoothed

with a Savitzky-Golay filter of order 3 and filter length of 41 frames, followed by a double smoothing of the Dtheta signal by moving the average of window length by three. Finally, all pauses and events longer than one second were removed. A one-sided Wilcoxon test was used to calculate the significance of each pooled group against random choice.

ACKNOWLEDGEMENTS

We are grateful for logistic and administrative support of Xim Cerda and his team at the Spanish National Research Council (CSIC Seville) and appreciate the help during field work preparation and data collection of Cornelia Buehlmann, Florent Le Moël and Christelle Gassama. This study was funded by the European Research Council 759817-EMERG-ANT ERC-2017-STG.

1. Kelso SJA (2009) Coordination dynamics. *Encyclopedia of Complexity and Systems Science*, ed Meyers RA (Springer, New York).
2. Sacks O (2003) The mind's eye. *The New Yorker* 28:48-59.
3. Barulli D & Stern Y (2003) Efficiency, capacity, compensation, maintenance, plasticity: emerging concepts in cognitive reserve. *Trends in cognitive sciences* 17(10):502-509.
4. Johansen-Berg H (2007) Structural plasticity: rewiring the brain. *Current Biology* 17:141-144.
5. Chklovskii DB, Mel BW, & Svoboda K (2004) Cortical rewiring and information storage. *Nature* 431:782-788.
6. Chittka L & Niven J (2009) Are bigger brains better? *Current Biology* 19:995-1008.
7. Wystrach A & Graham P (2012) What can we learn from studies of insect navigation? *Animal Behaviour* 84:13-20.
8. Steck K, Wittlinger M, & Wolf H (2009) Estimation of homing distance in desert ants, *Cataglyphis fortis*, remains unaffected by disturbance of walking behaviour. *The Journal of Experimental Biology* 212:2893-2901.
9. Delcomyn F (1991) Pertubation of motor system of freely walking cockraches. I. Rear leg amputation and the timing of motor activity in leg muscles. *The Journal of Experimental Biology* 156(1):483-502.
10. Graham D (1977) The effect of amputation and leg restraint on the free walking coordination of the stick insect *Carausius morosus*. *Journal of comparative physiology A* 116:91-116.
11. Barnes WJP (1975) Leg Co-OrdinationduringWalkingin the Crab, *Uca pugnax*. *Journal of Comparative Physiology* 96:237-256.
12. Wystrach A, Beugnon G, & Cheng K (2011) Landmarks or panoramas: what do navigating ants attend to for guidance? *Frontiers in Zoology* 8:21.
13. Graham P & Cheng K (2009) Ants use the panoramic skyline as a visual cue during navigation. *Current Biology* 19(20):935-937.
14. Wehner R, Michel B, & Antonsen P (1996) Visual navigation in insects: coupling of egocentric and geocentric information. *The Journal of Experimental Biology* 199:129-140.
15. Collett TS & Rees JA (1997) View-based navigation in Hymenoptera: multiple strategies of landmark guidance in the approach to a feeder. *Journal of Comparative Physiology A* 181:47-58.
16. Wystrach A, Schwarz S, Schultheiss P, Baniel A, & Cheng K (2014) Multiple sources of celestial compass information in the Central Australian desert ant *Melophorus bagoti*. *Journal of Comparative Physiology A* 200:591-601.
17. Dacke M, Baird E, Byrne M, Scholtz CH, & Warrent EJ (2013) Dung beetles use the Milky Way for orientation. *Current Biology* 23(4):298-300.
18. Homberg U, Heinze S, Pfeiffer K, Kinoshita M, & El Jundi B (2011) Central neural coding of sky polarization in insects. *Philosophical Transactions of the Royal Society B: Biological Sciences* 366(1565):680-687.
19. El Jundi B, *et al*. (2015) Neural coding underlying the cue preference for celestial orientation. *Proceedings of the National Academy of Sciences of the United States of America* 112(36):11395-11400.
20. Wehner R & Müller M (2006) The significance of direct sunlight and polarized skylight in the ant's celestial system of navigation. *Proceedings of the National Academy of Science of the USA* 103:1275-1279.
21. Steck K (2012) Just follow your nose: homing by olfactory cues in ants. *Current Opinion in Neurobiology* 22:231-235.
22. Bühlmann C, Hansson B, & Knaden M (2012) Path integration controls nest-plume following in desert ants. *Current Biology* doi:10.1016/j.cub.2012.02.029.

23. Wystrach A & Schwarz S (2013) Ants use a predictive mechanism to compensate for passive displacements by wind. *Current Biology* 23:1083-1085.
24. Wolf H & Wehner R (2000) Pinpointing food sources: olfactory and anemotactic orientation in desert ants, *Cataglyphis fortis The Journal of Experimental Biology* 203:857–868.
25. Buehlmann C, Hannson BS, & Knaden M (2012) Desert ants learn vibration and magnetic landmarks. *PLoS One* 7:33117.
26. Fleischmann PN, Grob R, Müller VL, Wehner R, & Rössler W (2018) The geomagnetic field is a compass cue in *Cataglyphis* ant navigation. *Current Biology* 28:1-5.
27. Seelig J & Jayaraman V (2015) Neural dynamics for landmark orientation and angular path integration. *Nature* 521:186-191.
28. Wehner R & Müller M (1985) Does interocular transfer occur in visual navigation by ants? *Nature* 315:228-229.
29. Woodgate JL, Perl C, & Collett TS (2021) The routes of one-eyed ants suggest a revised model of normal route following. *The Journal of Experimental Biology* 224(16):jeb242167.
30. Schwarz S, Narendra A, & Zeil J (2011) The properties of the visual system in the Australian desert ant *Melophorus bagoti*. *Arthropod Structure and Development* 40:128-134.
31. Knaden M & Wehner R (2005) Ant navigation: resetting the path integrator. *The Journal of Experimental Biology* 209:26-31.
32. Wystrach A, Schwarz S, Baniel A, & Cheng K (2013) Backtracking behaviour in lost ants: an additional strategy in their navigational toolkit. *Proceedings of the Royal Society B: Biological Sciences* 280:20131677.
33. Zeil J & Fleischmann PN (2019) The learning walks of ants (Hymenoptera: Formicidae). *Myrmecological News* 29:93-110.
34. Wystrach A, Philippides A, Aurejac A, & Graham P (2014) Visual scanning behaviours and their role in the navigation of the Australian desert ant *Melophorus bagoti*. *Journal of Comparative Physiology A* 200:615-626.
35. Fernandes ASD, Philippides A, Collett TS, & Webb B (2015) Acquisition and expression of memories of distance and direction in navigating wood ants. *The Journal of Experimental Biology* 218:3580-3588
36. Bolek S, Wittlinger M, & Wolf H (2012) Establishing food site vectors in desert ants. *The Journal of Experimental Biology* 215:653-656.
37. Schwarz S, Clement L, Gkanias E, & Wystrach A (2020) How do backward-walking ants (*Cataglyphis velox*) cope with navigational uncertainty? *Animal Behaviour* 164:133-142.
38. Freas CA & Spetch ML (2019) Terrestrial cue learning and retention during the outbound and inbound foraging trip in the desert ant, *Cataglyphis velox*. *Journal of Comparative Physiology A*:doi.org/10.1007/s00359-00019-01316-00356.
39. Schwarz S, Wystrach A, & Cheng K (2017) Ants' navigation in an unfamiliar environment is influenced by their experience of a familiar route. *Scientific Reports* 7:14161.
40. Murray T, *et al*. (2020) The role of attractive and repellent scene memories in ant homing (*Myrmecia croslandi*). *The Journal of Experimental Biology* 223:jeb210021.
41. Freas CA & Cheng K (2018) Landmark learning, cue conflict, and outbound view sequence in navigating desert ants. *Journal of Experimental Psychology: Animal Learning and Cognition* 44(4):409-421.
42. Giger AD & Srinivasan MV (1997) Honeybee vision: analysis of orientation and colour in the lateral, dorsal and ventral fields of view. *The Journal of Experimental Biology* 200:1271-1280.

43. Habenstein J, Amini E, Grübel C, El Jundi B, & Rössler W (2020) The brain of Cataglyphis ants: Neuronal organization and visual projections. *Journal of Comparative Neurology* 528(18):3479-3506.
44. Webb B & Wystrach A (2016) Neural mechanisms of insect navigation. *Current Opinion of Insect Science* 15:27-39.
45. Kamhi JF, Barron AB, & Narendra A (2020) Vertical lobes of the mushroom bodies are essential for view-based navigation in Australian Myrmecia ants. *Current Biology* doi.org/10.1016/j.cub.2020.06.030.
46. Buehlmann C, *et al*. (2020) Mushroom bodies are required for learned visual navigation, but not for innate visual behavior, in ants. *Current Biology* doi.org/10.1016/j.cub.2020.07.013.
47. Sommer S, Beeren von C, & Wehner R (2008) Multiroute memories in desert ants. *Proceedings of the National Academy of Science USA* 105:317-322.
48. Ardin P, Peng F, Mangan M, Lagogiannis K, & Webb B (2016) Using an insect mushroom body circuit to encode route memory in complex natural environments. *PLoS Computational Biology* 12(2):e1004683.
49. Le Möel F & Wystrach A (2020) Opponent processes in visual memories: a model of attraction and repulsion in navigating insects' mushroom bodies. *PLoS Computational Biology* 16(2):e1007631.
50. Cerda X (2001) Behavioural and physiological traits to thermal stress tolerance in two Spanish desert ants. *Etologia* 9:15-27.
51. Mangan M & Webb B (2012) Spontaneous formation of multiple routes in individual desert ants (*Cataglyphis velox*). *Behavioral Ecology* 23(5):944-954.
52. Haalck L, Mangan M, Webb B, & Risse B (2020) Towards image-based animal tracking in natural environments using a freely moving camera. *Journal of Neuroscience Methods* 330:108455.
53. Risse B, Mangan M, Del Pero L, & Webb B (2017) Visual Tracking of Small Animals in Cluttered Natural Environments Using a Freely Moving Camera. *International Conference on Computer Vision (ICCV)*:2840-2849.

Animal Behaviour 164 (2020) 133–142

Contents lists available at ScienceDirect

Animal Behaviour

journal homepage: www.elsevier.com/locate/anbehav

How do backward-walking ants (*Cataglyphis velox*) cope with navigational uncertainty?

Sebastian Schwarz [a, *], Leo Clement [a], Evripidis Gkanias [b], Antoine Wystrach [a]

[a] Centre de Recherches sur La Cognition Animale, CNRS, Université Paul Sabatier, Toulouse, France
[b] School of Informatics, University of Edinburgh, Edinburgh, U.K.

ARTICLE INFO

Article history:
Received 17 September 2019
Initial acceptance 22 January 2020
Final acceptance 5 March 2020

MS number 19-00627R

Keywords:
ants
backward movement
navigation
peeking
route following
uncertainty
view-based navigation

Current opinion in insect navigation assumes that animals need to align with the goal direction to recognize familiar views and approach it. Yet, ants sometimes drag heavy food items backwards to the nest and it is still unclear to what extent they rely on visual memories while doing so. In this study displacement experiments and alterations of the visual scenery revealed that ants indeed recognized and used the learnt visual scenery to guide their path towards the nest while walking backwards. In addition, the occurrence of forward-peeking behaviours revealed that backward-walking ants continually estimated their directional uncertainty by integrating multiple cues such as visual familiarity, the state of their path integrator and the time spent backwards. A simple mechanical model based on repulsive and attractive visual memories captured the results and explained how visual navigation can be performed backwards.

Central-place foragers, such as desert ants, exhibit formidable navigational skills to find food and their way back home during numerous daily foraging trips (Collett, Graham, & Durier, 2003; Heinze, Narendra, & Cheung, 2018; Wehner, 2003). These ground dwellers rely on a set of navigational strategies such as path integration (Wehner & Srinivasan, 2003; Wittlinger, Wehner, & Wolf, 2006) and visual scene navigation (Cheng, Narendra, Sommer, & Wehner, 2009; Zeil, 2012). Path integration (PI) is the capacity to return to a starting point by constantly updating the directional and distance information (based on celestial compass cues and a stride odometer) during an outbound trip whereas visual scene navigation provides directional information by comparing memorized and currently perceived views of terrestrial cues. The literature agrees that ants continuously integrate the directional dictates of these different strategies, rather than switching between them (Collett, 2012; Hoinville; Wehner, 2018; Legge; Wystrach; Spetch, & Cheng, 2014; Reid, Narendra; Hemmi, & Zeil, 2011; Wystrach; Mangan, & Webb, 2015).

Current models of insect visual navigation capture well the behaviour of forward-navigating ants (Baddeley, Graham, Husbands, & Philippides, 2012; Hoinville & Wehner, 2018; Wystrach, Beugnon, & Cheng, 2011; Wystrach, Cheng, Sosa, & Beugnon, 2011; Zeil, 2012); however, how ants navigate while dragging a heavy food item backwards remains unclear (Ardin, Mangan, & Webb, 2016; Pfeffer & Wittlinger, 2016; Schwarz, Mangan, Zeil, Webb, & Wystrach, 2017). Despite their irregular backward foot strides the ants' PI system seems as accurate as during forward movement (Pfeffer, Wahl, & Wittlinger, 2016; Pfeffer & Wittlinger, 2016); however, guidance based on terrestrial visual cues seems disrupted (Schwarz et al., 2017). Indeed, evidence suggests that to recognize the familiar terrestrial scenery ants need to align their body in the familiar forward direction (Narendra, Gourmaud, & Zeil, 2013; Wystrach, Cheng, et al., 2011; Zeil, 2012). This is probably why ants dragging a food item backwards occasionally display a so-called 'peeking' behaviour: the ant stops pulling, drops her food item and turns around to look forwards. If the scenery is familiar, the ant quickly returns to her food item and adjusts her backward path in the newly corrected homing direction. It seems clear that during these few moments facing forwards in a familiar direction, ants recover and store the correct direction and subsequently rely on celestial cues to maintain this

* Correspondence: S. Schwarz, Université Paul Sabatier, Centre de Recherches sur la Cognition Animale, CNRS, 31062, Toulouse, France.
E-mail address: sebastian.schwarz@univ-tlse3.fr (S. Schwarz).

https://doi.org/10.1016/j.anbehav.2020.04.006
0003-3472/

new bearing when travelling backwards (Schwarz et al., 2017). In this case navigation is discretized into different sources of information being used sequentially rather than simultaneously. Also, 'peeking' involves the decision to trigger a distinct and observable behaviour when navigational information is needed. This behaviour therefore provides a good opportunity to investigate how ants estimate their navigational uncertainty and, as a corollary, to which navigational information they have access.

Here two experiments with backward-walking ants were carried out to investigate the following questions. (1) Do ants still pay attention to visual terrestrial cues when walking backwards? (2) Does this visual information enable ants to guide their backward path? (3) Which information is used by ants to estimate uncertainty and trigger a peeking behaviour?

METHODS

Study Animal and Site

The experiments were carried out with Spanish desert ants, *Cataglyphis velox*, on a field site with diverse grass and bush vegetation on the outskirts of Seville (37°19′55″N, 5°59′20″W) during June 2017 and 2018. *Cataglyphis velox* show typical characteristics of a desert ant such as diurnality, thermophily and solitary foraging (Cerda, 2001). As in other ant species, navigation and orientation in *C. velox* is predominantly based on vision derived from terrestrial and celestial cues (Mangan & Webb, 2012; Wystrach, Mangan, & Webb, 2015).

General Methods

Two experiments were conducted: experiment 1 in 2017 and experiment 2 in 2018. Both set-ups shared the following methods. Ants were restricted to foraging on a straight route (for specific dimensions see below) between their nests and a feeder. The routes were cleared from all vegetation that could interfere with ant observations and enclosed by thin white plastic planks (10 cm high) that were dug halfway into the ground. The slippery surface of the planks prevented ants foraging elsewhere while minimizing the obstruction of surrounding views (Wystrach, Beugnon, & Cheng, 2012). Ants could freely travel between nest and feeder, which was a plastic bowl (ca. 15 × 15 × 15 cm) sunk into the ground that contained several kinds of sweet buttery biscuit crumbs. The walls of the bowl were covered with a thin layer of Fluon which prevented ants from climbing. Ants that dropped into the feeder and picked up a crumb were marked individually with coloured acrylic or enamel paint (Tamiya). During training, ants could leave the feeder via a small wooden ramp. Ants were considered trained and ready for testing once they had performed at least five foraging runs and were able to reach the feeder from the nest in a straight line (without colliding into any barriers). During tests (see below) the feeder ramp was removed to prevent other homing ants from interfering.

Experiment 1

Methods

Experiment 1 was conducted to assess the occurrence of peeking behaviour in backward-walking ants across four different test conditions with one nest of *C. velox* (summer 2017) located at the beginning of a straight foraging route (8.0 × 1.8 m long). The length of the route was chosen to be long enough for ants to build up proper PI information but short enough to enable them to drag a large crumb backwards along the whole distance without being too fatigued. Three thin (0.5 cm width), large wooden boards (2.4 × 1.2 m) were connected (7.2 × 1.2 m) and placed onto the foraging route (Fig. 1a, grey rectangles). These boards enhanced the tarsi grip of the ants and provided an even substrate that minimized potential interference from small grass haulms or pebbles during tests when ants dragged their food items backwards.

During training, the individually marked foragers scuttled (forwards) between the nest and feeder over the connected boards and familiarized themselves with the visual surroundings. After training, individual ants were subjected to one test condition. All tests comprised a forager that dragged a large biscuit crumb backwards. For that, trained foragers with a small food item (ca. 0.2 × 0.2 × 0.2 cm) were caught and transferred into a plastic vial. The food item was then carefully and manually removed and a larger crumb (ca. 2.0 × 0.5 × 0.2 cm) was offered to the ant instead. The crumb provided was large enough to force the ants to drag it backwards. After the ant had locked mandibles onto it, she was transferred from the vial to the appropriate release point. Four possible test conditions were carried out with either FV- (full-vector ants, i.e. ants with their PI vector information, captured at the feeder) or ZV-ants (zero-vector ants, i.e. foragers without PI information, captured just before they entered the nest; Fig. 1a). To test whether ants paid attention to the visual scenery during backward motion, FV ants were released at the feeder either within the familiar scenery (FV, condition 1) or within altered visual surroundings (FVA, condition 2), by adding large black plastic bags (ca. 0.8 × 0.6 m) on one side and a large dark tarp (0.9 × 3.4 m) on the other side of the route (Fig. 1a, unfamiliar test) to avoid potential obstructions. The objects were added a few seconds after the FVA-ant had started to home backwards to ensure that the ant did not perceive any alteration beforehand. To test the effect of route location, backward-walking ants were released either at the beginning (ZV, condition 3) or in the middle of the route (ZVmid, condition 4).

Note that upon release, the ants tested in experiment 1 had the chance to glimpse forwards while handling their large crumb before engaging in backward movements.

Data and analysis

For all tests, the distance between the release point and the location at which peeking behaviours occurred was noted with the help of a measuring tape placed on the side of the board that spanned form the feeder to the nest. Tests ended as soon as the backward-walking ants reached the end of the wooden boards (i.e. ca. 0.5 m in front of the nest entrance) or abandoned their food item for more than 1 min. Individual ants were tested only once per test but were subjected to different test conditions with at least one training trial, without interference, between tests. The sequence of tests was evenly counter-balanced across individuals (e.g. FV-FVA-ZV-ZVmid; FVA-ZV-ZVmid-FV; ZV-ZVmid-FV-FVA, etc.)

We compared FV- with FVA-ants and ZV- with ZVmid-ants (Fig. 1a). Given the large interindividual variation, we used paired data and thus individuals that were not tested in both FV and FVA or ZV and ZVmid conditions were excluded from the analysis. We compared both the distance at which the first peeking behaviour occurred (first-peek distance) and the overall peek rate of individuals (i.e. number of peeks/distance walked) using Wilcoxon rank sum tests, a nonparametric statistic for paired data. Given that all ants walked rather straight towards the nest along the route, distance walked could be simply approximated by the beeline distance walked along the route. Most ants walked the full route (7.2 m) except obviously ants in the ZVmid condition and some foragers that abandoned their crumb. For the comparison of peek rate, the 7.2 m long route on the boards was divided in half (Section 1: 0–3.4 m; Section 2: 3.4–7.2 m; Fig. 1a). Thus, during ZVmid tests ants ran only Section 2. We compared ZV- with ZVmid-ants to separate the effect of distance walked (i.e. ZVmid versus ZV on Section 1) from the actual location along the route (i.e. ZVmid

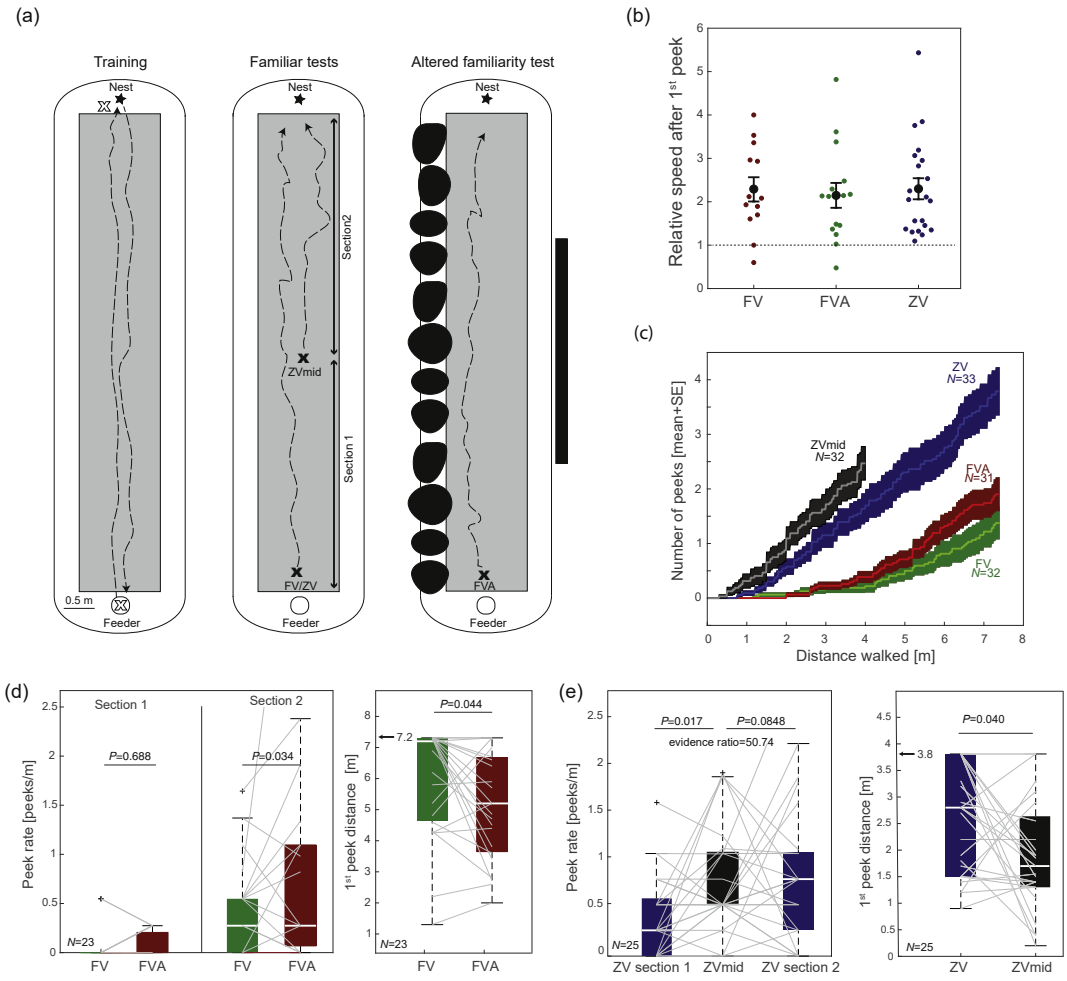

Figure 1. Dynamics of peeking behaviours in terms of path integration and visual familiarity (experiment 1). (a) Schematics of experimental set-up with training and test conditions. During training ants foraged between nest and feeder (ca. 8.0 m) on three thin wooden boards serving as an even substrate (grey rectangles). The route was divided into two sections corresponding to the first and second half of the route. For tests, trained ants were either captured at the feeder (full-vector ants, FV) or just before entering the nest after foraging (zero-vector ants, ZV; bold crosses) and released at the feeder (as FV-, FVA or ZV-ants) or on the middle of the route (ZVmid-ants; black crosses). For FVA (altered familiarity), the familiarity of the route was manipulated by adding large black objects (black blobs) on one side and a dark tarp (black vertical bar) on the other side of the route. Dashed lines depict example paths of the ants. (b) Change in speed after the first peek. Each dot shows the relative change in speed (5 s after/5 s before) for the first peek for each ant. Large dots and vertical bars indicate mean ± SE. Horizontal line at 1 indicates no change in speed. (c) Cumulated number of peeks displayed against the distance walked along the route (mean ± SE across individuals). (d) Overall peek rate and distance of the first peek for both FV-ants and FVA-ants. Boxes show the median and 25th and 75th percentiles; the whiskers indicate the values within 1.5 times the interquartile range and the crosses are outliers. Grey lines represent individually tested ants across conditions. The arrow indicates the end of the route. (e) As in (d), but for both ZV-ant conditions. Note that ZV-ant paths were truncated at 3.8 m to match the maximum homing distance of ZVmid-ants. See main text for statistical details.

versus ZV on Section 2). Bayesian statistics based on the *Z* values from these tests were applied to evaluate which of these alternative hypotheses explained peek rate best. We used f(*Z*), that is, the y values on the standard normal distribution obtained from each of the *Z* scores, to estimate evidence in favour of each hypothesis. The ratio of the f(*Z*) measures of the two hypotheses gives an estimate of the 'evidence ratio'. While evidence ratios under 5 are weak, ratios over 10 are very strong (see Wystrach, Schwarz, Schultheiss, Baniel, & Cheng, 2014 for more details).

Backward paths were recorded by using GoPro HERO3+ cameras which were manually held ca. 0.6 m above the tested ant. Therefore, the movement speed of the ants before and after peeking could be calculated. We measured the relative distance walked by the backward-walking ants during the 5 s preceding the onset of the first peek (i.e. before the moment when the ants released the crumb) and 5 s after the peek (i.e. after the ant resumed backward motion).

Experiment 2

Methods

Experiment 2 was conducted to test whether ants could guide their path backwards based on terrestrial cues. To do so, we recorded the paths of backward-walking ants captured near their nest and released at four different points (summer 2018). We used two different nests of *C. velox* ants. For each nest, a straight foraging route (5.0 × 2.0 m) was built with the nest entrance at one end and the feeder at the other (Fig. 2a). As in experiment 1, the route was enclosed by white plastic planks and ants were given a choice of biscuit crumbs inside the feeder to prompt foraging. However, here the ants scuttled back and forth directly on the natural ground during training. Once trained (see General methods), individual ants were captured on their way home 0.5 m before reaching their nest and subsequently released at one of four locations (Fig. 2a): (1) Feeder (F): ants were released 0.5 m after the feeder towards the

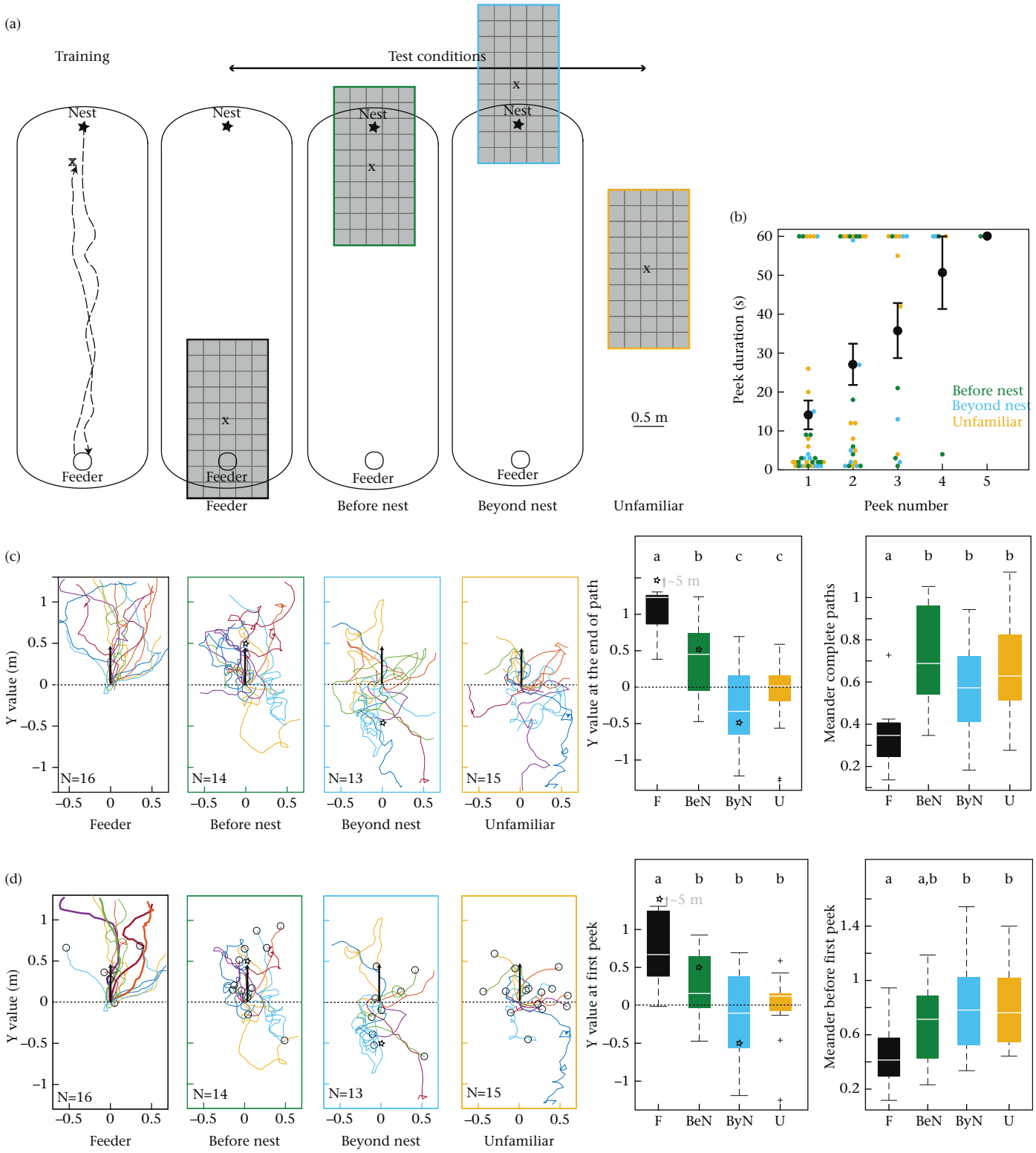

Figure 2. Backward path characteristics and peeking behaviour at different release points (experiment 2). (a) Schematics of experimental set-up with training and test conditions. During training ants foraged between the nest and feeder (ca. 5.0 m). Trained ants with a remaining homing vector of 0.5 m (bold cross depicts capture point) were tested backwards at different release points: feeder (F), before nest (BeN), beyond nest (ByN) and unfamiliar (U) test site. Ants were released (black crosses) on the middle of a thin wooden board (grey) to rule out the use of olfactory cues. Boards had a 0.25 × 0.25 m square pattern to enable path recording. Dashed lines depict example paths of ants during training. (b) Duration of peek (the time the ant spent away from the crumb) as a function of peek number for each individual. The maximum threshold of peek duration was set to 60 s and 'Feeder condition' was removed from this analysis as peek number correlates with position along the board. (c) Complete recorded backward paths of ants across conditions. Paths ended either because ants left the board or abandoned their crumb (peek duration > 60 s). Box plots show distance reached at the end of the path along the feeder–nest axis (*y* axis) and meander of the paths across individuals; boxes show the median and 25th and 75th percentiles; the whiskers indicate the values within 1.5 times the interquartile range and the crosses are outliers. Differences in top letters (a, b, c) indicate significant differences between groups (alpha = 0.05). Black dotted lines depict the release point, black arrows the remaining vector length (0.5 m) and open stars the nest position. (d) As in (c), except that paths were truncated at the first peek or when exiting the board. Hence all navigational information gathered by ants was obtained while walking backwards. Thick paths in the feeder condition represent four ants that displayed nest-directed backward paths without facing the nest direction. Open circles represent positions of first peeks. For statistical details see text.

nest direction; (2) Before nest (BeN): ants were released on the route, 0.5 m before their nest; (3) Beyond nest (ByN): ants were released 0.5 m beyond the nest in the feeder–nest direction; (4) Unfamiliar (U): ants were released ca. 30.0 m away from the nest in a visually unfamiliar location.

For all tests, ants were captured in a plastic vial, offered a large biscuit crumb to incite backward walking and, once the ant had grabbed it, released within a lampshade at the middle of a large wooden board (2.4 × 1.2 m). Individual ants were tested only once per test, but could be subjected to different test conditions, with at least one training trial, without interference, between tests. The wooden board was set in place just before and removed just after each test. It was centred on the current release location with the long side along the feeder–nest direction (Fig. 2a) as it represents the expected homing direction. The board provided an even substrate during tests and prevented ants using potential familiar olfactory cues from the ground or the nest (BeN and ByN tests). A grid pattern (0.25 × 0.25 m) drawn on the board enabled paths to be transcribed onto gridded paper. The lampshade (beige opaque fabric, 0.5 m diameter, 0.4 m height) surrounded the ant upon release and obstructed any familiar terrestrial views; the top of the lampshade was open providing the ant with celestial compass cues. Once the ant had pulled the large crumb backwards for 0.1 m, the lampshade was lifted and the visual surroundings were revealed. This ensured that the ants could not utilize any familiar scenes before starting their backward path. This sets experiment 2 apart from experiment 1 where tested ants could glimpse forwards before dragging the crumb backwards.

Data and analysis

The backward paths and locations of peeking behaviour were noted. For each peek, the duration (i.e. the time the ant was not dragging the crumb) was recorded. The actual trajectory of the path during forward motion was not recorded. Recording continued until the ants either reached the edge of the board or abandoned their large crumb for more than 1 min.

The recorded paths were digitized as (x, y) coordinates using GraphClick (Arizona Software, http://www.arizona-software.ch/). Path characteristics such as direction, meander and peek location were computed and analysed with Matlab (Mathworks, Matick, MA, U.S.A.). The meander index measures how much the path changed direction from segment to segment and was calculated as the mean angular deviation in direction between successive segments, each 0.3 m (Schwarz, Albert, Wystrach, & Cheng, 2011). Differences between test locations were determined using a generalized linear mixed-effect model (GLM) with repeated ants as a random effect and Tukey's post hoc corrections. For peek durations, a model for proportional (binomial) data was applied with 0–60 s (the duration at which recording was stopped) reported between 0 and 1.

RESULTS

Experiment 1

Experiment 1 was designed to investigate whether the occurrence of peeking behaviour in backward-walking ants depends on factors such as path integration, terrestrial cues, the location along the route or the distance walked.

Peeking and walking speed

In all conditions, and for most individuals, ants walked backwards on average twice as quickly after peeking than before peeking (Fig. 1b). This supports the idea that a peeking event increases the ant's directional certainty for some time.

FV versus ZV: effect of path integration

In both FV and ZV conditions, ants started to pull their crumb towards the nest and mostly maintained that direction. However, the PI state had a visible effect on the occurrence of peeking behaviours: ZV-ants peeked earlier (first peek distance ZV-ants: mean ± SD = 3.28 ± 2.19 m; FV-ants: mean ± SD = 5.90 ± 1.93 m; Wilcoxon rank sum test: $Z = -3.458$, $P < 0.001$) and thrice as much (overall peek rate ZV-ants: mean ± SD = 0.63 ± 0.63 peeks/m; FV-ants: mean ± SD = 0.19 ± 0.29 peeks/m; Wilcoxon rank sum test: $Z = -3.751$, $P < 0.001$) than FV-ants (Fig. 1c, blue versus green). Also, ZV-ants occasionally abandoned their large food item and did not resume backward movements (six of 33), whereas FV-ants never abandoned theirs (none of 32). This difference in proportion is significant (Fisher's exact test: $P = 0.032$). It seems clear that the lack of (or conflicting) PI information decreased the ant's directional certainty.

FV versus FVA: effect of altered visual familiarity

To test whether backward-walking ants pay attention to terrestrial cues, two conditions were conducted: (1) FV-ants homing backwards on the unaltered, usual route, and (2) FVA-ants homing backwards on the same route but with altered visual surroundings (Fig. 1a). The visual surroundings were changed only after the ants had started their journey backwards, so that differences indicate that ants paid attention to terrestrial cues while walking backwards. The FVA-ants peeked more often than FV-ants; however, this effect was weak, and reached significance only in Section 2 (Wilcoxon rank sum test: $Z = 3.751$, $P = 0.027$) but not in Section 2 of the route (Wilcoxon rank sum test: $Z \sim 0$, $P = 0.688$; Fig. 1d), owing to a statistical floor effect. Indeed, a low rate of peeking in the first section of the route was expected, given that the PI vector is longer and thus stronger at the beginning of the route home (Wystrach et al., 2015).

Second and most importantly, FVA-ants travelling in the altered visual environment displayed their first peek earlier along the route than FV-ants on the familiar route (Wilcoxon rank sum test: $Z = 2.016$, $P = 0.044$; Fig. 1d). Together, this suggests that backward-walking ants paid attention to terrestrial cues.

As for ZV-ants (see above), FVA-ants tested in the altered familiar condition abandoned their crumbs significantly more often than FV-ants (FVA: six of 31; FV: none of 32; Fisher's exact test: $P = 0.022$). Here again, it seems that the altered visual scenery decreased the directional certainty of backward-walking ants.

ZV versus ZVmid: effect of location

We investigated the potential effect of the location along the route by releasing ZV ants either at the beginning or in the middle of the familiar route (ZVmid; Fig. 1a, c). Consequently, ZVmid-ants walked only Section 2, while ZV-ants moved along both sections. Ants displayed their first peek on average slightly earlier when released in the middle of the route (ZVmid) than when released at the beginning of the route (ZV; Wilcoxon rank sum test: $Z = 2.062$, $P = 0.040$; Fig. 1e). Also, the peek rate of ZVmid-ants along Section 2 (the only section they walked) was higher than that of ZV-ants along Section 1 (Wilcoxon rank sum test: $Z = -2.814$, $P = 0.005$) but their peek rate was similar to that of ZV-ants along Section 2 of the route (Wilcoxon rank sum test: $Z = -0.2585$, $P = 0.796$; Fig. 1e). A Bayesian evidence ratio (see Methods) was computed to estimate whether Section 1 (i2.e. different location, same distance walked) or Section 2 (i.e. same location, different distance walked) of ZV-ants' peek rate resembled most ZVmid-ants' peek rate. The evidence ratio was 50.74 in favour of Section 2, which is 'overwhelming evidence' for an effect on peek rate of the location along the route rather than the distance walked.

Experiment 2

Experiment 2 was conducted to test whether ants could guide their path backwards using terrestrial cues. To do so, we recorded the paths of backward-walking ants captured near their nest and released at four different points. Unlike experiment 1, all tested ants in experiment 2 were prevented from monitoring the visual surroundings before dragging their food item backwards as a lampshade was blocking the whole panoramic view upon release (see Methods). Hence, any difference in the direction taken must result from visual information perceived while the ants were dragging their crumb backwards, at least until they peeked for the first time.

Ants can guide their backward path

To see whether ant paths were directed in different directions across release locations, we examined the y values, the end position along the feeder-to-nest line relative to the release point. The y values at the end of the foragers' paths varied across release locations (ANOVA: $F_{3, 55} = 21.96$, $P < 0.001$; Fig. 2c). Ants released at the feeder were directed towards the nest and hence obtained the highest y values (Tukey's post hoc test F versus BeN, ByN and U: Zs > 3.75, Ps < 0.001; Fig. 2c). Ants in unfamiliar tests (U) showed no directional preference along the *y* axis (Fig. 2c), as expected given the lack of familiar visual information at this location. Interestingly, ants from BeN and ByN conditions differed significantly in their final y values on the board (Tukey's post hoc test BeN versus ByN: $Z = 3.47$, $P = 0.003$). The medians of both groups are close to the actual nest location, showing that they used familiar visual cues to move towards the nest (Fig. 2c). Differences between conditions could also be observed in path meander (ANOVA: $F_{3, 54} = 9.07$, $P < 0.001$). Ants from the feeder test showed straighter paths than ants from all other conditions (Tukey's post hoc test F versus BeN, ByN and U: Zs > 3.68, Ps < 0.002; Fig. 2c). No difference in meander between the remaining test conditions could be determined. Indeed, BeN-, ByN- and U-ants were expected to search on the board: BeN- and ByN-ants due to the proximity of the nest and U-ants due to the lack of familiar visual information. Overall, these results show that ants could use familiar visual cues to adequately direct their backward paths.

Remarkably, analysis of the paths displayed purely backwards, before the first peek (or until the ant left the board if she did not peek), showed a similar pattern of results for both the y values reached (ANOVA: $F_{3, 55} = 11.37$, $P < 0.001$) and path meander (ANOVA: $F_{3, 37} = 3.52$, $P = 0.024$; Fig. 2d). Despite purely backward movements, ants released at the feeder travelled significantly longer distances along the feeder–nest direction (Tukey's post hoc test: F versus BeN, ByN and U: Zs > 3.29, Ps < 0.006; Fig. 2d) and displayed straighter paths (Tukey's post hoc test: F versus ByN and U: Zs > 2.65, Ps < 0.03; F versus BeN: $Z = 1.88$, $P = 0.235$; Fig. 2d) before peeking. The other three groups (BeN, ByN, U) were indeed expected to search on the board and to perform a similar level of path meander, as observed. Differences in the y values reached when released on each side of the nest did not reach significance using Tukey's post hoc test (BeN versus ByN: $Z = 2.084$, $P = 0.158$); however, the pattern of results followed what was expected if ants were using views to direct their path towards the nest. Ants released before (BeN) and beyond (ByN) their nest both moved on average towards the nest location, that is, in the opposite direction from their release points, and ants released at the unfamiliar test site (U) showed less directed paths (Fig. 2d). The differences in path characteristics are also apparent if one considers that the probability of obtaining the expected order of path endpoints across the four test conditions (y value: F > BeN > U > ByN) is $1/4! = 0.042$.

Because nest-directed path sections were completed before the ants carried out their first peek and the visual panorama was revealed to them only after they had started backward motion, the differences across locations show that ants recognized and used the familiar visual cues to guide their path while moving backwards and without the need to peek.

Interestingly, four of the 16 ants released at the feeder displayed nest-directed backward paths across the whole recording board without performing a single peek and by keeping their body orientation away from the feeder–nest direction by at least 90° (bold paths in Fig. 2d).

Peek duration and past information

We also tested whether peek duration was influenced by the test condition and the number of previously displayed peeks (Fig. 2b). The feeder condition was excluded from this analysis as these ants were expected to move in a straight line and exit the board so that the actual peek number of a given ant may correlate with the location where the ant peeks. The other three groups (BeN, ByN, U), on the other hand, were expected to search on the board so any effect of the peek number is unlikely to be attributed to a specific location on the board. Interestingly, peek duration, which was recorded for up to 60 s, was strongly influenced by the number of peeks previously displayed by the ant (GLM: peek number: $F = 17.09$, $P < 0.001$; Fig. 2b) and not the actual test condition (GLM: condition: $F = 0.17$, $P = 0.841$; Fig. 2b). The more peeks an ant had previously displayed the longer her current peeking lasted. This shows that the ant's peeking behaviour is also modulated by past information. Whether it was the time passed or the number of peeks previously displayed cannot be disentangled here.

DISCUSSION

Ants dragging a heavy food item backwards along their familiar route occasionally trigger a so-called 'peeking behaviour' or 'peek': ants drop their food and turn around to look forwards. Aligning their body in a familiar direction enables them to recognize the learnt visual panorama and store this direction to follow it during their subsequent backward path (Schwarz et al., 2017). Ants clearly gain directional information from learnt terrestrial cues when peeking forwards. However, whether, or not, they use terrestrial cues while dragging their food item backwards is less clear. Several of the current results demonstrate that ants are indeed able to do so, raising questions about the underlying mechanisms.

Backward-Walking Ants Recognize Terrestrial Cues

Experiment 1 shows that the visual scenery experienced while walking backwards influenced the occurrence of peeking behaviour. First, ZV ants (i.e. ants captured at the nest and thus deprived of useful PI information) displayed their first peek earlier when starting their backward journey halfway along the route than when starting at the beginning of the route (Fig. 1e). Second, FV ants (i.e. captured at the feeder and thus having a PI vector pointing towards the nest) displayed their first peek earlier along the route if the surrounding scenery was artificially altered (FVA, Fig. 1d). This was true even though the scene was manipulated only after the ants had started dragging their crumbs backwards indicating that ants paid attention to the familiar scenery while walking backwards. Note that this effect was weak (Fig. 1d), possibly because the alteration of the scene was not obvious enough (Schwarz et al., 2014).

In experiment 2, ants could guide their trajectories based on terrestrial cues while walking backwards. Ants were released on a board (ruling out the use of olfactory cues) and within a lampshade at different locations relative to the nest (Fig. 2). The visual world was revealed to them only after they had started their backward

journey. Nevertheless, and despite the lack of a PI homing vector, their paths were oriented in the expected direction (i.e. the nest) resulting in differences between test conditions. Importantly, this was also true for the portion of path displayed before their first peek, that is, displayed purely backwards (Fig. 2d).

In sum, ants can use learnt terrestrial visual cues while walking backwards to guide their path as well as decide whether and when to peek forwards. The next section discusses potential explanations.

Mental Rotation or Combining Attractive and Repulsive Views?

How can ants recognize views backwards? This is a puzzling question given that the assumption of current models of visual homing states that views must be retinotopically aligned to provide directional information (Ardin, Peng, Mangan, Lagogiannis, & Webb, 2016; Baddeley et al., 2012; Collett, Graham, & Collett, 2017; Le Möel & Wystrach, 2020; Möller, 2012; Murray et al., 2020; Narendra et al., 2013; Wystrach, Cheng, et al., 2011; Wystrach, Mangan, Philippides, & Graham, 2013; Zeil, Hofmann, & Chahl, 2003) although some other processes may also be at work (Wystrach et al., 2012). Recently, it has been suggested that ants may perform some sort of mental rotation to compare misaligned views (Ardin, Mangan, Wystrach, & Webb, 2015; Ardin, Mangan et al., 2016), which may be achieved if views are encoded in the frequency domain (Stone et al., 2017). However, one can wonder why, if they can achieve mental rotation, would they peek at all? A capacity for mental rotation is hard to reconcile with the result of previous experiments where ants would not adjust their backward trajectory at all unless they peeked to align their body in the correct direction (Schwarz et al., 2017).

An alternative hypothesis would be that backward-dragging ants may maintain their body alignment opposite to the nest direction by using the maximum, rather than the minimum, rather the minimum, of the rotational image difference function (Zeil et al., 2003). However, this fails to explain why ants successfully use terrestrial cues to guide their path backwards on a two-way route but not on a two-way route (as in the current experiments) but not on a one-way route (as in a previous experiment, Schwarz et al., 2017). Also to assess the maximum of the rotational image difference function without mental rotation (as for the minimum, Wystrach, Philippides, Aurejac, Cheng, & Graham, 2014) evaluate the relative mismatch across the different rotations; here, however, the ants could maintain a straight backwards path without scanning (Fig. 2d).

We suggest instead a third hypothesis: ants may still need to align their body in a familiar direction to recognize memorized views but possess a memory bank of views learnt while facing in multiple directions and not only towards the nest, as suggested in a related manner for learning and orientation walks (Jayatilaka et al., 2018; Zeil & Fleischmann, 2019). Notably, views learnt while facing away from the nest could be treated as repulsive when homing (Fig. 3a; Jayatilaka et al., 2018; Le Moël & Wystrach, 2019; Murray et al., 2020). Indeed, ants can treat learnt views as repulsive (Wystrach, Buehlmann, Schwarz et al., 2020). The familiarities resulting from the comparison of the currently perceived view with both attractive (nest facing) and aversive (feeder facing) visual memories could simply be compared in a way somewhat analogous to an opponent process, as recently modelled in the light of the insect's neural circuitry (Le Moël & Wystrach 2020). The signal resulting from this comparison informs the ant about whether to move towards or away from the currently faced direction, without the need for scanning (Le Moël & Wystrach 2020). The only additional assumption needed for this model to explain backward guidance is that, if the ant is holding a large food item, 'moving away' means going backwards because the ant cannot lift the crumb to turn her body. Fig. 3a illustrates the functionality of this simple model.

In the light of this model, we can wonder whether ants on the way home can also use the visual memories stored during their outbound trips (i.e. when they went from the nest to the feeder) as repulsive. This idea challenges the opinion that ants treat in- and outbound trips visually separately depending on the motivational state (Harris, Hempel de Ibarra, Graham, & Collett, 2005; Wehner, Boyer, Loertscher; Sommer, & Menzi, 2006). Instead, ants may always recall both their memorized in- and outbound-facing views but treat them as repulsive or attractive depending on their current motivational state.

This attraction/repulsion model explains several observed phenomena of the current and past studies. (1) In a previous experiment (Schwarz et al., 2017) backward-walking ants were not able to correct their path at all because, in this particular set-up, in- and outbound routes were spatially separated (as a one-way circuit) so that no outbound views were available to potentially help out backward-homing ants. (2) In the current experiment 2, backward-walking ants released at the feeder (F) carried on in the correct nest direction (Fig. 2d) because they recognized outbound views oriented towards the feeder, driving them away from (or opposite to) this direction (Fig. 3a). (3) Alteration of the visual surroundings would trigger earlier peeking behaviours because the familiarity of the feeder-facing (outbound) views would be equally altered, disrupting the repulsive effect and thus reducing the overall directional drive (Fig. 1d). (4) Assuming that outbound views near the feeder are more familiar than those in the middle of the route (ants perform learning walks at the feeder, Nicholson, Judd, Cartwright, & Collett, 1999), the repulsive effect would be stronger for ants released at the feeder than in the middle of the route, yielding to a stronger directional drive and hence less peeking near the feeder (Fig. 1d). (5) Further, it was surprising in experiment 2 that ants released close to the nest could direct their backward paths towards the nest (BeN, ByN; Fig. 2c and d). Although this verifies that they recognized familiar views, they nevertheless tended to peek often and even abandoned their crumb close to the nest (nine of 28 in the BeN- and four of 20 in the ByN-test). This seems counterintuitive because views near the nest should be extremely familiar and thus prevent the need for peeking, yet it can be explained in the light of the integration between 'attractive' and 'repulsive' views. During learning walks around the nest, ants indeed appear to store views oriented both towards and away from the nest (Jayatilaka, Murray, Narendra, & Zeil, 2018). Even though all these nest views may be extremely familiar, the integration of attractive (oriented towards the nest) and repulsive (oriented away from the nest) views would result in a low overall directional drive, and thus lead to high peek rates (and a high probability of abandoning the crumb) but nevertheless guide the ants towards the nest. This very same idea explained the recent puzzling observation that ants behaved similarly at the nest and in unfamiliar settings, but not on the foraging route (Murray et al., 2020). (6) Finally, two recent studies have revealed the importance of outbound trips for homing ants. Ants with outbound views during training were more efficient at homing than ants with only inbound views during training (Freas & Cheng, 2018; Freas; Spetch, 2019). Whether homing ants used their outbound view as suggested here, however, or simply learnt homing views by turning back during their outbound trips remains to be seen.

Ants Combine Multiple Directional Cues

Ants are known to combine the directional dictates of the current visual familiarity with their PI in a weighted fashion (Collett, 2012; Wehner, Hoinville, Cruse, & Cheng, 2018). Notably, the

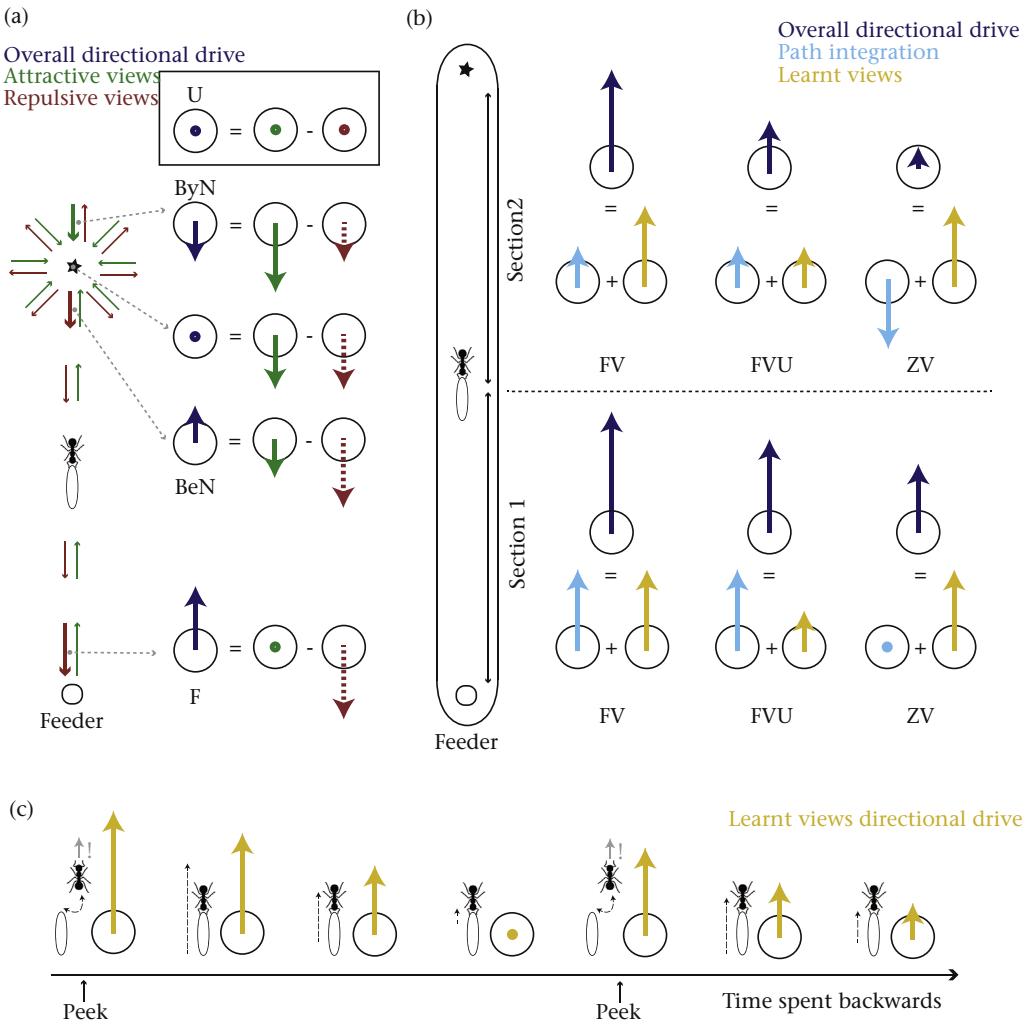

Figure 3. Models on how ants may combine navigational information. The longer the length of the drawn vectors the higher the directional drive. Dots represent cases with no directional drive and stars nest locations. (a) Illustration of the 'repulsive view hypothesis'. Overall directional drive results from the integration of attractive homing views (green arrows) minus repulsive outbound views (red arrows). Left-hand scheme represents theoretical positions and orientations of memorized views. The ant recognizes only views that are aligned with its current body orientation (here, always facing downwards). The larger the distance from the current location to the closest aligned view, the lower the familiarity and directional drive. This principle provides appropriate guidance towards the nest. Right-hand scheme shows examples of integration for different locations (grey dashed arrows) with the ant always facing downwards. For instance, when facing downwards at the BeN location, the closest aligned view is repulsive (bold red arrow on right- and left-hand schemes). Given that the neighbouring green arrow is not aligned, the closest aligned attractive view is further away, beyond the nest (bold green arrow on left-hand scheme). Overall, the ants at this position (still facing downwards) will be more repulsed than attracted by the current facing direction and thus walk backwards towards the nest. In contrast, when beyond the nest, ByN (still facing downwards), the attractive views will match better than the repulsive views and the ants will thus turn around and walk backwards towards the nest. Whatever the position and orientation of the ants around the nest, the agent will be drawn towards the nest. (b) Directional drive across test conditions of experiment 1 in Sections 1 and 2. Ants were tested in FV (full-vector), FVA (full-vector altered familiarity) and ZV (zero-vector) conditions. Overall directional drive (dark blue vectors) results from the integration of path integration (cyan vectors, the longer the path integration vector the stronger its directional drive) and learnt views (yellow vectors, the more familiar the view the stronger its directional drive). (c) Directional drive resulting from the recognition of a learnt view (yellow vectors) decreases with time spent facing in a different direction. Low directional drive results in lower speed (dashed arrow) and eventually peeking. Here memorized views are assumed to be facing upwards and are thus recognized only when facing upwards during peeking (small grey arrow) and not while facing downwards during backward motion. Note that the second peek triggers a lower directional drive than the first (see also Fig. 1b).

direction indicated by the current view is weighted more as the current view is familiar (Legge, Wystrach, Spetch, & Cheng, 2014) and the direction indicated by the PI is weighted more as the PI vector length increases (Wystrach et al., 2015). Backward-walking ants appear to weight these cues in the same fashion. Fig. 3b shows how this integration of cues captures the peek rate observed across our conditions and distance walked along the route. Notably, this explains why ZV-ants peeked earlier and more often than FV-ants (Fig. 1b), as observed in North African *Cataglyphis fortis* ants (Pfeffer & Wittlinger, 2016) and why peek rate increased as the distance walked along the route increased (Fig. 1d and e), as observed in *Myrmecia croslandi* ants (see Figure S2 in Schwarz et al., 2017).

Interestingly, such an estimate of directional certainty seems to influence not only the occurrence of peeking but also whether the peeking ants decided to return to their crumb or abandon it. All 32 FV-ants in familiar visual surroundings and therefore with the highest directional certainty dragged their crumb all the way along the 7.20 m route. In contrast, some ants abandoned their crumbs in both FVA (six of 31) and ZV (six of 33) conditions.

Finally, ants clearly increased the speed of their backward motion after peeking (Fig. 1b). The increase in speed is likely to be not only a mere consequence of a short recovery from the dragging activity but also a gain in navigational certainty as this sudden speed increase is also apparent when displaced foragers reach their familiar route and recognize the familiar scenery (S. Schwarz, A.

Wystrach & M. Mangan, personal observation). Furthermore, a decrease in speed when ants run off their PI has been described (Buehlmann, Fernandes, & Graham, 2018). Hence it seems that the speed of movement reflects the strength of the directional drive and therefore directional certainty (however, see Buehlmann, Aussel, & Graham, 2020). If peeking behaviour seems to increase directional certainty, the latter seems to decrease with time spent backwards (Fig. 3c), which also makes functional sense.

Ants Gather Information About Time Spent Backwards

Recently, it has been shown that directional information based on terrestrial cues is obtained when ants face forwards during peeks and must therefore be stored in a short-term memory while the ant is subsequently walking backwards (Schwarz et al., 2017). Our results suggest that short-term memory also influences the ants' navigational certainty. The time spent peeking forwards varied (as already noted by Pfeffer & Wittlinger, 2016) with some ants 'peeking' for less than 1 s while others spent more than 60 s (after which recording was stopped) without returning to their crumb. Interestingly, the more an ant had peeked before during a test run, the longer her current peek lasted (Fig. 2b). This shows that ants somehow gather information across time to adjust their current certainty: either information about the overall time spent backwards or information about the number of peeks previously displayed (see also Fig. 3c).

Previous experiments have already shown that the behaviour of ants can be modulated by recent experience in the order of seconds to minutes, a form of hysteresis (Graham & Mangan, 2015). For instance, ants display a so-called backtracking behaviour only if they have recently perceived the nest surroundings (Wystrach, Schwarz, Baniel, & Cheng, 2013). Also, homing ants meander more along their paths when recapitulating a well-known route for the second time in a row (Collett, 2014; Wystrach, Schwarz, Graham, & Cheng, 2019). Finally, ants can remember the compass direction of a wind gust that blows them off course (Wystrach & Schwarz, 2013). In the present case, ants also seemed to build up information about the recent past. Even though it makes functional sense, it remains to be seen what neural or physiological mechanisms underlie this phenomenon.

Conclusion

This study confirmed that ants walking backwards are not just paying attention to celestial cues but combine multiple information from their PI, the recognition of terrestrial cues and temporal information such as the time they spent backwards. All this information seems to be integrated in an overall directional drive. This drive, which reflects the current directional certainty, seems to (1) guide the ants' backward path, (2) trigger peeking behaviour if too low and, finally, (3) dictate whether, or not, to return to their food item during peeks. Importantly, this study shows that ants use familiar terrestrial cues while navigating backwards. In addition to using the attractive memories facing towards the nest, the hypothesis that homing ants use a collection of repulsive visual memories facing away from the nest and possibly stored during their outbound trip has been put forward (Jayatilaka et al., 2018; Le Moël & Wystrach, 2020; Zeil & Fleischmann, 2019; Murray et al., 2020). In the light of this hypothesis, visual navigation forwards or backwards can then be achieved simply by using the relative familiarity between both sets of opposite valence memories. As often with research on insect navigation, remarkably flexible behaviours incite researchers to endorse the simplest explanations (Wystrach & Graham, 2012).

Author Contributions

S.S. and A.W. conceptualized the study and performed the analysis; S.S., L.C., E.G. and A.W. carried out the experiments; S.S. wrote the original draft of the manuscript and S.S., L.C., E.G. and A.W. reviewed and edited it; A.W. obtained the funding.

Acknowledgments

We are grateful to Xim Cerda and his helpful team at CSIC Seville for permanent assistance in logistics and administration during field work. We also thank Cornelia Buehlmann, Scarlett Dell-Cronin, Cody Freas and Michael Mangan for manual and moral support during field preparation and data collection. Finally, we are grateful for the constructive feedback of Paul Graham on the manuscript and the comments of two anonymous referees. The study was partly financed by The European Research Council, 759817-EMERG-ANT ERC-2017-STG.

References

Ardin, P., Mangan, M., Wystrach, A., & Webb, B. (2015). How variation in head pitch could affect image matching algorithms for ant navigation. *Journal of Comparative Physiology, 201*, 585–597.

Ardin, P., Peng, F., Mangan, M., Lagogiannis, K., & Webb, B. (2016). Using an insect mushroom body circuit to encode route memory in complex natural environments. *PLoS Computational Biology, 12*, e1004683.

Ardin, P. B., Mangan, M., & Webb, B. (2016). Ant homing ability is not diminished when traveling backwards. *Frontiers in Behavioral Neuroscience, 10*, 69.

Baddeley, B., Graham, P., Husbands, P., & Philippides, A. (2012). A model of ant route navigation driven by scene familiarity. *PLoS Computational Biology, 8*, 1002336.

Buehlmann, C., Aussel, A., & Graham, P. (2020). Dynamic multimodal interactions in navigating wood ants: What do path details tell us about cue integration? *Journal of Experimental Biology, 223*. https://doi.org/10.1242/jeb.221036. jeb221036.

Buehlmann, C., Fernandes, A., & Graham, P. (2018). The interaction of path integration and terrestrial visual cues in navigating desert ants: What can we learn from path characteristics? *Journal of Experimental Biology, 221*.

Cerda, X. (2001). Behavioural and physiological traits to thermal stress tolerance in two Spanish desert ants. *Etología, 9*, 15–27.

Cheng, K., Narendra, A., Sommer, S., & Wehner, R. (2009). Traveling in clutter: Navigation in the central Australian desert ant *Melophorus bagoti*. *Behavioural Processes, 80*, 261–268.

Collett, M. (2012). How navigational guidance systems are combined in a desert ant. *Current Biology, 22*, 927–932.

Collett, M. (2014). A desert ant's memory of recent visual experience and the control of route guidance. *Proceedings of the Royal Society B: Biological Sciences, 281*, 20140634.

Collett, M., Graham, P., & Collett, T. S. (2017). Insect navigation: What backward walking reveals about the control of movement. *Current Biology, 27*, 141–143.

Collett, T., Graham, P., & Durier, V. (2003). Route learning by insects. *Current Opinion in Neurobiology, 13*, 718–725.

Freas, C. A., & Cheng, K. (2018). Landmark learning, cue conflict, and outbound view sequence in navigating desert ants. *Journal of Experimental Psychology: Animal Learning and Cognition, 44*, 409–421.

Freas, C. A., & Spetch, M. L. (2019). Terrestrial cue learning and retention during the outbound and inbound foraging trip in the desert ant, *Cataglyphis velox*. *Journal of Comparative Physiology, 205*, 177–189.

Graham, P., & Mangan, M. (2015). Insect navigation: Do ants live in the now? *Journal of Experimental Biology, 218*, 819–823.

Harris, R. A., Hempel de Ibarra, N., Graham, P., & Collett, T. S. (2005). Priming of visual route memories. *Nature, 438*, 302.

Heinze, S., Narendra, A., & Cheung, A. (2018). Principles of insect path integration. *Current Biology, 28*, 1023–1058.

Hoinville, T., & Wehner, R. (2018). Optimal multiguidance integration in insect navigation. *Proceedings of the National Academy of Sciences of the United States of America, 115*(11), 2824–2829.

Jayatilaka, P., Murray, T., Narendra, A., & Zeil, J. (2018). The choreography of learning walks in the Australian jack jumper ant *Myrmecia croslandi*. *Journal of Experimental Biology, 221*, 185306.

Le Möel, F., & Wystrach, A. (2020). Opponent processes in visual memories: A model of attraction and repulsion in navigating insects' mushroom bodies. *PLoS Computational Biology, 16*, e1007631.

Legge, E., Wystrach, A., Spetch, M., & Cheng, K. (2014). Combining sky and earth: desert ants (*Melophorus bagoti*) show weighted integration of celestial and terrestrial cues. *Journal of Experimental Biology, 217*, 4159–4166.

Mangan, M., & Webb, B. (2012). Spontaneous formation of multiple routes in individual desert ants (*Cataglyphis velox*). *Behavioral Ecology, 23*, 944–954.

Möller, R. (2012). A model of ant navigation based on visual prediction. *Journal of Theoretical Biology, 305*, 118–130.
Murray, T., Zoltán, K., Dahmen, H., Le Möel, F., Wystrach, A., & Zeil, J. (2020). The role of attractive and repellent scene memories in ant homing (*Myrmecia croslandi*). *Journal of Experimental Biology, 223*, jeb210021.
Narendra, A., Gourmaud, S., & Zeil, J. (2013). Mapping the navigational knowledge of individually foraging ants, *Myrmecia croslandi*. *Proceedings of the Royal Society B: Biological Sciences, 280*, 20130683.
Nicholson, D. J., Judd, S. P. D., Cartwright, B. A., & Collett, T. S. (1999). Learning walks and landmark guidance in wood ants (*Formica rufa*). *Journal of Experimental Biology, 202*, 1831–1838.
Pfeffer, S., Wahl, V., & Wittlinger, M. (2016). How to find home backwards? Locomotion and inter-leg coordination during rearward walking of *Cataglyphis fortis* desert ants. *Journal of Experimental Biology, 219*, 2110–2118.
Pfeffer, S., & Wittlinger, M. (2016). How to find home backwards? Navigation during rearward homing of *Cataglyphis fortis* desert ants. *Journal of Experimental Biology, 219*, 2119–2126.
Reid, S. F., Narendra, A., Hemmi, J. M., & Zeil, J. (2011). Polarised skylight and the landmark panorama provide night-active bull ants with compass information during route following. *Journal of Experimental Biology, 214*, 363–370.
Schwarz, S., Albert, L., Wystrach, A., & Cheng, K. (2011). Ocelli contribute to the encoding of celestial compass information in the Australian desert ant *Melophorus bagoti*. *Journal of Experimental Biology, 214*, 901–906.
Schwarz, S., Julle-Daniere, E., Morin, L., Schultheiss, P., Wystrach, A., Ives, J., et al. (2014). Desert ants (*Melophorus bagoti*) navigating with robustness to distortions of the natural panorama. *Insectes Sociaux, 61*, 371–383.
Schwarz, S., Mangan, M., Zeil, J., Webb, B., & Wystrach, A. (2017). How ants use vision when homing backward. *Current Biology, 27*, 401–407.
Stone, T., Webb, B., Adden, A., Weddig, N., Honkanen, A., Templin, R., … Heinze, S. (2017). An anatomically constrained model for path integration in the bee brain. *Current Biology, 27*, 3069–3085. e3011.
Wehner, R. (2003). desert ant navigation: How miniature brains solve complex tasks. *Journal of Comparative Physiology, 189*, 579–588.
Wehner, R., Boyer, M., Loertscher, F., Sommer, S., & Menzi, U. (2006). Ant navigation: One-way routes rather than maps. *Current Biology, 16*, 75–79.
Wehner, R., Hoinville, T., Cruse, H., & Cheng, K. (2018). Steering intermediate courses: desert ants combine information from various navigational routines. *Journal of Comparative Physiology, 202*, 459–472.
Wehner, R., & Srinivasan, M. V. (2003). Path integration in insects. In K. K. Jeffrey (Ed.), *The neurobiology of spatial behaviour* (pp. 9–30). Oxford, U.K.: Oxford University Press.
Wittlinger, M., Wehner, R., & Wolf, H. (2006). The ant odometer: Stepping on stilts and stumps. *Science, 312*, 1965–1966.
Wystrach, A., Beugnon, G., & Cheng, K. (2011). Landmarks or panoramas: What do navigating ants attend to for guidance? *Frontiers in Zoology, 8*, 21.
Wystrach, A., Beugnon, G., & Cheng, K. (2012). Ants might use different view-matching strategies on and off the route. *Journal of Experimental Biology, 215*, 44–55.
Wystrach, A., Buehlmann, C., Schwarz, S., Cheng, K., & Graham, P. (2020). Rapid aversive and memory trace learning during route navigation in desert ants. *Current Biology*. https://doi.org/10.1016/j.cub.2020.02.082.
Wystrach, A., Cheng, K., Sosa, S., & Beugnon, G. (2011). Geometry, features, and panoramic views: Ants in rectangular arenas. *Journal of Experimental Psychology: Animal Behavior Processes, 37*, 420–435.
Wystrach, A., & Graham, P. (2012). What can we learn from studies of insect navigation? *Animal Behaviour, 84*, 13–20.
Wystrach, A., Mangan, M., Philippides, A., & Graham, P. (2013). Snapshots in ants? New interpretations of paradigmatic experiments. *Journal of Experimental Biology, 216*, 1766–1770.
Wystrach, A., Mangan, M., & Webb, B. (2015). Optimal cue integration in ants. *Proceedings of the Royal Society B: Biological Sciences, 282*, 20151484.
Wystrach, A., Philippides, A., Aurejac, A., Cheng, K., & Graham, P. (2014). Visual scanning behaviours and their role in the navigation of the Australian desert ant Melophorus bagoti. *Journal of Comparative Physiology A, 200*, 615–626.
Wystrach, A., & Schwarz, S. (2013). Ants use a predictive mechanism to compensate for passive displacements by wind. *Current Biology, 23*, 1083–1085.
Wystrach, A., Schwarz, S., Baniel, A., & Cheng, K. (2013). Backtracking behaviour in lost ants: An additional strategy in their navigational toolkit. *Proceedings of the Royal Society B: Biological Sciences, 280*, 20131677.
Wystrach, A., Schwarz, S., Graham, P., & Cheng, K. (2019). Running paths to nowhere: Repetition of routes shows how navigating ants modulate online the weights accorded to cues. *Animal Cognition, 22*, 213–222.
Wystrach, A., Schwarz, S., Schultheiss, P., Baniel, A., & Cheng, K. (2014). Multiple sources of celestial compass information in the Central Australian desert ant *Melophorus bagoti*. *Journal of Comparative Physiology, 200*, 591–601.
Zeil, J. (2012). Visual homing: An insect perspective. *Current Opinion in Neurobiology, 22*, 285–293.
Zeil, J., & Fleischmann, P. N. (2019). The learning walks of ants (Hymenoptera: Formicidae). *Myrmecological News, 29*, 93–110.
Zeil, J., Hofmann, M. I., & Chahl, J. S. (2003). Catchment areas of panoramic snapshots in outdoor scenes. *Journal of the Optical Society of America A, 20*, 450–469.

A lateralised design for the interaction of visual memories and heading representations in navigating ants.

Antoine Wystrach[1*], Florent Le Moël[1], Leo Clement[1], Sebastian Schwarz[1]

[1]Centre de Recherches sur la Cognition Animale, Centre de Biologie Intégrative, Université de Toulouse, CNRS, Université Paul Sabatier, 31062 Toulouse cedex 9, France

[*]Corresponding author:

Antoine Wystrach: antoine.wystrach@univ-tlse3.fr

***Abstract*:**

The navigational skills of ants, bees and wasps represent one of the most baffling examples of the powers of minuscule brains. Insects store long-term memories of the visual scenes they experience [1], and they use compass cues to build a robust representation of directions [2,3]. We know reasonably well how long-term memories are formed, in a brain area called the Mushroom Bodies (MB) [4–8], as well as how heading representations are formed in another brain area called the Central Complex (CX) [9–12]. However, how such memories and heading representations interact to produce powerful navigational behaviours remains unclear [7,13,14]. Here we combine behavioural experiments with computational modelling that is strictly based on connectomic data to provide a new perspective on how navigation might be orchestrated in these insects. Our results reveal a lateralised design, where signals about whether to turn left or right are segregated in the left and right hemispheres, respectively. Furthermore, we show that guidance is a two-stage process: the recognition of visual memories – presumably in the MBs – does not directly drive the motor command, but instead updates a "desired heading" – presumably in the CX – which in turn is used to control guidance using celestial compass information. Overall, this circuit enables ants to recognise views independently of their body orientation, and combines terrestrial and celestial cues in a way that produces exceptionally robust navigation.

Bilaterally decorrelated input to the CX produces goal-oriented paths.

We first investigated how information about the visual familiarity of the scenes – as computed in the MB – could plausibly be sent to the CX for guidance given the known circuitry of insect brains. Even though our current approach is an experimental one, the CX circuitry is understood and conserved enough to make such effort possible using biologically constrained neural modelling [12,15–17].

Recent studies have shown that the CX circuits can: 1) track the current heading, in two substructures called Ellipsoid Body (EB) and Protocerebral Bridge (PB) [10,11,18]; 2) retain a desired heading representation for tens of seconds in the Fan-shaped Body (FB) [14]; and 3) compare both current and desired headings to output compensatory left/right steering commands [14,19]. The desired heading can be updated by bilateral signals to the FB from external regions [14]. Such a signal can plausibly come from the recognition of long-term visual memories in the MB, which sends bilateral input to the FB through one relay in the Superior Intermediate Protocerebrum (SIP). These observations led to the idea that navigation, such as learnt route following, could emerge by having the MBs signalling to the CX when the insect is facing its familiar route direction or not [7,13,14].

We thus tested the viability of this hypothesis by building a model of the CX, strictly based on this connectivity (Fig. 1). Contrary to what was expected, our model shows that having the bilateral 'visual familiarity' signals to the FB correspond with the moments when the agent is facing the correct route direction did not allow straight routes to emerge. A thorough search through the parameter space revealed that this configuration produces a mediocre directionality at best, and is very sensitive to parameter change (Extended data fig. 1). Contrastingly, route following becomes extremely stable and robust to parameter changes as soon as the signals to the FB from the left and right brain hemispheres correspond to moments where the agent is oriented to the right or the left of its goal, respectively (Fig. 1). Impressively, varying parameters (such as the time during which FB neurons sustain their activity, or the heading angle away from the goal for which left or right input signals are strongest) hardly has any effect: straight routes emerge as long as left and right hemispheric inputs roughly correlate with a right and left heading bias, respectively (Fig. 1, Extended data fig. 1). As a corollary, if left and right hemispheric inputs correlate instead with left and right (rather than right and left) heading biases, a straight route in the

reverse direction emerges (Fig. 1). Thus, having the input signal correlate with moments where the agent faces the goal direction corresponds to a zone of transition between two stable regimes of route-following in opposite directions.

In other words, this suggests that recognising views when facing the goal may not be a good solution, and instead, it shows that the CX circuitry is remarkably adapted to control a visual course as long as the input signals from the visual familiarity of the scene to both hemispheres are distinct, with one hemisphere signalling when the agent's heading is biased towards the right and the other, towards the left. This model makes particular predictions, which we next tested with behavioural experiments.

The recognition of familiar views triggers compensatory left or right turns.

Previous studies assumed that ants memorise views while facing the goal [20–22] and anti-goal [23–25]) directions, and that they must consequently align their body in these same directions to recognise a learnt view as familiar [26–28]. On the contrary, our modelling effort suggests that ants should rather recognise views based on whether the route direction stands on their 'left or right' rather than 'in front or behind'. We put this idea to the test using an open-loop trackball system enabling the experimenter to choose both the position and body orientation of tethered ants directly in their natural environment [29]. We trained ants along a route and captured homing individuals just before they entered their nest to ensure that these so-called zero-vector ants (ZV) could no longer rely on their path integration homing vector [30]. We recorded the motor response of these ants while mounted on the trackball system, in the middle of their familiar route, far from the catchment area of the nest, when fixed in eight different body orientations (Fig. 2a, b). Results show that, irrespective of their body orientation, ants turned mostly towards the correct route direction (Fig. 2c). When the body was oriented towards (0°, nest direction) or away (180°) from the route direction, ants still showed a strong preference for turning on one side (to the left or to the right, depending on individuals) (Fig. 2d). This was not the case when ants were tested in unfamiliar surroundings (Fig. 2c, d), showing that the lateralised responses observed on the familiar route was triggered by the recognition of the visual scene. This implies that ants can recognise their route independently of their body orientation, and can derive whether the

route direction is towards their left or their right. Importantly, even when facing the route or anti-route direction, recognition of familiar views appears to trigger a 'left vs. right' decision rather than a 'go forward vs. turn' decision.

Guidance based on memorised views involves the celestial compass.

We showed that the recognition of familiar views indicates whether the goal direction is towards the left or right. In principle, guidance could thus be achieved by having these left/right signals directly trigger the left or right motor command. An alternative would be, as in our model, that such left/right signals can be used to update the 'desired heading directions' in the CX, which in turn uses its own compass information to control steering (Fig. 1). This makes a counterintuitive prediction: if the recognition of familiar views triggers a turn towards the correct side, reversing the direction of the compass representation in the CX should immediately reverse the motor decision. We tested this prediction by mirroring the apparent position of the sun in the sky by 180° to *Cataglyphis velox* ants tethered to our trackball system. A previous study had shown that this manipulation was sufficient to shift this species' compass heading representation [31].

We first tethered well-trained ZV ants (i.e., captured just before entering the nest) on our trackball system with their body orientation fixed perpendicularly to their familiar route direction. As expected, ants in this situation turned towards the correct route direction (Fig. 3, left panels, natural sun), indicating that they correctly recognised familiar visual terrestrial cues. When mirroring the apparent sun's position by 180°, these ants responded by turning in the opposite direction within one second (Fig. 3, left panel, mirrored sun). We repeated the experiment by placing such ZV ants in the same compass direction but in an unfamiliar location. In this situation, the ants turned in random directions (Fig. 3, middle panels), showing that the direction initially chosen by the ants on their familiar route (Fig. 3, left panels) was based on the recognition of terrestrial rather than celestial cues. It however remains unclear whether the sun rotation had an impact on ants in unfamiliar terrain, as ants in this situation regularly alternate between left and right turns anyway [25]. Finally, to ensure that the observed effect on route was not due to an innate bias at this particular location, we repeated this experiment with ants tethered at the exact same route location

and body orientation, but this time only with ants that were trained to an alternative straight route, which was aligned with the tethered direction of the trackball (Fig. 3, right panel). As expected, these ants showed no preference in turning direction at the group level, although most individuals still strongly favoured one side rather than walking straight (Fig. 3 right panels). Interestingly, mirroring the sun significantly reversed the individual's chosen direction (even though they were aligned with their goal direction) (Fig. 3c right panels).

Taken together these results show that guidance based on learnt views is a two-stage process: the recognition of visual memories – presumably through the MBs – does not directly drive the motor command, but it instead signals a desired heading – presumably through the CX –, which in turn is used to control guidance using celestial compass information.

A complex interaction between terrestrial and celestial guidance

The results from above point at a complex interaction between the use of long-term memory of terrestrial cues – indicating whether the goal is left or right – and the heading estimate based on compass cues. To further endorse the credibility of our proposed guidance system, we used our model to explore how agents navigating along their familiar route would react to a sudden 135° shift of the CX current celestial compass estimate, and compared their behaviour to that of real homing ZV ants tested in a similar scenario, where we shifted the sun position by 135° using a mirror (Fig. 4). Impressively, and despite the nonlinear dynamics at play, the simulated shift in the CX model closely resembled the response of the ants to the sun manipulation, adding credibility to the model and helping us grasp the mechanisms at play (Fig. 4).

General discussion

We showed that during view-based navigation, ants recognise views when oriented left and right from their goal to trigger left and right turns. Facing in the correct route direction does not trigger a 'go forward' command, but marks some kind of labile equilibrium point in the system. Also, we show that the recognition of left or right familiar views does not drive the

motor decision directly but is perfectly suited to inform the CX, which in turn maintains the desired heading using its own compass information. The advantage of this design is clear considering that the recognition of learnt visual terrestrial cues is sensitive to variables such as body orientation [31,32] or partial visual obstructions that must happen continuously when navigating through grassy or leafy environments, making the visual familiarity signal mediated by the MBs inherently noisy. In contrast, the CX provides a stable and sustained heading representation by integrating self-motion [11] with multiple wide-field celestial [10] and terrestrial cues [9,33]. The CX is thus well suited to act as a heading buffer from the noisy MBs signal, resulting in smooth and stable guidance control. In addition, the compass representation in the CX enables to steer the direction of travel independently of the actual body orientation [12]. Our results thus explain how ants visually recognise a view using the MBs and subsequently follow such direction backwards using the CX [31] or how ants can estimate the actual angular error between the current and goal directions before initiating their turn [34]. Also, in addition to route following, such a lateralised design can produce remarkably robust homing in complex environments (Wystrach et al., 2020 in prep).

Finally, the proposed circuit offers an interesting take on the evolution of navigation. Segregating 'turn left' and 'turn right' signals between hemispheres evokes the widespread tropotaxis, where orientation along a gradient is achieved by directly comparing the signals intensities between physically distinct left and right sensors (e.g., antennae or eyes) in bilateral animals [35–41]. Comparing signals between hemispheres could thus be an ancestral strategy in arthropods; and ancestral brain structures such as the CX accommodates well such a bilateral design and may be constrained to receive such lateralised input to function properly. The evolution of visual route-following in hymenoptera is a relatively recent adaptation, and it cannot be achieved by directly comparing left and right visual inputs – which is probably why each eye can afford to project to both hemispheres' MBs [42,43]. Categorising learnt views as indicators of whether the goal is to the left or to the right, and subsequently segregating this information in the left and right hemispheres may thus be an evolutionary adaptation to fit the ancestrally needed bilateral inputs to the CX (Fig. 1).

How left and right visual memories are acquired and learnt when naive insects explore the world for the first time remains to be seen. During their learning flights, wasps regularly alternate between moments facing 45° to the left and 45° to the right of their goal, strongly

supporting our claim that insect form such left and right memories [44]. During their meandering learning walks, ants tend to reverse turning direction when facing the nest or anti-nest direction [21,23,45], however, they do expose their gaze in all directions, providing ample opportunities to form a rich set of left and right visual memories [45]. Our model shows that the angle at which views are learnt does not need to be precisely controlled (Fig. 1c,d). Views facing the nest may as well be included during learning and categorised as left, right or both, explaining why most ants facing their goal usually choose to turn in one particular direction while others turned less strongly. During learning, the first source of information about whether the current body orientation is left or right from the goal probably results from path integration. Interestingly, lateralised dopaminergic feedback from the Lateral Accessory Lobes (LAL, a pre-motor area) to the MBs could represent an ideal candidate to orchestrate such a categorisation of left/right memories (Wystrach et al., 2020 in prep). Revisiting current questions in insect and robot navigation such as early exploration, route following and homing [20,46–49]; the integration of aversive memories [8,24,50], path integration and views ([51–54] or other sensory modalities ([55–58] as well as seeking for underlying neural correlates [5–7] – with such a lateralised design as a framework promises an interesting research agenda.

Acknowledgments: We thank the Profs. Jochen Zeil and Xim Cerda to provide us access to field sites in ANU Canberra, Australia and Sevilla, Spain, respectively. We are grateful to the Prof. Hansjuergen Dahmen for helping us setting the trackball device. We thank the Profs. Rüdiger Wehner, Tom Collett and Paul Graham for fruitful discussions and comments on earlier versions of the manuscript.

Authors contributions

Research design: AW. Data collection: AW, SS, FLM, LC. Trackball system design: FLM. Data analysis: AW, SS, FLM. Modelling: AW. Manuscript writing: AW.

Funding

This work was funded by the ERC Starting Grant EMERG-ANT no. 759817 to AW.

Method

The trackball setup:

For both experiments (fig 2 and 3) we used the air-suspended trackball setup as described in Dahmen et al., 2017 [29]; and chose the configuration where the ants are fixed in a given direction and cannot physically rotate (if the ant tries to turn, the ball counter-rotates under its legs). To fix ants on the ball, we used a micro-magnet and metallic paint applied directly on the ant's thorax. The trackball air pump, battery and computer were connected to the trackball through 10 m long cables and hidden in a remote part of the panorama. The trackball movements were recorded using custom software in C++, data was analysed with Matlab and can be provided upon request.

Routes setups and ant training in Cataglyphis velox:

For all experiments (fig. 2 and 3 and 4), *Cataglyphis velox* ants were constrained to forage within a route using dug wood planks that prevented them to escape, while leaving the surrounding panoramic view of the scenery intact (as described in Wystrach et al., 2012[59]). Cookie crumbs were provided ad libitum in the feeder positions for at least two days before any tests. Some barriers dug into the ground created baffles, enabling us to control whether ants were experienced with the route. Ants were considered trained when able to home along the route without bumping into any such obstacle. These ants were captured just before they entered their nest to ensure that they could not rely on path integration (so-called ZV ants), marked with a metallic paint on the thorax and a colour code for individual identification, and subjected to tests (see next sections).

Routes setups and ant training in Myrmecia croslandi:

For the experiment with *Myremcia croslandi* ants (fig. 2), we used each individual's natural route, for which these long-lived ants have extensive experience [60]. Individuals were captured on their foraging trees, marked with both metallic paint and a colour code for individual identification, given a sucrose solution or a prey and released where they had been captured (on their foraging tree). Upon release, most of these ants immediately started

to return home. We followed them while marking their route using flag pins every 50 cm (so that their exact route was known). We captured the ants just before they entered their nests and subjected them to the test on the trackball (see next section).

Experimental protocol for the left/right trackball experiment (figure 2):

1- An experienced ant was captured just before entering its nest, and marked with a drop of metallic paint on the thorax.
2- A large opaque ring (30 cm diameter, 30 cm high) was set around the trackball setup.
3- The ant was fixed on the trackball within the opaque ring, which prevented her to see the surroundings. Only a portion of sky above was accessible to the ant.
4- The trackball system (together with the opaque ring and the fixed ant within) was moved to the desired position and rotated so that the ant was facing the desired direction.
5- One experimenter started recording the trackball movements (from the remote computer), when another lifted the ring (so the ant could see the scenery) before leaving the scene, letting the ant behave for at least 15 seconds post ring lifting.
6- The experimenter came back, replaced the ring around the trackball system, and rotated the trackball system (following a pre-established pseudo random sequence) for the ant to face in a novel direction.
7- We repeated steps 5 and 6 until the 8 possible orientations were achieved (the sequence of orientations were chosen in a pseudo-random order so as to counter-balance orientation and direction of rotation).
The data shown in fig. 2 for each orientation is averaged across 12 sec of recording (from 3 sec to 15 sec assuming ring lifting is at 0 sec). We decided to let 3 sec after ring lifting, as the movements of the experimenter before he leaves the scenery might disturb the ants).
In all experiments, ants were tested only once.

Experimental protocol for the mirror trackball experiments (figure 3):

1- An experienced ant was captured just before entering its nest, and marked with a drop of metallic paint on the thorax.

2- A large opaque ring (30 cm diameter, 30 cm high) was set around the trackball setup.
3- The ant was fixed on the trackball within the opaque ring, which prevented her to see the surroundings. Only a portion of sky above was accessible to the ant.
4- The trackball system (together with the opaque ring and the fixed ant within) was moved to the desired position and rotated so that the ant was facing the desired direction.
5- One experimenter started recording the trackball movements, when another lifted the ring (so the ant could see the scenery) before leaving the scene, letting the ant behave for at least 10 seconds post ring lifting.
5- Two experimenters simultaneously hid the real sun and projected the reflected sun using a mirror, so that the sun appeared in the opposite position of the sky to the ant for at least 8 seconds.
Ants were tested only once, in one of the conditions.

Experimental design and protocol for the mirror experiment with ants on the floor *(figure 4):*

Cataglyphis velox ants were trained to a 10 meters-long route for at least two consecutive days. A 240 × 120 cm thin wood board was placed on the floor in the middle of the route, ensuring that the navigating ants walked smoothly without encountering small clutter over this portion of the route. Homing ants were captured just before entering their nest and released at the feeder as ZV ants. Upon release, these ZV ants typically resume their route homing behaviour; at mid-parkour (halfway along the board section) the real sun was hidden by one experimenter and reflected by another, using a mirror, for the sun to appear to the ant 135° away from its original position in the sky. To ensure that each individual was tested only once, tested ants were marked with a drop of paint after the procedure.

The ZV ants walking on the board were recorded using a Panasonic Lumix DMC-FZ200 camera on a tripod, and their paths were digitised frame by frame at 10 fps using image J. We used four marks on the board to correct for the distortion due to the tilted perspective of the camera's visual field. Analysis of the paths were achieved with Matlab.

The CX neural model.

The CX model circuitry and input signals are described in Extended data figure 2 (a-d), and the different parameters used to obtain the output (motor command) are described in Extended data figure 1. All the modelling has been achieved with Matlab, and can be provided upon request.

References

1. Collett, M., Chittka, L. & Collett, T. S. Spatial memory in insect navigation. *Current biology : CB* **23**, R789–R800 (2013).
2. Collett, T. S. & Collett, M. Path integration in insects. *Current Opinion in Neurobiology* **10**, 757–762 (2000).
3. Wystrach, A., Schwarz, S., Schultheiss, P., Baniel, A. & Cheng, K. Multiple sources of celestial compass information in the central Australian desert ant Melophorus bagoti. *Journal of Comparative Physiology A* 1–11 (2014).
4. Ardin, P., Peng, F., Mangan, M., Lagogiannis, K. & Webb, B. Using an Insect Mushroom Body Circuit to Encode Route Memory in Complex Natural Environments. *PLOS Computational Biology* **12**, e1004683 (2016).
5. Buehlmann, C. *et al.* Mushroom Bodies Are Required for Learned Visual Navigation, but Not for Innate Visual Behavior, in Ants. *Current Biology* (2020) doi:10.1016/j.cub.2020.07.013.
6. Kamhi, J. F., Barron, A. B. & Narendra, A. Vertical Lobes of the Mushroom Bodies Are Essential for View-Based Navigation in Australian Myrmecia Ants. *Current Biology* (2020) doi:10.1016/j.cub.2020.06.030.
7. Webb, B. & Wystrach, A. Neural mechanisms of insect navigation. *Current Opinion in Insect Science* **15**, 27–39 (2016).
8. Wystrach, A., Buehlmann, C., Schwarz, S., Cheng, K. & Graham, P. Rapid Aversive and Memory Trace Learning during Route Navigation in Desert Ants. *Current Biology* **30**, 1927-1933.e2 (2020).
9. Kim, S. S., Hermundstad, A. M., Romani, S., Abbott, L. F. & Jayaraman, V. Generation of stable heading representations in diverse visual scenes. *Nature* **576**, 126–131 (2019).
10. Pfeiffer, K. & Homberg, U. Organization and Functional Roles of the Central Complex in the Insect Brain. *Annual Review of Entomology* **59**, null (2014).
11. Seelig, J. D. & Jayaraman, V. Neural dynamics for landmark orientation and angular path integration. *Nature* **521**, 186–191 (2015).

12. Stone, T. *et al.* An Anatomically Constrained Model for Path Integration in the Bee Brain. *Current Biology* **27**, 3069-3085.e11 (2017).
13. Collett, M. & Collett, T. S. How does the insect central complex use mushroom body output for steering? *Current Biology* **28**, R733–R734 (2018).
14. Honkanen, A., Adden, A., Freitas, J. da S. & Heinze, S. The insect central complex and the neural basis of navigational strategies. *Journal of Experimental Biology* **222**, jeb188854 (2019).
15. Franconville, R., Beron, C. & Jayaraman, V. Building a functional connectome of the Drosophila central complex. *eLife* **7**, e37017 (2018).
16. Le Moël, F., Stone, T., Lihoreau, M., Wystrach, A. & Webb, B. The Central Complex as a Potential Substrate for Vector Based Navigation. *Front. Psychol.* **10**, (2019).
17. Pisokas, I., Heinze, S. & Webb, B. The head direction circuit of two insect species. *eLife* **9**, e53985 (2020).
18. Heinze, S. & Homberg, U. Maplike representation of celestial E-vector orientations in the brain of an insect. *Science* **315**, 995–997 (2007).
19. Green, J., Vijayan, V., Pires, P. M., Adachi, A. & Maimon, G. A neural heading estimate is compared with an internal goal to guide oriented navigation. *Nature neuroscience* **22**, 1460–1468 (2019).
20. Fleischmann, P. N., Rössler, W. & Wehner, R. Early foraging life: spatial and temporal aspects of landmark learning in the ant Cataglyphis noda. *Journal of Comparative Physiology A* **204**, 579–592 (2018).
21. Müller, M. & Wehner, R. Path Integration Provides a Scaffold for Landmark Learning in Desert Ants. *Current Biology* **20**, 1368–1371 (2010).
22. Wystrach, A., Mangan, M., Philippides, A. & Graham, P. Snapshots in ants? New interpretations of paradigmatic experiments. *The Journal of Experimental Biology* **216**, 1766–1770 (2013).
23. Jayatilaka, P., Murray, T., Narendra, A. & Zeil, J. The choreography of learning walks in the Australian jack jumper ant Myrmecia croslandi. *Journal of Experimental Biology* **221**, jeb185306 (2018).
24. Möel, F. L. & Wystrach, A. Opponent processes in visual memories: A model of attraction and repulsion in navigating insects' mushroom bodies. *PLOS Computational Biology* **16**, e1007631 (2020).
25. Murray, T. *et al.* The role of attractive and repellent scene memories in ant homing (Myrmecia croslandi). *Journal of Experimental Biology* (2019) doi:10.1242/jeb.210021.
26. Baddeley, B., Graham, P., Husbands, P. & Philippides, A. A model of ant route navigation driven by scene familiarity. *PLoS Comput Biol* **8**, e1002336 (2012).

27. Wystrach, A., Cheng, K., Sosa, S. & Beugnon, G. Geometry, features, and panoramic views: Ants in rectangular arenas. *Journal of Experimental Psychology: Animal Behavior Processes* **37**, 420–435 (2011).
28. Zeil, J. Visual homing: an insect perspective. *Current Opinion in Neurobiology* **22**, 285–293 (2012).
29. Dahmen, H., Wahl, V. L., Pfeffer, S. E., Mallot, H. A. & Wittlinger, M. Naturalistic path integration of Cataglyphis desert ants on an air-cushioned lightweight spherical treadmill. *Journal of Experimental Biology* **220**, 634–644 (2017).
30. Wehner, R., Michel, B. & Antonsen, P. Visual navigation in insects: Coupling of egocentric and geocentric information. *Journal of Experimental Biology* **199**, 129–140 (1996).
31. Schwarz, S., Mangan, M., Zeil, J., Webb, B. & Wystrach, A. How Ants Use Vision When Homing Backward. *Current Biology* **27**, 401–407 (2017).
32. Zeil, J., Hofmann, M. I. & Chahl, J. S. Catchment areas of panoramic snapshots in outdoor scenes. *Journal of the Optical Society of America a-Optics Image Science and Vision* **20**, 450–469 (2003).
33. Fisher, Y. E., Lu, J., D'Alessandro, I. & Wilson, R. I. Sensorimotor experience remaps visual input to a heading-direction network. *Nature* **576**, 121–125 (2019).
34. Lent, D. D., Graham, P. & Collett, T. S. Image-matching during ant navigation occurs through saccade-like body turns controlled by learned visual features. *Proceedings of the National Academy of Sciences of the United States of America* **107**, 16348–16353 (2010).
35. Borst, A. & Heisenberg, M. Osmotropotaxis inDrosophila melanogaster. *Journal of comparative physiology* **147**, 479–484 (1982).
36. Cain, W. S. Differential sensitivity for smell:" noise" at the nose. *Science* **195**, 796–798 (1977).
37. Duistermars, B. J., Chow, D. M. & Frye, M. A. Flies require bilateral sensory input to track odor gradients in flight. *Current Biology* **19**, 1301–1307 (2009).
38. Jékely, G. *et al.* Mechanism of phototaxis in marine zooplankton. *Nature* **456**, 395–399 (2008).
39. Martin, H. Osmotropotaxis in the honey-bee. *Nature* **208**, 59–63 (1965).
40. Matsuo, Y., Uozumi, N. & Matsuo, R. Photo-tropotaxis based on projection through the cerebral commissure in the terrestrial slug Limax. *Journal of Comparative Physiology A* **200**, 1023–1032 (2014).
41. Porter, J. *et al.* Mechanisms of scent-tracking in humans. *Nature neuroscience* **10**, 27–29 (2007).
42. Habenstein, J., Amini, E., Grübel, K., el Jundi, B. & Rössler, W. The brain of Cataglyphis ants: neuronal organization and visual projections. *Journal of Comparative Neurology* (2020).
43. Rössler, W. Neuroplasticity in desert ants (Hymenoptera: Formicidae)–importance for the ontogeny of navigation. *Myrmecological News* **29**, (2019).
44. Stürzl, W., Zeil, J., Boeddeker, N. & Hemmi, J. M. How Wasps Acquire and Use Views for Homing. *Current Biology* **26**, 470–482 (2016).

45. Zeil, J. & Fleischmann, P. N. The learning walks of ants (Hymenoptera: Formicidae). (2019).
46. Denuelle, A. & Srinivasan, M. V. Bio-inspired visual guidance: From insect homing to UAS navigation. in *2015 IEEE International Conference on Robotics and Biomimetics (ROBIO)* 326–332 (IEEE, 2015).
47. Kodzhabashev, A. & Mangan, M. Route Following Without Scanning. in *Biomimetic and Biohybrid Systems* 199–210 (Springer, 2015).
48. Möller, R. Insect visual homing strategies in a robot with analog processing. *Biological Cybernetics* **83**, 231–243 (2000).
49. Philippides, A., de Ibarra, N. H., Riabinina, O. & Collett, T. S. Bumblebee calligraphy: the design and control of flight motifs in the learning and return flights of Bombus terrestris. *The Journal of Experimental Biology* **216**, 1093–1104 (2013).
50. Schwarz, S., Clement, L., Gkanias, E. & Wystrach, A. *How do backward walking ants (* Cataglyphis velox *) cope with navigational uncertainty?* http://biorxiv.org/lookup/doi/10.1101/2019.12.16.877704 (2019) doi:10.1101/2019.12.16.877704.
51. Freas, C. A. & Cheng, K. Limits of vector calibration in the Australian desert ant, Melophorus bagoti. *Insect. Soc.* **65**, 141–152 (2018).
52. Hoinville, T. & Wehner, R. Optimal multiguidance integration in insect navigation. *Proceedings of the National Academy of Sciences* **115**, 2824–2829 (2018).
53. Wehner, R., Hoinville, T., Cruse, H. & Cheng, K. Steering intermediate courses: desert ants combine information from various navigational routines. *J Comp Physiol A* **202**, 459–472 (2016).
54. Wystrach, A., Mangan, M. & Webb, B. Optimal cue integration in ants. *Proceedings of the Royal Society of London B: Biological Sciences* **282**, (2015).
55. Buehlmann, C., Mangan, M. & Graham, P. Multimodal interactions in insect navigation. *Animal Cognition* 1–13 (2020).
56. Buehlmann, C., Graham, P., Hansson, B. S. & Knaden, M. Desert ants locate food by combining high sensitivity to food odors with extensive crosswind runs. *Current Biology* **24**, 960–964 (2014).
57. Knaden, M. & Graham, P. The sensory ecology of ant navigation: from natural environments to neural mechanisms. *Annual review of entomology* **61**, 63–76 (2016).
58. Wystrach, A. & Schwarz, S. Ants use a predictive mechanism to compensate for passive displacements by wind. *Current biology : CB* **23**, R1083–R1085 (2013).
59. Wystrach, A., Beugnon, G. & Cheng, K. Ants might use different view-matching strategies on and off the route. *The Journal of Experimental Biology* **215**, 44–55 (2012).

433 60. Narendra, A., Gourmaud, S. & Zeil, J. Mapping the navigational knowledge of individually
434 foraging ants, Myrmecia croslandi. *Proceedings of the Royal Society B: Biological Sciences* **280**,
435 (2013).
436 61. Green, J. & Maimon, G. Building a heading signal from anatomically defined neuron types in the
437 Drosophila central complex. *Current Opinion in Neurobiology* **52**, 156–164 (2018).
438

439 **Figure 1**

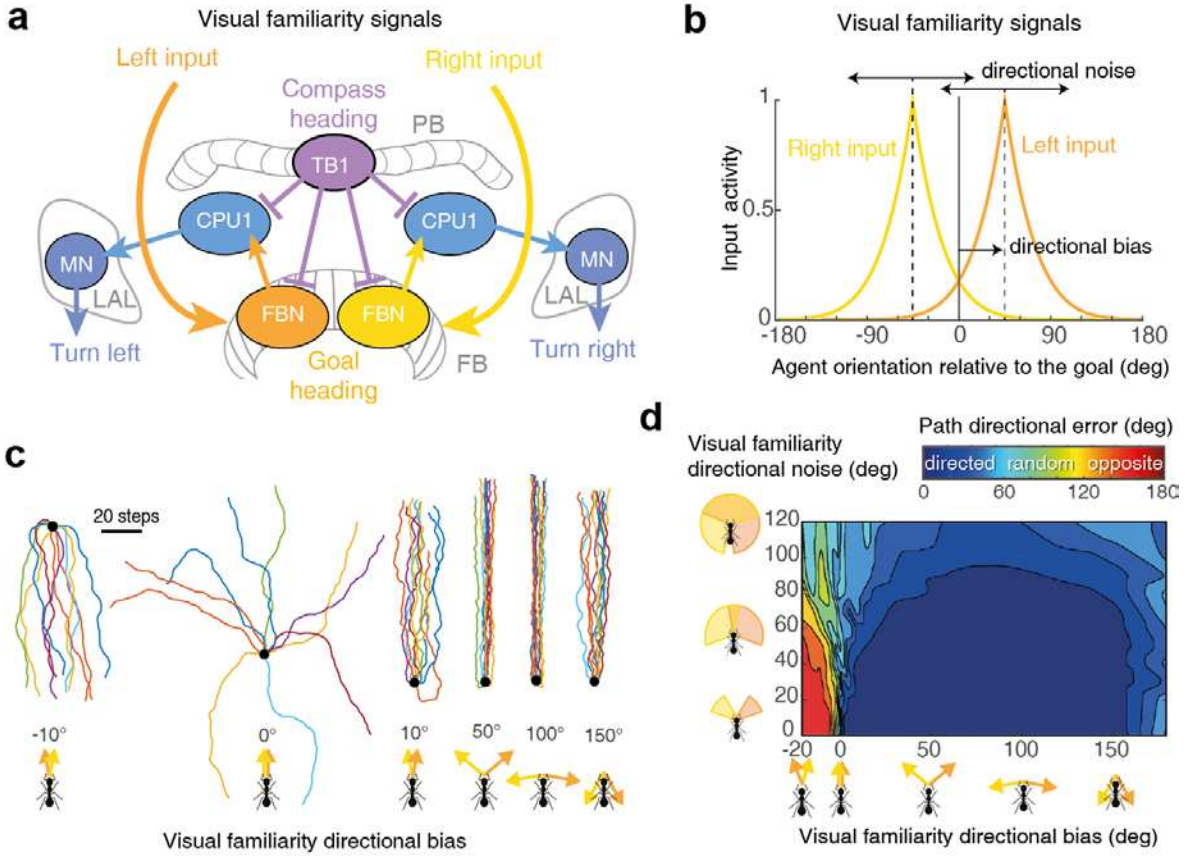

440

441 **Figure 1.** ***Bilaterally decorrelated input to Central Complex produces stable route heading.***

442 ***a****. The* central complex (CX) sits at the centre of the brain but is wired to both hemispheres.
443 It receives bilateral inputs in the Fan-shaped Body (FB), where sustained activity of the FB
444 neurons (FBN) forms two representations of the goal heading. CPU1 neurons compare such
445 'goal heading' representations to the 'compass-based current heading' representation of the
446 Protocerebral Bridge (PB) neurons (TB1) and outputs bilateral signals to the left and right
447 Lateral Accessory Lobes (LALs), where they modulate motor neurons (MN) descending to the
448 thorax to control left and right turns, respectively (see **extended figure 2, d, g** for details of
449 the circuitry). **b.** Simulated inputs to the FBN neurons. We assumed that the input signals to
450 the FBN are body-orientation-dependant (as expected if resulting from visual familiarity of
451 the scene [28] such as outputted by the MBs [4]. 'directional bias' indicates the direction relative
452 to the goal direction (0°) at which the left visual familiarity signals is highest in average (+45°
453 in this example). Right signal responds symmetrically for the other direction (-directional
454 bias). 'Directional noise' in the visual familiarity was implemented by shifting the input curve
455 response around its mean (i.e. the 'directional bias') at each time step by a random value

(normal distribution with standard deviation given by 'directional noise'). **c.** Paths resulting given different directional biases. **d.** Path directional error (absolute angular error between start-to-arrival beeline, and start-to-goal direction) after 200 steps, as a function of the visual familiarity 'directional bias' (x axis) and 'directional noise' (y axis). **c, d.** Straight route headings robustly emerge as long as left and right inputs send a signal when the body is oriented right and left from the goal, respectively (i.e., directional bias > 0°) but not if both inputs send a signal when facing the goal (i.e., directional bias = 0°). Orientation towards the opposite direction emerges if left and right inputs signal inversely, that is, when the body is oriented right and left from the goal respectively (i.e., directional bias < 0°). Robustness to visual familiarity directional noise indicate that the direction in which views are learnt does not need to be precisely controlled. See further analysis in Extended Data Fig. 1.

468 **Figure 2.**

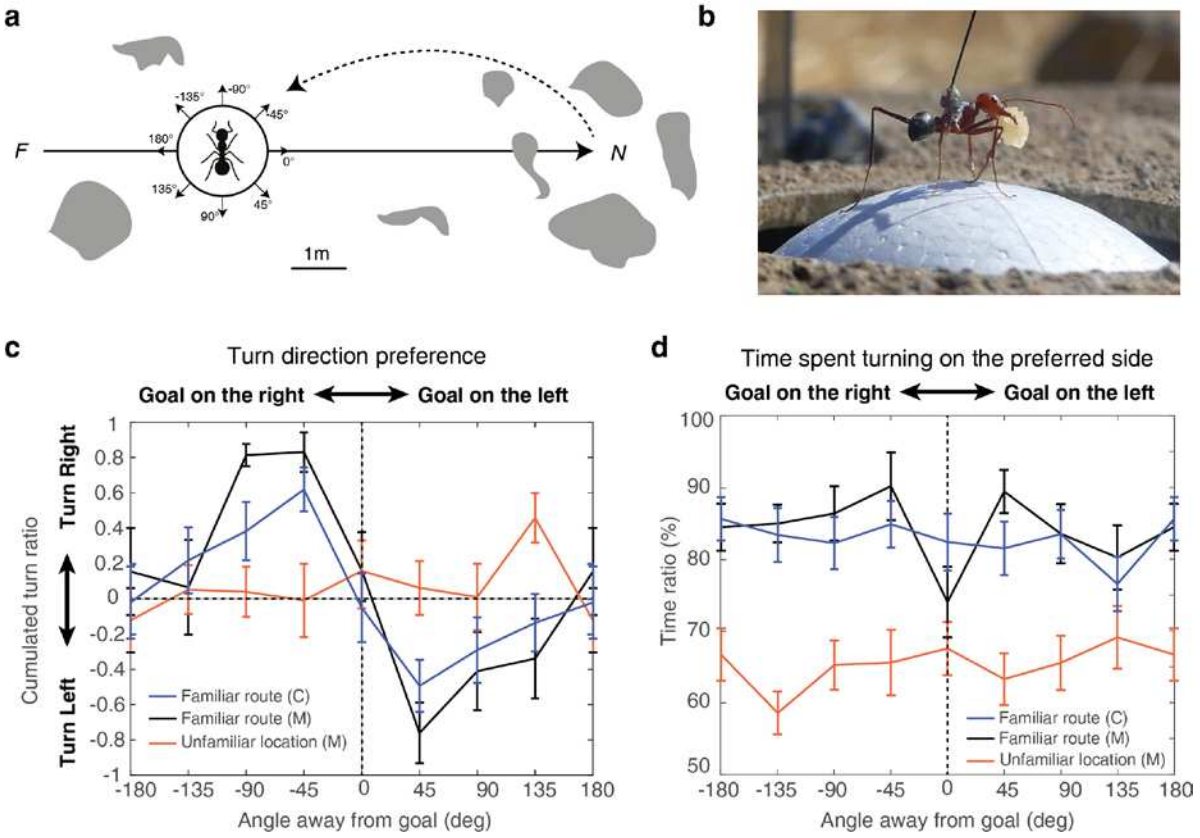

469

470 **Figure 2. Ants visually recognise whether the goal direction is left or right. a.** Homing ants
471 were captured at the end of their familiar route and fixed on the trackball (**b**) in 8 different
472 compass orientations. The route was rich in visual terrestrial cues (grey blobs). *F*: feeder, *N*:
473 nest. **b**. An individual *Cataglyphis velox* mounted on the trackball setup, holding its precious
474 cookie crumb. **c.** Turn ratio (degrees *(right - left) / (right + left)*; mean ± se across individuals)
475 for the eight compass directions, on the familiar route or in the unfamiliar location (same
476 compass directions but unfamiliar surroundings) across 12 seconds of recording. **d**.
477 Proportion of time spent turning on the preferred side of each individual (mean ± se across
478 individuals). C: *Cataglyphis velox (n=17)*, M: *Myrmecia crosslandi (n=11*).

479

480 **Figure 3**

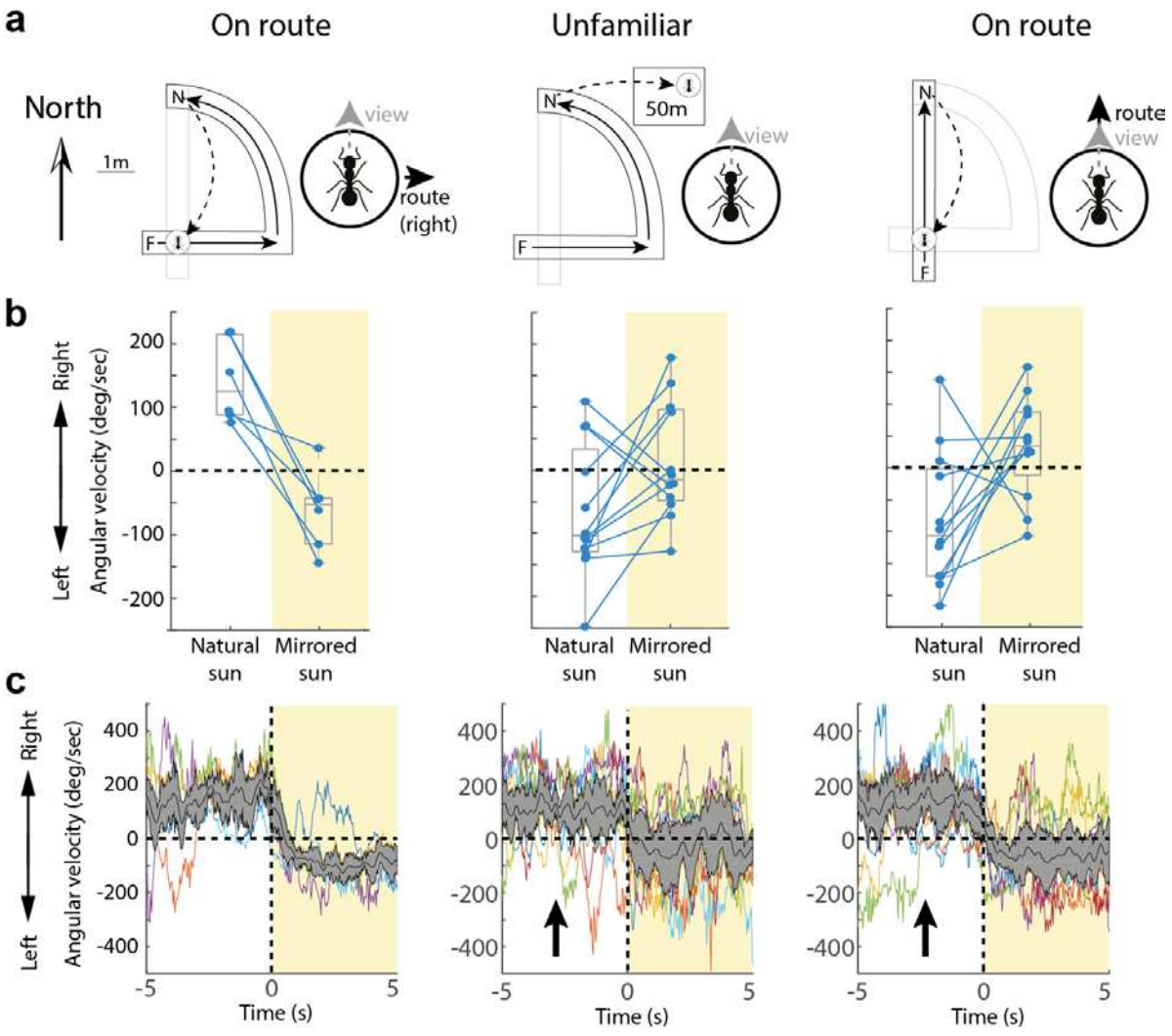

481

482 **Figure 3. Rotation of celestial cues shift turning direction based on familiar terrestrial cues.**
483 **a**. Schemes of the training and test condition. Homing ants were captured at the end of their
484 familiar route (black arrows: familiar route, F: feeder, N: nest) and fixed on the trackball with
485 their body always facing north, either on their route with the route direction 90° to the right
486 (left panel); or within unfamiliar surroundings (middle panel); or ants were trained along a
487 route oriented 90° to the previous one and released on their familiar route in the same
488 location and orientation, which this time is facing their route direction. **b.** Box plots indicate
489 average angular velocity (positive = right turn) each ant (dots) 5s before (white) and 5s after
490 (yellow) the apparent sun's position is mirrored by 180°. Wilcoxon test for: 'turn towards
491 the right with natural sun' (left panel: n=6, p=0.0156; middle panel: n=12 p=0.9788; right
492 panel: n=12 p=0.9866), 'mirror effect: turn direction reversal' (left panel: n=6, p=0.0156,
493 power=0.9994; middle panel: n=12 p=0.3955; right panel: n=12 p=0.0320). **c.** Turning

494 velocities (individuals in colour; median ± iqr of the distribution in grey) across time, before
495 and after the sun manipulation (t_0). Arrows in the middle and left panels: the velocities of
496 some individuals have been inverted so that all individuals' mean turn directions before the
497 manipulation are positive.

498

499 **Figure 4**

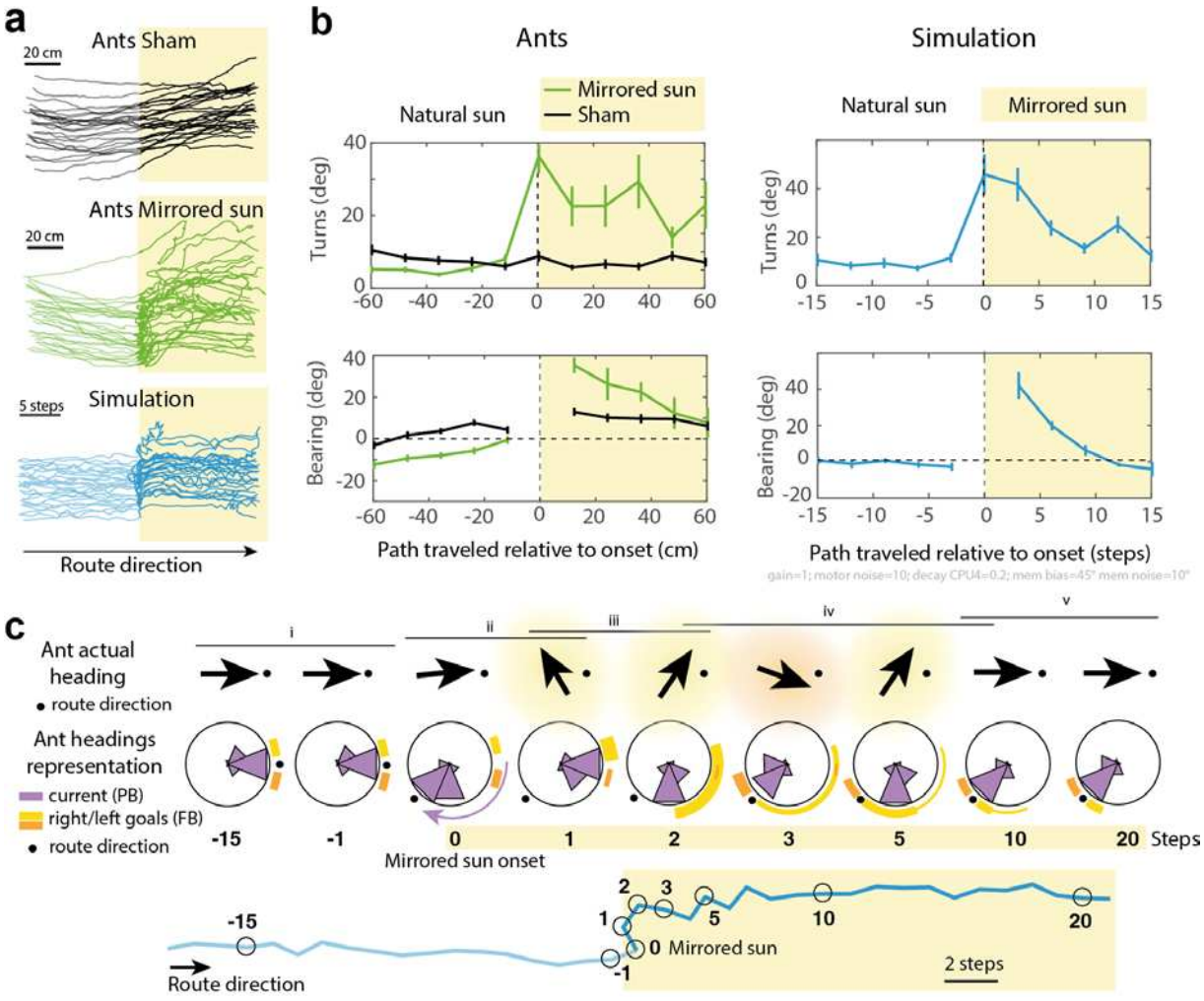

500

501 **Figure 4. Rotation of celestial cues affect ants route following as predicted.** Paths (**a**) and
502 quantification of bearing and turns (**b**) of real (black and green) and simulated (blue) zero-
503 vector ants (i.e., deprived of path integration information) recapitulating a familiar straight
504 route while entering an area where we manipulated celestial compass cues (yellow). For the
505 'Mirrored sun' condition (green) the real sun was hidden from the ants and mirrored so as to
506 appear rotated by 135° counter clockwise in the sky. For the 'sham' condition (black), the
507 experimenters were standing in the same place and the real sun was also hidden, but only a
508 small piece of the sky (close to, but not including the sun) was mirrored for the ants.
509 Simulated ants (blue) result from the model presented in fig. 1. Sun rotation was modelled
510 as a 135° shift in the current heading representation (3-cell shift of the bump of activity in
511 the Protocerebral Bridge). Paths of both real and simulated ants were discretised (segments
512 of 12 cm for real ants, and of 3 steps for the simulations), before and after the sun rotation
513 onset point. Turns correspond to the absolute angle between two successive segments,

bearing indicates the direction of segments relative to the route (0°). Turns at '0' on the x-axes correspond to the angle between the segment preceding and following the shift of the celestial compass. **c.** The effect observed in the simulations is quantitatively dependant on the model's parameters (here gain=1; motor noise=10; decay FBN=0.2; visual familiarity directional bias ± noise=45°±10° see Extended Data Fig. 1 for a description of parameters), but its key signature can be explained qualitatively. (i) Under normal situation the current heading is maintained between the right and left goal heading representation in the Fan-shaped Body (FB) (yellow and orange marks) and updated by right and left visual familiarity signals. (ii) The sun rotation creates a sudden shift of the current heading representation in the Protocerebral Bridge (PB) (purple curved arrow), although the agent is still physically facing the actual route direction (black dot). This leads the agent to display a sudden left turn to re-align its shifted heading representation with the FB goal heading that is held in short term memory. (iii) This novel direction of travel is visually recognised as being 'left of the goal', causing a strong lateralised signal in the right FB's goal heading representation (yellow). This biased activity triggers right turns, exposing the agent to new headings recognised as 'right of the goal', and thus more signal sent to the right FB (yellow arcs), favouring further right turns. (iv) Turning right eventually leads the agent to overshoot the actual goal direction, recognise view as 'right from the goal' and thus signalling in the left FB (orange). These signals are, at first, superimposed with the previous desired heading representation, resulting in a period of conflicting guidance information causing meandering. (v) The agent progressively updates its novel goal heading representation as the trace of the previous desired heading fades out and the new one strengthens due to the incoming signals from visual familiarity. In sum, motor decision results from complex dynamics between two main factors: 1- how strong are the left and right visual familiarity signals updating the goal heading representations (orange and yellow glow around the 'Ant actual heading' arrows), which depend on whether the agent is oriented left or right from its goal; and 2- how well the current heading representation (PB) matches the goal heading representation (more detail in Extended Data Fig. 2).

Extended data figure 1.

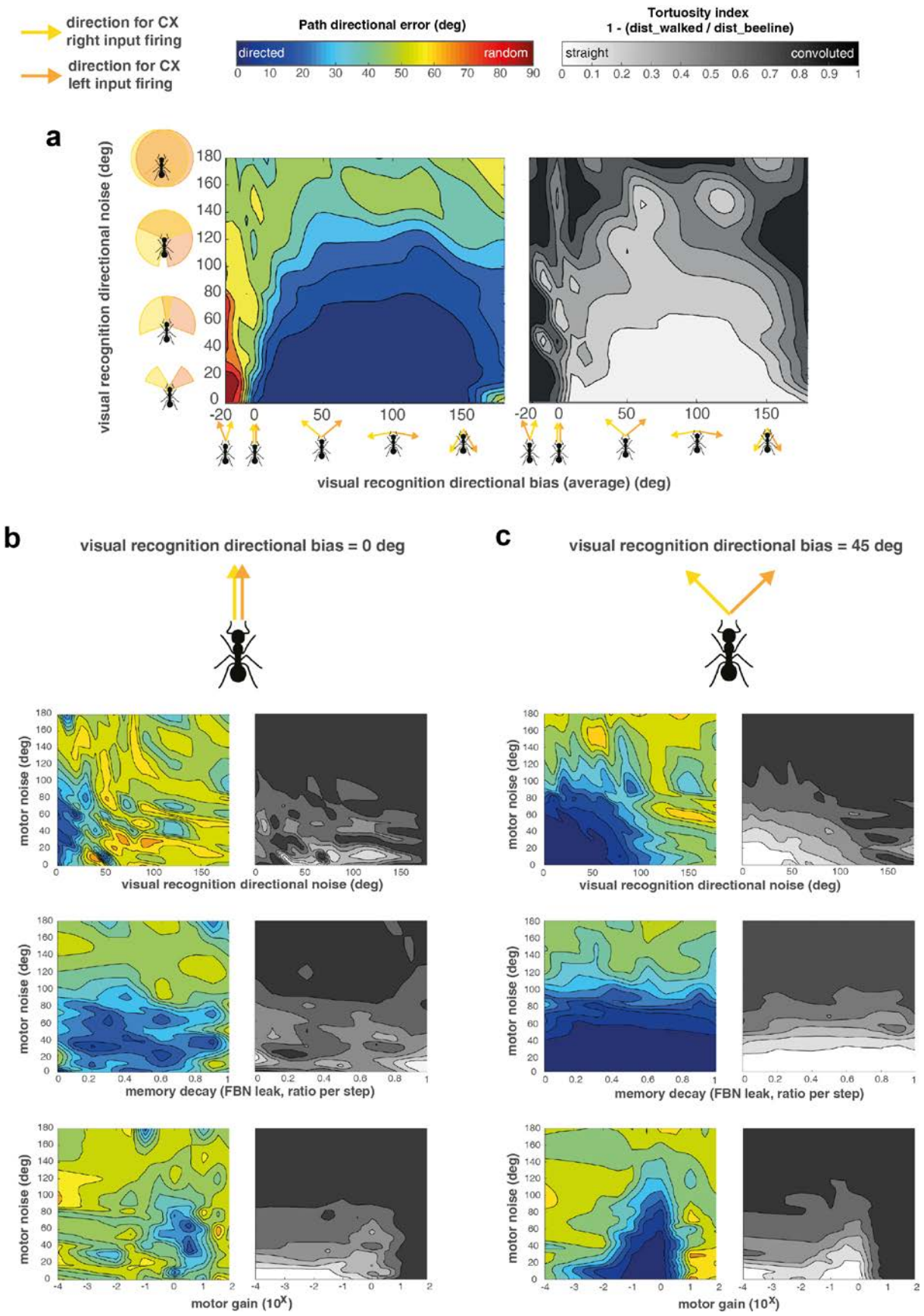

Extended data figure 1. Parameter exploration of the Central Complex model (see fig 3). a.

This shows a parameter exploration for the CX model presented in **Fig. 1** (see **extended fig. 2** for details of the circuitry). - Path directional error (absolute angular error between start-to-arrival and start-to-goal directions) and path tortuosity (index = *1 - (beeline_distance/distance_walked)*) after 200 steps are shown according to various parameter ranges. For each point on the map, all the other parameters are chosen to maximise for lowest path directionality error.

a. Same as **Fig. 1d**, except that for each point of the map, the other parameters are chosen to maximise for lowest path directionality error instead of being fixed at an average range. Note that in **Fig. 1d**, visual familiarity direction bias < 0 typically results in routes leading to the opposite direction (i.e., path directional error close to 180°, **see Fig. 1**). Here, maximising for lowest path directional error did not result in goal-oriented path, but selected parameters yielding very high tortuosity, thus indicated that no parameter regime can yield straight, directed route when visual familiarity bias is < 0. Note that straight, goal-oriented paths emerge as long as the visual familiarity direction bias is > 0, that is, if the left hemisphere inputs correlate with moments when the nest is on the left, and vice versa.

b. Visual familiarity directional bias is fixed at a value of 0°, meaning that both CX inputs respond maximally when the agent is facing the goal direction. Note that in this condition, regions of low path directional errors (blue) and region of low path tortuosity (white) do not overlap. This means that one cannot obtain straight, goal-directed paths if left and right CX inputs respond when the nest is located in front.

c. Visual familiarity directional bias is fixed at a value of +45°, meaning that left and right CX inputs respond maximally when the agent is oriented 45° to the right or left from the goal direction, respectively. Note that regions with low path directional errors (blue) and regions of low path tortuosity (white) overlap well, showing a very large range of parameters for which we can obtain straight, goal-directed paths. We found the robustness to parameters remarkable: the model copes with motor noise up to 80°, visual familiarity direction noise up to 90°, is insensitive to its vector-memory decay and operates across several orders of magnitude for the gain.

Parameters' description:

Visual familiarity directional bias: Indicates the absolute angle away from the goal at which visual familiarity signals (i.e., the CX inputs) are highest, assuming 0° indicates the correct goal direction. 0° indicates that both left and right inputs fire when the nest direction is aligned with the current body orientation. Inversely, 180° indicates that left and right input fire when the nest is right behind. Positive values (between 0° and 180°) indicate that the left and right inputs fire when the nest direction is on the left and right hand side respectively (the extent of the angular bias is given by the value). Negative values (between 0° and -180°) indicate a reversal, so that left and right input fire when the nest direction is on the right and left hand side respectively. ***Visual familiarity directional noise:*** Represents the extent of a systematic deviation from the visual familiarity directional bias angle. It is implemented by shifting the input curve response (horizontal arrows in **Fig. 1b**) around its mean (given by the 'directional bias') at each time step by random values drawn from a normal distribution with standard deviation given by 'directional noise'. It can be seen as representing a directional noise when storing visual memories. High directional noise means that the input signal will occasionally respond strongest when oriented in the other direction than indicated by the visual familiarity directional bias. Robustness to visual familiarity directional noise indicates that the orientation of the body does not need to be precisely controlled during memory acquisition. ***Motor noise*****:** at each time step, a directional 'noise angle' is drawn randomly from a Gaussian distribution of *± SD = motor noise*, and added to the agent's current direction. ***Memory decay*****:** proportion of Fan-shaped Body Neurons (FBN, see extended fig 2 for details) activity lost at each time step: For each FBN: $\text{Activity}_{(t+1)} = \text{Activity}_{(t)} \times (1 - \textit{memory decay})$. This corresponds to the speed at which the memory of the vector representation in the FBN decays. A memory decay = 1 means that the vector representation in the FBN is used only for the current time step and entirely overridden by the next inputs. A memory decay = 0 means that the vectors representation acts as a perfect accumulator across the whole paths (as in PI), which is probably unrealistic. ***Motor gain***: Sets the gain to convert the motor neuron signals (see extended fig 2 for details) into an actual turn amplitude (*turn amplitude = turning neuron signal × gain*). Note that here, the motor gain is presented across orders of magnitude. One order of magnitude higher means that the agent will be one order of magnitude more sensitive to the turning signal.

607 **Extended data figure 2.**

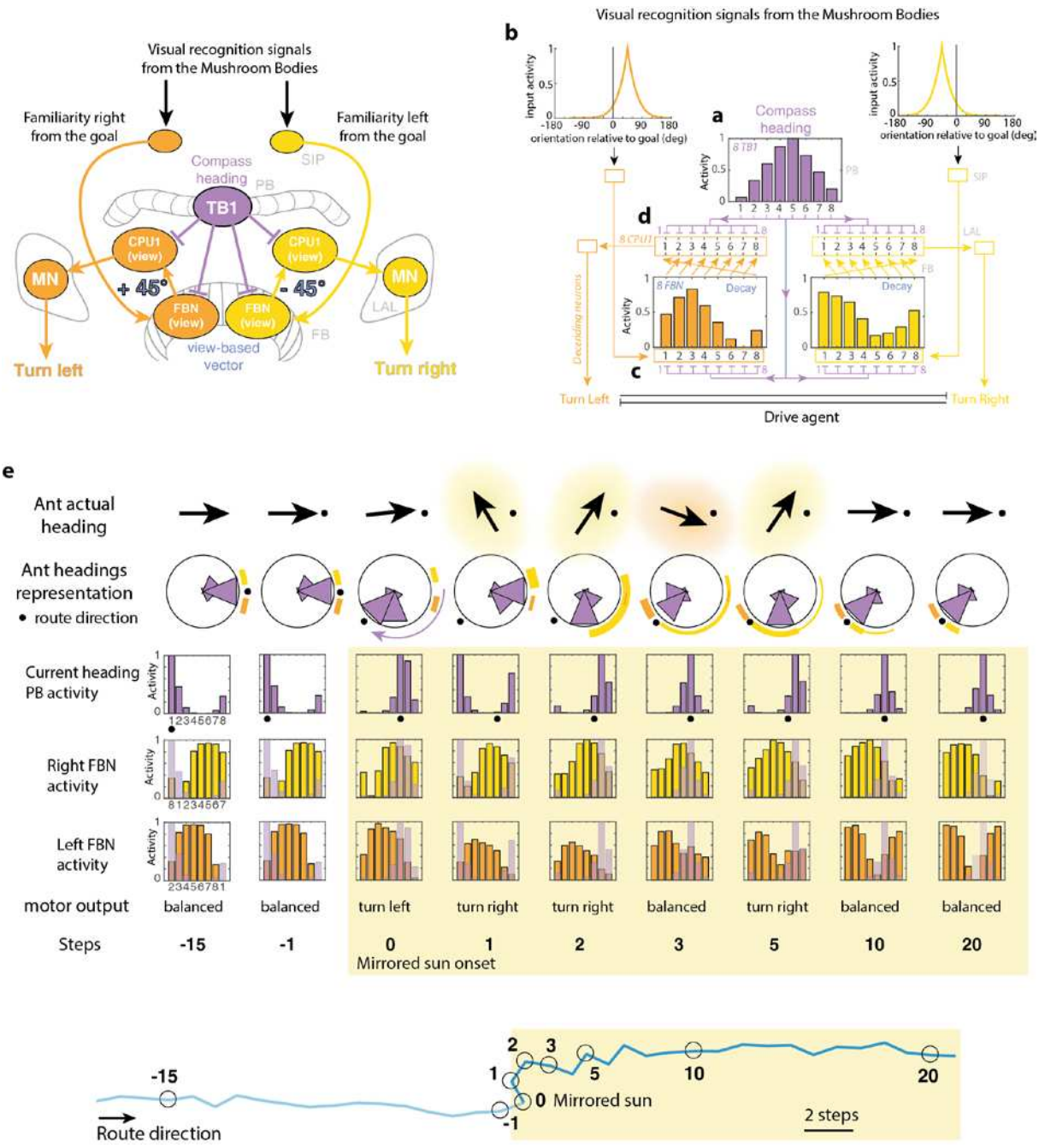

608

609

610 **Extended data figure 2. Details of the CX model's circuitry.**

611 **a-d.** General scheme of the CX model as presented in figure 1 (left panel) and the
612 corresponding detailed circuitry (right panel). This model exploits the same circuit as the CX
613 model used for PI [12,14], except that FB input indicate visual familiarity rather than speed of
614 movement.

615 **a**. Current heading direction is modelled in the Protocerebral Bridge (PB) as a bump of
616 activity across 8 neurons forming a ring-attractor (purple), as observed in insects [14]. Each
617 neuron responds maximally for a preferred compass direction, 45° apart from the neighbour
618 neurons (neuron 1 and 8 are functionally neighbours, closing the ring structure). Change in
619 the agent's current compass orientation results in a shift of the bump of activity across the 8
620 neurons (we did not model how this is achieved from sensory cues, see [9,10,61] for studies
621 dedicated on this.

622 **b.** Visual familiarity signals fire according to the agent orientation relative to the goal
623 direction. Here the input curve indicates that right and left signals fire maximally when the
624 agent is oriented 50° (in average) left and right from its goal respectively (but see Fig. 1 and
625 Extended fig. 1 for variation of these parameters: 'directional bias' and 'directional noise').

626 **c.** These lateralised input signals excite two dedicated sets of FBN. These FBNs are
627 simultaneously inhibited by the current heading representation (purple), resulting in two
628 negative imprints of the current heading activity across the FBNs, which can be viewed as
629 two 'view-based vectors'. FBNs show some sustained activity so that, across time, successive
630 imprints are superimposed, thus updating the 'view-based-vectors' (as for Path integration,
631 except that this sustained activity is not crucial). The sustainability of such a 'view-based
632 vector' depends on the FBN activity's decaying rate, which can be varied in our model and
633 has little incidence on the agent's success (Extended figure 1, parameter decay).

634 **d.** Motor control is achieved using the same circuitry as for Path integration [12]. On each brain
635 hemisphere, neurons (called CPU1 in some species), compare the current compass heading
636 (purple) with their version of the FBN 'view-based-vector'. Crucially, both FBN
637 representations are neurally shifted by 1 neuron (as if rotating the view-based-vector by 45°
638 clockwise or counter-clockwise depending on the hemisphere), resulting in an overall activity
639 in the CPU1 (sum of the 8 CPU1) indicating whether the view-based-vector points rather on
640 the left- (higher resulting activity in the left hemisphere) or right-hand side (higher resulting
641 activity in the right hemisphere). The CPU1 neurons sum their activity on descending motor
642 neurons (MN), which difference in activity across hemispheres triggers a left or right turn of
643 various amplitude, given a 'motor gain' that can be varied to make the agent more or less
644 reactive (Extended figure 1 for detailed parameter description). Numbers on the left indicate
645 neurons numbers. Letters on the right indicate brain areas (SIP: Superior Intermediate

Protocerebrum, PB: Protocerebral Bridge, FB: Fan-shaped Body, LAL: Lateral Accessory Lobe).

e. Same as Fig. 4c, with added details of the PB (purple) and right and left FB (yellow and orange) neural activity. Note that the FBNs order has been shifted (2,3,4,5,6,7,8,1 and 8,1,2,3,4,5,6,7) and inhibition exerted by the PB is represented (overlaid transparent purple, 1,2,3,4,5,6,7,8) as happens in the left and right CPU1 neuron (**d**). This way, the strength of the motor signal for turning right and left– which correspond to the sum of non-inhibited right and left CPU1 activity – can be inferred by looking at the area covered by non-occluded yellow and orange FBN columns respectively.

With manipulation such as rotating the current compass information, it becomes apparent that motor decision results from complex dynamics between two main factors: 1- how strong are the left and right visual input signal updating the view-based-vectors representation (represented by orange and yellow glow around the actual ant heading arrows), which depend on whether the agent is oriented left or right from its goal and 2- how well the current heading representation (PB) matches the rotated left and right shifted FB view-based-vector current representations.

ECOLOGY

CATER: Combined Animal Tracking & Environment Reconstruction

Lars Haalck[1]†, Michael Mangan[2]†, Antoine Wystrach[3]†, Leo Clement[3], Barbara Webb[4], Benjamin Risse[1]*

Quantifying the behavior of small animals traversing long distances in complex environments is one of the most difficult tracking scenarios for computer vision. Tiny and low-contrast foreground objects have to be localized in cluttered and dynamic scenes as well as trajectories compensated for camera motion and drift in multiple lengthy recordings. We introduce CATER, a novel methodology combining an unsupervised probabilistic detection mechanism with a globally optimized environment reconstruction pipeline enabling precision behavioral quantification in natural environments. Implemented as an easy to use and highly parallelized tool, we show its application to recover fine-scale motion trajectories, registered to a high-resolution image mosaic reconstruction, of naturally foraging desert ants from unconstrained field recordings. By bridging the gap between laboratory and field experiments, we gain previously unknown insights into ant navigation with respect to motivational states, previous experience, and current environments and provide an appearance-agnostic method applicable to study the behavior of a wide range of terrestrial species under realistic conditions.

INTRODUCTION

For more than 50 years (*1*), researchers have sought technologies to accurately quantify the behavior of animals in their natural habitats. Advances in imaging technology, computer vision, and machine learning have enabled a variety of breakthroughs in the computational analysis of animal behavior in recent years (*2*–*5*) with different tracking systems developed for model organisms such as *Drosophila melanogaster* flies (*6*, *7*), larvae (*8*, *9*), *Caenorhabditis elegans* (*10*), zebrafish (*11*), and mice (*12*, *13*).

Animal tracking approaches are usually divided into two categories, namely, pose estimation and positional detections over time (*14*). In particular, deep learning algorithms have enabled fully automatic pose estimations from video recordings. Prominent examples are DeepPoseKit (*15*), DeepLabCut (*16*), and LEAP (*17*). Recently, extensions of these algorithms have improved the applicability of these algorithms for multi-animal pose estimation (*18*, *19*). For positional detection of animals over time, both conventional computer vision and deep learning algorithms have been used. For example, Ctrax (*20*), idTracker (*11*), Multi-Worm Tracker (*10*), and FIMTrack (*9*) are well-known examples for conventional tracking algorithms using background subtraction and dedicated foreground identification strategies. In contrast, machine learning–based detection algorithms usually use (fully) convolutional neural networks to identify the objects of interest such as the idTracker.ai (*21*), Mouse Tracking (*22*), fish CNNTracker (*23*), and anTraX (*24*).

Because the difficulty of visual tracking typically increases with the complexity and variability of the scenery (*25*), these systems have primarily been developed for controlled laboratory conditions (*18*, *19*, *21*, *26*). The difficulty is further aggravated for small animals like insects, which do not provide visually distinctive features (limiting feature-based methods such as deep learning approaches), while navigating unpredictably in a cluttered and highly ambiguous environment (preventing background modeling and requiring camera motion compensation) (*27*). Moreover, the lack of unique features and visual ambiguities challenge the capabilities of state-of-the-art tracking algorithms, which often use discriminative correlation filters, Siamese correlation, or transformer-based machine learning architectures (*28*). To provide a general purpose in-field animal tracker, three fundamental challenges must be addressed. First, animals must be detected consistently over time, even when occupying few pixels, providing low contrast, and across periods of occlusion. Second, these detections must be linked and warped into a camera motion compensated trajectory in a common frame of reference. Third, trajectories must be embedded in an environment reconstruction, allowing researchers to relate trajectories to environmental features, such as obstacles. At the time of writing, there is no software that addresses all three challenges in an end-to-end pipeline, facilitating long-range and unconstrained in-field animal tracking (table S1) (*25*).

The visual tracking of individually foraging ants provides an excellent example of these challenges. These insects are comparatively small and often visually indistinguishable from each other and their complex natural habitat (background). On the other hand, ants exhibit highly complex navigation strategies such as path integration (PI) and visual memory mechanisms, which are best studied under natural conditions in the field (*29*). Desert ant behavior is currently quantified over longer ranges, either using hand annotation with reference to a preinstalled grid (*30*, *31*) or by following individuals with differential Global Positioning System (GPS) device (*32*). Complementary analysis of the fine-scale movement patterns in small areas [from fixed cameras stationed at the nest, e.g., (*33*, *34*) or using data from trackballs placed at discrete locations, e.g., (*35*)] have inspired new hypotheses regarding how

[1]Institute for Geoinformatics and Institute for Computer Science, University of Münster, Heisenbergstraße 2, 48149 Münster, Germany. [2]Department of Computer Science, University of Sheffield, Western Bank, Sheffield S102TN, UK. [3]Research Center on Animal Cognition, Center for Integrative Biology, CNRS - Université Paul Sabatier - Bât 4R4, 169, avenue Marianne Grunberg-Manago, Toulouse 31062, France. [4]School of Informatics, University of Edinburgh, Crichton St, Edinburgh EH8 9AB, UK.
†These authors contributed equally to this work.
*Corresponding author. Email: b.risse@uni-muenster.de

visual memories are learned (*36*) and used (*37*), respectively. However, many questions remain unresolved. For example, how quickly can visual route memories be learned? How is foraging behavior affected by motivational state and environmental interactions? What are the underlying control strategies that govern motion during navigation? To tackle these questions, there is a need for in-field quantification techniques that enable unconstrained measurement of microscale behavior in the animal's natural habitat.

In this work, we bridge the gap between laboratory experiments and in-field studies by demonstrating how new visual tracking methods provide unique insights into the natural navigation behavior of ants. Our core contribution is a combined solution for unconstrained visual animal tracking and environment reconstruction framework [called Combined Animal Tracking & Environment Reconstruction (CATER)], capable of detecting small targets in video data captured in complex settings while embedding their locomotion path within a high-resolution environment reconstruction in moving camera conditions. This has been achieved by:

1) An unsupervised probabilistic animal detection mechanism, which identifies the object of interest in the images based on motion alone, making its appearance agnostic, robust to occlusions and camera motion, and capable of localizing even tiny insects in cluttered environments.

2) A dense and globally optimized environment reconstruction algorithm, which can process millions of frames to calculate a high-resolution image mosaic from multiple freely moving camera videos.

3) A unified and highly parallelized tracking framework combining the detection and reconstruction algorithm to generate full frame rate animal locations projected onto the very high-resolution environment reconstruction.

4) Integrated routines and graphical interfaces for user interactions to enable efficient corrections and manual annotations to contextualize the behavioral measurements.

5) The application of this framework to obtain a uniquely high-resolution (time and position) dataset describing the entire foraging history of individual desert ants in their complex desert-shrub habitat.

Evaluations of our framework yield excellent spatial and temporal accuracy. We demonstrate its applicability in a setting beyond the capabilities of existing approaches by successfully integrating 1.8 million images from multiple recordings into a unique high-resolution environment reconstruction while achieving a median tracking accuracy of 0.6 cm evaluated on more than 300,000 manually annotated images. CATER enables us to obtain detailed trajectories, which revealed a number of original insights into ant navigation.

RESULTS

Data collection

Our test scenario is a study of the foraging ontogeny of desert ants (*Cataglyphis velox*). For video recording, an off-the-shelf camcorder (Panasonic HDC-TM900) was used to capture uncompressed 1920 by 1080 video recordings at 50 frames per second. A custom-made camera rig with a 1.5-m horizontal arm was used to capture video from directly above the ant (approximately 1 m) without the experimenter disturbing the forager (Fig. 1A). To simplify the capture process, four standard red laser pointers were secured around the camera pointing downwards to create a visible light pattern on the ground to aid camera/ant alignment (Fig. 1, A and B). Given that ants blend in with the background and only cover approximately 30 by 6 pixels in the image (Fig. 1C), they are barely visible for human observers and can only be identified in zoomed croppings (Fig. 1, D and E). This clearly presents a major challenge for any existing tracking algorithm.

We followed each individual ant (having marked them) from the first time that they exited the nest (Fig. 1F). The ant was free to forage in any direction, interact with other ants and vegetation, and return to the nest as it wished. Only when its foraging path reached approximately 8 m from the nest was it provided with a food morsel. Foraging ants will more or less rapidly establish visually guided idiosyncratic routes if they discover a site with a regular food supply (*30*, *31*). Following their second homeward trip from the same feeding site, individuals were subjected to a series of displacement tests to assess their visual memory performance given minimal experience (details are in "Data capture" section in Supplementary Text). The resultant dataset totals 151 videos (1.8 million individual frames) documenting the complete foraging history and displacement trials of 14 foragers in their natural habitat (details of complete dataset are in "The ant ontogeny dataset" section in Supplementary Text).

Tracking and reconstruction framework

Our framework consists of several modules processed in an interleaved fashion, as summarized in Fig. 2A. For all frames I_i, a similarity graph is generated by extracting and matching features across all frames from all videos (Fig. 2B). The frames and resultant transformations are then passed to two parallelized tracking and reconstruction tasks.

In the first task, matches from consecutive images are used to calculate pairwise transformations $T_{i,i+1}$ (*38*). These transformations are used to compensate the camera motion and to extract motion residuals between consecutive images called unaries Φ_i (Fig. 2C; details are in "Tracking and reconstruction algorithm" section in Materials and Methods). That is, each unary represents the probability distribution of animal movement as a two-dimensional (2D) heatmap. Assuming a moving ant in the majority of the frames, the motion residuals can be interpreted as 2D probability distributions of potential ant locations. These locations $\mathbf{p_i} = (x, y)$ are connected by a motion model (i.e., pairwise potentials $\Psi_{p_i \to p_{i+1}}$ between two consecutive detections $\mathbf{p_i}$ and $\mathbf{p_{i+1}}$) to encourage smooth pixel transitions and temporal consistency for all possible locations in each frame. By combining all unaries and pairwise potentials into a factor graph (which is a graphical representation of the underlying belief network; Fig. 2D), the most probable ant locations $\mathbf{p_i^*}$ for all frames $i = 1, ..., T$ can be computed by using the globally optimal max-sum algorithm (*39*)

$$\arg\max_{p_1^*,\cdots,p_T^*} E(p_1,\cdots,p_T \mid I_1,\cdots,I_T) = \sum_{i=1}^{T}\Phi_i + \sum_{i=1}^{T-1}\Psi_{p_i \to p_{i+1}}$$

This global probabilistic inference formulation can be solved independently of the object and background appearance, does not require any initialization or manually labeled training data (unsupervised), and is capable of resolving ambiguities such as occlusions automatically.

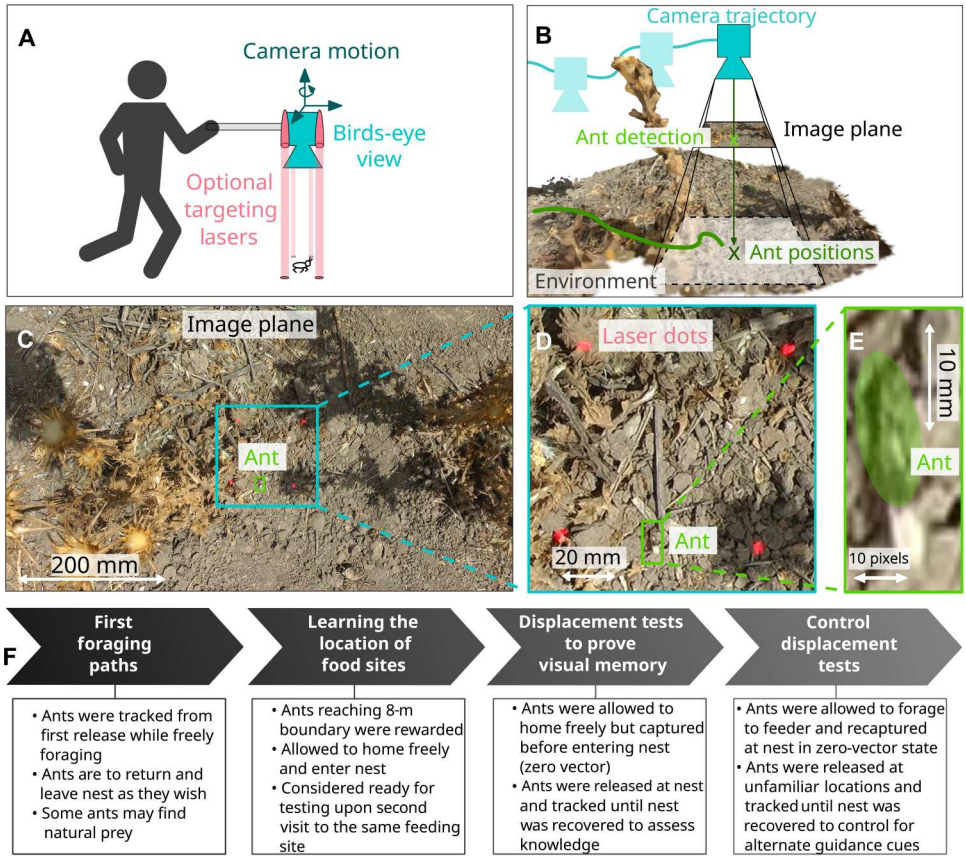

Fig. 1. Data capture and visual in-field tracking overview. (**A**) Ant paths were recorded using an off-the-shelf camera augmented with downward facing laser pointers to aid camera/ant alignment. (**B**) From these recordings, camera trajectories and ant detections are estimated and combined to compute the ant position (animal trajectory) with respect to the environment reconstruction. (**C** to **E**) Example image from the dataset at full resolution and zoomed in around the ant. (**F**) Flow chart outlining the experimental protocol to assess the minimal learning and memory requirements for visual route following in desert ants ("Data capture" section in Supplementary Text provides additional information).

In the second task, 2D environment reconstructions are extracted by identifying key frames from any number of video sequences and warping these frames I_i into a unified image mosaic coordinate system $\hat{I}_i$ based on their pairwise transformations $T_{i,i+1}$ (Fig. 2E). Subsequently, introduced drift is mitigated by minimizing an optimization problem using the transformations between all frames. Afterwards, all intermediate frames need to be reintegrated to enable full frame rate trajectories. This is done using geodesic interpolation followed by a refinement step resulting in dense transformations T_i for all frames (Fig. 2F) (*40*). In the following, we refer to the resultant globally optimized image mosaic as environment reconstruction or map to emphasize that this mosaic recovers visual characteristics in two dimensions.

Last, ant locations $\mathbf{p_i}$ need to be projected onto the image mosaic via T_i to embed the trajectories into the environment reconstructions (Fig. 2G). The approaches are thus combined into a unified unsupervised tracking framework that yields high-accuracy paths and environmental maps without initialization or calibration routines.

In contrast to nonvisual tracking methods [such as telemetry (*41*)], our resulting dataset preserves all visual environment information, allowing post hoc augmentations that both improve the data quality (e.g., through human-in-the-loop tracker corrections) and allow emergent research questions to be tackled after data collection. In particular, labels can be added to individual frames (e.g., to note behavioral changes such as acquisition of food) or specific locations tagged in the background image mosaics (e.g., feeding sites). The entire framework as well as the interaction functionality is embedded into a unified graphical user interface and offers a variety of convenient and usable features and visualizations for fast data interaction (details are in "Tracking and reconstruction algorithm" section in Materials and Methods and fig. S2).

Tracking and reconstruction performance evaluation

Our object detection and tracking algorithm is appearance agnostic and can be used to detect all kinds of animals and artificial objects in a variety of different environments and lighting conditions (*39*). Here, we use this localization pipeline to successfully recover the position of ants in all 1.8 million images of our ontogeny dataset.

Our reconstruction pipeline registers background scenes to create high-resolution top-down image mosaics of the ant habitat on which the complete foraging paths of multiple ants can be plotted (Fig. 3A and fig. S6). Previous evaluation has shown that our registration mechanism can achieve millimeter spatial accuracy and a median angular error of 3° (*40*). The resultant data are particularly unique: The high-temporal resolution (50 Hz) allows

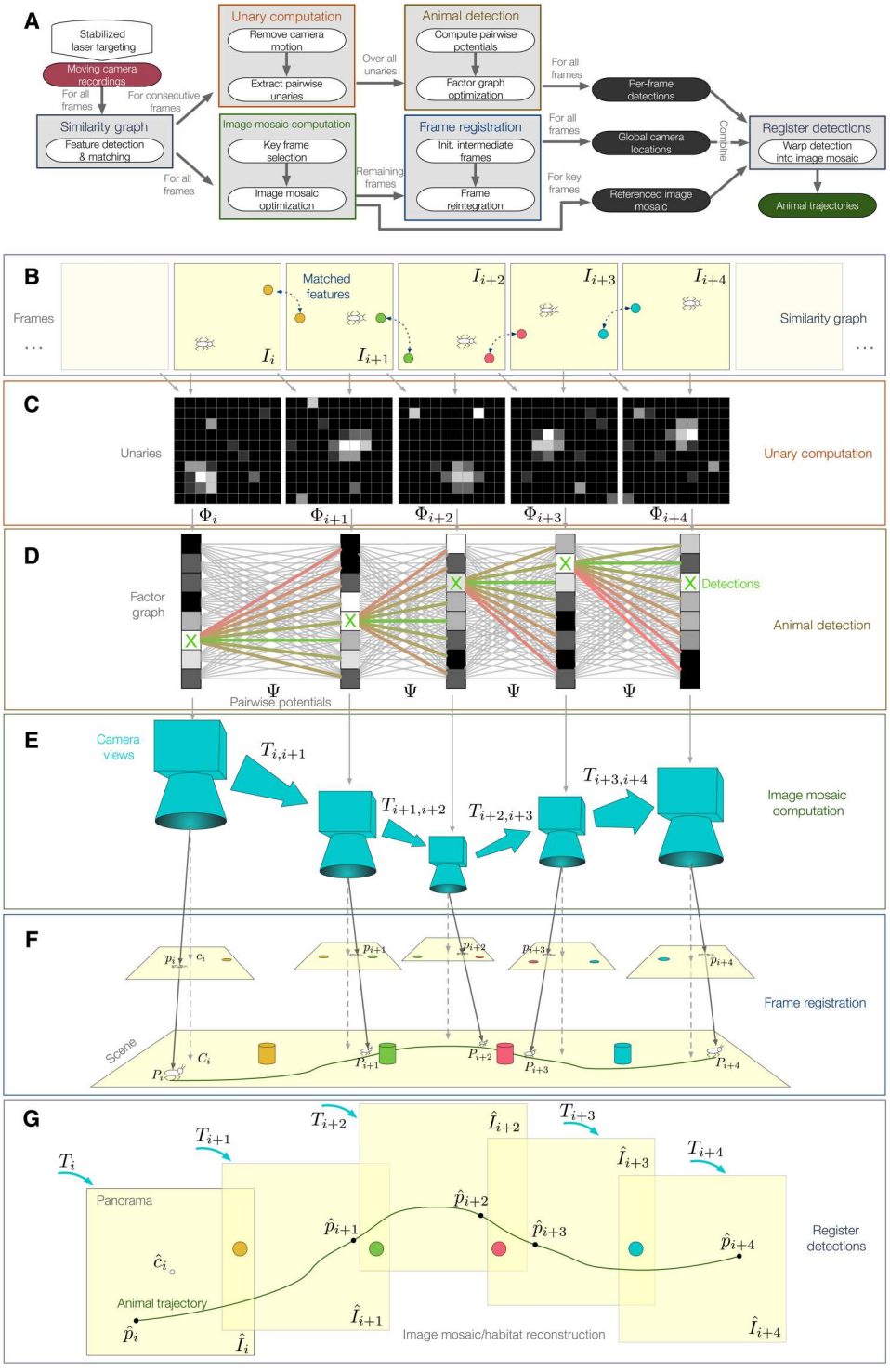

Fig. 2. Insect tracking and environment reconstruction framework. (**A**) Overview of the detection and tracking framework. Consecutive frames I_i are used (**B**) to compute camera motion compensated unaries Φ_i (**C**), which are connected by pairwise potentials Ψ to build a factor graph (**D**). In-frame ant detections p_i are then computed using the factor graph and projected based on the camera views (**E**) into a unified reference system $\hat{p}_i$ using globally referenced frame transformations T_i (**F**) to project the images $\hat{I}_i$ into a unified image mosaic (**G**) to generate animal tracks.

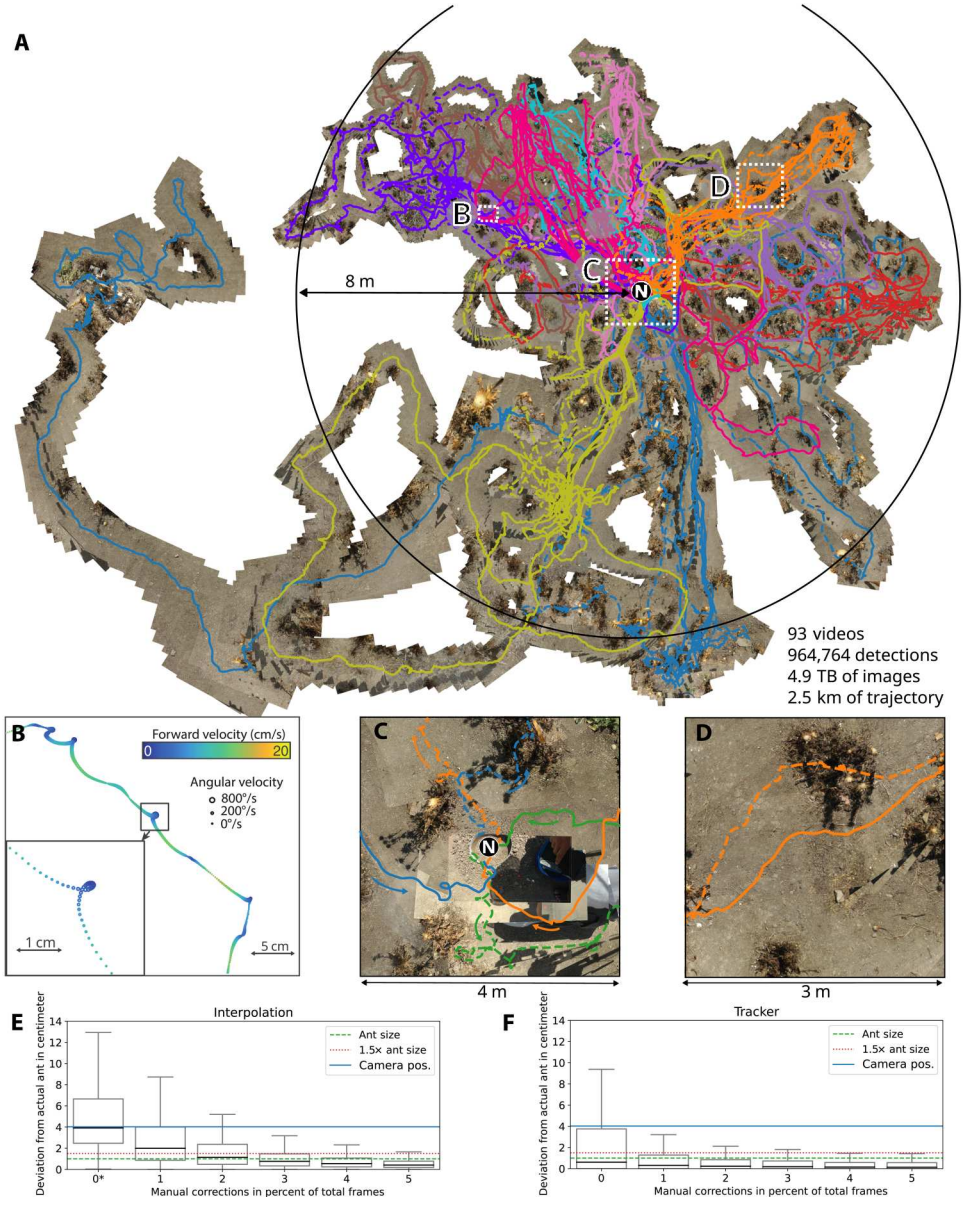

Fig. 3. Reconstructing the foraging history of desert ants in the wild. (**A**) A unified high-resolution (41,248 by 30,351 pixels) top-down image mosaic incorporating 93 videos on which the recovered paths of their respective ants are plotted. (**B**) The 50-Hz temporal resolution allows accurate forward and angular velocities to be measured and fine-scale behavioral motifs such as loops to be mapped. (**C**) Behavior with respect to key locations [here, the first departures (dashed lines) and returns (solid lines) of three ants from the nest (N)] can be compared across individuals. (**D**) Environmental interaction with terrain features (here, bushes) can be recovered. (**E**) Deviation of tracking results per frame using linear interpolation between equidistant points. 0∗ stands for two points being the minimum for successful linear interpolation. (**F**) Deviation of tracking results per frame using the tracker. The points are selected on the basis of high deviation from the ground truth.

observation of fine-scale behavior across the animals complete foraging path in their natural habitat (Fig. 3B); the embedding of paths into a shared frame of reference allows high-resolution comparison of behaviors within and across individuals (Fig. 3C). Moreover, the ability to add labels while reviewing the videos permits retrospective analysis; i.e., conditions of interest such as interactions with vegetation or other ants (Fig. 3D) do not need to be explicitly recorded by the experimenter at the time of data collection, provided that they can be observed in the video data.

Figure 3 (E and F) compares the performance of the tracking algorithm with respect to the amount of manual positional estimates versus a linear interpolation between the same amounts of evenly spaced points. We evaluated the tracking performance using 307,956 manually annotated images and achieved a median accuracy of 0.6 cm. Integrating just 1% of these manual annotations into the globally optimized probabilistic inference task further improves the accuracy to 0.31 cm median accuracy. In contrast, the results using linear interpolation needs more points to achieve similar median accuracy. We note that this is the accuracy of the true ant

position rather than an estimate of position of the tracking device (e.g., GPS unit) as a proxy for the animal position and that the behavioral statistics do not change substantially if manually specified corrections are included to the probabilistic inference task (cf. fg. S5). Performance is particularly robust for homing ants that travel quickly over open terrain while carrying a clearly visible food morsel. These results are in line with previous evaluations of the detection mechanisms in which a localization accuracy above 96% was achieved on the publicly available Small Targets within Natural Scenes dataset (*39*). On the basis of accurate (in-frame) localizations, the accuracy of camera motion compensated trajectories can be estimated based on the precision of the image mosaic algorithm, which has been estimated under laboratory conditions in a separate publication (*40*).

Tracking yields insights from detailed route comparisons

A crucial and novel outcome of our processing framework is that it allows successive routes of the same ant to be precisely registered through anchoring on the terrain. This allows us to probe how accurately an ant can follow a route using visual memory alone after minimal experience. This was tested by tracking individual ants until they had returned twice from the same feeding site. The first-time ants were permitted to enter the nest and deposit the food; the second time, they were captured just before nest entry and (still holding the food item) released back at the feeding site. This eliminates PI information, and as these ants do not use chemical trails, it allows us to test visual navigation in isolation.

An example of the entire foraging history of an individual ant as it progressed through our experimental protocol is provided in Fig. 4. This example clearly demonstrates that after just two visits to the same feeding site, the displaced ant was capable (after an initial search) of retracing its homeward path, a result replicated by all 14 ants tested in this way. There is notable overlap in each return path. Excluding any initial search segment (i.e., trimmed), we quantitatively compared the homing route taken after displacement to the same ant's immediately previous homeward route, for all ants (see "Trajectory processing" section in Materials and Methods). We observed a close similarity in the precise path taken; substantially more similar than would be expected if the ant was just trying to run in the nest direction (e.g., if attracted by a beacon or using a local vector), or if it was retracing its outward route (Fig. 4, ridgeline plot). The same ants were subsequently displaced to a location, which they had not previously experienced (3 to 4 m from the nest in a perpendicular or 180° direction from their feeding location), and were observed to engage in search, only able to home if their search path crossed over a previous inward route (Fig. 4, right).

These data provide strong evidence that *C. velox* desert ants need to experience a route no more than twice (and only once successfully reaching the nest) to have committed it to memory with sufficient reliability to be able to use it to return home in the absence of PI information. This supports previous reports of one-time route learning either in isolated instances (*31*) or over short route segments (*42*, *43*).

We note that the ant shown in Fig. 4 foraged to the 8 m boundary and returned with food on its first outing, as did two other ants; that is, they did not appear to perform "learning walks." This lack of recent experience of the nest surrounds (all ants that had foraged in the previous 2 days were excluded) did not affect their homing ability either on their first homeward trip (Fig. 3C and "Homing performance of ants without exploratory paths" section in Supplementary Text) or in their route displacement test for which they ranked second, third, and fifth of the 14. Nine of the ants made at least one initial exploratory path (returning without food) in the nest vicinity (explorations: mean = 2.2, SD = 1.9; see "The ant ontogeny dataset" section in Supplementary Text). However, unlike the usual characterization of learning walks (*33*, *36*, *44*–*46*), we saw no consistent growth in the duration (mean/SD, first: 27/23 s and last: 36/53 s) or distance covered (mean/SD, first: 0.60/0.32 m and last: 0.64/0.34 m) in these paths. Although the angular coverage increased over trips (mean/SD, first: 98°/37° and last: 191°/78°), foraging was generally restricted to a specific angular sector (Fig. 4 and "Characterization of initial exploratory forages" section in Supplementary Text). This puts into doubt an assumption frequently made in recent computational models of ant visual memory (including our own) (*47*–*51*) that all foraging ants use learning walks to acquire views from multiple directions and a range of distances around the nest as a basis for reliable homing behavior.

Reconstructions enable habitat interaction studies

The ability to reexamine the behavior of ants in the context of the merged video information allows us to identify the effect of habitat features. Upon locating food, ants will return directly to the nest (using PI) and are then assumed to return to the location where the food was found to scavenge further (using a vector memory, that is, inverting the PI information) (*52*). Our data reveal clear differences between paths taken when returning to either a known feeding location or the nest implying different strategies depending on the motivational context. Outward paths of ants to the 8 m boundary gradually increased in their similarity, directness, and speed of travel over successive journeys indicating that they are refined over time, which contrasts with homeward paths that were fixed, direct, and travelled quickly from their first instance ("Differences in outward and inward route learning" section in Supplementary Text).

Closer examination shows that some ants entered bushes much more often on their outward trips than homing trips (ratio of time in bush; Fig. 5), suggesting different strategies driven by motivational state. Foraging ants may target bushes to locate prey (e.g., snail carcasses) or shelter from the sun, while homing ants aim to get home as quickly as possible and thus avoided the bushes (Fig. 5). This is supported by the fact that, when in a bush, foraging (outbound) ants slow down considerably and spent time searching (higher search index), whereas homing ants (which rarely entered a bush) continued moving at their usual rapid pace through bushes (Fig. 5, boxplot). Incorporation of such adaptive strategies into computational models will be important in maintaining their explanatory power in more realistic settings.

High spatiotemporal data yields mechanistic insights

Our dataset provides the spatiotemporal resolution (50Hz positioning at centimeter accuracy) necessary for revealing the mechanisms that underpin guidance behavior in insects. For example, a host of competing hypotheses have been proposed regarding the encoding, storage location, and use of visual route memories in insects (*51*, *53*, *54*). One way to tease apart these models is to reveal the precise circumstances under which navigating insects recognize their location (e.g., the change in distance and orientation at which a view is

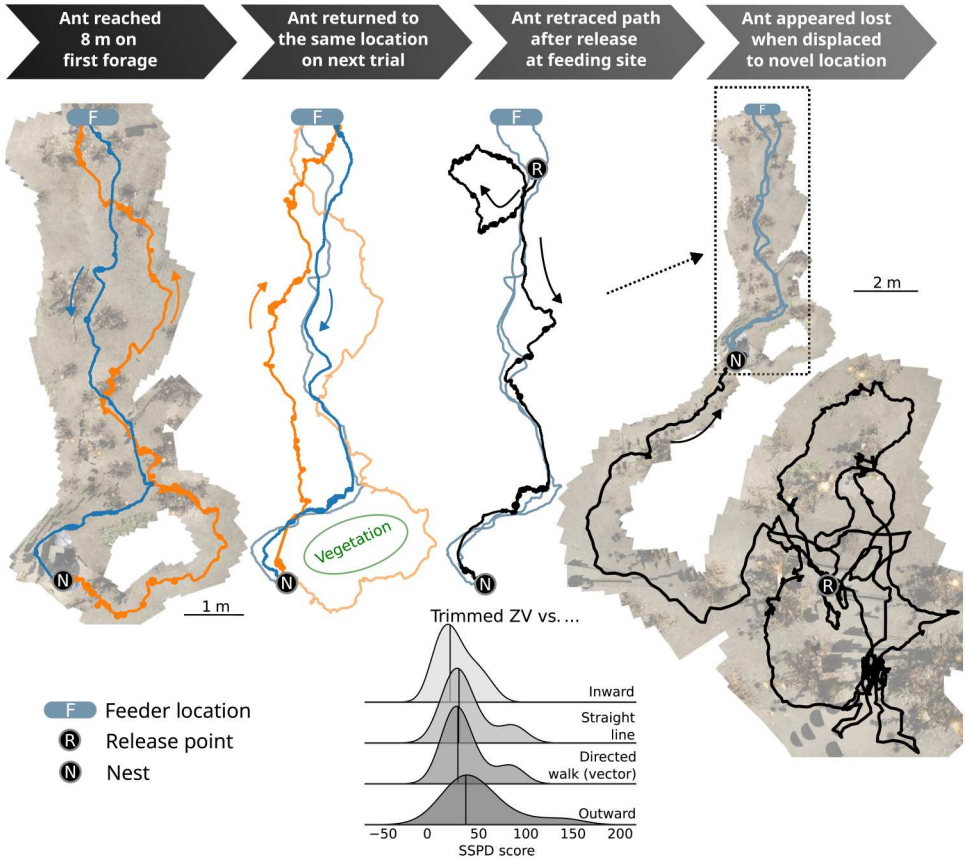

Fig. 4. Tracking results indicate that homeward route memories are acquired rapidly. The foraging history of an individual ant is shown (left to right). On the second return (second from left), it is captured before nest entry and displaced back to the feeding site and is able to retrace the same homeward route without path integration (PI) information (third from left). Ridgeline plot (below): The similarity to its previous route is higher than to a straight line [as measured by symmetrized segment-path distance (SSPD) as defined in the section "Trajectory Preprocessing" in Materials and Methods"], a directed walk with realistic noise, or to its outward path. Control (far right): Displacement to a location not previously experienced results in lengthy search indicating the absence of any long-range cues to the nest position.

recognized is likely to be specific to an individual model). Our data demonstrates local bursts of forward speed when the ant trajectory becomes aligned in a "familiar" direction (Fig. 6, A and B), that is, along a route it has previously taken toward the nest. We can thus infer the locations and conditions under which ants recognize a previously traversed route. We also observe instances of scanning movements (sharply reduced forward speed and increased angular velocity) (*55*) immediately following moments when the ant strays from a previously traversed route (Fig. 6, A and B), allowing us to infer when there is a failure of recognition. Unexpectedly —and not captured by recent models (*37*, *51*, *54*)—some ants moved much faster and displayed less local meander when searching in a completely unfamiliar environment (Fig. 6B, bottom left panel). This suggests that slowing and scanning behaviors may be triggered by sharp (phasic) changes in familiarity, rather than the tonic familiarity level of the current location, as has previously been assumed.

We also observe, in ants moving freely in natural conditions, the expression of regular lateral oscillations (Fig. 6C). These have previously been seen in laboratory conditions (*56*) and in tethered ants running on a trackball in the field (*35*, *57*) but have not been reported for ants moving over natural terrain, as they are hard to perceive by eye. The oscillation frequency is remarkably conserved (around 0.9 Hz) across conditions, but their regularity (magnitude of the Fourier peak) is modulated by the familiarity of the visual environment (Fig. 6C and fig. S10). Oscillations are most regular with zero-vector (ZV) ants in unfamiliar environment (Fig. 6C and fig. S10). This fits nicely the idea that an intrinsic neural oscillator is constantly at play in navigating ants but that both PI [available in full-vector (FV) ants] and visual scene recognition (available when on the familiar route) modulate these oscillations and thus interfere with their regularity (*35*, *57*) by adding externally driven left and right motor commands (*37*, *56*, *58*). Overall, this shows how detailed kinematic data at the natural scale can shed light on the mechanisms at play during an ecological task.

DISCUSSION

The ability to track animal behavior over the natural range of foraging distances has been transformative in our understanding of navigation behavior. For bees, it provided definitive evidence that dance communication provides new foragers with a vector to find the food location (*59*). In bats, it revealed the pin-point accuracy with which animals could target a particular foraging location (a single tree) over large distances (kilometers) (*60*). Even in laboratory rats, the use of a larger arena was a critical factor in the discovery of grid

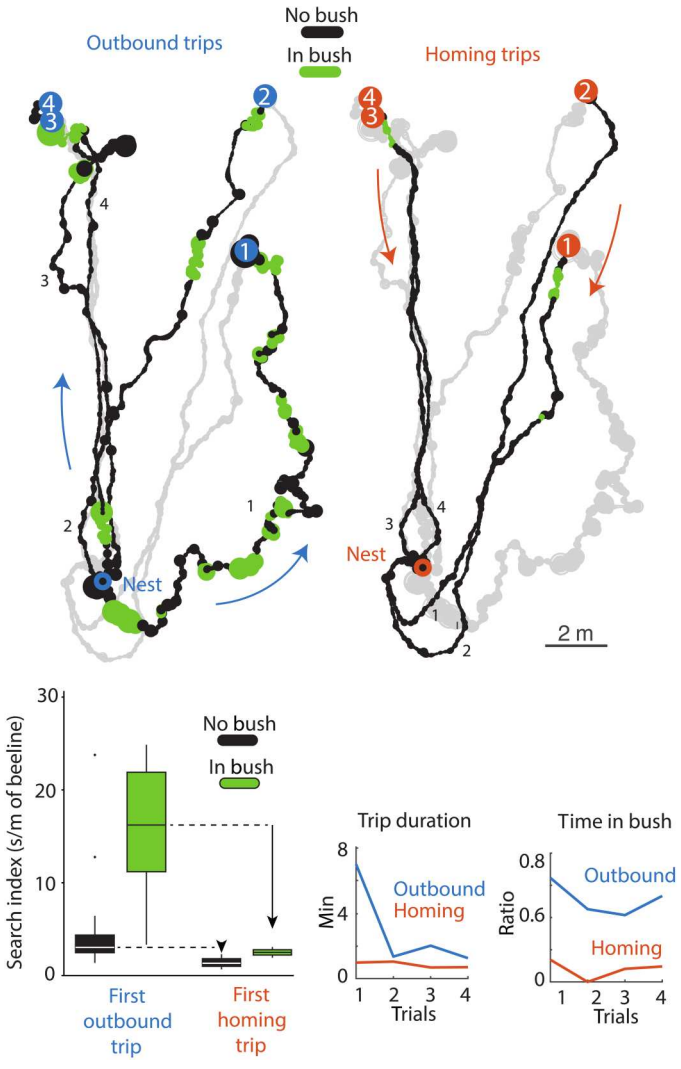

Fig. 5. Environment reconstruction enables post hoc habitat interaction studies. The first four foraging trips of an ant to the 8 m boundary are shown with sections spent within vegetation highlighted in green. The ant entered bushes significantly more during its outward (13 bushes, 334 s) than its homing trips (two bushes, 10 s). The boxplot depicts the search index (a measure of amount of local searching; see "Trajectory processing" section in Materials and Methods for search index calculation) of the ant for route sections within bushes compared to those in open terrain for both the first outbound and first homing trip. Only on outward trips did the ant engage in search behaviors, and search increased within bushes. The duration and ratio of time spent in bushes shows a clear tendency to enter bushes on outbound trips versus a tendency to avoid bushes when homing (bottom right).

cells (*61*). However, until now, substantially increasing the range while maintaining the spatial and temporal resolution of laboratory tracking conditions (*18*) was not possible, particularly under natural conditions where the computer vision challenges are substantially increased (*25*, *27*).

Here, we have shown that, using a single camera to follow a foraging animal, we can reconstruct both detailed tracks and natural habitats. CATER is a general visual tracking and reconstruction framework capable of extracting dense movement patterns of unmarked animals irrespective of their size (even down to a few pixels), camera motion (both static and moving), or setting (controlled laboratory to natural habitats). It combines algorithms for small object detection (*39*) and full frame rate–optimized reconstruction (*40*) into a novel and fully automatic tracking framework, which is applicable to extremely challenging datasets. As a result, animal locations and habitat reconstructions from potentially multiple videos are incorporated in a global reference frame, enabling a wide range of behavioral quantifications and studies. We show its application to data from freely foraging ants in a complex desert-shrub habitat, consisting of multiple videos from handheld cameras with more than 1.8 million frames and a total of more than 2 km of insect tracks. The tracking module achieved centimeter-level precision without any manual correction, with tracks embedded in a shared reconstructed image mosaic. Note that this processing pipeline is designed to provide high-precision trajectories of individual animals followed by the camera. It has therefore been developed for tracking a single animal of interest with no built-in multi-animal tracking capabilities and can only be used in a post hoc fashion (no real-time tracking). The resulting output documents the entire foraging history of desert ants, as they learned to navigate their local environment at unprecedented spatiotemporal resolution.

As a result of these methodological advances, we have already gained important new insights into the visual navigation capabilities of ants. The combination of accuracy within tracks and consistent registration between tracks has revealed that ants follow previous routes very tightly. From instantaneous speed data, we could directly confirm that slowing and scanning—which have been assumed to indicate uncertainty about the route—are associated directly with points at which the ant has deviated from its previous route, and clear increases in speed can be observed when the route is regained. We found that visual memory for the inbound path is obtained very rapidly and appears equally accurate along the whole course of the path, and accuracy in return is independent of time spent in "learning walks" around the nest. We believe this is indicative of "one-shot" learning of visual scenes by the ant. By contrast, the outward path evolves more gradually, under the influence of alternative foraging instincts such as approach to bushes. The ability to retrospectively annotate the video footage to identify such environmental influences and relate them to behavior is an important contribution of our approach. Last, the high temporal resolution provided by video tracking provides additional mechanistic insight by revealing a steady underlying oscillation in the ant's paths, observed under all conditions (foraging, homing, and searching), which appears to be an intrinsic active strategy controlling visual steering.

Robust motion tracking as a behavioral readout is fundamental to fields from neuroscience (*62*) through genetics (*63*, *64*) to medicine (*65*) and ecology (*5*, *25*). Although this study focused on tracking insects from handheld camera footage, the methods described are widely generalizable. For example, drones are increasingly being used to capture video of different animals in distinct settings [e.g., large terrestrial mammals (*66*, *67*) or fishes in shallow water (*68*)], and the data produced are remarkably similar to that presented here and thus can be processed in our framework to obtain detailed paths projected onto their territory. Similarly, multicamera systems and structure from motion pipelines could be added to capture the 3D structure of animal habitats (*69*), which combined with new biologically realistic sensing (*70*) and brain models (*51*, *54*, *71*) would

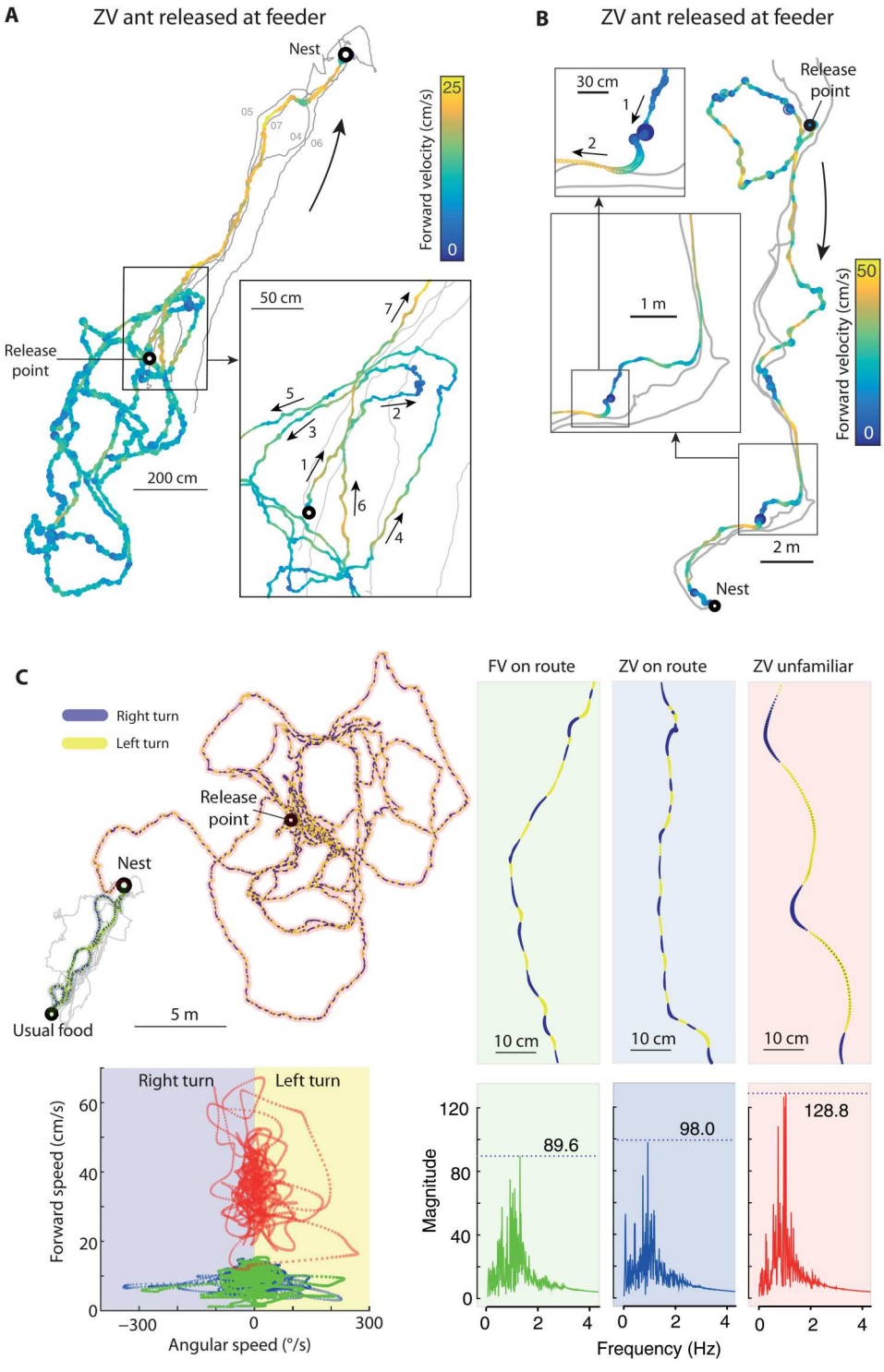

Fig. 6. Mechanistic insight from high spatio-temporal data resolution. (**A** and **B**) Tracks of ants after displacement to the feeding site, with forward velocity indicated by color and angular velocity by line thickness. Previous tracks are in gray. In (A), the ant's initial search is slow with extensive rotation compared to the straight and fast movement once the familiar route is found. Inset, zoomed section of search: A similar transition to faster, straighter motion can be seen in detail each time the ant faces in the direction of the route (arrows 1, 4, 6, and 7), suggesting moments of visual recognition. (B) Zooming in on another ant mid-route, we can identify a "scan," where forward velocity falls to zero and angular velocity exceeds 500°/s (arrow 1) immediately preceding its regaining of the route (arrow 2). (**C**) Comparison of movement dynamics for an ant homing from her usual feeding location with [full-vector (FV) on route, green] or without [zero-vector (ZV) on route, blue] a PI vector or when released in an unfamiliar area without a PI vector (ZV unfamiliar, red). For this ant, there is a clear increase in forward velocity in the unfamiliar environment (bottom left). Highlighting right (blue) and left (yellow) turning reveals regular lateral oscillations. Zooming in (top right) shows that oscillation amplitude increases markedly in the unfamiliar environment. The Fourier spectrum of the angular velocity (bottom left) shows similar frequency of oscillations (around 1 Hz) but variation in their regularity (magnitude) across conditions.

allow hypotheses to be verified in real-world conditions. In the future, we will integrate additional features such as multi-animal tracking and real-time user feedback during recording. The applications of such general tracking methods thus extend beyond behavioral analyses and include habitat management (*72*) and conservation (*2*, *66*).

MATERIALS AND METHODS

Tracking and reconstruction algorithm

Overview

The proposed method consists of several interacting modules that are explained in more detail below. Transformations between consecutive images are used to rectify the camera motion in the unary computation stage or between all frames in the image mosaic

computation stage to find key frames and to generate a 2D background representation. Following the unary computation, animal detections are computed using factor graph optimization. These animal coordinates in per-frame pixel space are transformed using the global camera locations resulting from camera registration and following the image mosaic generation. An abstract overview of the complete framework is outlined in Fig. 2A.

Unary computation and detection

Consecutive images are transformed using their pairwise transformation. To minimize the reprojection error and thus the noise in the resulting unaries, we use homographies in this stage, since they have the highest degree of freedom. Given images I_i, I_{i+1} and their estimated homography $H_{i,i+1}$, image I_{i+1} can be warped into the same coordinate system as I_i using

$$\hat{I}_{i+1} = H_{i,i+1}^{-1} \cdot I_{i+1} \tag{1}$$

effectively removing camera motion between those two images. The remaining motion is calculated by subtracting the warped image $\hat{I}$ and I

$$D_i = |\hat{I}_{i+1} - I_i| \tag{2}$$

The difference D_i contains only moving objects like the moving animal as well as plants moving in the wind, shadows, and noise due to errors in the estimation of the transformation or due to parallax.

The objective of the following optimization problem is to find a probable and temporally consistent path of a single animal through the full video. The optimization problem is formulated as a probabilistic inference problem estimating animal positions $\mathbf{p_i} = (x_i, y_i)$ for all frames $i \in \{1, ..., T\}$ for a total of T images given the frame differences as observations $\mathcal{D} = \{D_1, ..., D_T\}$. The energy function to be maximised is defined as follows (*39*)

$$E(p|D) = \left[\sum_{i=1}^{T} \Phi(p_i|D_i)\right] + \left[\sum_{i=1}^{T} \Psi(p_i, p_{i+1})\right] \tag{3}$$

The first functional $\Phi(\cdot)$ defines the unary potential and is described in terms of the remaining motion D_i weighted by a centered Gaussian distribution to amplify regions in the center and reduce motion cues at the edge of the images

$$\Phi(p_i|D_i) = \mathcal{N}(\mu, \sigma^2) \cdot D_i \tag{4}$$

for some predefined mean μ and variance σ^2 [see (*39*) for details].

The second functional $\Psi(\cdot)$ defines the pairwise potential and encourages temporal consistency by coupling detections between consecutive images

$$\Psi(p_i, p_{i+1}) = \mathcal{N}(p_{i+1}|p_i, \sigma^2) \tag{5}$$

Intuitively, the optimization maximizes areas of motion while enforcing smooth transitions by limiting the step size between images. The functional from Eq. 3 problem is maximized using factor graphs (*39*).

Image mosaic computation and registration

To decrease the computational complexity of the image mosaic computation and reduce visual artifacts, the first step is a key frame selection. Starting with the first image as the first key frame, the following key frames are selected using multiple metrics. A candidate must have enough overlap with the previously selected key frame and should have a small reprojection error (i.e., the error of the transformation) with a high amount of good quality feature points covering a substantial portion of the image. Exhaustive feature matching is done on all key frames to find recurring places in the full scene. For consecutive key frames, transformations are estimated warping them into them same coordinate system.

For this stage of the pipeline, similarities are used instead of homographies, encoding scale, rotation around the viewing direction, and a translation for a camera that is directed perpendicular toward the ground. The goal of the image mosaic generation is to find the best globally consistent reconstruction of the environment, whereas the goal of the unary computation was to minimize noise between consecutive images. Because of the additional degrees of freedom, the later optimization of the transformation is more unstable and often results in unusable image mosaics.

Let $\mathcal{F} = \{I_1, ..., I_N\}$ be the set of all N images and let

$$\mathcal{F} = \{F_i \subset \mathbb{R}^2 \,|\, i \in \{1, \ldots, N\}\}$$

be their corresponding feature vectors, where F_i is a set of 2D feature points.

Given K key frames $\{\tilde{I}_1, \ldots, \tilde{I}_K\} \subset \mathcal{I}$ and their corresponding pairwise similarity $\tilde{T}_{i,i+1}$ for a consecutive pair of key frames $\tilde{I}_i$ and $\tilde{I}_{i+1}$, we can define transformations with respect to the first key frame by a multiplication of the transformation matrices

$$\begin{aligned} \tilde{T}_j &= \prod_{i=1}^{j-1} \tilde{T}_{i,i+1}^{-1} \text{ for } 2 \le j \le N \\ \tilde{T}_1 &= 1 \end{aligned} \tag{6}$$

We call these matrices global transformations, as they project a certain frame into a common reference coordinate system. The multiplication leads to an error manifesting itself in a drift where points of revisiting do not align between earlier and later frames in the videos.

Subsequently, an optimization problem is solved, where common feature points in all frames are used to mitigate errors in the initial estimates

$$\begin{aligned} \min J(\tilde{T}_1, \ldots, \tilde{T}_K) = \sum_{1 \le i \le K} \sum_{i \le j \le K} \sum_{(f_k f_l) \in \tilde{M}_{i,j}} \\ \| (\tilde{T}_j^{-1} \tilde{T}_i) \cdot f_k - f_l \|_2^2 + \| (\tilde{T}_i^{-1} \tilde{T}_j) \cdot f_l - f_k \|_2^2 \end{aligned} \tag{7}$$

For feature matches $\tilde{M}_{i,j} \subset \tilde{F}_i \times \tilde{F}_j$ between key frames $\tilde{I}_i$and $\tilde{I}_j$, minimizing the symmetric reprojection error of the global transformations.

Given two key frames $\tilde{I}_i$ to $\tilde{I}_j$, this energy function reduces the difference between directly transforming from $\tilde{I}_i$ to $\tilde{I}_j$ by using $\tilde{T}_{i,j}$ and using $\tilde{T}_i$ to transform $\tilde{I}_i$ to the reference coordinate system and then using $\tilde{T}_j^{-1}$ to transform to frame $\tilde{I}_j$. The direction of this transformation can also be reversed leading to the above functional. These transformations can then be used to align the images to generate a common image mosaic.

With these optimized transformations of the key frames alone, animal detections in frames between two key frames cannot be projected onto the generated image mosaic. To calculate transformations for all frames, the omitted frames from the preceding key frame selection are reintegrated using geodesic interpolation and are subsequently refined using feature matches between the previous and next key frame, resulting in dense and accurate

transformations T_i for each frame $i \in \{1, ..., T\}$. The optimization and subsequent reintegration and refinement can also be generalized to multiple videos by combining key frames of all videos in the optimization in Eq. 7. Reintegration and refinement is subsequently done for all videos simultaneously. Details for the optimization, reintegration, and multiple video extension can be found in (*40*). The registration process is illustrated in fig. S1.

Trajectory generation

The last step is to overlay per-frame detections onto the image mosaic, which can be achieved by matrix vector multiplication with the transformation estimate of the corresponding frame. Given per-frame detections $\mathbf{p_i} = (x_i, y_i)$ for a frame I_i for all $i \in \{1, ..., T\}$ and their respective transformations T_i mapping them into the common coordinate system, we transform p_i according to

$$\hat{p}_i = T_i \cdot p_i \tag{8}$$

To generate the full animal trajectory, detections of all frames—intermediate and key frames—have to be used. This is possible, since we have one transformation for each frame and not only for the sparse set of key frames after performing reintegration and refinement. The described transformation can also be used to overlay camera trajectories onto the generated image mosaic by transforming points $\mathbf{c_i} = (w/2, h/2)$ for images with a width of w and a height of h for all for all $i \in \{1, ..., T\}$.

GUI, human interactions, and parallelization

The tracking and reconstruction algorithms are combined into a single framework that can be accessed via a graphical user interface (GUI). This GUI can be used to load and process the video frames and provides a variety of visualization strategies and user feedbacks to simplify the tracking process. The graphical interface can also be used to attach labels and provides a summary indicating the quality of the frames with respect to the tracking task. See fig. S2 for more details.

The method described in "Unary computation and detection" section supports two types of human interaction. First, the user can manually correct the animal position by manually clicking on correct animal positions. Note that because of the factor graph optimization, a single click can correct multiple frames (*39*). Second, the user can also easily add labels to a video to allow more complex behavioral analysis. For example, in this study, we added labels indicating the visibility of the ant, whether the ant was within shadows or bushes, plus the ant's current state (foraging versus homing).

The computational time used to solve the optimization problem in Eq. 3 across all frames made manual corrections cumbersome. To alleviate this, after initial global optimization, videos were chunked into smaller subsections, which were processed in parallel to let the user see the impact of their manual correction more quickly. After revising the whole video, the full optimization can be performed again.

Trajectory preprocessing

The generated raw trajectory is smoothed by using a Savitzky-Golay smoothing filter (*73*) with a polynomial order of 3 and a window size of 50, which equals to 1 s in our recordings. Trajectories in pixel space on the generated image mosaics were scaled to real-world space in centimeters using an object with known scale.

Velocity metrics from the paths were obtained by first calculating "instantaneous velocities vectors" as the vectors connecting each two subsequent trajectory points. Forward velocity values were then obtained as the norm of the instantaneous velocity vectors (Euclidean distances between successive points). Angular velocity values were obtained as the angle between two subsequent instantaneous velocity vectors. Determining the sign of angular velocity (whether the ant is turning clockwise or counterclockwise) is intrinsically ambiguous. However, here, the frame rate (50 Hz) can resolve angular velocities up to 180°/0.02 s (i.e., 9000°/s), which is by far higher than the maximum angular velocity displayed by ants. Therefore, the sign of angular velocity values between two consecutive frames could be easily disambiguated by choosing the comparison ($n \rightarrow n + 1$ or $n + 1 \rightarrow n$) that yielded an angle smaller than 180°. Velocity values presented in Fig. 6 were smoothed using first a median filter (sliding window of 10 frames, 0.2 s, to remove aberration data) and then an average filter (sliding window of 10 frames, 0.2 s, to reduce noise). Absolute angular velocity values in Fig. 6 were converted linearly into dot thickness of a scatter plot.

Straightness of a trajectory is defined by the ratio of its total path length (sum of the length of all segments between consecutive trajectory points) divided by the distance between its start and end point as discussed in (*74*). Distance between trajectories is quantified using the symmetrized segment-path distance (SSPD), which is based on point to segment distances as described in (*75*) rather than dynamic time warping (DTW), which is based on point-to-point correspondences. SSPD is therefore less dependent on the velocity of the two compared trajectories. Higher velocity results in fewer points on the trajectory, which leads to higher distances when using DTW.

The search index presented in Fig. 5 corresponds to the time spent within a bush (or between bushes) divided by the Euclidian distance between the path's entrance point in a bush and subsequent exit point (or the exit point of one bush to the entrance point of the next bush for between-bushes indexes). Directed random walks are defined by a realistic step size determined by the average velocity of the model species and an angle sample from a random distribution centered around the target angle determined by the angle from the current position to the nest. Directed walks are then generated with a same straightness as the corresponding trimmed zero vector path using the metric from above. This is done by repeatedly sampling random walks until a desired straightness is achieved.

Supplementary Materials

This PDF file includes:

Supplementary Text
Figs. S1 to S11
Table S1
Legend for movie S1
References

Other Supplementary Material for this manuscript includes the following:

Movie S1

REFERENCES AND NOTES

1. South African Correspondent, Biotelemetry: Tracking of wildlife. *Nature* **234**, 508–509 (1971).
2. D. Tuia, B. Kellenberger, S. Beery, B. R. Costelloe, S. Zuffi, B. Risse, A. Mathis, M. W. Mathis, F. van Langevelde, T. Burghardt, R. Kays, H. Klinck, M. Wikelski, I. D. Couzin, G. van Horn,

M. C. Crofoot, C. V. Stewart, T. Berger-Wolf, Perspectives in machine learning for wildlife conservation. *Nat. Commun.* **13**, 1 (2022).
3. S. E. R. Egnor, K. Branson, Computational analysis of behavior. *Annu. Rev. Neurosci.* **39**, 217–236 (2016).
4. N. C. Manoukis, T. C. Collier, Computer vision to enhance behavioral research on insects. *Ann. Entomol. Soc. Am.* **112**, 227–235 (2019).
5. B. G. Weinstein, A computer vision for animal ecology. *J. Anim. Ecol.* **87**, 533–545 (2018).
6. H. Dankert, L. Wang, E. D. Hoopfer, D. J. Anderson, P. Perona, Automated monitoring and analysis of social behavior in *Drosophila*. *Nat. Methods* **6**, 297–303 (2009).
7. A. D. Straw, K. Branson, T. R. Neumann, M. H. Dickinson, Multi-camera real-time three-dimensional tracking of multiple flying animals. *J. R. Soc. Interface* **8**, 395–409 (2011).
8. A. Gomez-Marin, N. Partoune, G. J. Stephens, M. Louis, automated tracking of animal posture and movement during exploration and sensory orientation behaviors. *PLOS ONE* **7**, e41642 (2012).
9. B. Risse, D. Berh, N. Otto, C. Klämbt, X. Jiang, FIMTrack: An open source tracking and locomotion analysis software for small animals. *PLOS Comput. Biol.* **13**, e1005530 (2017).
10. N. A. Swierczek, A. C. Giles, C. H. Rankin, R. A. Kerr, High-throughput behavioral analysis in *C. elegans*. *Nat. Methods* **8**, 592–598 (2011).
11. A. Pérez-Escudero, J. Vicente-Page, R. C. Hinz, S. Arganda, G. G. de Polavieja, idTracker: Tracking individuals in a group by automatic identification of unmarked animals. *Nat. Methods* **11**, 743–748 (2014).
12. S. L. Reeves, K. E. Fleming, L. Zhang, A. Scimemi, M-Track: A new software for automated detection of grooming trajectories in mice. *PLOS Comput. Biol.* **12**, e1005115 (2016).
13. A. Weissbrod, A. Shapiro, G. Vasserman, L. Edry, M. Dayan, A. Yitzhaky, L. Hertzberg, O. Feinerman, T. Kimchi, Automated long-term tracking and social behavioural phenotyping of animal colonies within a semi-natural environment. *Nat. Commun.* **4**, 2018 (2013).
14. V. Panadeiro, A. Rodriguez, J. Henry, D. Wlodkowic, M. Andersson, A review of 28 free animal-tracking software applications: Current features and limitations. *Lab Animal* **50**, 246–254 (2021).
15. J. M. Graving, D. Chae, H. Naik, L. Li, B. Koger, B. R. Costelloe, I. D. Couzin, DeepPoseKit, a software toolkit for fast and robust animal pose estimation using deep learning. *eLife* **8**, e47994 (2019).
16. A. Mathis, P. Mamidanna, K. M. Cury, T. Abe, V. N. Murthy, M. W. Mathis, M. Bethge, DeepLabCut: Markerless pose estimation of user-defined body parts with deep learning. *Nat. Neurosci.* **21**, 1281–1289 (2018).
17. T. D. Pereira, D. E. Aldarondo, L. Willmore, M. Kislin, S. S.-H. Wang, M. Murthy, J. W. Shaevitz, Fast animal pose estimation using deep neural networks. *Nat. Methods* **16**, 117–125 (2019).
18. J. Lauer, M. Zhou, S. Ye, W. Menegas, S. Schneider, T. Nath, M. M. Rahman, V. di Santo, D. Soberanes, G. Feng, V. N. Murthy, G. Lauder, C. Dulac, M. W. Mathis, A. Mathis, Multi-animal pose estimation, identification and tracking with DeepLabCut. *Nat. Methods* **19**, 496–504 (2022).
19. T. D. Pereira, N. Tabris, A. Matsliah, D. M. Turner, J. Li, S. Ravindranath, E. S. Papadoyannis, E. Normand, D. S. Deutsch, Z. Y. Wang, G. C. McKenzie-Smith, C. C. Mitelut, M. D. Castro, J. D'Uva, M. Kislin, D. H. Sanes, S. D. Kocher, S. S. H. Wang, A. L. Falkner, J. W. Shaevitz, M. Murthy, SLEAP: A deep learning system for multi-animal pose tracking. *Nat. Methods* **19**, 486–495 (2022).
20. K. Branson, A. A. Robie, J. Bender, P. Perona, M. H. Dickinson, High-throughput ethomics in large groups of *Drosophila*. *Nat. Methods* **6**, 451–457 (2009).
21. F. Romero-Ferrero, M. G. Bergomi, R. C. Hinz, F. J. H. Heras, G. G. de Polavieja, idtracker.ai: Tracking all individuals in small or large collectives of unmarked animals. *Nat. Methods* **16**, 179–182 (2019).
22. B. Q. Geuther, S. P. Deats, K. J. Fox, S. A. Murray, R. E. Braun, J. K. White, E. J. Chesler, C. M. Lutz, V. Kumar, Robust mouse tracking in complex environments using neural networks. *Commun. Biol.* **2**, 124 (2019).
23. Z. XU, X. E. Cheng, Zebrafish tracking using convolutional neural networks. *Sci. Rep.* **7**, 42815 (2017).
24. A. Gal, J. Saragosti, D. J. C. Kronauer, anTraX, a software package for high-throughput video tracking of color-tagged insects. *eLife* **9**, e58145 (2020).
25. A. I. Dell, J. A. Bender, K. Branson, I. D. Couzin, G. G. de Polavieja, L. P. J. J. Noldus, A. Pérez-Escudero, P. Perona, A. D. Straw, M. Wikelski, U. Brose, Automated image-based tracking and its application in ecology. *Trends Ecol. Evol.* **29**, 417–428 (2014).
26. P. Karashchuk, J. C. Tuthill, B. W. Brunton, The DANNCE of the rats: A new toolkit for 3D tracking of animal behavior. *Nat. Methods* **18**, 460–462 (2021).
27. L. Haalck, M. Mangan, B. Webb, B. Risse, Towards image-based animal tracking in natural environments using a freely moving camera. *J. Neurosci. Methods* **330**, 108455 (2020).
28. M. Kristan, J. Matas, A. Leonardis, M. Felsberg, R. Pflugfelder, J.-K. Kämäräinen, H. J. Chang, M. Danelljan, L. Cehovin, Alan Lukežič, O. Drbohlav, J. Käpylä, G. Häger, S. Yan, J. Yang, Z. Zhang, G. Fernández, The ninth visual object tracking VOT2021 challenge results, in *Proceedings of the IEEE/CVF International Conference on Computer Vision* (IEEE/CVF, 2021), pp. 2711–2738.
29. R. Wehner, in *Desert navigator: The Journey of an Ant* (Harvard University Press, Cambridge, 2020).
30. M. Kohler, R. Wehner, Idiosyncratic route-based memories in desert ants, melophorus bagoti: How do they interact with path-integration vectors? *Neurobiol. Learn. Mem.* **83**, 1–12 (2005).
31. M. Mangan, B. Webb, Spontaneous formation of multiple routes in individual desert ants (*Cataglyphis velox*). *Behav. Ecol.* **23**, 944–954 (2012).
32. A. Narendra, S. Gourmaud, J. Zeil, Mapping the navigational knowledge of individually foraging ants, *Myrmecia croslandi*. *Proc. Biol. Sci.* **280**, 20130683 (2013).
33. P. N. Fleischmann, R. Grob, R. Wehner, W. Rössler, Species-specific differences in the fine structure of learning walk elements in *Cataglyphis* ants. *J. Exp. Biol.* **220**, 2426–2435 (2017).
34. P. Jayatilaka, T. Murray, A. Narendra, J. Zeil, The choreography of learning walks in the Australian jack jumper ant *Myrmecia croslandi*. *J. Exp. Biol.* **221**, jeb185306 (2018).
35. T. Murray, Z. Kócsi, H. Dahmen, A. Narendra, F. L. Möel, A. Wystrach, J. Zeil, The role of attractive and repellent scene memories in ant homing (*Myrmecia croslandi*). *J. Exp. Biol.* **223**, jeb210021 (2020).
36. J. Zeil, P. N. Fleischmann, The learning walks of ants (*Hymenoptera:* Formicidae). *Myrmecological News*, (2019).
37. A. Wystrach, F. Le Moël, L. Clement, S. Schwarz, A lateralised design for the interaction of visual memories and heading representations in navigating ants. *bioRxiv*, 2020.08.13.249193 (2020).
38. R. Hartley, A. Zisserman, in *Multiple view geometry in computer vision* (Cambridge University Press, Cambridge, 2011).
39. B. Risse, M. Mangan, L. D. Pero, B. Webb, Visual Tracking of Small Animals in Cluttered Natural Environments Using a Freely Moving Camera, in *Proceedings of the 2017 IEEE International Conference on Computer Vision Workshops* (ICCVW, 2017), pp. 2840–2849.
40. L. Haalck, B. Risse, Embedded Dense Camera Trajectories in Multi-Video Image Mosaics by Geodesic Interpolation-Based Reintegration, in *Proceedings of the IEEE/CVF Winter Conference on Applications of Computer Vision* (WACV, 2021), pp. 1849–1858.
41. R. Kays, M. C. Crofoot, W. Jetz, M. Wikelski, Terrestrial animal tracking as an eye on life and planet. *Science* **348**, aaa2478 (2015).
42. C. A. Freas, K. Cheng, Learning and time-dependent cue choice in the desert ant, *Melophorus bagoti*. *Ethology* **123**, 503–515 (2017).
43. C. A. Freas, M. L. Spetch, Terrestrial cue learning and retention during the outbound and inbound foraging trip in the desert ant, *Cataglyphis velox*. *J. Comp. Physiol. A Neuroethol. Sens. Neural Behav. Physiol.* **205**, 177–189 (2019).
44. M. Müller, R. Wehner, Path integration provides a scaffold for landmark learning in desert ants. *Curr. Biol.* **20**, 1368–1371 (2010).
45. P. N. Fleischmann, M. Christian, V. L. Müller, W. Rössler, R. Wehner, Ontogeny of learning walks and the acquisition of landmark information in desert ants, *Cataglyphis fortis*. *J. Exp. Biol.* **219**, 3137–3145 (2016).
46. T. S. Collett, J. Zeil, Insect learning flights and walks. *Current Biology* **28**, R984–R988 (2018).
47. B. Baddeley, P. Graham, P. Husbands, A. Philippides, A model of ant route navigation driven by scene familiarity. *PLoS Comput. Biol.* **8**, e1002336 (2012).
48. A. Wystrach, M. Mangan, A. Philippides, P. Graham, Snapshots in ants? New interpretations of paradigmatic experiments. *J. Exp. Biol.* **216**, 1766–1770 (2013).
49. A. D. Dewar, A. Philippides, P. Graham, What is the relationship between visual environment and the form of ant learning-walks? An in silico investigation of insect navigation. *Adapt. Behav.* **22**, 163–179 (2014).
50. W. Stürzl, J. Zeil, N. Boeddeker, J. M. Hemmi, How wasps acquire and use views for homing. *Curr. Biol.* **26**, 470–482 (2016).
51. F. Le Moël, A. Wystrach, Opponent processes in visual memories: A model of attraction and repulsion in navigating insects' mushroom bodies. *PLoS Comput. Biol.* **16**, e1007631 (2020).
52. S. E. Pfeffer, S. Bolek, H. Wolf, M. Wittlinger, Nest and food search behaviour in desert ants, *Cataglyphis*: A critical comparison. *Anim. Cogn.* **18**, 885–894 (2015).
53. P. Ardin, F. Peng, M. Mangan, K. Lagogiannis, B. Webb, Using an insect mushroom body circuit to encode route memory in complex natural environments. *PLOS Comput. Biol.* **12**, e1004683 (2016).
54. X. Sun, S. Yue, M. Mangan, A decentralised neural model explaining optimal integration of navigational strategies in insects. *eLife* **9**, e54026 (2020).
55. A. Wystrach, A. Philippides, A. Aurejac, K. Cheng, P. Graham, Visual scanning behaviours and their role in the navigation of the Australian desert ant *Melophorus bagoti*. *J. Comp. Physiol. A* **200**, 615–626 (2014).
56. D. D. Lent, P. Graham, T. S. Collett, Phase-dependent visual control of the zigzag paths of navigating wood ants. *Curr. Biol.* **23**, 2393–2399 (2013).

57. L. Clement, S. Schwarz, A. Wystrach, An intrinsic oscillator underlies visual navigation in ants. *bioRxiv*, 2022.04.22.489150 (2022).
58. J. R. Riley, U. Greggers, A. D. Smith, D. R. Reynolds, R. Menzel, The flight paths of honeybees recruited by the waggle dance. *Nature* **435**, 205–207 (2005).
59. A. Kodzhabashev, M. Mangan, Route Following Without Scanning, in *Biomimetic and Biohybrid Systems*, S. Wilson, P. Verschure, A. Mura, T. Prescott, Eds. (Springer, Cham, 2015), vol. 9222.
60. S. Toledo, D. Shohami, I. Schiffner, E. Lourie, Y. Orchan, Y. Bartan, R. Nathan, Cognitive map–based navigation in wild bats revealed by a new high-throughput tracking system. *Science* **369**, 188–193 (2020).
61. T. Hafting, M. Fyhn, S. Molden, M.-B. Moser, E. I. Moser, Microstructure of a spatial map in the entorhinal cortex. *Nature* **436**, 801–806 (2005).
62. T. D. Pereira, J. W. Shaevitz, M. Murthy, Quantifying behavior to understand the brain. *Nat. Neurosci.* **23**, 1537–1549 (2020).
63. M. Reiser, The ethomics era? *Nat. Methods* **6**, 413–414 (2009).
64. M. B. Sokolowski, *Drosophila*: Genetics meets behaviour. *Nat. Rev. Gen.* **2**, 879–890 (2001).
65. R. Hajar, Animal testing and medicine. *Heart Views* **12**, 42 (2011).
66. R. Schiffman, Drones flying high as new tool for field biologists. *Science* **344**, 459 (2014).
67. B. Kellenberger, M. Volpi, D. Tuia, Fast Animal Detection in UAV Images Using Convolutional Neural Networks, in *Proceedings of the 2017 IEEE International Geoscience and Remote Sensing Symposium* (IGARSS, 2017), pp. 866–869.
68. V. Raoult, L. Tosetto, J. E. Williamson, Drone-based high-resolution tracking of aquatic vertebrates. *Drones* **2**, 37 (2018).
69. P. C. Brady, Three-dimensional measurements of animal paths using handheld unconstrained GoPro cameras and VSLAM software. *Bioinspir. Biomim.* **16**, 026022 (2021).
70. B. Millward, S. Maddock, M. Mangan, CompoundRay, an open-source tool for high-speed and high-fidelity rendering of compound eyes. *eLife* **11**, –e73893 (2022).
71. R. Goulard, C. Buehlmann, J. E. Niven, P. Graham, B. Webb, A unified mechanism for innate and learned visual landmark guidance in the insect central complex. *PLOS Comput. Biol.* **17**, e1009383 (2021).
72. L. Schad, J. Fischer, Opportunities and risks in the use of drones for studying animal behaviour. *Methods Ecol. Evol.*, 10.1111/2041-210X.13922 (2022).
73. A. Savitzky, M. J. E. Golay, Smoothing and differentiation of data by simplified least squares procedures. *Anal. Chem.* **36**, 1627–1639 (1964).
74. E. Batschelet, in *Circular Statistics in Biology* (Academic Press, Cambridge, 1981).
75. P. Besse, B. Guillouet, J.-M. Loubes, F. Royer, Review and perspective for distance-based clustering of vehicle trajectories. *IEEE Trans. Intell. Transp. Syst.* **17**, 3306–3317 (2016).
76. M. Ratnayake, A. Dyer, A. Dorin, Tracking individual honeybees among wildflower clusters with computer vision-facilitated pollinator monitoring. *PLOS ONE* **16**, e0239504 (2021).
77. G. Bhat, M. Danelljan, L. Van Gool, R. Timofte, Learning Discriminative Model Prediction for Tracking, in *Proceedings of the 2019 IEEE/CVF International Conference on Computer Vision* (ICCV, 2019).
78. G. Jocher, YOLOv5 by Ultralytics, https://github.com/ultralytics/yolov5 (2020).
79. F. Francesco, P. Nührenberg, A. Jordan, High-resolution, non-invasive animal tracking and reconstruction of local environment in aquatic ecosystems. *Mov. Ecol.* **8**, 27 (2020).

Acknowledgments: We thank X. Cerda and his research group at Estación Biológica de Doñana, Sevilla for hosting our field study. We also thank to P. Ardin for assisting in data capture and the technicians at University of Edinburgh for designing and building the custom camera tracking rig. **Funding:** L.H. thanks the Heinrich Böll Foundation. B.R. and L.H. acknowledge the Human Frontier Science Program (RGP0057/2021). B.R. thanks the WildDrone MSCA Doctoral Network funded by EU Horizon Europe under grant agreement no. 101071224. A.W. thanks the Fyssen Foundation. A.W. and L.C. acknowledge the financial support from the European Research Council (ERC StG: EMERG-ANT 759817). B.W. and M.M. acknowledge the financial contribution of the Biotechnology and Biological Sciences Research Council (BB/I014543/1) and the Engineering and Physical Sciences Research Council [EP/M008479/1 (B.W. and M.M.), EP/P006094/1 (M.M.), and EP/S030964/1]. **Author contributions:** Conceptualization: B.W., M.M., A.W., and B.R. Methodology: L.H., B.R., and M.M. Investigation: M.M., A.W., B.R., B.W., and L.C. Visualization: L.H., B.R., A.W., and M.M. Supervision: B.R., B.W., and M.M. Writing: L.H., M.M., A.W., L.C., B.W., and BR. **Competing interests:** M.M. also holds position as Research Director at Opteran Technologies, UK. All other authors declare that they have no competing interests. **Data and materials availability:** All data needed to evaluate the conclusions in the paper are present in the paper and/or the Supplementary Materials. The Ontogeny dataset and the source code of CATER can be found at https://cater.cvmls.org.

Submitted 12 December 2022
Accepted 22 March 2023
Published 21 April 2023
10.1126/sciadv.adg2094